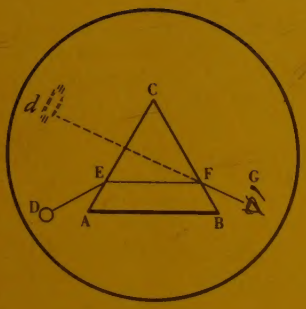

UNIVERSITY OF ILLINOIS
LIBRARY
MAY 11 1961
CHICAGO

optics and spectroscopy

volume x
number 1
january 1961

OPTICAL SOCIETY OF AMERICA

USSR ACADEMY OF SCIENCES

RUSSIAN EDITORIAL STAFF FOR
OPTIKA I SPEKTROSKOPIYA sponsored by
USSR ACADEMY OF SCIENCES

Editor: S. E. FRISH

Assistant Editor: P. P. FEOFILOV
Corresponding Secretary: L. S. SAZONOV

Associate Editors:

M. M. GUREVICH M. A. EL'IASHEVICH A. A. LEBEDEV V. P. LINNIK
S. L. MANDEL'SHTAM I. V. OBREIMOV V. K. PROKOF'EV
N. N. SOBOLEV A. N. TERENIN A. I. TUDOROVSKII

Translated from *OPTIKA I SPEKTROSKOPIYA* on the initiative of THE OPTICAL SOCIETY OF AMERICA, INC. with a grant-in-aid from THE NATIONAL SCIENCE FOUNDATION. *Optics and Spectroscopy* is a cover-to-cover translation of *Optika i Spektroskopiya* and no attempt is made to edit the material other than to correct obvious misprints. The views are those of the original authors and do not represent the Optical Society of America.

TRANSLATION EDITORIAL STAFF

Scientific Editors

CYRUS FELDMAN, *Oak Ridge National Laboratory*

CARL W. GARLAND, *Massachusetts Institute of Technology*

MATHEW G. GIBBONS, *Oakland, California*

Administrative Editor: PATRICIA R. WAKELING, *OSA*

Published monthly by the Optical Society of America, Inc. Executive office: 1155 Sixteenth Street, N.W., Washington, D.C. Subscriptions for one year to members of the Society: Associates $13.00; Regular members and Fellows $17.00. Subscriptions for non-members of the Society: One year U. S. and Possessions, $25.00; Foreign $28.00. Back numbers: $3.00 per copy. Subscriptions, changes of address and undeliverable copies should be referred to the Executive offices in Washington, D.C. The office of publication is 2500 South State Street, Ann Arbor, Michigan. Second class postage paid at Ann Arbor, Michigan.

Printed in the U.S.A. by Edwards Brothers, Inc., Ann Arbor, Michigan.

THE SIZE OF ATOMIC ELECTRON SHELLS AS A FUNCTION OF ATOMIC NUMBER

V. S. Korol'kov (pp. 3-7)

Received 8 January 1960

The dependence of $\overline{r}^k(n, l)$ on the atomic number and degree of ionization of an atom is discussed. On the basis of the function investigated, relative values of $\overline{r}^k(4f)$ are calculated for the rare earth ions with k = −3, +1, +2, +4, and +6. The results are compared with the experimental data.

For the approximate determination of the relationips among the various properties of the atoms, the an values of the distance r(n, l) of the electron in a ven shell from the nucleus, expressed in various rwers k, are used as parameters, $\overline{r}^k(n, l)$. For a satisctory theoretical calculation of the values of $\overline{r}^k(n, l)$, iis necessary to have a fairly accurate knowledge of the dial wave functions of the atom. At the present time, e best functions are those obtained by the method of e self-consistent field with exchange. It is regrettable at this method has been applied to only a relatively all number of light atoms and ions (Z ≤ 30). Radial ve functions obtained by means of the self-consistent ld without exchange give poor agreement with experient, especially for the outer shells. For a solution to s problem, it is necessary to investigate the dependce of $\overline{r}^k(n, l)$ on Z and on the degree of ionization of e atom; i.e., to find the relative values of $\overline{r}^k(n, l)$ for atoms and ions having a given shell n, l. It is easier find relative values of $\overline{r}^k(n, l)$ than sufficiently reliе absolute values, because even crude methods (e.g., e Thomas-Fermi method) give good descriptions of the riation of atomic properties which depend monotonously Z. It can also be expected that the relative values will t change substantially when an atom is included in a ystal, although the absolute values of $\overline{r}^k(n, l)$ can dend to a considerable degree on the surroundings. The istence of even a few experimental values of $\overline{r}^k(n, l)$ ll obviously make it possible to convert from relative absolute values.

For the hydrogenlike wave functions, the following lation is satisfied

$$[r^k(n, l)]^{-\frac{1}{k}} = C(n, l, k)\, Z,$$

ere the coefficient C is independent of Z.

Therefore, it can be expected that in the case of onectron wave functions for complex atoms, the quantities $^k(n, l)]^{-1/k}$ will be fairly simple functions of Z. To exore the nature of this dependence, we will use values 2p) and $\overline{r}(3d)$ obtained by the method of the self-constent field with exchange.[2] Figures 1 and 2 represent e dependence of $1/\overline{r}$ on Z for 2p and 3d shells rectively. It is easy to see that in the case of 2p shell, $\overline{r}$ depends linearly on the atomic number of an atom th for isoelectronic sequences and for ions of a given gree of ionization. The linear dependence is especially arked for an isoelectronic sequence corresponding to e completion of a shell. The straight lines correspondg to different isoelectronic sequences (i.e., different grees of completion of the shell form a system of equistant parallel lines. The straight lines which correond to a given stage of ionization of atoms also form a stem of equidistant parallel lines, but with a different ope.

The simple form of the dependence of $[\overline{r}(2p)]^{-1}$ on Z d on the degree of ionization of the atom is explained

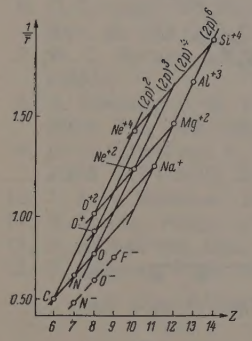

Fig. 1

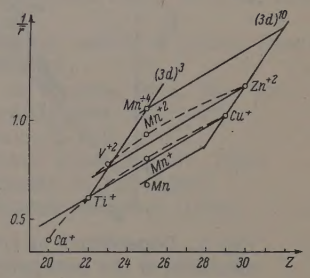

Fig. 2

Fig. 1. Dependence of $[\overline{r}(2p)]^{-1}$ on Z.
Fig. 2. Dependence of $[\overline{r}(3d)]^{-1}$ on Z for elements of the iron group.

in this case by the small degree of interaction between configurations (in most cases, the closest excited level with which the ground level can interact is several hundred thousand cm^{-1} away). The interaction of electrons among themselves can be neglected when we consider the motion of each electron in some averaged field having central symmetry. In this approximation, many properties of a radial wave function are similar to the properties of a hydrogenlike wave function when Z is replaced by Z_{eff} (Z_{eff} depends not only on n and l but also on the atomic properties which we wish to describe with a hydrogenlike wave function). For a hydrogenlike wave function, $[\overline{r}^k(n, l)]^{-1/k}/\overline{r}(n, l)$ depends linearly on k and is entirely independent of Z. For wave functions of the non-hydrogenlike type, this ratio is not a strictly linear function of k, and even though it depends on Z (linearly), it is only a weak dependence. For this reason, it is not necessary to make a detailed investigation of the dependence of $[\overline{r}^k(n, l)]^{-1/k}$ on Z at $k \neq 1$, since this will be similar to the dependence of $[\overline{r}(n, l)]^{-1}$ on Z (only the slopes of corresponding lines will be slightly different).

Deviations of the values of $[\overline{r}^k(n, l)]^{-1/k}$ from the above described function were observed for the 3d shell of the transition elements of the iron group. This is explained quite naturally by the interaction of the $3d^x$ configurations with the configurations of the $3d^{x-1}4s$ and $3d^{x-2}4s^2$ types. The terms of these configurations overlap considerably, and this leads to a significant interaction among them. For example, for the Ca^+ ion, the configuration $3\overline{p}^6 3d$ is not even the ground state, and interacts strongly with the $3\overline{p}^6 4d$ configuration. This leads to a significant deviation of the value of $\overline{r}^k(3d)$ from the predicted value. For the remaining ions of the transition elements of the iron group, the deviations are much smaller and only in special cases exceed 5%. Quite similar deviations from linear dependence occur at k = −3 (Fig. 3). The similarity of Figs. 2 and 3 indicates

the linear dependence of $[r^k(n, l)]^{-1/k}/r$ on Z in this case also. A comparison of the values of $\overline{r}^{-3}(3d)$ calculated using the wave functions of a self-consistent field with exchange with the values of $\overline{r}^{-3}(3d)$ obtained from hyperfine structure[3] shows (Table 1) that the calculated absolute values are about 20% higher than the experimental ones. The relative values agree quite satisfactorily when the inaccuracy of the experimental data is taken into account.

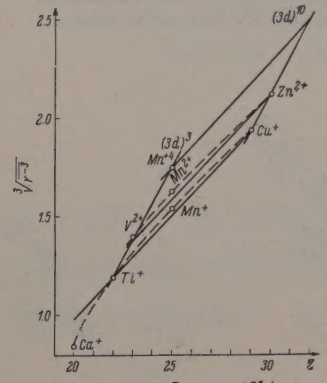

Fig. 3. Dependence of $[\overline{r}^{-3}(3d)]^{1/3}$ on Z for elements of the iron group.

Table 1. Comparison of the Values of $\overline{r}^{-3}(3d)$ Calculated from Wave Functions of a Self-Consistent Field with Exchange with Experimental Data[3]

Symbol	Z	Doubly ionized				Neutral
		Calculated		Experimental		
		$\sqrt[3]{\overline{r^{-3}}}$ (a.u.)	Relative values	$\sqrt[3]{\overline{r^{-3}}}$ (a.u.)	Relative values	Relative values
V	23	2.74	1.00	2.3	1.0	1.0
Mn	25	4.34	1.58	3.5	1.5	1.5
Co	27	6.20	2.26	5.2	2.3	2.3
Cu	29	8.35	3.05	6.3	2.7	3.2

As an example of the application of these results, we will calculate the relative values of $\overline{r}^k(4f)$ for triply ionized rare earth atoms. For the 4f shell of rare earth ions, the configuration interaction should be weak because of the great difference of energies between the ground configuration and the closest excited configuration of the same parity (several hundred thousand cm^{-1}). As a result the dependence of $[\overline{r}^k(4f)]^{-1/k}$ on Z can be expected to be quite linear (as in the case of the 2p shell). On this basis, the relative values of $\overline{r}^k(4f)$ of all rare earth ions for k = −3, +1, 2, 4, 6 (Table 3) were calculated, using the values of $\overline{r}^k(4f)$ for Pr^{3+} and Tm^{3+} (Table 2), which were determined employing the wave functions of a self-consistent field without exchange.[5] Because of the lack of experimental data on free ions, we used the data on crystalline compounds of the rare earth ions. In a crystal, the external shells are distorted by the surroundings. However, experiments on the paramagnetic diffuse scattering of neutrons on Mn salts,[6] indicated that the maximum of the radial function of the outer shell electron distribution shifts only slightly. A substantial deviation from the distribution in a free ion occurs only on the boundaries of the outer shell. In the rare earth ions, the f-shell is screened from external influences by the $5s^2$ and $5p^6$ shells which are also affected by the surrounding atoms. There are also direct indications of the weakness of the interaction between the f shell of the rare earth ions and the surrounding atoms; for example, the sharpness of spectral lines corresponding to transitions inside the shell, even at room temperature;[4] the lack of temperature-dependence of the paramagnetic scattering of neutrons over a wide range of temperatures;[7] the data on the magnetic susceptibility;[4] the absence of any influence of surrounding ions on the hyperfine structure of spectral lines corresponding to transitions inside the shell,[8] etc.

Table 2. Values of $r^{-k}(4f)$ for Pr^{+3} and Tm^{+3} Ions (in Atomic Units)

k	Pr^{+3}	Tm^{+3}
1	1.067	0.7636
2	1.464	0.7606
4	5.34	1.57
6	39.5	7.26
−3	4.36	10.50

It can be expected that the relative values of $\overline{r}^k(n, l)$ obtained are correct for the rare earth ions which are contained in crystals and solutions. In order to check this statement, we used the $\{A_6^m \overline{r}^6\}$ parameters of Stark splitting of the levels of the rare earth ethyl-sulfates[9] and the x-ray data on the dimensions d of the unit cells of these crystals[10] to find the relative values of $\overline{r}^6(4f)$ for Ce, Nd, Sm, and Dy according to the approximate formula

$$\frac{\overline{r^k}(Z)}{\overline{r^k}(Z_0)} = \left[\frac{d(Z)}{d(Z_0)}\right]^{k+2} \frac{\{A_k^m \overline{r^k}\}_z}{\{A_k^m \overline{r^k}\}_{z_0}}.$$

When dipole surroundings predominate it is easy to derive this formula, because A_k^m is inversely proportional to the (k + 2) power of the size of the elementary cell of a crystal (see ref. 4 for explicit expressions for the coefficients A_k^m). Figure 4 shows that the theoretical values agree with the experimental data within the limits of experimental error. From calculations of the Pr^{3+} and Nd^{3+} spectra, Murao[11] obtained Z_{eff} values of 10.5 and 11.0 respectively. The ratio $\overline{r}^2(Pr)/\overline{r}^2(Nd) \equiv 1.10$ calculated from these data agrees within the limits of error with the value 1.08 obtained from the data in Table 3. It follows from this that the values of $\overline{r}(4f)$ for Ho(0.68 A) and Er(0.76 A), as given by Afanas'eva,[12] are incorrect. As Z increases, the size of any shell decreases,[1,2] which contradicts the data in ref. 12. On the other hand, the values of $\overline{r}^{-3}(4f)$ calculated from the fine structure of the spectra of the trivalent rare earth ions[13] agree with the data presented in Table 3 to within 5%.

As a result of this analysis, the following conclusions can be drawn: (a) fairly satisfactory relative values of $\overline{r}^k(n, l)$ can be obtained using the wave functions of a self-consistent field without exchange when configuration

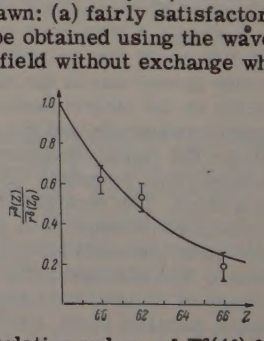

Fig. 4. Relative values of $\overline{r}^6(4f)$ for trivalent rare earth ions. Solid line—theory; circles—experiment.

Table 3. Relative Values of $[\overline{r}^{-k}(4f)]$ for Triply Ionized Rare Earth Atoms

Z	Symbol	$\overline{r}^{-3}$	$\overline{r}$	$\overline{r}^{2}$	$\overline{r}^{4}$	$\overline{r}^{6}$
58	Ce	1.00	1.00	1.00	1.00	1.0
59	Pr	1.12	0.960	0.924	0.861	0.83
60	Nd	1.26	0.923	0.856	0.748	0.68
61	Pm	1.40	0.889	0.796	0.654	0.56
62	Sm	1.56	0.858	0.741	0.575	0.47
63	Eu	1.72	0.829	0.691	0.504	0.39
64	Gd	1.90	0.801	0.647	0.446	0.34
65	Tb	2.09	0.775	0.608	0.398	0.28
66	Dy	2.29	0.751	0.571	0.354	0.24
67	Ho	2.50	0.729	0.538	0.315	0.22
68	Er	2.72	0.707	0.507	0.283	0.19
69	Tm	2.96	0.687	0.479	0.254	0.16
70	Yb	3.22	0.668	0.454	0.229	0.14

eraction is small (in the opposite case, one should use e wave functions of a self-consistent field with exchange); the relative values $\overline{r}^{k}(n, 1)$ depend weakly on the de- ee of ionization of the atom; (c) for the 4f-shell of the re earth ions, the relative values of $\overline{r}^{k}(4f)$ change only ghtly when a free ion enters into a crystal or solution.

It can be expected that a knowledge of relative values $\overline{r}^{k}(n, 1)$ will facilitate the finding of the absolute values the sizes of the shells of atoms and ions from experi- ental data.

The author is grateful to M. A. El'yashevich for his erest in this work and his valuable advice.

REFERENCES

1. E. Condon and Shortley, "Teoriya Atomnykh Spektrov" (Theory of Atomic Spectra). Izd. Inostrannoi Lit., Moscow-Leningrad, 1949. Cambridge Univ. Press, 1935.
2. D. Hartree, "The Calculation of Atomic Structures." Wiley, New York, 1957.
3. A. Abragam, J. Horowitz, and M. H. L. Pryce, Proc. Roy. Soc. **230**, 169 (1955).
4. M. A. El'yashevich, "Spektry Redkikh Zemel'" (Rare Earth Spectra). Gosudarst. Tekh. Teoret. Izd., Moscow, 1953.
5. E. C. Ridly, Proc. Cambridge Phil. Soc. **56**, 41 (1960).
6. C. L. Shull, W. A. Strauser, and E. O. Wollan, Phys. Rev. **83**, 333 (1951).
7. W. C. Kochler and E. O. Wollan, Phys. Rev. **92**, 1380 (1953).
8. B. Bleaney, P. M. Llewellyn, and D. A. Jones, Proc. Phys. Soc. **B69**, 860 (1956).
9. B. J. Elliott and K. W. H. Stevens, Proc. Roy. Soc. **A215**, 447 (1952); Ibid. **A219**, 287, 387 (1953).
10. J. A. A. Ketelaar, Physica **4**, 619 (1937).
11. T. Murao, Progr. Theoret. Phys. **20**, 287 (1958).
12. N. Afanas'eva, Opt. i Spektr. **5**, 110 (1958).
13. B. Bleaney, Proc. Phys. Soc. **A68**, 937 (1955).

MEASUREMENT OF THE ABSOLUTE VALUES OF THE OSCILLATOR STRENGTHS FOR THE RESONANCE LINES OF CALCIUM, STRONTIUM, AND BARIUM IONS

Yu. I. Ostrovskii and N. P. Penkin (pp. 8-14)

Received 30 March 1960

D. S. Rozhdestvenskii's "hook" method was used to measure the absolute values of f for the doublet resonance lines of Ca II ($f_{3933} = 0.78$, $f_{3968} = 0.40$), Sr II ($f_{4078} = 0.75$, $f_{4215} = 0.39$) and Ba II ($f_{4554} = 0.70$, $f_{4934} = 0.35$). The values obtained were checked by measuring the ratios $f_{Ca\,II(3933)}/f_{Ba\,II(4554)}$ and $f_{Sr\,II(4078)}/f_{Ba\,II(4554)}$ in mixtures of vapors of these alkaline earth elements. Our data confirm Saha's equation to an accuracy better than 20%.

TRODUCTION

One of us had previously studied the processes of mic excitation[1] and ionization[2] in a King oven, when it s shown that the atoms were distributed among their ergy levels according to the Boltzmann law, and that degree of ionization observed corresponds to that culated from Saha's equation. Consequently, conditions se to thermodynamic equilibrium prevail in the King en. This result was confirmed by the work of Frish, nkin, and Shukhtin[3] which established that arc and spark es of strontium and barium, irrespective of the series which they belong, have an identical reversal tempera- e, corresponding to the temperature of the inner wall the graphite tube of the oven.

The fact that the ion concentration in the King oven be calculated from Saha's equation was also used in present investigation to measure the absolute values he oscillator strengths of the doublet resonance lines Ca II, Sr II, and Ba II.

On the other hand, the measured oscillator strengths independent of the oven temperature, which must in- ate the validity of Saha's equation in our conditions.

MEASUREMENT OF THE ABSOLUTE VALUES OF f

It is easily shown that if the absolute f value of the atomic line is known, the oscillator strength of the line of the corresponding ion can be found. To do this it is sufficient to simultaneously photograph the hooks adjacent to the lines and measure the oven temperature. Hereafter we will use the subscript a to indicate values relating to the normal state of the atom and its resonance line, and the subscript i to indicate values relating to the normal state of the ion and its resonance line. As is well known, the hook method leads to the following expression for the oscillator strength (f_i) of a spectral line:

$$f_i = \frac{\pi mc^2 k_i}{e^2 \lambda_i^3 l_i N_i} \Delta_i^2, \qquad (1)$$

where e and m are the charge and mass of the electron, λ_i is the wavelength of the resonance line of the ion, l_i and N_i are the length and concentration of the column of ions, k_i is a constant of the method depending on the thickness and refractive index of the plane-parallel plate inserted into the interferometer to form the hooks, and

Δ_i is the distance between the turning points of the hooks on either side of the spectral line.

Saha's equation, from which the concentration of ions in the King oven can be calculated, will be written in the following form:

$$\frac{N_i N_e}{N_a} = \left(\frac{2\pi mk}{h^2}\right)^{\frac{3}{2}} \frac{g_e g_i}{g_a} T^{\frac{3}{2}} 10^{-\frac{5040 V_i}{T}} \qquad (2)$$

where N_i and N_a are the concentrations of ions and atoms; g_i, g_a, and g_e are the statistical weights for ion, atom, and electron, respectively; N_e is the electron concentration; V_i is the atomic ionization potential, expressed in volts; T is the absolute temperature; k and h are the Boltzmann and Planck constants, and m is the mass of the electron.

We will assume that electrons in the oven originate from ionization of one type of atom only, that is, that there are no foreign ionizing impurities and no other sources of electrons (photoeffect, thermal emission). Then we have:

$$N_i = N_e. \qquad (3)$$

This assumption, as we will see later, is borne out in practice.

Taking into consideration that for alkaline earth atoms and ions $g_a = 1$ and $g_i = 2$ ($g_e = 2$), we find:

$$N_i^2 = 4N_a \left(\frac{2\pi mk}{h^2}\right)^{\frac{3}{2}} T^{\frac{3}{2}} 10^{-\frac{5040 V_i}{T}} \qquad (4)$$

For the concentration of normal atoms (N_a), we can write an expression analogous to Eq. (1):

$$N_a = \frac{\pi m c^2 k_a}{e^2 \lambda_a^3 f_a l_a} \Delta_a^2. \qquad (5)$$

Equations (1), (4), and (5) give:

$$f_i = A \left(\frac{10^{\frac{2520 V_i}{T}}}{T^{\frac{3}{4}}} \right) \frac{\Delta_i^2}{\Delta_a}. \qquad (6)$$

If we bear in mind that the lengths of the columns of atoms and ions are identical and equal to the heated length of the graphite tube in the oven, that is, $l_a = l_i = l$, the expression for A becomes:

$$A = \frac{h^{\frac{3}{2}} k_i \lambda_a^{\frac{3}{2}} f_a^{\frac{1}{2}}}{2^{\frac{7}{4}} \pi^{\frac{1}{4}} m^{\frac{1}{4}} e k^{\frac{3}{4}} k_a^{\frac{1}{2}} \lambda_i^3 l^{\frac{1}{2}}}. \qquad (7)$$

From Eqs. (6) and (7) it follows that the accuracy of the f_i value depends only on the errors of measurement of f_a, l, Δ_i, Δ_a, and T, since the remaining quantities entering into the equations are known to a much greater accuracy ($\approx 0.1\%$). The greatest error in the value of f_i is thus introduced by the temperature measurements, since the temperature is in the exponent. The values of V_i for calcium, strontium, and barium are 6.111, 5.692, and 5.209 respectively, according to ref. 4.

THE MEASUREMENT OF RELATIVE VALUES OF f

The errors caused by inaccuracies in temperature measurement can be considerably reduced if we investigate the ionization of mixtures of vapors of alkali earth elements. Equation (3) need no longer be used. However, using mixtures, we can determine only relative oscillator strengths of ionic lines.

Russel[5] has represented the ionization of mixtures in analytical form. However, Saha's equation in the form of Eq. (2) applies irrespective of the existence of other degrees of ionization or the presence of other elements, which makes it far simpler to use when considering ionization in mixtures. From this equation we can obtain the following expression for the concentration of atoms and ions of two types, present in the oven in the normal states:

$$\frac{N_{i1}}{N_{i2}} = \frac{N_{a1}}{N_{a2}} 10^{\frac{-5040 \Delta V_i}{T}}, \qquad (8)$$

where ΔV_i is the difference in ionization potential of the atoms.

Equations (1), (5), and (8) give:

$$\frac{f_{i1}}{f_{i2}} = \frac{k_{i1}}{k_{i2}} \cdot \frac{k_{a2}}{k_{a1}} \left(\frac{\lambda_{i2}\lambda_{a1}}{\lambda_{i1}\lambda_{a2}}\right)^3 \left(\frac{l_{i2} l_{a1}}{l_{i1} l_{a1}}\right) \frac{f_{a1}}{f_{a2}} \left(\frac{\Delta_{a2}\Delta_{i1}}{\Delta_{a1}\Delta_{i2}}\right)^2 10^{\frac{-5040 \Delta V_i}{T}} \qquad (9)$$

If we assume that the different types of atoms and their ions are each distributed along the oven tube in the same way, the quantity $(l_{i2} l_{a1} / l_{i1} l_{a2})$ can be set equal to unity.

In our case ΔV_i does not exceed 0.9 volt, which greatly reduces the error in f caused by errors in temperature measurement. However, in this case, as follows from Eq. (9), errors enter from the measurement of the hooks.

In this investigation, we measured the relative oscillator strengths of ionic lines in various mixtures; our object was to check the data obtained by measuring the absolute f values of these lines and also to confirm the validity of Saha's equation for ionization processes in mixtures.

THE EXPERIMENT. RESULTS

The experimental arrangement that we used was described in detail in refs. 1, 6, and 7. Metallic calcium, strontium, and barium (singly or in binary mixtures) were placed in the graphite tube of the oven, which had previously been heated under vacuum to the highest temperature attainable. The oven was filled with argon ($p \approx$ 100-200 mm Hg) and slowly heated to the melting point of the metal; the temperature was then rapidly raised to the maximum. After this, the oven was switched off and the argon evacuated with a backing pump. This procedure was followed to prevent metal from sputtering onto the oven window. The oven was then rapidly heated to a temperature at which the hooks being measured appeared clearly, and these were immediately photographed. We obtained a large number of photographs of hooks adjacent to ionic and atomic lines of calcium, strontium, and barium. Figure 1 shows one of these photographs.

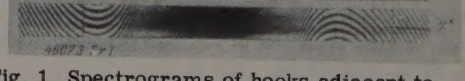

Fig. 1. Spectrograms of hooks adjacent to atomic and ionic lines of strontium, obtained at 2960° K.

This type of spectrogram can be used to obtain an accurate (to within 1-3%) measurement of the distances between the turning points of the hooks. The dispersion around the resonance lines of Ca, Sr, and Ba was enormous (see Fig. 1). Therefore, in making measurements on the spectrograms we took into account its effect on the dispersion around the weaker ionic lines. This calculation was made by using the well-known equations[6] of the hook method. The oven temperature was measured with an optical pyrometer calibrated at the All-Union Scientific Research Institute of Metrology. The absolute values of the oscillator strengths were calculated from Eq. (6) and the relative values from Eq. (9).

We will now estimate the accuracy of our measurements. We indicated above that the accuracy of the determination of the oscillator strengths depends only on the measurement error in f_a, l, Δ_l, Δ_a, and T, since the remaining quantities entering into the equations are known to a much greater degree of accuracy. The absolute f values of the resonance lines of alkaline earth atoms are known to an accuracy of 15% from measurements made by us together with Shabanova.[8]

In obtaining Eq. (7) we assumed that $l_a = l_i = l$. This is an approximation, as is shown in ref. 9. In order to observe the effect of differences in l_a, l_i, and l on the measurements of f, we determined the oscillator strength of the ionic barium line using graphite tubes 10 and 20 mm long. The oscillator strengths were identical, to within the experimental error.

Prolonged operation of the oven leads to an increase in the difference between l_a and l_i, so the photographs of the spectrograms were taken shortly after the dispersion reached an easily measured value. The magnitudes of f_a and l enter Eq. (6) as square roots. Consequently, errors made in measuring these quantities have little effect on the accuracy of the oscillator strength determinations.

The errors in measuring the oven temperature averaged about 25°C, which caused an error of about 25% in the absolute oscillator strengths and an error of 5% in the relative f values.

We made measurements on a large number of spectrograms taken under different experimental conditions, in order to reduce the random experimental error. Not less than 80 plates were measured for each line; for some lines, the figure reached 180.

Figures 2-4 show the experimental results graphically; in these figures, the absolute oscillator strengths of the ionic lines are plotted on the y-axis and the oven temperature at which the measurements were made is plotted on the x-axis. The scatter in the points is an indication of the accuracy of our measurements. The broken lines on the graphs show the mean oscillator strengths. These mean values are also given in the fourth column of Table 1.

The number of photographs measured for each line, n, is given in the last column of the table. For f_{3933} Ca II, the error of an individual measurement averages 20%,

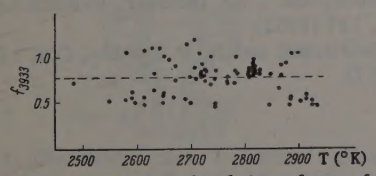

Fig. 2. Experimental absolute values of f for the λ_{3933} Ca II line.

Table 1

Ion	λ (A)	Transition	f	n
Ca II	3933.67 *	$4^2S_{1/2} - 4^2P_{3/2}$	0.78	86
	3968.47	$4^2S_{1/2} - 4^2P_{1/2}$	0.40	—
Sr II	4077.71 *	$5^2S_{1/2} - 5^2P_{3/2}$	0.75	93
	4215.52	$5^2S_{1/2} - 5^2P_{1/2}$	0.38	—
Ba II	4554.04	$6^2S_{1/2} - 6^2P_{3/2}$	0.70	—
	4934.09 *	$6^2S_{1/2} - 6^2P_{1/2}$	0.35	100

for f_{4078} Sr II it averages 17%, and for f_{4934} Ba II it averages 16%. The mean square error of the data of Table 1 does not exceed 3% for any line. Naturally, the possible systematic errors discussed above are not included in this figure (in particular that arising from errors in the values of f_a).

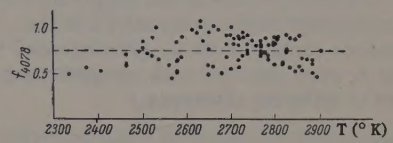

Fig. 3. Experimental absolute values of f for the λ_{4078} Sr II line.

In Table 1, the asterisks indicate lines whose absolute oscillator strengths were determined directly. The values of f for the remaining lines were calculated from the relative oscillator strengths of doublet resonance lines of Ca II, Sr II, and Ba II. These values were reported in refs. 2 and 10.

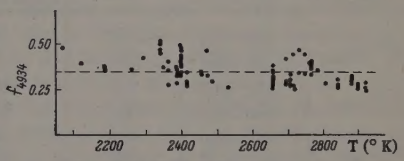

Fig. 4. Experimental absolute values of f for Ba II 4934.

We repeated the measurements on the doublets of Ca II and Sr II since we had at our disposal a large number of very good spectrograms (see Fig. 5) and consequently we could obtain more accurate results. Our results were:

for Ca II $f_{3933}/f_{3968} = 1.94$ (±1%)
for Sr II $f_{4078}/f_{4215} = 1.98$ (±1%).

These ratios and the data given in ref. 2 were used to calculate the absolute oscillator strengths for Ca II 3968, Sr II 4215, and Ba II 4554.

The sum of the f values for the resonance doublet of Ca II was 1.18, which agrees well with Hartree's theoretical value of 1.19.[11] The sums of the oscillator strengths of the Sr II and Ba II lines are 1.13 and 1.05 respectively—also greater than unity. We note that similar results were obtained for the resonance doublets of atomic sodium,[12] rubidium,[13] cesium,[14] and copper.[15]

The absolute oscillator strengths of the ionic lines were measured at different oven temperatures (see Figs. 2-4). This means that the factor in brackets in Eq. (6) varied considerably (for example, in the calcium and strontium experiments, it varied by a factor of approximately 12-17, and in the barium experiments by a factor of 60). Nevertheless, the mean values of the oscillator strengths remained constant to an accuracy of better than 10% (see Table 2) which shows that the Saha equation is

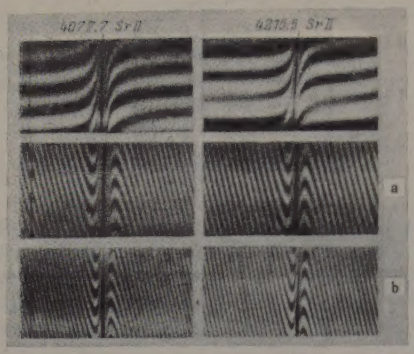

Fig. 5. Spectrograms of the dispersion and hooks adjacent to the components of the resonance doublet of Sr II. (Photographs a and b were obtained with compensating plates of different thickness.)

satisfied in the conditions existing in the King oven.

We also studied ionization in Ca + Ba and Sr + Ba mixtures. Photographs of the spectra were obtained at oven temperatures between 2400 and 2950° K.

The ratio of the oscillator strengths of the ionic lines was calculated from Eq. (9).

Table 2

Ion and wavelength (A)	Temperature interval (° K)	f_{mean}	Number of photographs measured
Ca II λ_{3933}	2500—2650	0.73	18
	2650—2800	0.80	34
	2800—2950	0.78	34
Sr II λ_{4078}	2300—2550	0.71	14
	2550—2750	0.79	49
	2750—2950	0.72	30
Ba II λ_{4934}	2100—2400	0.39	24
	2400—2700	0.36	39
	2700—2950	0.33	37

The results of the measurements are shown in Figs. 6 and 7. The scatter of the points indicates the accuracy of our data. The mean ratios of the f values are shown on the graphs by the broken lines. For the Ca + Ba mixture, the mean value of $f_{Ca(3933)}/f_{Ba\,II\,(4554)}$ obtained from measurement of 103 photographs was 1.14 (±20%), instead of the 1.11 indicated by Table 1.

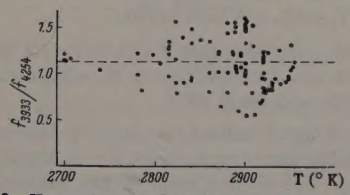

Fig. 6. Experimental values of the ratio of the oscillator strengths of ionic calcium and barium lines.

The mean value of the ratio $f_{Sr\,II\,(4078)}/f_{Ba\,II\,(4554)}$ = 0.93 (±19%) was obtained from measurements on 182 photographs.

According to the data of Table 1, this ratio is 1.07.

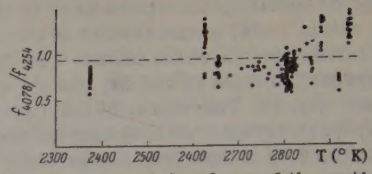

Fig. 7. Experimental values of the ratio of oscillator strengths of ionic lines of strontium and barium.

We see that the values coincide, within the experimental error (indicated in brackets).

The experimental absolute values of the oscillator strengths of the Ca II, Sr II, and Ba II resonance lines are thus confirmed by measurements of the relative f values in mixtures of the vapors of alkaline earth elements. The results also show that the Saha equation accurately describes the ionization processes which occur in mixtures.

We measured the mean absolute and relative f values of the doublet resonance lines of Ca II, Sr II, and Ba II over a wide range of oven temperatures. These values remained constant to an accuracy better than 10%. This confirms the validity of the Saha equation and shows that it is satisfied to an accuracy of better than 20% under the conditions of the King oven.

REFERENCES

1. N. P. Penkin, Zhur. Eksptl. i Teoret. Fiz. 17, 355 (1947).
2. N. P. Penkin, Izvest. Akad. Nauk SSSR, Ser. Fiz. 11, 217 (1947).
3. S. E. Frish, N. P. Penkin, and A. M. Shukhtin, Zhur. Eksper. i Teoret. Fiz. 18, 734 (1948).
4. C. E. Moore, "Atomic Energy Levels as Derived from the Analysis of Optical Spectra," Vols. 1-3, Natl. Bur. Standards (U.S.), Circ. No. 467 (1949-1958).
5. H. Russel, Astrophys. J. 15, 119 (1922).
6. D. S. Rozhdestvenskii and N. P. Penkin, J. Phys. USSR 5, 319 (1941).
7. Yu. I Ostrovskii, G. F. Parchevskii, and N. P. Penkin, Opt. i Spektr. 1, 821 (1956).
8. Yu. I. Ostrovskii, N. P. Penkin, and L. N. Shabanova, Doklady Akad. Nauk SSSR 120, 66 (1958), Soviet Phys.-Doklady 3, 538 (1958).
9. Yu. I. Ostrovskii and N. P. Penkin, Opt. i Spektr. 9, 703 (1960), Optics and Spectroscopy 9, 371 (1960).
10. E. I. Nikonova and V. K. Prokof'ev, Opt. i Spektr. 1, 290 (1956).
11. Landolt-Börnstein Tabellen, Part I, 1950.
12. G. S. Kvater, Izvest. Akad. Nauk SSSR, Ser. Fiz. 9, 236 (1945).
13. G. I. Gol'dberg, Izvest. Glavnoi Astron. Observat. No. 156, 126 (1956).
14. G. S. Kvater and T. G. Meister, Vestnik Leningrad. Univ. 9, 137 (1952).
15. Yu. I. Ostrovskii and N. P. Penkin, Opt. i Spektr. 3, 193 (1957).

SPECTRAL DETERMINATION OF THE ISOTOPIC COMPOSITION OF LITHIUM*

*The work was done in 1956-1957.

A. N. Zaidel', A. N. Raxumovskii, and M. P. Chaika (pp. 15-18)

Received 16 April 1960

A method is described for determining the isotopic composition of Li. The method is based on the measurement of the intensities of the components of the resonance doublet. A hollow cathode was used as the light source. The spectrum was scanned with a Fabry-Perot etalon housed in a pressure chamber. The calibration curves were constructed with the aid of standards. Five to ten μg (~0.05 mg LiCl) of lithium were needed for an analysis. The method was sensitive to ~0.5% Li^6. The coefficient of variation was 0.15-0.7% for Li^6 contents between 40 and 90%. The time required for an analysis was 10-15 min.

A number of articles[1-6] have been devoted to methods for the spectral determination of the isotopic composition of lithium.

The purpose of this work was the development of a method of analysis which could fully utilize the optical speed of a photoelectric spectrometer with a Fabry-Perot interferometer. This would give fast, accurate results with low consumption of sample.

EXPERIMENTAL PROCEDURE

Light Source. The line λ = 6707.8 A, which has a large isotopic shift (0.16 A) and lies in a convenient spectral region, was used for the analysis. A hollow cathode discharge served as the light source. The width of the line emitted by the discharge depends on the operating parameters of the discharge tube, and most of all on the temperature of the cathode. It was found experimentally that cooling the cathode with circulating water gave satisfactory resolution of the components.

The construction of the tube is shown in Fig. 1, where 1 and 2 are the cathode and anode sections of the tube respectively. The cathode is tumbler-shaped, having a wide flange. It is connected to the anode section by an insulating rubber ring which also serves as a vacuum seal. The two sections of the tube are fastened together by a "vinyl-plast" collar. A water-cooled metal jacket is installed around the protruding part of the cathode. For better thermal contact, the joints between the cooling jacket and the cathode are wetted with water, which does not have sufficient time to evaporate during the experiment. The anode section of the tube is cone-shaped and made of steel. The tube is equipped with two outlets through which the carrier gas circulates. The end of the tube is closed by a glass window resting on a rubber seal. The iron insert of the anode section directs the flow of gas toward the cathode in order to secure an intense purification of the gas in the discharge zone.

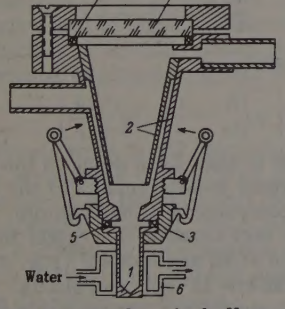

Fig. 1. Discharge tube. 1—hollow cathode; 2—anode section of the tube; 3—"vinyl-plast" color; 4—glass window; 5—rubber gasket; 6—cooler.

Any inert gas can be used as a discharge carrier. The intensity of the spectrum of lithium is approximately the same in He, Ne, and Ar. We selected helium because the closest line of this gas is farther away from the lithium line than are the lines of the other gases. This permits the use of a wider monochromator slit, which increases the light flux conveyed to the photomultiplier.

The vacuum system serving the discharge tube was composed of a circulating section and an evacuating section.[7] The pressure was measured by means of a U-shaped oil manometer. The working pressure of the gas was 1.6 mm Hg.

The direct current for the discharge tube was supplied by a high voltage rectifier with an output potential of 1500 volts. The rectifier was provided with a stabilizer[8] which provided a current of ~50 ma through the discharge tube with an accuracy of ~0.2%. At the discharge current used, it appeared that the brightness of the radiation was sufficient for measuring the intensities of the components with the required precision. The self-absorption was not strong enough to appreciably increase the error of analysis.

The accuracy of the analysis is greatly influenced by the stability of the light source. The latter depends appreciably on the condition of the inner surface of the cathode, where the discharge is concentrated, and on the method of introducing the sample into the cathode. The best results are obtained by electrolytic deposition of metallic lithium on the inner surface of the cathode.[6,9] It seems to be important that the walls of the hollow cathode be covered by an extremely homogeneous and uniform layer of the substance. After the inner surface of the duralumin cathode was polished with a GOI paste, lithium was electrolytically deposited from a 0.1% solution of lithium chloride in anhydrous acetone. The anode was a platinum wire. In 15 sec, ~1μg of lithium was deposited by a current of 1 ma. This amount was sufficient for the analysis.

The tube, after being evacuated and then filled with helium, gives bright lines of lithium as soon as the discharge current is turned on. The intensity, although de-

creasing with time, remains fairly high for a long period of time.

Spectroscopic Arrangement. A Fabry-Perot interferometer, described previously,[10] was employed for recording the isotopic structure of the lithium line. A grating monochromator was used to isolate the line from the spectrum. The grating with shaped grooves was mounted in such a way as to operate at its blaze angle and give the greatest angular dispersion. The angles of incidence and diffraction were calculated for these conditions. The remaining parameters of the optical system were calculated according to ref. 10 and are given in Fig. 2.

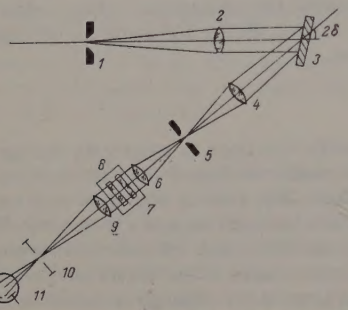

Fig. 2. Diagram of the spectrometer. 1,5—Slits; 2—objective (F_1 = 300 mm); 3—diffraction grating; 4,6—objectives ($F_{2,3}$ = 120 mm); 7—Fabry-Perot interferometer; 8—pressure chamber; 9—objective (F_4 = 600 mm); 10—Iris diaphragm; 11—radiation detector (FEU-22). The diameters of all the objectives are 6 cm.

The Fabry-Perot interferometer with dielectric layers was 4 mm thick. The reflection coefficient of the mirrors was relatively low (~ 80%). The resolving power was sufficient to solve the given problem, and the gain in light flux was significant when compared to the beam obtained with high-reflecting mirrors (R ≅ 90%). The interferometer was placed in a pressure chamber in which the air pressure was varied periodically. The valve on the chamber was switched automatically by a simple device 1 shown in Fig. 3. The mercury level in the manometer 5 changes with the changing air pressure in the chamber until the electric circuit of one of the coils 4 is closed by the mercury. As a result, the electromagnet 3 turns the valve 2, cuts off the pump 7, and in turn opens the air intake 8 or vice-versa. The air pressures in the chamber at which the switching occurs are regulated by means of the movable contacts 6. The contacts were adjusted in such a manner that the components

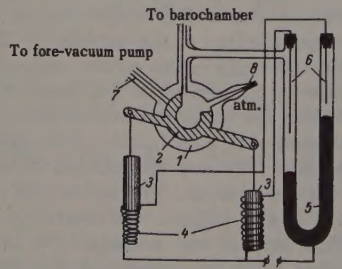

Fig. 3. Arrangement of the automatic switch for air intake and evacuation.

necessary for the measurement could be recorded in only one order of interference.

Recording of the Light Beam. The light beam emerging from the spectrometer was directed onto the cathode of an FEU-22 photomultiplier whose sensitivity was fairly good in the spectral region in question. A VS-9 rectifier furnished 1000-1100 volts dc to the photomultiplier. The signal from the photomultiplier was amplified by a dc amplifier and then fed to an EPP-09 automatic recorder. The recorder's carriage traversed the full scale in 1 sec. A sample recording of the structure of the line is given in Fig. 4.

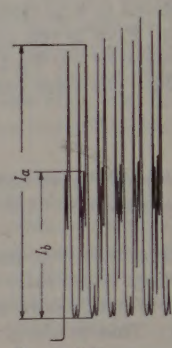

Fig. 4. A recording of the components of Li 6707.8 (sample contains ~ 2% Li^6).

THE METHOD OF ANALYSIS

The concentrations of the lithium isotopes in a sample were determined by comparing the relative intensities of the components of the isotopic structure in a sample and in standards.

The 6707.8 A line of lithium has a fine structure composed of two components whose intensities are in a 1:2 ratio. The isotopic shift is of the same magnitude as the splitting. As a result, one of the components of the fine structure of Li^6 is superimposed on a component which belongs to Li^7 (Fig. 5). The isotope concentration can be determined from the ratio of the intensities of the outer components, or from the ratio of the middle component (b) to one of the outer components (a or c). Since the weak component c was poorly resolved at low Li^6 concentrations, the ratio of the intensities of the b and a components was used. If self-absorption and other effects influencing the relative intensities of the lines are disregarded, then the following equation should be satisfied:

$$\frac{C_{Li^6}}{C_{Li^7}} = \frac{I_b}{I_a} - \frac{1}{2}.$$

The coordinates

$$\left[\lg\left(\frac{I_b}{I_a} - \frac{1}{2}\right),\ \lg\frac{C_{Li^6}}{C_{Li^7}}\right]$$

were used for the graph. Each point on the graph is the mean value of twenty measurements of the relative intensities of the components of one sample. The graph is a curve which is very close to a straight line passing through the origin at an angle of 45° (Fig. 6). The greatest deviations exist at low Li^6 concentrations. This can be explained by self-absorption and by a partial distortion of the profiles of the components.

Accuracy. The error of the analysis of determined by the error in the standards, the variability of the ana-

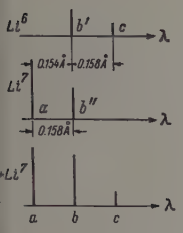

Fig. 5

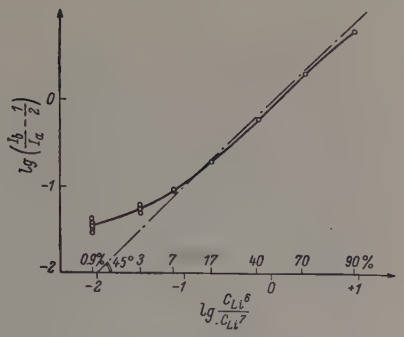

Fig. 6

Fig. 5. Diagram of the structure of the line Li 6707.8.
Fig. 6. Calibration curve

ytical results, and the error related to possible differences in the chemical composition of the sample and the standards. In this case, the first and the last errors can be made much smaller than the second. Consequently, the accuracy of the method is practically the same as its reproducibility. The coefficient of variation did not exceed 6% at low Li^6 contents and was only 0.15-0.7% in the 40-90% Li^6 range. In order to decrease the influence of the recording error, the line structure for each sample was recorded 5-10 times.

Time Required for an Analysis. The time for preparing the sample, recording the spectrum, and calculating the concentration using the calibration curve amounted to about 15 min. After the preliminary preparation of the samples for the analysis, each successive analysis can be accomplished in 5-6 min. It was found experimentally that it was not necessary to clean the discharge tube after the analysis.

The authors express their gratitude to T. N. Krylova for the preparation of the reflecting layers of the interferometer plates, and also to G. M. Malyshev for his cooperation at different stages of the work.

REFERENCES

1. G. L. Stukenbrocker, D. D. Smith, G. K. Werner, and J. R. McNally, J. Opt. Soc. Am. **41**, 870 (1951); Ibid. **42**, 383 (1952).
2. G. K. Werner, D. D. Smith, S. J. Ovenshine, O. B. Rudolf, and J. R. McNally, J. Opt. Soc. Am. **42**, 870 (1952); Ibid. **45**, 202 (1955).
3. J. K. Brody, M. Fred, and F. S. Tomkins, J. Opt. Soc. Am. **42**, 870 (1952); Ibid. **46**, 383 (1956).
4. V. A. Fassel and H. J. Hettel, Spectrochim. Acta **7**, 175 (1955).
5. J. Artaud, J. Blaise, and S. Gerstenkorn, Spectrochim. Acta **10**, 110 (1957).
6. F. F. Gavrilov, Opt. i Spektr. **7**, 285 (1959), Optics and Spectroscopy **7**, 185 (1959).
7. S. Tolansky, "Spektroskopiya vysokoi razreshayushchei sily" (High Resolution Spectroscopy) Izd. Inostrannoi Lit., Moscow, 1955.
8. A G. Zhiglinskii, Opt. i Spektr. **3**, 9 (1957).
9. N. A. Izgaryshev and S. V. Gorbachev, "Kurs Teoreticheskoi electrokhimii" (A Course in Theoretical Electrochemistry) Goskhimizdat, Moscow, 1951.
10. M. P. Chaika, Opt. i Spektr. **3**, 372 (1957).

STUDY OF EQUILIBRIA IN NONAQUEOUS SOLUTIONS OF ELECTROLYTES USING ABSORPTION SPECTRA

I. Picric Acid and Sodium Picrate in Water and in Methyl, Ethyl, and Normal-Butyl Alcohols

N. A. Izmailov and E. L. Gurevich (pp. 19-26)

Received 8 April 1960

A study has been made of the spectra of solutions of picric acid and sodium picrate in water and in methyl, ethyl, and n-butyl alcohols and of the equilibria established between ions and molecules and between ions and ion pairs. We have calculated the thermodynamic dissociation constants in all the solvents mentioned. A comparison of the value of the dissociation constant of picric acid calculated from our data with electrometrically determined values shows that in alcohols (especially in n-butyl alcohol) there occurs a significant ionic association, which is practically nonexistent in water. It has also been determined that the spectra of the limiting equilibrium forms of picric acid in water and in the alcohols differ only slightly.

From previous work in our laboratories, it was known that the strength of electrolytes in solution (their dissociation) depends on the chemical nature of the solvent, the dielectric constant, the dipole moment of its molecules, and also on the characteristics of the products of interaction of the solvent with the molecules and ions of the dissolved substance.

The dissociation of an electrolyte KA in a solvent M may be considered to be a process occurring in several stages:

$$KA + (n+m)\,M \underset{}{\overset{K^{*}_{solv.}}{\rightleftharpoons}} KAMn + mM \overset{K_D}{\rightleftharpoons} K^{+}_{s} + A^{-}_{s}$$
$$+ \qquad\qquad\qquad\qquad \uparrow\downarrow K^{-1}_{ass.}$$
$$yM \underset{K_{pr.}}{\rightleftharpoons} K^{+}_{s}A^{-}_{s} + xM,$$

where $K^{*}_{solv.}$, $K_{diss.}$, $K^{-1}_{ass.}$, and $K_{pr.}$ are constants for the respective equilibria. Depending on the properties of the dissolved electrolyte and of the solvent, any one of these equilibria may predominate, and in a series of cases the dissolved substance may be involved in all the equilibria.

For substances of acid-base character, it is known[1,2] that absorption spectra, especially fluorescence spectra and yields, indicate clearly the nature of the interaction of the solvent with the ions and molecules of the dissolved substance, and also the influence of the basicity and the physical properties of the solvent. For the purpose of obtaining a more detailed explanation of the influence of the solvent on the dissociation of electrolytes, we have undertaken an investigation of the absorption spectra of picric acid and sodium picrate in various media: water and alcohols (leveling solvents); acetone, acetonitrile, and dioxane (differentiating solvents); benzene, carbon tetrachloride, chloroform, and dichloroethane (aprotic solvents); and also in oxalic acid, pyridine, dioxane-water mixtures, and in other solvents.

The spectra of picric acid and of picrates in various solvents (water, dioxane-water mixtures, and in several aprotic solvents) have been determined by Halban and co-workers.[3-5] In ethyl alcohol the spectrum of picric acid was studied by Gross and co-workers.[6]

In the present work we set as our goal the study of the equilibria between the ions and molecules of picric acid and sodium picrate in water and in methyl, ethyl, and n-butyl alcohols, and the influence of these solvents on the spectra of the various equilibrium forms of picric acid and sodium picrate.

Water and the alcohols are solvents of similar chemical nature. The similarity of properties of these solvents is explained by the fact that they are all associated, they have similar values of the dipole moment, and contain hydroxyl groups. Water and alcohols give identical addition compounds with dissolved substances. However, regardless of the existence of considerable similarity, water differs to an appreciable extent from the alcohols in a large number of chemical and physical properties. Thus, one of the present authors[7,8] has shown that water and alcohols have different proton affinities, and that the character of the ion-dipole interaction is identical for all alcohols and is different from that of water. Furthermore, all the solvents mentioned, viz., water and methyl, ethyl, and n-butyl alcohols, have different dielectric constants, the values being, respectively, 78.54, 31.5, 24.3, and 17.4.

It is natural to assume that the spectra of picric acid and of sodium picrate in water and in alcohols should be somewhat different.

METHOD OF INVESTIGATION

Absorption spectra were investigated with the use of an SF-4 spectrophotometer. All substances were subjected to careful purification: Chemically pure picric acid was recrystallized twice from water and sodium picrate from alcohol. The alcohols were purified and dried by standard methods; water was treated by boiling with alkaline potassium permanganate and then distilled three times. All solutions were prepared in the same calibrated volumetric flask at 25°C, after which all dilutions were carried out with the same calibrated pipet. To avoid photolysis[9] all work was carried out with freshly prepared solutions. In the investigation the following concentrations of picric acid and of sodium picrate were used: 5.0×10^{-5}, 1.0×10^{-3}, and 8.8×10^{-3} moles/liter, and the corresponding sample thicknesses were, respectively, 1, 0.05, and 0.0057 cm, such that the product of concentration and sample thickness was in all cases a constant quantity.

DISCUSSION OF RESULTS

The absorption spectra of picric acid and of sodium picrate in water are identical at concentrations of 5×10^{-5}, 1×10^{-3}, and 8.8×10^{-3} moles/liter (Fig. 1) and exhibit a maximum in the 355-356 mμ region. The applicability of Beer's law to this case indicates that at the concentrations mentioned only one kind of particle is absorbing (in this case, ions). Analogous spectra for solutions of picrates in water were obtained by Halban and co-workers.[3-5]

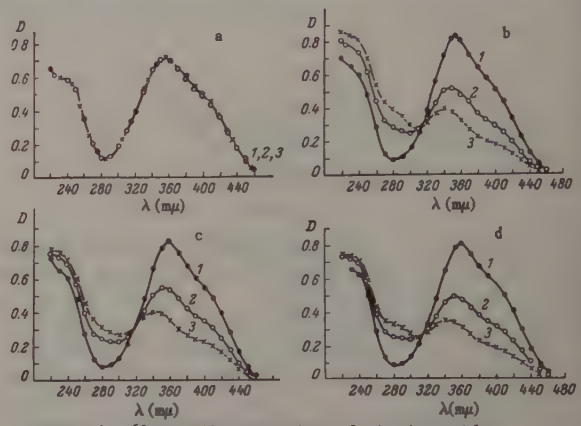

Fig. 1. Absorption spectra of picric acid (HPi) and sodium picrate (NaPi) in various solvents and at various concentrations. Solvents: a—H_2O, b—CH_3OH; c—C_2H_5OH; d—n-C_4H_9OH. Concentrations (in moles/liter) and substance: a: 1—5×10^{-5} HPi and NaPi; 2—1×10^{-3} HPi and NaPi; 3—8.8×10^{-3} HPi and NaPi. b–d: 1—5×10^{-5} HPi and NaPi; 2—1×10^{-3} HPi; 3—8.8×10^{-3} HPi. Abscissae for all curves are λ (mμ).

In the alcohols three different spectral curves are obtained for picric acid at the concentrations of 5×10^{-5}, 1×10^{-3}, and 8.8×10^{-3} moles/liter, the curves intersecting in a single point lying in the 310 mμ region. Figure 1 shows that the nature of the spectral curves is identical for all the alcohols at a given concentration. The identity of the spectra of picric acid and sodium picrate at a concentration of 5×10^{-5} moles/liter and the presence of a maximum in the 355-358 mμ region indicates complete dissociation of the picric acid in the alcohols at low concentrations. It should be noted that in water and in methyl alcohol the ion spectrum is characterized by a maximum at 355-356 mμ, while in ethyl alcohol it is at 357 mμ, and in n-butyl alcohol at 358 mμ.

The departure from Beer's law in these cases may be caused by the appearance of some new species not as absorbing as ions, since the point of intersection indicates an equilibrium among these particles. In order to show the nature of the particles involved in this equilibrium, we suppressed the dissociation of the picric acid by the addition of sulfuric acid in the case of aqueous solutions and by saturating the alcohols with dry hydrogen chloride. In this way spectra of undissociated acid in water and in alcohols were obtained, reminiscent of the absorption spectra of picric acid in dioxane, dichloroethane, chloroform, and other aprotic solvents.

In water, picric acid is a strong electrolyte, and consequently in order to suppress its dissociation it was necessary to provide a high concentration of sulfuric acid

[15 moles/liter). In order to obtain the spectrum of undissociated picric acid in alcohol, it was sufficient to add 0.1 gram equivalent of hydrogen chloride per liter of solution.

Spectral curves for solutions of picric acid with added nonabsorbing mineral acid intersect at a point lying in the 310 mμ region (Fig. 2), analogous to the previously discussed case. This indicates an equilibrium between the ions and molecules of picric acid. From Fig. 2 one sees that to the right of the intersection point the spectral curves are gradually lowered and the position of the maximum, corresponding to the ionic spectrum (355-358 mμ), is gradually shifted towards the short wavelength region; while to the left of the intersection point, on the other hand, there is a gradual rise in the spectral curves, and there appears a maximum in the spectrum of the undissociated acid in the 230-240 mμ region. In water this maximum occurs at 240 mμ, in methanol at 235-237 mμ, in ethanol at 230-232 mμ, and in n-butanol at 230 mμ. One can conclude that the situation is similar to the picture for aqueous solutions[4] and for dioxane-water mixtures[5] as obtained by Halban and co-workers, who studied equilibria between the ions and molecules of picric acid. The above-mentioned authors have investigated the spectrum of undissociated picric acid in dioxane, in water with the addition of large amounts of hydrochloric acid (up to 12 N), and in other solvents. However, all these spectra were studied only as far down as the region of 250 mμ, and consequently they did not observe the maximum at 230-240 mμ.

The applicability of Beer's law for solutions in alcohols with the addition of 0.1 N hydrogen chloride indicates that we actually obtained spectra of undissociated picric acid.

In Fig. 3 are presented the spectra of sodium picrate

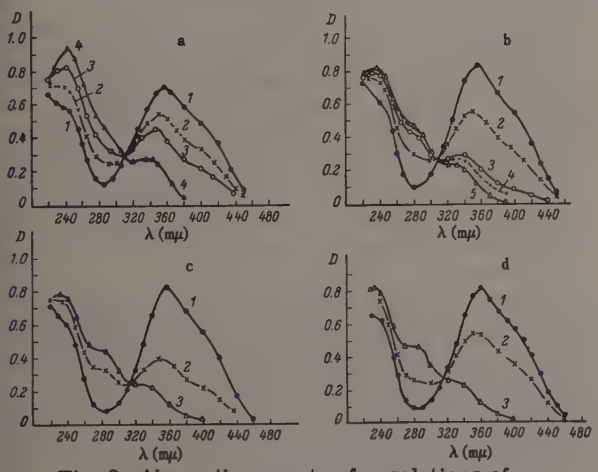

Fig. 2. Absorption spectra for solutions of picric acid in various solvents and with the addition of mineral acids. Solvents: a-d, see description of Fig. 1. Concentration of HPi (in moles/liter and amount of added mineral acid: a: 1—1×10^{-3} HPi; 2—same + 0.5 M H_2SO_4; 3—same + 1 M H_2SO_4; 4—same + 15 M H_2SO_4. b: 1—5×10^{-5} HPi; 2—same + 0.0005 N HCl; 3—same + 0.005 N HCl; 4—same + 0.01 N HCl; 5—same + 0.1 N HCl. c: 1—5×10^{-5} HPi; 2—same + 0.001 N HCl; 3—same + 0.1 N HCl. d: 1—5×10^{-5} HPi; 2—same + 0.0005 N HCl; 3—same + 0.1 N HCl.

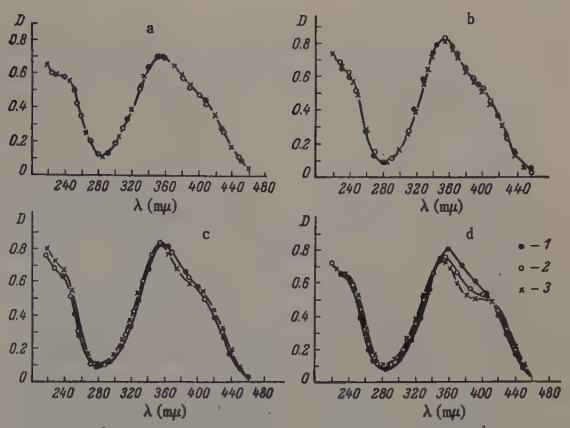

Fig. 3. Absorption spectra of solutions of sodium picrate in various solvents at different concentrations. Solvents a-d, see description in Fig. 1. Concentration (in moles/liter): 1—5×10^{-5}; 2—1×10^{-3}; 3—8.8×10^{-3}.

solutions at concentrations of 5×10^{-5}, 1×10^{-3}, and 8.8×10^{-3} moles/liter in water and in alcohols. In methyl alcohol, as in water, sodium picrate at all these concentrations is characterized by one spectral curve, peculiar to the ion spectrum. The applicability of Beer's law shows that there is complete dissociation of sodium picrate in methyl alcohol over the entire concentration range from 5×10^{-5} to 8.8×10^{-3} moles/liter. In ethyl alcohol sodium picrate has the ion spectrum at concentrations of 5×10^{-5} and 1×10^{-3} moles/liter but at 8.8×10^{-3} moles/liter a slight spectral shift is observed (i.e., a deviation from Beer's law occurs). In n-butyl alcohol deviations from Beer's law are also observed at 1×10^{-3} moles/liter as a result of which for all three investigated concentrations of sodium picrate, three different spectral curves, which overlap at two points, are obtained. The nonapplicability of Beer's law can be explained as the appearance of a new kind of absorbing species.

When the alcoholic solutions of sodium picrate were treated with the nonabsorbing salt $NaClO_4$ (sodium perchlorate), whose ions are quite similar to those of sodium picrate, an analogous displacement of the spectra occurs (Fig. 4). This same effect is observed when the dielectric constant of the solvent is decreased by the addition of benzene to the alcoholic solutions. Thus, in the limit we obtained in all cases (Figs. 3 and 4) the spectrum of sodium picrate in alcohol, analogous to the spectrum of sodium picrate in dioxane (cf. Fig. 5—ionic association). This spectrum is obviously closely related to that of solutions of undissociated sodium picrate in alcohols.

Many investigators,[4,5,10-14] in studying absorption spectra of solutions of thiosulfates, sulfates, nitrates, and picrates of metals, have postulated the existence of ion pairs. However, other authors (for example, Popov,[15] Kolthoff,[16] and others) came to the conclusion that the formation of ion pairs was not indicated by the absorption spectra. Halban and co-workers obtained the undissociated picrate spectrum in water by adding to the solutions large amounts of nonabsorbing salts.[3,4] These spectra are very similar to the analogous spectra obtained by us in alcoholic solutions. Moreover, undissociated picrates, as indicated by Halban, undoubtedly have a heteropolar nature. The dipole moment of ammonium

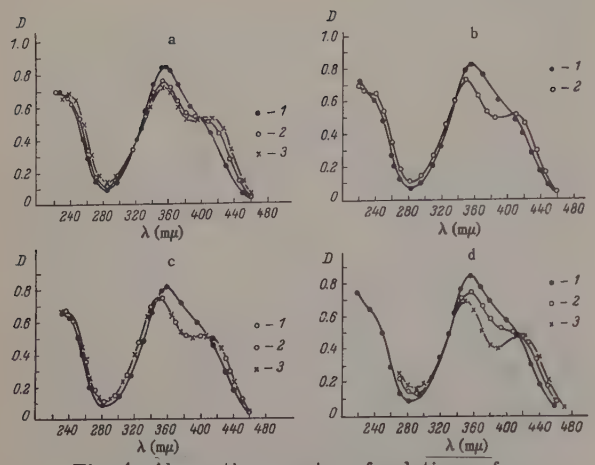

Fig. 4. Absorption spectra of solutions of sodium picrate in various solvents upon addition of sodium perchlorate or benzene. Solvents: a—CH_3OH; b—C_2H_5OH; c—n-C_4H_9OH; d—$C_2H_5OH + C_6H_6$. Concentration of NaPi (in moles/liter) and amount of added sodium perchlorate or benzene: a: 1—5×10^{-5} NaPi; 2—same + 1 N $NaClO_4$; 3—same + 2.63 N $NaClO_4$. b: 1—5×10^{-5} NaPi; 2—same + 1 N $NaClO_4$. c: 1—5×10^{-5} NaPi; 2—same + 0.005 N $NaClO_4$; 3—same + 0.12 N $NaClO_4$. d: 1—1×10^{-3} NaPi in C_2H_5OH; 2—same in 50% C_2H_5OH and 50% C_6H_6; 3—same in 16% C_2H_5OH + 84% C_6H_6.

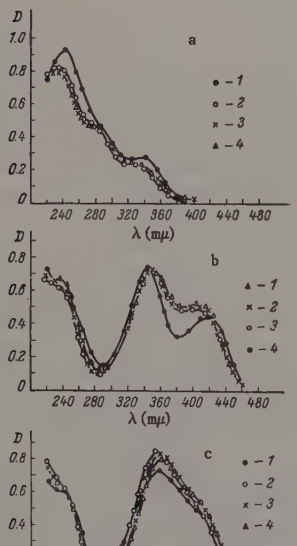

Fig. 5. The absorption spectra of solutions of various equilibrium forms of HPi and NaPi in different solvents. a—HPi (undissociated); b—NaPi (ion associations); c—HPi and NaPi (ions). Solvents: a, c: 1—H_2O, 2—CH_3OH, 3—C_2H_5OH, 4—n-C_4O_9OH; b: 1—CH_3OH, 2—C_2H_5OH, 3—n-C_4H_9OH, 4—dioxane.

picrate in dioxane, measured by Kraus et al,[3] proved to be larger than expected for a homopolar molecule. It follows from this, according to Halban, that undissociated picrates are composed of ion pairs.

In the present work we have shown that the spectrum of associated sodium picrate differs from the spectrum of dissociated sodium picrate in that the intersection points observed by us indicate the existence of an equilibrium between ions and ion pairs.

As a consequence of the varying dissociative properties of the alcohols for the conversion of a 5×10^{-5} moles/liter solution of sodium picrate into the undissociated state, in methyl alcohol there is required 2.63 gm eq./liter of $NaClO_4$, in ethyl alcohol 1 gm eq./liter, and in n-butyl alcohol only 0.005 gm eq./liter. This is evidence that the value of $pK = -\log K^{-1}_{ass.}$ ($K^{-1}_{ass.} = a_{Na} + a_{Pi^-}/a_{Na^+Pi^-}$) increases on going from methyl alcohol to n-butyl alcohol. Upon further additions of the salt $NaClO_4$ (0.05 and 0.12 gm eq./liter the spectrum does not change appreciably. This fact, together with the applicability of Beer's law to alcoholic solutions of sodium picrate at concentrations from 5×10^{-5} to 8.8×10^{-3} moles/liter with additions of $NaClO_4$, indicates that in this case sodium picrate is completely transformed into associated ions. The spectrum of the associated picrate is characterized by two maxima in the 350 and 410 mμ range in alcohols and in the 345 and 417-420 mμ range in dioxane.

In order to characterize the influence of the solvent on the acid strength[17-19] of picric acid and on the solution equilibria involved, we have calculated dissociation constants for picric acid in water and in methyl, ethyl, and n-butyl alcohols by using molar extinction coefficients for the ionic and molecular forms of picric acid and data on activity coefficients of sulfuric acid in water[20] and hydrochloric acid in alcohols.[7,20]

The values of $pK_{diss.}$ of picric acid obtained by us for solutions in the above-mentioned solvents proved to be identical in all spectral regions from 230 to 390 mμ, differing by only about one percent (average values of $pK_{diss.}$ are presented in the Table.

Solvent	Water	CH_3OH	C_2H_5OH	n.-C_4H_9OH
pK of picric acid (average values)	0.82	3.09	3.27	3.26

The dissociation constants for picric acid can be calculated by an alternative method, not using activity coefficients but rather utilizing molar extinction coefficients of the ionic and molecular forms of picric acid and the optical density of picric acid at concentrations of 1×10^{-3} moles/liter in pure alcohols. This calculation was made only at low concentrations (no higher than 1×10^{-3} moles/liter.) In calculating $pK_{diss.}$ of picric acid in alcohol solutions, when the concentration reached 8.8×10^{-3} moles/liter there had already occurred an appreciable alteration, as a result of which it was necessary to determine the activity of the picric acid.

The values of $pK_{diss.}$ for picric acid for a concentration of 1×10^{-3} moles/liter, calculated without computing the activity coefficient, over the 230-390 mμ wavelength interval for solutions in methyl, ethyl, and n-butyl alcohols, were, respectively, 3.15, 3.12, and 3.16.

For solutions of picric acid in methyl alcohol we calculated the value of $pK_{diss.}$ by the method suggested by Komar',[21] and obtained the value of 3.08. This agrees

th the value of $pK_{diss.}$ in methyl alcohol presented in e Table.

Gross and co-workers, using data at 436 mμ to calulate $pK_{diss.}$ of picric acid in ethyl alcohol, obtained the lue of 3.74.[6] This constant, calculated from data at a ngle wavelength (occurring at the steep portion of the ectral curve) appears to us to be quite imprecise.

The value of $pK_{diss.}$ for picric acid in methyl and hyl alcohols, obtained from electrical conductivity data e, respectively, 3.81[22] and 3.99,[23] and the value of $K_{diss.}$ in n-butyl alcohol, obtained from emf data, is 84.[24] From this it is obvious that the values obtained us for $K_{diss.}$ of picric acid in alcohols are several nes larger than the dissociation constants calculated by her authors from data on electrical conductivity and nf. This can be explained in the following way: Ions d ion pairs absorb in the same spectral region, and as result, in the presence of ion association, the value of $K_{diss.}$ calculated from absorption spectra is larger than at based on electrical conductivity and emf data, since e ion pairs do not take part in carrying current and do t influence the emf, behaving in this respect like unssociated molecules. This phenomenon has already en noted by Halban and Litmanowitsch[14] in an investiation of the degree of dissociation of nitric acid in diane 20% water.

As a result of the high dielectric constant of water, cric acid exhibits practically no ionic association in ueous solution. Consequently, the value of $pK_{diss.}$ of cric acid in water, calculated by us from absorption ectra (see Table) agrees with the values calculated om emf data[24] (0.82) and from water-benzene distribun data[25] (0.78).

Without the data on the activity coefficients of $LiClO_4$ in alcohols, we would not have been able to calulate equilibrium constants for sodium picrate in ethyl and ethyl alcohols. We found the value of $K_{ass.}$ n-butyl alcohol at a concentration of 1×10^{-3} oles/liter ($pK = -\log K^{-1}_{ass.} = 3.23$).

Until now we have considered the influence of the olvent on the equilibrium between the various equilibum forms of picric acid and sodium picrate. It is inresting to trace how the solvent influences the spectra the limiting equilibrium forms of picric acid and of odium picrate, i.e., the ions, molecules, and associated ns. Thus, in different solvents the ions, molecules, and ssociated ions are solvated with various molecules of olvent, and one could expect a difference in the absorpon spectra of the limiting equilibrium forms.

Figure 5 shows spectra of solutions of undissociated icric acid in water and in alcohols. In methyl, ethyl, nd n-butyl alcohols the absorption spectra of undissoci-ed picric acid are very similar, but the form and the tensity are appreciably different in water. On this same iagram are also presented data for ionic association, hich, as in the case of molecules of picric acid, yield ery similar spectra in the various alcohols. Here the odium picrate spectrum in dioxane is shown for comarison.

Furthermore, Fig. 5 shows the absorption spectra f the ions of picric acid in water and in alcohols, the difference between them being only their intensities. Thus, it is easily seen that the spectra of ions are appreciably different from the spectra of undissociated molecules of picric acid and from the spectra of associated ions.

REFERENCES

1. N. A. Izmailov and V. A. Kremer, Uchenye Zapiski, Kharkov. Gosudarst. Univ. **38**; Trudy Nauch.-Issledovatel. Khim. Inst. **9**, 307 (1951).
2. N. A. Izmailov and V. A. Kremer, Izvest. Akad. Nauk SSSR, Ser. Fiz. **15**, 565 (1951).
3. H. Halban and B. Stigeti, Helv. Chim. Acta **20**, 746 (1937).
4. H. Halban and M. Litmanowitsch, Helv. Chim. Acta **24**, 38 (1941).
5. H. Halban and M. Litmanowitsch, Helv. Chim. Acta **26**, 771 (1943).
6. P. Gross and A. Goldstern, Monatsh. Chem. **55**, 316 (1930).
7. N. A. Izmailov and V. V. Aleksandrov, Zhur. Fiz. Khim. **31**, 2619 (1957).
8. V. V. Aleksandrov and N. A. Izmailov, Zhur. Fiz. Khim. **32**, 404 (1958).
9. W. Jackel, Z. phys. Chem. **207**, 296 (1957).
10. F. G. R. Gimblett and C. B. Monk, Trans. Faraday Soc. **51**, 793 (1955).
11. G. O. Thomas and C. B. Monk, Trans. Faraday Soc. **52**, 685 (1956).
12. H. M. Hershenson, M. E. Smith, and D. N. Hume, J. Am. Chem. Soc. **75**, 507 (1953).
13. E. W. Davies and C. B. Monk, J. Am. Chem. Soc. **80**, 5032 (1958).
14. H. V. Halban and M. Litmanowitsch, Helv. Chim. Acta **31**, 1963 (1948).
15. A. J. Popova and R. E. Humphrey, J. Am. Chem. Soc. **81**, 2043 (1959).
16. J. M. Kolthoff, D Stocesca, and T. S. Lee, J. Am. Chem. Soc. **75**, 1834 (1953).
17. N. A. Izmailov, Doct. dissertation, Kharkov, 1948.
18. N. A. Izmailov and I. F. Zabara, "Sbornik Rabot po Fiz. Khim." (Collected Works in Physical Chemistry), p. 310. Izd. Akad. Nauk SSSR, 1947.
19. N. A. Izmailov and E. I. Vail', Ukrain. Khim. Zhur. **23**, 662 (1957).
20. N. S. Harned and B. Owen, "Physical Chemistry of Solutions of Electrolytes," pp. 511, 569. Izd. Inostrannoi Lit., Moscow, 1952. 3rd ed., Reinhold, New York, 1958.
21. N. P. Komar', Uchenye Zapiski, Kharkov. Gosudarst. Univ. **37**; Trudy Nauch.-Issledovatel. Inst. Khimii **8**, 57 (1951).
22. H. Goldschmidt and H. Aarflot, Z. phys. Chem. **117**, 312 (1925).
23. H. Goldschmidt, Z. phys. Chem. **91**, 46 (1916).
24. L. Wooten and L. Hammet, J. Am. Chem. Soc. **57**, 2289 (1935).
25. V. Rothmund and R. Drucker, Z. phys. Chem. **46**, 827 (1903).

ON THE USE OF THE CURVES $\nu = f(Z_X)$ IN THE STUDY OF THE VIBRATIONAL SPECTRA OF TETRAHEDRAL MOLECULES AND IONS OF THE FORM $X(Hal)_4$

I. N. Godnev and A. M. Aleksandrovskaya (pp. 27-32)

Received 26 April 1960

It has been shown that simultaneous study of the dynamic coefficients of the $X(Hal)_4$ neutral molecules (X is an element of the fourth group with the electronic configuration s^2p^2) and of the corresponding isoelectronic ions enables one to explain the regular pattern of the curves $\nu = f(Z_X)$, which proves to be useful for predicting the frequencies of ions.

A work by Woodward[1] was recently published, in which the results of measurement of the normal vibration frequencies of certain isoelectronic molecules and ions of the form XY_4 were compared, and the dependence of the force constant of the valence vibration on the ionic charge was studied.

It is interesting to carry out a study and comparison of the other four dynamic coefficients of molecules and ions of the form XY_4. The results of such an investigation relative to the halides are set forth below; unlike Woodward, we have not only carried out the study of the dynamic coefficients of separate triads, but have also considered the behavior of these coefficients among the elements X of the fourth group with the electronic configuration s^2p^2 * as a function of the atomic number of the

*X = C, Si, Ge, Sn, Pb.

central atom Z_X. The study of this dependence enables us to clarify the functional relationship $\nu_i = f(Z_X)$ and will be useful for prediction of the unknown frequencies of a number of ions.*

*Hildebrand[2] discovered a regular change in the frequencies ν_1 and ν_2, at Y = const., as a function of the distance r_{X-Y}.

Study of the dynamic coefficients and interaction coefficients of neutral molecules of the form XY_4 was begun earlier in our laboratory.[3-7] The equations ensuing from the method of progressive rigidity[8-10] (compare with refs. 3 and 11) have rendered substantial help in this study; they make it possible to calculate five linearly independent reduced coefficients in terms of the four frequency values $\nu_1(A_1)$, $\nu_2(E)$, $\nu_3(F_2)$, and $\nu_4(F_2)$:

$$k_1 = \frac{\nu_1^2}{\varepsilon_Y}, \quad (1)$$

$$k_2 = \frac{\nu_2^2}{3\varepsilon_Y\sigma^2}, \quad (2)$$

$$k_{11} \approx \frac{\nu_3^2}{A_{11}} + \frac{A_{12}^2\nu_4^2}{A_{11}|A|}, \quad (3)$$

$$k_{12} \approx -\frac{A_{12}\nu_4^2}{|A|}, \quad (4)$$

$$k_{22} \approx \frac{A_{11}\nu_4^2}{|A|}, \quad (5)$$

where k_1, k_2, k_{11}, k_{12}, and k_{22} are the reduced dynamic coefficients, A_{11}, A_{12}, and A_{22} are the kinematic coefficients of a two-dimensional block, and

$$\varepsilon_Y = \frac{m_H}{m_Y}, \quad \sigma = \frac{r_{C-H}}{r_{X-Y}}.$$

Analogous equations are obtained for the reduced interaction coefficients by inversion of the (k) matrix.* The

*Compare with ref. 3.

curves of these coefficients, $k^* = f(A_{central})$ (and also $k = f(A_{central})$), have been used by us to determine the normal vibration frequencies of some tetrahedral molecules.[6,7]

Equations (1)-(5) have been used by us for the evaluation of the dynamic coefficients* of a series of ions on

*For the determination of unknown interatomic distances, a procedure analogous to that previously described[6,7] was employed.

the basis of the experimental frequency values[12-15]; analogously to Woodward, who studied the dependence of the one coefficient k_1 on the ionic charge, we discovered a rapid increase in all 5 coefficients as Z_X increases for each isoelectronic series (see Table 1, in which are presented the 5 dynamic coefficients for two triads).

Table 1. Reduced Dynamic Coefficients of Two Triads (10^5 cm^{-2})

XY_4	Z_X	k_1	k_2	k_{11}	k_{12}	k_{22}
$AlCl_4^-$	13	3.97	(0.77)	4.29	0.58	0.89
$SiCl_4$	14	5.88	0.83	5.02	0.81	1.18
PCl_4^+	15	6.63	1.07	5.71	0.96	1.45
$ZnBr_4^{--}$	30	2.17	0.44	1.40	0.30	0.53
$GaBr_4^-$	31	3.24	0.58	2.50	0.45	0.81
$GeBr_4$	32	4.03	0.66	3.51	0.52	0.91

Construction of the curves of the change in dynamic coefficients of the ions (together with the analogous curves for the neutral molecules) as a function of Z_X (X is an element of the fourth group with the electronic configuration s^2p^2) at Y = const. has shown that a regular change is observed in the ionic and molecular coefficients; this change is schematically represented in Fig. 1 (the curve 00′ corresponds to the neutral molecules and the curves 11′, 22′, and 33′ to the isoelectronic ions).

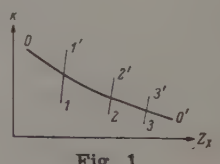

Fig. 1

To explain the regularity found, let us first consider the change in $k = f(Z_X)$ along the curve 00′, and then the change in k along the ionic curves 11′, 22′, and 33′. The first consideration corresponds to the transition ... Si → Ge → Sn → Pb, the second to the transition from the molecules listed to the positive and negative ions.

As an example, let us consider the "cross" corresponding to $GeCl_4$,

$$\begin{array}{c} AsCl_4^+ \\ | \\ \ldots-SiCl_4-GeCl_4-SnCl_4-\ldots \\ | \\ GaCl_4^- \end{array} \qquad (6)$$

In this case we shall have the transition $Z_X = 14, 32, \ldots$ along the horizontal chain. The addition of 18 electrons (Si → Ge → Sn) does not essentially change the structure of the electronic envelope, and consequently we may expect a weak decrease in the coefficients k_1, k_{11}, k_{12}, and k_{22} as Z_X increases. This is observed actuality for all the molecules indicated (see, for example, Fig. 2, which shows the independence of k_1 and k_{22} on Z_X for the chlorides).*

*For the elements with the electronic configuration d^2s^2 (Ti-Zr-Hf), small breaks are observed on curve 00′, but the general character of this curve is preserved. Unfortunately, we have no data for the construction of the ionic curves 11′, 22′, ... for this case.

Another picture must be observed along an ionic series, for example $GaCl_4^-$-$GeCl_4$-$AsCl_4^+$ (number of electrons 100) or another analogous isoelectronic series. On going over to the ions, we shall have vibrations in the field of an uncompensated electric charge, the action of which must strongly influence the value of the dynamic coefficients.

Actually, from a comparison of diagrams of the structure of the X—Y bond (Fig. 3), we must expect that

$$k_{As^+} > k_{Ge} > k_{Ga^-},$$

i.e., as Z_X of the central atom increases along an isoelectronic series, not a fall but a rise in the dynamic coefficients must be observed, and this rise must be marked. This is also observed in all the cases studied by us (see e.g. 2).

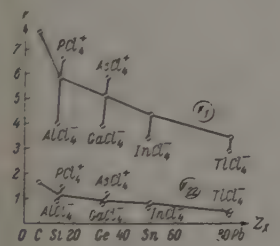

Fig. 2

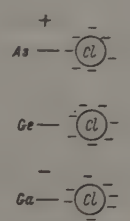

Fig. 3

The regularities found in the behavior of the dynamic coefficients enable us to give a basis also for the dependence of the frequencies ν_1, ν_2, ν_3, and ν_4 on Z_X.*

*We have studied a relatively simple case. For example, for octahedral molecules and ions, the curves $\nu = f(Z_X)$ must have a more complicated appearance.

Actually, solution of Eqs. (1)-(5) for the frequencies gives

$$\nu_1^2 = \frac{m_H}{m_Y} k_1, \qquad (7)$$

$$\nu_2^2 = 3\frac{m_H}{m_Y} \cdot \frac{r_{C-H}^2}{r_{X-Y}^2} k_2, \qquad (8)$$

$$\nu_3^2 = m_H\left(\frac{1}{m_Y} + \frac{4}{3}\cdot\frac{1}{m_X}\right)\cdot\left(k_{11} - \frac{k_{12}^2}{k_{22}}\right), \qquad (9)$$

$$\nu_4^2 = \frac{6r_{C-H}^2 m_H (m_X + 4m_Y)}{r_{X-Y}^2 m_Y (3m_X + 4m_Y)} \cdot k_{22}. \qquad (10)$$

From (7) it can be seen that m_Y does not depend on Z_X (along the line 00′, m_Y = const.), and the behavior of the curve $\nu_1 = f(Z_X)$ is determined by the behavior of k_1, which falls off slightly. From this it follows that the value of ν_1 as Z_X changes along 00′ must describe a curve of Hildebrand's type, but on going over to the ions we must observe a sharp increase in ν_1 with Z_X. This is observed in actuality (see Fig. 4 for the chlorides). An analogous result is obtained for ν_2. The slow fall in this quantity along the line 00′ is governed by the slow fall of k_2 and the increase in r_{X-Y} (see formula (8)), while the rapid increase along the ionic curves is governed by the rapid increase in k_2 and the diminution of r_{X-Y}. In the case of ν_3, the fall along 00′ is governed by the increase in m_X and the diminution of k_{11} (the change in k_{12}^2/k_{22} may be neglected, see formula (9)), while the rapid growth for the ions is governed by the sharp increase in k_{11} with an increase in Z_X. The behavior of $\nu_4 = f(Z_X)$ is explained in an analogous way (see formula (10)).

The predicted relationships are well verified by experiment. Using the data of Table 2, we have constructed 12 curves characterizing the dependence of ν_1, ν_2, ν_3, and ν_4 for the molecules and ions on Z_X. They all have the same appearance. Such curves for the chlorides are presented in Figs. 4 and 5. The frequencies of the bromides and iodides behave analogously.

The dependences $\nu = f(Z_X)$ may be used to predict

Table 2. Normal Vibration Frequencies of Molecules and Ions of the Form XY_4 (cm^{-1})

No.	XY_4	$\nu_1(A_1)$	$\nu_2(E)$	$\nu_3(F_2)$	$\nu_4(F_2)$	References
1	CCl_4	457	216	798	311	[16]
2	PCl_4^+	451	173	627	244	[12]
3	$SiCl_4$	424	150	610	221	[17]
4	$AlCl_4^-$	349	136—146	575	180	[13]
5	$GeCl_4$	396	132	453	172	[17]
6	$GaCl_4^-$	346	114	386	149	[18]
7	$ZnCl_4^{--}$	282	82?	?	116	[14]
8	$SnCl_4$	367	104	403	129	[17]
9	$PbCl_4$	327	90 (85)	348	90 (93)	[19]
10	CBr_4	268	128	673	182	[20]
11	$SiBr_4$	249	90	487	137	[17]
12	$GeBr_4$	235	80	327	112	[17]
13	$GaBr_4^-$	210	71	278	102	[15]
14	$ZnBr_4^{--}$	172	61	210	82	[14]
15	$SnBr_4$	220	64	279	88	[17]
16	$InBr_4^-$	197	55	239	79	[21]
17	$CdBr_4^{--}$	166	53	183	62	[22, 26]
18	$PbBr_4$	207	59	231	73	[7]
19	$TlBr_4^-$	190	51	209	64	[23]
20	CJ_4	207	86	598	118	[3]
21	SiJ_4	168	63	405	94	[17]
22	GeJ_4	159	60	264	80	[24]
23	GaJ_4^-	145	52	222	73	[25]
24	ZnJ_4^{--}	122	44	170	62	[14]
25	SnJ_4	149	47	216	63	[24]
26	InJ_4^-	139	42	185	58	[25]
27	CdJ_4^{--}	117	36	145	44	[22, 26]
28	PbJ_4	137	37	168	48	[7]

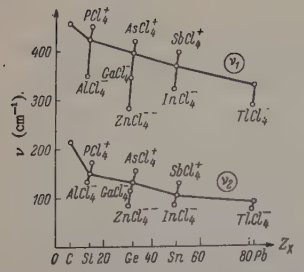

Fig. 4

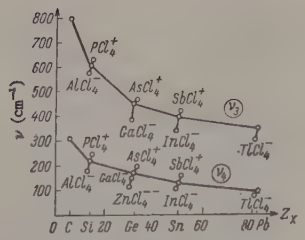

Fig. 5

the frequencies of a number of ions. For example, on the basis of the indicated graphs we have found the normal vibration frequencies of $InCl_4^-$, $TlCl_4^-$, TlI_4^-, and $AsCl_4^+$ (see Table 3). To verify the frequency values found, the latter were computed by the method described previously[6]: curves of the interaction coefficients as a function of $A_{central}$ were constructed; the interaction coefficients were determined from them, and then the frequency values were computed (see the second column of Table 3). They proved to be close to the frequencies found graphically.

Thus the method of $\nu = f(Z_X)$ curves (the method of Hildebrand-type curves) proves to be useful for the study of tetrahedral ions and molecules containing halogens.

Table 3. Normal Vibration Frequencies of Ions of the Form XY_4 (cm^{-1})*

Frequencies	$InCl_4^-$		$TlCl_4^-$		TlJ_4^-		$AsCl_4^+$	
	I	II	I	II	I	II	I	I
$\nu_1(A_1)$	320	314	285	292	127	133	420	42
$\nu_2(E)$	86	89	75	79	30	38	155	15
$\nu_3(F_2)$	340	342	300	320	140	156	467	46
$\nu_4(F_2)$	109	114	80	92	43	47	195	19

*The frequency values were determined with the help of the $\nu = f(Z_X)$ curves (were computed by the method described in ref. 6 (II).

REFERENCES

1. L. A. Woodward, Trans. Faraday Soc. **54**, 1271 (1958).
2. J. H. Hildebrand, J. Chem. Phys. **15**, 727 (1947).
3. A. S. Sverdlin, Zhur. Fiz. Khim. **32**, 659 (1958).
4. I. N. Godnev, A. S. Sverdlin, and N. I. Ushanova, Opt. i Spektr. **2**, 704 (1957).
5. N. I. Ushanova, I. N. Godnev, and I. V. Orlova, Opt. i Spektr. **5**, 567 (1958).
6. I. N. Godnev, A. M. Aleksandrovskaya, and I. V. Rigina, Opt. i Spektr. **7**, 271 (1959), Optics and Spectroscopy **7**, 172 (1959).
7. A. M. Aleksandrovskaya, I. V. Rigina, and I. N. Godnev, Opt. i Spektr. **7**, 844 (1959), Optics and Spectroscopy **7**, 495 (1959).
8. P. Torkington, J. Chem. Phys. **17**, 357 (1949).
9. M. Larnaudie, J. phys. radium **15**, 365 (1954).
10. I. V. Orlova and I. N. Godnev, Opt. i Spektr. **6**, 447 (1959), Optics and Spectroscopy **6**, 284 (1959).
11. A. S. Sverdlin, Kand. diss., Ivanovskii, Khim.-Tekhnol. Inst., 1956.
12. H. Gerding and H. Hautgraaf, Rec. trav. chim. **74**, 5 (1955).
13. H. Gerding and H. Hautgraaf, Rec. trav. chim. **72**, 21 (1953).
14. M. L. Delwaulle, Compt. rend. Acad. Sci. **240**, 213 (1955).
15. L. A. Woodward and A. A. Nord, J. Chem. Soc. 265 (1955).
16. H. H. Claassen, J. Chem. Phys. **22**, 50 (1954).
17. M. L. Delwaulle, F. Francois, and M. Delhaye-Bui J. phys. radium **15**, 206 (1954).
18. L. A. Woodward and A. A. Nord, J. Chem. Soc. 372 (1956).
19. J. T. Neu and W. D. Gwinn, J. Am. Chem. Soc. **70**, 3463 (1948).
20. M. L. Delwaulle, J. Phys. Chem. **56**, 355 (1952).
21. M. L. Woodward and P. T. Bill, J. Chem. Soc. 1699 (1
22. M. L. Delwaulle, F. Francois, and J. Wiemann, Compt. rend. Acad. Sci. **208**, 1818 (1939).
23. M. L. Delwaulle, Compt. rend. Acad. Sci. **238**, 252 (1954).
24. H. Stammreich, R. Forneris, and Y. Tavares, J. Chem. Phys. **25**, 1278 (1956).
25. L. A. Woodward and G. H. Singer, J. Chem. Soc. 7 (1958).
26. J. A. Rolfe, D. E. Shepard, and L. A. Woodward, Trans. Faraday Soc. **50**, 1275 (1954).

CALCULATION OF THE INTEGRATED INTENSITIES OF THE INFRARED BANDS OF ISOTOPICALLY SUBSTITUTED METHANES. VIII

L. M. Sverdlov (pp. 33-40)

Received 5 April 1960

A theoretical calculation of the integrated intensities of the infrared bands of 11 isotopically substituted methanes (CH_3D, CH_2D_2, CHD_3, CD_4, CH_3T, CH_2T_2, CHT_3, CT_4, CD_3T, CD_2T_2, and CDT_3) has been carried out in the first approximation of the valence-optical scheme. The high accuracy of the intensity calculation is confirmed by the good fulfillment of the sum rules for intensities.

1. In connection with the widespread application of otopes in science and engineering, the working out of ethods for checking the purity of various isotopic prep- rations, and also for determining the composition of otopic mixtures, takes on important significance. One the most effective methods of such checking is the ethod based on the study of vibrational spectra. Infra- ed spectra are most frequently used for this purpose; uantitative isotopic analysis must be based on the meas- rement of the integrated intensities of the infrared nds of the various isotopic molecules, since this re- ases one from the necessity of using standard samples.[1] consideration of this circumstance, theoretical calcu- tions of the integrated intensities of the infrared spec- a of the most important sets of isotopic molecules are great interest.

In the present work, a calculation of the integrated tensities of the infrared bands of a series of isotopi- lly substituted methanes has been carried out in the rst approximation of the valence-optical scheme[2]: $CH_{\alpha}D_{4-\alpha}$, $CH_{\alpha}T_{4-\alpha}$, and $CD_{\alpha}T_{4-\alpha}(\alpha = 0\text{-}3)$.

We have previously[3] evaluated the electro-optical rameters of methane. In doing so, we used the experi- ental values of the absolute integrated intensities of e infrared bands of CH_4 [4] and the values of the force nstants calculated with the help of the zero-order fre- encies presented in ref. 5 for the CH_4 and CD_4 mole- les. However, in a recently published work by Jones d McDowell,[6] the values of the zero-order frequencies methane were somewhat altered as a result of an in- estigation of the infrared spectra of tritium- and itium-deuterium-substituted methanes. Along with is, the set of methane force constants was also changed. the work at hand, these new results have also been sed for the evaluation of the electro-optical parameters.

2. For the computation, we introduce the vibrational ordinates q_i, α_{ij}, and δ, and the angular valence-optical coordinates β_{ni}. The symbols for the coordinates and e directions of the axes are shown in Figs. 1, 2 and 3.

Molecules of types CX_4, CX_3Y, and CX_2Y_2 (X, Y = , D, T) belong respectively to the symmetry groups T_d, $_v$, and C_{2v}.

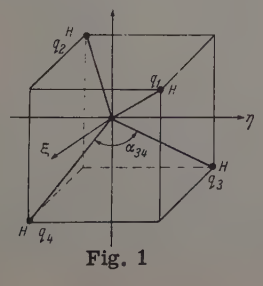

Fig. 1

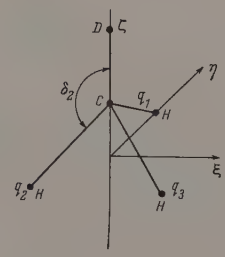

Fig. 2

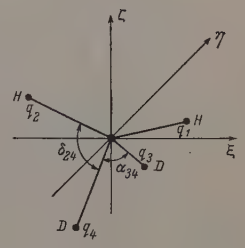

Fig. 3

In terms of the normal coordinates Q_l, the symmetry coordinates ($S_k = \Sigma L_{kl} Q_l$) are expressed in the form:

for CH_3D

$$q_d^{A_1} = \sum_l C_{dl}^{A_1} Q_l;\quad q_H^{A_1} = \sum_l C_{Hl}^{A_1} Q_l;\quad \alpha^{A_1} = \sum_l D_{al}^{A_1} Q_l;$$

$$q_H^{E\,II} = \sum_l C_{Hl}^{E\,II} Q_l;\quad \alpha^{E\,II} = \sum_l D_{al}^{E\,II} Q_l;\quad \delta^{E\,II} = \sum_l D_{\delta l}^{E\,II} Q_l;$$

for CH_2D_2

$$q_H^{A_1} = \sum_l C_{Hl}^{A_1} Q_l;\quad q_d^{A_1} = \sum_l C_{dl}^{A_1} Q_l;\quad \alpha_H^{A_1} = \sum_l D_{Hl}^{A_1} Q_l;\quad \alpha_d^{A_1} = \sum_l D_{dl}^{A_1} Q_l;$$

$$q_H^{B_1} = \sum_l C_{Hl}^{B_1} Q_l;\quad \delta^{B_1} = \sum_l D_{\delta l}^{B_1} Q_l;\quad q_d^{B_2} = \sum_l C_{dl}^{B_2} Q_l;\quad \delta^{B_2} = \sum_l D_{\delta l}^{B_2} Q_l.$$

In the first approximation of the valence-optical scheme, the derivatives of the dipole moment with respect to the normal coordinates, $\partial P_i/\partial Q_l$, have the form:

for CH_4*

*In ref. 3, we omitted interactions of types $\partial\alpha/\partial q$ and $\partial\mu/\partial\alpha$.

$$\left.\begin{aligned}\frac{\partial P_\zeta}{\partial Q_l^{F_2}} = \left\{\frac{\partial P_\zeta}{\partial q^{F_2}} C_l + \frac{\partial P_\zeta}{\partial \alpha^{F_2}} D_l\right\} = \left\{\left[\frac{2}{\sqrt{3}}\left(\frac{\partial \mu_{CH}^{(1)}}{\partial q_1} - \frac{\partial \mu_{CH}^{(2)}}{\partial q_1}\right) - \right.\right.\\ \left. - \sqrt{\frac{8}{3}}\,\mu_{CH}\left(\frac{\partial \alpha_{12}}{\partial q_1} - \frac{\partial \alpha_{34}}{\partial q_1}\right)\right] C_l + \left[-\frac{2}{\sqrt{3}}\frac{\mu_{CH}}{r_{CH}} + \\ \left. + \sqrt{\frac{8}{3}}\left(\frac{\partial \mu_{CH}^{(1)}}{\partial \alpha_{12}} - \frac{\partial \mu_{CH}^{(3)}}{\partial \alpha_{12}}\right)\right] D_l\right\};\quad \frac{\partial P_\zeta}{\partial Q_l^{F_2}} = \frac{\partial P_\eta}{\partial Q_l^{F_2}} = 0\ (l = 3, 4);\end{aligned}\right\} \quad (1)$$

for CH_3D

$$\left.\begin{aligned}\frac{\partial P_\zeta}{\partial Q_l^{A_1}} = \left\{\frac{\partial P_\zeta}{\partial q^{F_2}}\left(\frac{\sqrt{3}}{2} C_{dl}^{A_1} - \frac{1}{2} C_{Hl}^{A_1}\right) - \sqrt{2}\,\frac{\partial P_\zeta}{\partial \alpha^{F_2}} \cdot D_{al}^{A_1}\right\};\\ \frac{\partial P_\xi}{\partial Q_l^{A_1}} = \frac{\partial P_\eta}{\partial Q_l^{A_1}} = 0\ (l = 1,\ 3a,\ 4a);\\ \frac{\partial P_\eta}{\partial Q_l^{E\,II}} = \left\{\frac{\partial P_\zeta}{\partial q^{F_2}} C_{Hl}^{E\,II} - \frac{1}{\sqrt{2}}\frac{\partial P_\zeta}{\partial \alpha^{F_2}}\left(D_{al}^{E\,II} - D_{\delta l}^{E\,II}\right)\right\};\\ \frac{\partial P_\xi}{\partial Q_l^{E\,II}} = \frac{\partial P_\zeta}{\partial Q_l^{E\,II}} = 0\ (l = 2,\ 3b,\ 4b);\end{aligned}\right\} \quad (2)$$

Table 1. C_1 and D_1 Coefficients of Isotopically Substituted Methanes of Types CX_4 and CX_2Y_2 (in units of 10^{12} gm$^{-1/2}$)

Molecule	Coordinate	Symmetry type A_1				Coordinate	Symmetry type B_1		Symmetry type B_2	
		Q_1	Q_{2a}	Q_{2c}	Q_{4c}		Q_{2b}	Q_{4b}	Q_{2c}	Q_{4c}
CH_2D_2	q_d	0.5758	0.0067	—0.0427	—0.0055	q_H	0.8148	—0.026	—	—
	α_H	0.0986	1.1167	—0.0586	—0.2631	δ	—0.1324	0.9987	—	—
	q_H	—0.0108	—0.0151	0.7936	0.0143	q_d	—	—	0.6048	—0.0139
	α_d	—0.1064	0.0911	0.071	0.8413	δ	—	—	—0.1953	1.1293
CH_2T_2	q_T	0.4816	—0.0083	—0.0414	0.0033	q_H	0.8148	—0.0234	—	—
	α_H	0.1609	1.1267	—0.0584	—0.1737	δ	—0.1378	0.9203	—	—
	q_H	—0.0091	—0.0161	0.7939	0.011	q_T	—	—	0.5163	0.0057
	α_T	—0.1397	0.0187	0.0744	0.7132	δ	—	—	—0.2714	1.091
CD_2T_2	q_T	0.4685	—0.0026	—0.1167	0.0026	q_d	0.6049	—0.0084	—	—
	α_d	0.1177	0.8132	—0.1232	—0.2037	δ	—0.2099	0.8202	—	—
	q_d	0.0711	—0.0046	0.5722	0.005	q_T	—	—	0.5163	0.0037
	α_T	—0.1153	0.0485	0.1254	0.7084	δ	—	—	—0.2853	0.8635

Molecule	Coordinate	Symmetry type F_2		Molecule	Coordinate	Symmetry type F_2		Molecule	Coordinate	Symmetry type F_2	
		Q_3	Q_4			Q_3	Q_4			Q_3	Q_4
CH_4	q_H	0.8145	—0.0336	CD_4	q_d	0.6049	—0.0097	CT_4	q_T	0.5163	—0.0031
	α_H	—0.1147	1.204		α_d	—0.2067	0.9072		α_T	—0.2638	0.7758

for CH_2D_2

$$\left.\begin{aligned}
&\frac{\partial P_\zeta}{\partial Q_l^{A_1}} = \frac{1}{\sqrt{2}}\left[\frac{\partial P_\zeta}{\partial q^{F_2}}\left(C_{Hl}^{A_1} - C_{dl}^{A_1}\right) + \frac{\partial P_\zeta}{\partial \alpha^{F_2}}\left(D_{Hl}^{A_1} - D_{dl}^{A_1}\right)\right];\\
&\frac{\partial P_\xi}{\partial Q_l^{A_1}} = \frac{\partial P_\eta}{\partial Q_l^{A_1}} = 0 \quad (l = 1,\ 2a,\ 3a,\ 4a);\\
&\frac{\partial P_\xi}{\partial Q_l^{B_1}} = \left[\frac{\partial P_\zeta}{\partial q^{F_2}} C_{Hl}^{B_1} + \frac{\partial P_\zeta}{\partial \alpha^{F_2}} D_{Hl}^{B_1}\right];\quad \frac{\partial P_\eta}{\partial Q_l^{B_1}} = \frac{\partial P_\zeta}{\partial Q_l^{B_1}} = 0 \ (l = 3_B,\ 4_B);\\
&\frac{\partial P_\eta}{\partial Q_l^{B_2}} = \left[\frac{\partial P_\zeta}{\partial q^{F_2}} C_{dl}^{B_2} + \frac{\partial P_\zeta}{\partial \alpha^{F_2}} D_{dl}^{B_2}\right];\quad \frac{\partial P_\xi}{\partial Q_l^{B_2}} = \frac{\partial P_\zeta}{\partial Q_l^{B_2}} = 0 \ (l = 3c,\ 4c);\\
&\frac{\partial P_\xi}{\partial Q_{2b}^{A_2}} = \frac{\partial P_\eta}{\partial Q_{2b}^{A_2}} = \frac{\partial P_\zeta}{\partial Q_{2b}^{A_2}} = 0.
\end{aligned}\right\} \quad (3)$$

To evaluate the form coefficients L_{kl}, the mechanical problem was solved on the basis of the zero-order frequencies ω_i and the force constants presented in ref. 6: $K_q = 9.3313$, $h = 0.2016$, $K_\alpha - O_{\alpha\alpha} = 0.7794$, $a_\alpha - b_\alpha = 0.2564$, $l_{\alpha\alpha} - O_{\alpha\alpha} = -0.0263$ (in units of 10^6 cm^{-2}). The secular equations were solved by Mayants's iteration method.[7] In Tables 1 and 2 are presented the normalized C_1 and D_1 coefficients of methane and its 11 isotopic substitution products. These coefficients have been computed with high accuracy—the good fulfillment of the relations $\| L \| \cdot \| L^* \| = \| A_{ij} \|$, where $\| A_{ij} \|$ is the matrix of the kinematic coefficients, testifies to this.

Using the experimental values of the integrated intensities for methane,[4] we have obtained the following values for the electro-optical parameters of the molecule.*

*In ref. 3, the corresponding parameters are equal to 0.6763 D/A and −0.3382 D/A; i.e., they differ from the new values by only a few percent in all.

Table 2. C_1 and D_1 Coefficients of Isotopically Substituted Methanes of Type CX_3Y (in units of 10^{12} gm$^{-1/2}$)

Molecule	Coordinate	Symmetry type A_1			Coordinate	Symmetry type E II		
		Q_1	Q_{2a}	Q_{4a}		Q_3	Q_{3b}	Q_{4b}
CH_3D	q_d	0.5896	—0.0377	0.0129	α_H	1.2009	0.0806	—0.423
	q_H	0.0013	0.7836	—0.0167	q_H	0.0149	0.8146	—0.026
	α_H	0.1178	—0.0425	0.8452	δ	0.4846	—0.094	0.967
CD_3H	q_d	0.5607	—0.0363	—0.0043	δ	1.1323	—1.1379	—0.167
	q_H	0.0006	0.8046	0.0202	q_d	—0.0087	0.6048	0.008
	α_d	—0.074	0.0856	0.6481	α_d	0.1667	0.1464	0.912
CH_3T	q_T	0.4985	—0.0364	—0.0089	α_H	1.2296	0.0805	—0.330
	q_H	—0.0012	0.7836	—0.0166	q_H	0.0174	0.8147	—0.023
	α_H	0.1763	—0.0424	0.8358	δ	0.3915	—0.098	0.932
CT_3H	q_T	0.4638	—0.0354	0.0037	δ	1.0912	—0.1919	—0.045
	q_H	—0.0013	0.8047	0.0171	q_T	0.004	0.5163	—0.002
	α_T	—0.0997	0.0898	0.5617	α_T	0.0366	0.1864	0.772
CD_3T	q_T	0.4852	—0.12	—0.0041	α_d	0.8746	0.1461	—0.305
	q_d	0.078	0.5565	—0.0055	q_d	0.0043	0.6049	—0.008
	α_d	0.1496	—0.0998	0.6329	δ	0.318	—0.1484	0.780
CT_3D	q_T	0.4566	—0.089	0.0026	δ	0.8557	—0.1875	—0.12
	q_d	0.0512	0.5887	0.0072	q_T	0.0023	0.5163	—0.00
	α_T	—0.0797	0.1394	0.5548	α_T	0.1095	0.1864	0.76

$$\left.\begin{aligned}
&\left[\left(\frac{\partial \mu_{CH}^{(1)}}{\partial q_1} - \frac{\partial \mu_{CH}^{(2)}}{\partial q_1}\right) - \sqrt{2}\,\mu_{CH}\left(\frac{\partial \alpha_{12}}{\partial q_1} - \frac{\partial \alpha_{34}}{\partial q_1}\right)\right] = 0.6994\ \frac{D}{A};\\
&\frac{\mu_{CH}}{r_{CH}} - \frac{\sqrt{2}}{r_{CH}}\left(\frac{\partial \mu_{CH}^{(1)}}{\partial \alpha_{12}} - \frac{\partial \mu_{CH}^{(3)}}{\partial \alpha_{12}}\right)\Bigg] = -0.3133\ \frac{D}{A}
\end{aligned}\right\} \quad (4)$$

(these values correspond to the sign combination $+\partial P/\partial Q_3$ $+\partial P/\partial Q_4$).

Table 3. Integrated Intensities of the Infrared Bands (I_1) and the Quantities $\partial P/\partial Q_1$ for the Molecules CH_4, CD_4, and CT_4*

No. of the vibration	Symmetry	CH_4				CD_4				CT_4			
		Observed frequency, ν	Zero-order frequency, ω	$\frac{\partial P}{\partial Q_l}$	I_1	Observed frequency, ν	Zero-order frequency, ω	$\frac{\partial P}{\partial Q_l}$	I_1	Observed frequency, ν	Zero-order frequency, ω	$\frac{\partial P}{\partial Q_l}$	I_1
1	A	2917	3143	0	0	2108	2224	0	0	1738	1817	0	0
2	E	1534	1573	0	0	1092	1113	0	0	896	910	0	0
3	F_2	3019	3154	61.63	356.2585	2259	2333	41.3717	160.5419	1937	1990	32.157	96.9912
4	F_2	1306	1357	40.84	156.4417	996	1027	32.0304	96.229	858	880	27.8121	72.5519

*ν and ω are in cm^{-1}; $\partial P/\partial Q_l$ is in chs units/cm·gm$^{1/2}$; I_l is in cm^{-1}/cm·atm.

Table 4. Integrated Intensities of the Infrared Bands (I_1) and the Quantities $\partial P_1/\partial Q_1$ for Molecules of Type CX_3Y (X, Y = H, D, T)*

No. of the vibration	Symmetry	Observed frequency, ν	Zero-order frequency, ω	$\frac{\partial P_\zeta}{\partial Q_1}$	I_1	Observed frequency, ν	Zero-order frequency, ω	$\frac{\partial P_\zeta}{\partial Q_1}$	I_1	Observed frequency, ν	Zero-order frequency, ω	$\frac{\partial P_\zeta}{\partial Q_1}$	I_1
		CH_3D				CH_3T				CD_3T			
1	A_1	2200	2306	35.1611	38.653	1877	1949	25.8955	20.9656	1865	1937	23.1367	16.7364
3a	A_1	2945	3146	—32.1033	32.2224	2952	3146	—32.0199	32.0552	2165	2262	—25.7635	20.7524
4a	A_1	1300	1352	—41.6604	54.2632	1296	1346	—42.7075	57.0252	990	1018	—32.4486	32.9193
				$\frac{\partial P_\eta}{\partial Q_1}$				$\frac{\partial P_\eta}{\partial Q_1}$				$\frac{\partial P_\eta}{\partial Q_1}$	
2	E	1471	1512	—17.1148	18.316	1463	1503	—20.0281	25.0823	1066	1086	—13.8862	12.0574
3b	E	3021	3154	61.3244	235.1554	3024	3153	61.2286	234.4213	2260	2333	41.3153	106.7358
4b	E	1155	1197	33.4658	70.031	1088	1124	30.4056	57.809	929	956	27.2082	46.2901
		CD_3H		$\frac{\partial P_\zeta}{\partial Q_1}$		CT_3H		$\frac{\partial P_\zeta}{\partial Q_1}$		CT_3D		$\frac{\partial P_\zeta}{\partial Q_1}$	
1	A_1	2142	2251	—18.8147	11.0676	1796	1862	—13.7186	5.8841	1786	1853	—10.7806	3.6337
3a	A_1	2993	3151	53.3643	89.0349	2983	3150	53.1157	88.2072	2230	2313	37.6374	44.2892
4a	A_1	1003	1035	—31.5652	31.1513	876	899	—27.6892	23.9706	868	890	—27.9808	24.4782
				$\frac{\partial P_\eta}{\partial Q_1}$				$\frac{\partial P_\eta}{\partial Q_1}$				$\frac{\partial P_\eta}{\partial Q_1}$	
2	E	1291	1327	—26.9379	45.3749	1236	1265	—21.2094	28.1284	984	1002	—22.8714	32.7095
3b	E	2263	2333	41.5747	108.0803	1939	1991	32.0247	64.1296	1939	1991	32.1356	64.5745
4b	E	1036	1063	23.9946	36.0011	875	894	27.2959	46.589	873	893	19.2666	23.2113

Table 5. Integrated Intensities of the Infrared Bands (I_1) and the Quantities $\partial P_1/\partial Q_1$ for the Molecules CH_2D_2, CH_2T_2, and CD_2T_2*

No. of the vibration	Symmetry	CH_2D_2 Observed frequency, ν	CH_2D_2 Zero-order frequency, ω	$\frac{\partial P}{\partial Q_1}$	I_1	CH_2T_2 Observed frequency, ν	CH_2T_2 Zero-order frequency, ω	$\frac{\partial P_\zeta}{\partial Q_1}$	I_1	CD_2T_2 Observed frequency, ν	CD_2T_2 Zero-order frequency, ω	$\frac{\partial P_\zeta}{\partial Q_1}$	I_1
1	A_1	2202	2279	—28.2533	24.9573	1852	1906	—20.3364	12.9302	1841	1893	—16.7408	8.7622
2a	A_1	1436	1477	24.9882	19.5222	1426	1467	27.8944	24.3272	1049	1071	19.4424	11.8184
3a	A_1	2976	3149	44.4421	61.7515	2976	3149	44.3074	61.3778	2203	2290	32.9792	34.0047
4a	A_1	1033	1061	—27.1195	22.9944	879	899	—22.2416	15.4664	875	895	—23.1896	16.813
				$\frac{\partial P_\xi}{\partial Q_1}$				$\frac{\partial P_\xi}{\partial Q_1}$				$\frac{\partial P_\xi}{\partial Q_1}$	
3b	B_1	3013	3153	61.0126	116.3851	3003	3153	60.8244	115.6682	2251	2333	41.2594	53.2236
4b	B_1	1090	1126	34.0249	36.1953	1005	1038	31.3956	30.8174	903	929	28.9873	26.2708
				$\frac{\partial P_\eta}{\partial Q_1}$				$\frac{\partial P_\eta}{\partial Q_1}$				$\frac{\partial P_\eta}{\partial Q_1}$	
3c	B_2	2234	2333	41.777	54.5674	1932	1991	31.8825	31.7807	1935	1991	32.1018	32.2194
4c	B_2	1234	1278	39.7261	49.3413	1203	1244	39.9261	49.8393	957	984	31.53	31.0818
2b	A_2	1329	1363	0	0	1255	1285	0	0	997	1016	0	0

*For the dimensions of all quantities, see note to Table 3.

Table 6. Fulfillment of the Sum Rules for the Intensities of the Infrared Bands of Isotopically Substituted Methanes

$\frac{1}{6}[\sum I_1(CX_4)+\sum I_1(CY_4)]=\sum I_1(CX_3Y,\ \text{Sym. type}\ A_1)$			Δ
(X = H; Y = D)	128.2452	129.2254	—0.9802
(X = H; Y = T)	113.7072	114.1016	—0.3944
(X = D; Y = T)	71.0523	71.3983	—0.346
$\frac{1}{6}[\sum I_1(CX_4)+\sum I_1(CY_4)]=\sum I_1(CX_2Y_2)$ (Sym. type B_1, B_2)			
(X = H; Y = D)	256.4904	256.4891	0.0013
(X = H; Y = T)	227.4144	228.1056	—0.6912
(X = D; Y = T)	142.1047	142.7956	—0.6909
$\sum I_1(CX_4)+\frac{1}{4}\sum I_1(CY_4)=\sum I_1(CX_3Y)$ (Sym. type A_1, E)			
(X = H; Y = D)	448.7179	448.641	0.0769
(X = D; Y = H)	320.7532	320.7101	0.0431
(X = H; Y = T)	426.9109	427.3586	—0.4477
(X = T; Y = H)	255.3324	256.9089	—1.5765
(X = D; Y = T)	234.964	235.4914	—0.5274
(X = T; Y = D)	191.3501	192.8964	—1.5463
$\frac{1}{3}[\sum I_1]^2(CX)_4+[\sum I_1]^2(CX_2Y_2)=[\sum I_1]^2(CX_3Y)+\frac{1}{3}[\sum I_1]^2(CXY_3)$			
(X = H; Y = D)	236396.1739	235563.7363	832.4376
(X = D; Y = H)	170752.7739	169947.8838	804.8901
(X = H; Y = T)	204726.2661	204636.1006	90.1655
(X = T; Y = H)	126687.3886	126880.6406	—193.252
(X = D; Y = T)	67856.1252	67859.2065	—3.0813
(X = T; Y = D)	55460.6477	55694.4209	—233.7732

Substituting in formulas (1)-(3) the numerical values of the coefficients C_1 and D_1 and of the electro-optical parameters $\partial P/\partial q^{F_2}$ and $\partial P/\partial \alpha^{F_2}$ of methane, we obtain the derivatives of the dipole moments with respect to the normal coordinates of isotopically substituted methanes.

In Tables 3-5 are presented the computed values of $\partial P/\partial Q_1$ and of the integrated intensities I_1 of the molecules under consideration. The high accuracy of the computation of the intensities is confirmed by the good fulfillment of the first-[8] and second-order[9] sum rules for intensities. As follows from Table 6, the difference between the two sides of the equations does not exceed 0.5% of the values of the quantities entering into these formulas.

REFERENCES

1. V. M. Chulanovskii, Uspekhi Fiz. Nauk 68, 147 (1959), Soviet Physics Uspekhi 2, 444 (1959).
2. M. V. Vol'kenshtein, M. A. El'yashevich, and B. I. Stepanov, "Kolebaniya molekul" (Molecular Vibrations), Vol. 2. Gosudarst. Izd. Tekh. i Teoret. Lit., Moscow-Leningrad, 1949.
3. L. M. Sverdlov, Opt. i Spektr. 7, 21 (1959), Optics and Spectroscopy 7, 11 (1959).
4. H. L. Welsh et al., J. Chem. Phys. 19, 340 (1951); Ibid. 20, 1646 (1952).
5. H. H. Kaylor and A. H. Nielsen, J. Chem. Phys. 23, 2139 (1955).
6. L. H. Jones and R. S. McDowell, J. Mol. Spectrosc. 3, 632 (1959).
7. L. S. Mayants, Trudy Fiz. Inst. Akad. Nauk SSSR 5, 63 (1950).
8. J. C. Decius, J. Chem. Phys. 20, 1039 (1952).
9. L. M. Sverdlov, Opt. i Spektr. 8, 253 (1960), Optics and Spectroscopy 8, 129 (1960).

CALCULATION AND INTERPRETATION OF THE VIBRATIONAL SPECTRA OF ISOBUTANE

T. I. Kuznetsova and M. M. Sushchinskii

Received 8 April 1960

The vibration frequencies and form coefficients for the molecules of isobutane and partially deuterated isobutane $DC(CH_3)_3$ have been computed. An interpretation of the observed spectra is given. The effect of variations in the values of a number of force constants and geometrical parameters of the molecule on the vibrational frequencies has been elucidated.

1. Isobutane is the simplest representative of the branched hydrocarbons. Therefore, a detailed study of its spectra is of great interest for the theory of the vibrations of polyatomic molecules. In addition, a calculation of the vibrational frequencies of isobutane has been carried out in only one work.[1] In the other works devoted to isobutane an experimental study of its vibrational spectra has been made.[2-8] In these works, and also in a review[9] and refs. 10 and 11, an interpretation of the vibrational spectra of isobutane is given, but since this interpretation does not rest on calculation of the vibrational frequencies, it cannot be considered as final.

In view of the fact that, in ref. 1, the calculation of the isobutane frequencies was carried out by a rather crude method and the results of the calculation were not compared with the infrared spectral data, we considered it necessary to carry out a more rigorous calculation of the vibrational frequencies, and also of the form coefficients of this molecule. There has recently appeared a work[8] in which new data on the Raman and infrared spectra of isobutane $HC(CH_3)_3$ and partially deuterated isobutane $DC(CH_3)_3$ are reported. The possibility of using these new data in a theoretical examination imparts additional interest to the isobutane calculation.

Because of the fact that the isobutane molecule is relatively simple and possesses high symmetry, it is also a suitable object for the elucidation of the effect of variations in the values of certain force constants and geometrical parameters on the vibrational spectra.

2. In the calculation, an isobutane model with symmetry C_{3v} was taken. Partially deuterated isobutane $DC(CH_3)_3$ also possesses the same symmetry. According to this model, the molecule possesses vibrations of the the following symmetry types.

$$\Gamma = 8A_1 + 4A_2 + 12E \qquad (1)$$

The vibrations of types A_1 and E are active in both Raman and infrared spectra, the Raman lines of type A_1 vibrations being polarized, those of type E depolarized. Type A_2 vibrations are inactive.

The secular equations were set up according to the well-known procedure of El'yashevich and Stepanov,[1] the coordinates corresponding to rotation of the CH_3 groups, as usual, not being taken into account. The solution of the secular equations was carried out by the method of progressive diagonalization with the help of an "Arrow" electronic computer.[12] The form coefficients were computed according to Mayants's method.[13]* The normalization of the form coefficients was carried out with the condition that any vibration should have a unique energy (see ref. 1).

*In the computation of the form coefficients, we made use of a program set up by A. M. Bogomolov.

In order to simplify the procedure for setting up the secular equations, we did not carry out an elimination of the redundant coordinates. In the calculation, zero values of the frequencies corresponded to these redundant coordinates. The form coefficients were computed with respect to coordinates connected with the ordinary "approximate symmetry coordinates" by simple linear relationships. For convenience of discussion in the tables presented below, the form coefficients are given, as usual, with respect to the approximate symmetry coordinates (see ref. 1), transformed in accordance with the complete symmetry of the molecule.

3. A comparison of the experimentally observed frequency values in the Raman and infrared spectra of isobutane with the computed frequencies is presented in

Table 1. Interpretation of the Vibrational Spectrum of Isobutane

Coordinate	$HC(CH_3)_3$ Experimental Ram. $\Delta\nu$ (cm^{-1})	Ram. I	Ram. ρ	$HC(CH_3)_3$ Experimental IR $\Delta\nu$ (cm^{-1})	IR I	$HC(CH_3)_3$ Calculated $\Delta\nu$ (cm^{-1})	$DC(CH_3)_3$ Experimental Ram. $\Delta\nu$ (cm^{-1})	Ram. I	Ram. ρ	$DC(CH_3)_3$ Experimental IR $\Delta\nu$ (cm^{-1})	IR I	$DC(CH_3)_3$ Calculated $\Delta\nu$ (cm^{-1})
Vibrations of type A_1												
γ^+_{tert}	433	3	0.35	426	m	395	426	3	0.23	432	m	391
Q_{tert}	799	76	0.24	797	s	789	796	70	0.17	793	s	785
β'_{CH_3}	1184	8	—	1177	m	1147	1166	10	p	—	—	1132
$\alpha^+_{CH_3}$	1373	3	—	1394	m	1381	1358	2	—	1367	m	1381
α'_{CH_3}	1468	16	—	1477	s	1469	1463	30	0.8	1477	s	1466
$q^+_{CH_3}$	2907	103	0.18	2904	s	2898	2903	108	0.25	2904	s	2899
q_{CH}	2880	—	—	2880	m	2952	2146	50	0.41	2152	s	2201
q'_{CH_3}	2958	116	d	2962	s	2981	2956	116	d	2962	s	2976
Vibrations of type E												
γ'_{tert}	367	8	d	—	—	354	370	9	d	—	—	353
β'_{tert}	917	3	d	918	s	925	1065	6	d	—	—	1034
β^2_{tert}	966	16	d	—	m	956	944	18	d	952	s	937
Q'_{tert}	1169	15	d	1166	—	1148	1229	25	d	1233	s	1257
β'_{CH}	1327	13	d	1330	m	1333	813	5	d	812	m	821
$\alpha^+_{CH_3}$	1373	3	—	1371	s	1380	1380	6	d	1390	s	1380
$\alpha^2_{CH_3}$	1450	35	d	1475	s	1460	1450	28	d	1475	s	1459
α'_{CH_3}	1468	16	—	1477	s	1475	1463	30	0.8	1477	s	1473
$q^+_{CH_3}$	2889	87	0.38	2894	s	2899	2882	42	0.25	2894	s	2899
q'_{CH_3}	2958	116	d	2962	s	2975	2956	116	d	2962	s	2975
$q^2_{CH_3}$	2958	116	d	2962	s	2977	2956	116	d	2962	s	2977
Vibrations of type A_2												
	—	—	—	—	—	965	—	—	—	—	—	965
	—	—	—	—	—	1473	—	—	—	—	—	1473
	—	—	—	—	—	2965	—	—	—	—	—	2965

Note: Ram. – Raman spectrum (d – depolarized line); IR – infrared absorption spectrum (symbols for band intensities: s – strong; m – medium intensity).

Table 1. In the calculations, we adopted the set of force constants constructed by Stepanov on the basis of the calculation of ethane and propane.[1] It can be seen that the agreement between the experimental and computed frequency values is satisfactory and the matching of the two sets of values is entirely unequivocal (except for the valence vibrations of the CH_3 groups, a discussion of which will be carried out in a subsequent section). Some weak lines in the spectra of heavy isobutane are apparently due to the presence of admixtures of other deuterio derivatives.

In Tables 2 and 3 are presented the form coefficients calculated with the use of the same set of force constants as was used for the frequencies (Table 1). Here we do not give the data for those frequencies whose assignment to definite vibrational coordinates is self-evident, and the computation of the form coefficients gives nothing new for them. The coordinates q and α, which describe the internal vibrations of the CH_3 groups, belong to this class. Computation of the form coefficients only confirms that these coordinates are weakly coupled with the remaining coordinates.

Table 2. Form Coefficients of the Vibrations of Type A_1

Coordinate	$HC(CH_3)_3$			$DC(CH_3)_3$		
	Frequency (cm^{-1})			Frequency (cm^{-1})		
	395	789	1147	391	785	1132
β'_{CH_3}	0.14	—0.28	0.95	0.13	—0.26	0.95
Q^+	0.02	0.28	0.14	0.02	0.28	0.12
γ^+	0.26	—0.08	—0.28	0.26	—0.08	—0.26

As can be seen from Table 2, the form coefficients in the case of the totally symmetric vibrations give quite a clear representation of the corresponding vibrations. A certain difficulty arises only for the frequency 789 cm^{-1} (or 785 cm^{-1} in the case of heavy isobutane). The coordinates Q^+ and β'_{CH_3} are involved almost equally in the vibration with this frequency. One may, however, ask the question of which frequency is most strongly coupled with the coordinate Q^+. For the answer to this question, it is sufficient to compare the numbers in the corresponding row. From such a comparison, one concludes that the totally symmetric skeletal vibrations (coordinate Q^+) are most directly characterized by the 789 cm^{-1} frequency.

Table 3. Form Coefficients of the Vibrations of Type E

Coordinate	$HC(CH_3)_3$					$DC(CH_3)_3$				
	Frequency (cm^{-1})					Frequency (cm^{-1})				
	354	925	956	1148	1333	353	821	937	1034	1257
$\beta^2_{CH_3}$	—0.07	—0.46	—0.56	—0.56	—0.30	—0.07	—0.06	—0.68	—0.45	—0.54
β'_{CH_3}	0.01	—0.68	—0.59	0.17	—0.31	0.01	—0.48	—0.20	0.75	—0.30
Q'	0.01	—0.16	—0.15	0.27	0.23	0.01	0.03	—0.23	0.08	0.34
β'_{CH}	—0.01	0.34	—0.26	0.52	—1.11	—0.02	0.73	0.00	0.38	—0.57
γ'	—0.32	—0.02	0.05	0.26	0.23	—0.31	—0.01	0.01	0.14	0.32

The interpretation of the degenerate vibrations presents a more difficult problem. As can be seen from Table 3, the form coefficients for a series of frequencies of type E have closely-grouped values, while these coefficients change substantially on going from light to heavy isobutane. Therefore, only the interpretation of the frequency 354 cm^{-1} as a deformation vibration frequency of the skeleton is here entirely unequivocal. For the remaining four frequencies, the coordinates β (of different types) and Q' simultaneously have substantial significance.* The establishment of the correspondence

*We note that the discussion existing in refs. 1 and 9-11 concerning the assignment of one or another frequency to the coordinate Q' appears, in the light of the foregoing, to be to a considerable degree fruitless, although a certain preference may be granted to the frequency 1148 cm^{-1}.

of the frequencies of light and heavy isobutane also proves to be provisional in some cases, since the form of the vibrations for these two molecules is substantially different.

It follows from the examination which we have conducted that, in the case of isobutane, there exists a group of vibrational coordinates which are closely coupled with one another and weakly coupled with the remaining coordinates. This group of coordinates describes the tertiary carbon atom as a characteristic structural element of the molecule. The following may be designated as coordinates which are characteristic for the tertiary carbon atom:

$$\text{totally symmetric} - Q_{tert}(Q^+,\ \beta');\ \gamma^+_{tert};$$

$$\text{degenerate} - \beta^2_{tert}(\beta^2_{CH_3},\ \beta'_{CH_3},\ \beta'_{CH});$$

$$\beta'_{tert}(\beta^2_{CH_3},\ \beta'_{CH_3},\ \beta'_{CH});\ Q'_{tert}(Q',\ \beta^2_{CH_3},\ \beta'_{CH});\ \beta'_{CH};\ \gamma_{tert}$$

(these coordinates are indicated in Table 1).

Certain of the frequencies corresponding to the indicated coordinates were noted by Stepanov[1] as characteristic frequencies for simple branching. The examination conducted in ref. 14 has shown that the lines in the Raman spectra with frequencies in the region 910, 950, 1145, 1170, and 1340 cm^{-1} are characteristic lines of the tertiary carbon atom.

4. In calculating the vibration frequencies of polyatomic molecules, there always remains a certain indeterminacy associated with the fact that a set of force constants is used which has been set up for simpler molecules. For a particular molecule, this set may, generally speaking, change in some way, which introduces an unknown error into the results of the calculation. This also applies to the geometrical parameters: The lengths of the valence bonds and the angles between them change, generally speaking, on going over from one molecule to another, which it is not always possible to allow for in the calculation of the vibration frequencies.

The isobutane molecule appeared to us to be a suitable object for the elucidation of the extent to which variations in the force constants used in the calculation are significant, and also for establishing the magnitude of certain constants which are specific for the tertiary carbon atom. We have carried out the calculations in the following variants.

(1) The constant for the interaction of C—C bonds with each other (H) = 0.1.

(2) The constant for the interaction of C—C bonds and C—H bonds with a common C atom (H′) = 0.1.

(3) The constant for the interaction of the angles β and γ with a common vertex and a common side (w) = −0.1.

(4) The constant for the interaction of the angles β with a common vertex and a common C—H bond (w′) = −0.1.

(5) The constant for the interaction of adjacent angles γ (l_γ) = −0.1.

(6) The constant for the interaction of the angles β with a common C—C bond and vertices on different C atoms (the angles lie in one plane) (m) = 0.

(7) The constant for the interaction of the angles β

Table 4. Results of Variation of the Force Constants and Geometrical Parameters

ν_{exp} (cm^{-1})	$\nu_{exp} - \nu_0$ (cm^{-1})		$\nu - \nu_0$ in the different variants of the calculation (cm^{-1})																	
			1		2		3		4		5		6		7		8	9	10	
	H	D	H	D	H	D	H	D	H	D	H	D	H	D	H	D	H	H	H	D
A_1																				
433	38	35	0	0	0	0	33	33	1	−18	−19	−18	8	9	5	5	1	2	14	15
799	10	11	1	1	1	1	2	2	1	−1	−1	−1	3	3	3	3	1	1	1	1
1184	37	34	2	1	0	1	14	12	−22	−6	−6	−6	−22	−21	−24	−23	4	0	8	6
1373	−8	−23	1	1	−1	−1	0	0	0	0	0	0	0	0	3	2	0	0	0	0
E																				
367	13	17	0	0	0	0	−2	0	0	0	15	14	1	0	1	1	4	1	13	14
917	−8	−8	−2	0	0	0	−1	0	1	25	0	0	3	32	3	29	1	0	−1	0
966	10	7	−1	−2	0	0	−2	0	6	5	0	0	25	3	24	0	0	1	−2	0
1169	21	31	−3	−1	0	0	12	5	13	8	2	1	−6	−26	−14	−26	2	−1	14	6
1327	−6	−28	−3	−5	0	0	−18	−15	40	12	2	4	−39	−16	−52	−17	2	−1	−16	−11
1373	−7	0	0	0	0	−1	0	0	4	0	0	0	14	4	37	1	0	0	0	0

with a common C—C bond and vertices on different C atoms (the angles do not lie in one plane)(n) = 0.1.

Furthermore, calculations were carried out with altered values for the C—C bond length (variant 8) and CCC valence angle (variant 9). Here the values obtained for isobutane in ref. 15 by the method of microwave spectroscopy were taken for the indicated quantities, namely: C—C bond length, 1.525 A; CCC angle, 111.2°.

In Table 4 are presented the results of the calculations of the frequency values in the variants listed. Here ν_0 is the frequency value calculated in the "zeroth" variant, i.e., with the basic set of force constants (these values are presented in Table 1). The symbols H and D indicate light and heavy isobutane respectively. In the column $\nu_{exp.}$ are presented the experimental frequency values for light isobutane.

As can be seen from Table 4, fairly large variations in the bond interactions (variants 1 and 2) and in the geometrical parameters (variants 8 and 9) do not lead to substantial change in the frequency values. Thus the indicated factors may apparently be left out of account in the calculation of the frequencies. Change in the angle interactions is more significant. Here the discrepancy between the experimental and calculated values may be reduced by simultaneously varying the values of the constants w and l_γ (variants 3 and 5), taking, for example, w = −0.10, l_γ = −0.1. The frequency values obtained with these values of the constants are also presented in Table 4 (variant 10). In this variant, a certain improvement in the agreement between the experimental and calculated frequency values is achieved. However, the values found for the constants must still be verified on other molecules.

5. The frequencies lying in the region of the CH valence vibrations require special consideration. According to the calculation (see Table 1), one might expect here the appearance of three frequencies: ~2899, 2975-2981 (three coalescing bands), and 2952 (in heavy isobutane, 2201 cm^{-1}). Actually, at least 5 or 6 frequencies are observed in this region (see Table 5). The excess of the number of experimentally observed frequencies over that theoretically expected in the region of the CH valence vibrations is not a specific peculiarity of the isobutane spectrum, inasmuch as it is observed in the spectra of a large number of hydrocarbons. An explanation of this phenomenon may be found by taking account of the following two factors: (1) interaction of the C—H bonds on different C atoms leads to displacement and splitting of the frequencies in this region; (2) resonance interaction of the frequencies of the CH valence vibrations with overtones of the α deformation frequencies leads to splitting of the frequencies and change in their intensities.

Table 5. Frequencies Lying in the Region of the CH Valence Vibrations

$HC(CH_3)_3$					$DC(CH_3)_3$			
Experiment*			Calculation		Experiment*			Calculation
$\Delta\nu$ (cm^{-1})	I	ρ	$\Delta\nu$ (cm^{-1})	Interpretation	$\Delta\nu$ (cm^{-1})	I	ρ	$\Delta\nu$ (cm^{-1})
2869	167	0.13	—	A_1, CH_3 (sym.)+overtone	2864	87	0.23	—
2880	—	—	2966	A_1, CH	2146	50	0.41	2200
2889	87	0.38	2886	E, CH_3 (sym.)	2882	42	0.25	2886
2907	103	0.18	2900	A_1, CH_3 (sym.)+overtone	2903	108	0.25	2915
2933	94	0.27	—	TOH E, CH_3 (degen.) + overtone	2927	80	0.43	—
—	—	—	—	—	2938	74	0.57	—
2958	116	d	2992	A_1, CH_3 (degen.)	2956	116	d	2988
2958	116	d	2973	E, CH_3 (degen.)	2956	116	d	2972
2958	116	d	2983	E, CH_3 (degen.) + overtone	2956	116	d	2987

*According to the data of ref. 8. For symbols, see note to Table 1.

In refs. 14 and 16, the interaction constants of CH bonds situated on different C atoms were found. Using these values, we have carried out the corresponding calculations, the results of which are presented in Table 5. It is easy to see that, as a result of the interaction of the C—H bonds, the value of the 2899 cm^{-1} type E frequency was lowered to 2886 cm^{-1}, while the remaining frequencies changed relatively slightly.

In the interpretation of the spectrum of isobutane in the region under consideration, it is desirable first of all to find the band corresponding to the vibrations of the isolated C—H bond. The marked decrease in the intensity of the 2864 and 2882 cm^{-1} bands of heavy isobutane in comparison with the 2869 and 2889 cm^{-1} lines of light isobutane attracts the attention. At the same time, no band has disappeared from the spectrum. This compels us to assume that the band corresponding to vibrations of the isolated C—H bond (which goes over into the 2146 cm^{-1} band of heavy isobutane) does not coincide with the 2869 or 2889 cm^{-1} bands of light isobutane, but is characterized by an intermediate frequency value (~2880 cm^{-1}). We note that in the infrared spectrum of isobutane there is a band with the frequency 2880 cm^{-1}, while there is no such band in the spectrum of deuterated isobutane (see ref. 8).

The remaining bands may be interpreted in the following way. The totally symmetric vibration with a frequency ~2900 cm^{-1} gives, as a result of resonance interaction with the overtone 1450 · 2, the bands 2907 and 2869 cm^{-1} which are observed in the spectrum. Analogously, the vibration with a frequency around 2990 cm^{-1}, interacting with the overtone 1468 · 2, gives the bands 2933 and 2958 cm^{-1}. The interpretation of the 2889 cm^{-1} band was given above.

The investigation presented here enables us to interpret all the bands in the isobutane spectra. However, this interpretation must by all means be considered as preliminary, since no calculation of the resonance interaction has been carried out.

REFERENCES

1. M. V. Vol'kenshtein, M. A. El'yashevich, and B. I. Stepanov, "Kolebaniya molekul" (Molecular Vibra-

tions). Gosudarst. Tekh. i Teoret. Izd., Moscow-Leningrad, 1949.
2. K. W. F. Kohlrausch, "Spektry kombinatsionnogo rasseyaniya" Izd. Inostrannoi Lit., Moscow, 1952. "Ramanspektren." Edwards, Ann Arbor, Michigan.
3. R. S. Rasmussen, J. Chem. Phys. **16**, 712 (1948).
4. F. E. Condon, H. L. McMurry, and V. Thornton, J. Chem. Phys. **19**, 1010 (1951).
5. S. Bhagavantam, Ind. J. Phys. **6**, 695 (1931).
6. K. W. F. Kohlrausch and F. Köppl, Z. phys. Chem. **26**, 209 (1934).
7. R. Ananthakrishnan, Proc. Indian Acad. Sci. **A3**, 527 (1936).
8. J. C Evans and H. J. Bernstein, Can. J. Chem. **34**, 1037 (1956).
9. N. Sheppard and D. M. Simpson, Quart. Rev. **7**, 19 (1953).
10. G. B. B. M. Sutherland and D. M. Simpson, J. Chem. Phys. **15**, 153 (1947).
11. D. M. Simpson and G. B. B. M. Sutherland, Proc. Roy. Soc. **A199**, 169 (1949).
12. R. I. Podlovchenko and M. M. Sushchinskii, Opt. i Spektr. **2**, 49 (1957).
13. L. S. Mayants, Trudy Fiz. Inst. Akad. Nauk SSSR **5**, 63 (1950).
14. M. M. Sushchinskii, Dokt. diss. (Dissertation), Fiz. Inst., Akad. Nauk SSSR, Moscow, 1957.
15. D. R. Lide, IV Meeting on Molecular Spectroscopy, Bologna, 1959.
16. M. M. Sushchinskii, Izvest. Akad. Nauk SSSR, Ser. Fiz. **22**, 1073 (1958).

ON THE TEMPERATURE DEPENDENCE OF THE INTENSITIES OF VIBRATIONAL ABSORPTION BANDS IN GASES

M. P. Lisitsa and V. L. Strizhevskii

Received 30 March 1960

Certain theoretical questions relating to the temperature dependence of the integrated intensities of vibrational absorption bands in gases are considered. Formulas have been obtained describing the dependence of the integrated absorption on temperature which differ somewhat from those generally accepted. A comparison of theory with experiment has been carried out and certain experimental aspects of the question are discussed.

INTRODUCTION

One may point out the following factors whose influence makes itself felt on the temperature dependence of the absorption in vibrational bands of gaseous substances: (1) the Boltzmann factor;* (2) radiation (spontaneous and induced); (3) collisions; (4) anharmonicity of the vibrations; (5) Doppler effect; and so on.

*Strictly speaking, by "Boltzmann factor" one should understand the general formula of statistical theory which completely determines the temperature dependence. The specific appearance of this formula depends on the corresponding quantum transition and the choice of a model to describe the motion of the particles. Taking account of the terminology which has become established in the literature, we shall, in the present work, understand by "Boltzmann factor" (in the narrower sense) the law for the temperature dependence of absorption which arises from the general formula, and is accurate for an ensemble of nonradiating harmonic oscillators which are subject to no external influences (except for processes of absorption of a light quantum).

Comparison of the experimental data[1-3] (to be sure, they are not numerous) with the results of statistical theory,[4] which principally takes account of the Boltzmann factor, shows that in some of the vibrational bands the absorption intensity increases more sharply with an increase in temperature[2] than follows from the theory. Such deviations testify to the necessity of taking account of other factors as well. Under various experimental conditions and for various molecules, the influence of the latter will, of course, not be uniform. Thus, for example, according to the estimates of Smirnov and Bazhulin,[2] the anharmonicity of the vibrations in the case of diatomic molecules gives a negligibly small correction. It is possible that for more complex molecules its role may become substantial. By the experiments of Stepanov and Khvashchevskaya,[5] a marked influence of spontaneous radiation on the general intensity of an absorption band was established only when working with low-temperature light sources. As for induced radiation, it may, in our opinion, prove to be significant. At very low pressures, there is no reason to take account of molecular collisions and the like. Skillful choice of the conditions of experimentation and of a method of theoretical investigation makes it possible to exclude the influence of some factors and to enhance the action of other, thus allowing us to investigate closely the character of the temperature dependence.

Aside from the Boltzmann factor, the effect of which is known from statistical theory,[4] we have considered in the present work the influence of radiation and of the anharmonicity of intramolecular vibrations on the absorption band intensity.

THEORY

As is well known, small intramolecular vibrations may be described with the help of normal coordinates.[4,6] In the harmonic approximation, the wave functions $u_{v_i}(Q)$ which correspond to vibrational motion consist of products of the functions of linear harmonic oscillators (Q and v_i denote respectively the set of normal coordinates and the set of quantum numbers of the oscillators corresponding to the normal vibrations of the molecules). Those components V′ of the potential energy of vibrational motion whose order with respect to Q is higher than second make up the mechanical anharmonicity[6] and are considered as a small perturbation, allowance for which leads to the following expressions for the wave functions:

$$\psi_{v_i}(Q) = u_{v_i}(Q) + \sum_{v_s} a_{v_i v_s} u_{v_s}, \qquad (1)$$

where the $a_{v_i v_s}$ are certain constants. If we use the

known formulas of perturbation theory,[7] the latter may be linked with the mechanical anharmonicity constants and the differences in energy levels in the unperturbed problem.

The probabilities of the phototransitions $\psi_{v_j} \rightarrow \psi_{v_i}$, in which light quanta are absorbed or radiated, are determined by the squares of the matrix elements

$$P_{v_j v_i} = \int \psi_{v_j}(Q)\, P(Q)\, \psi_{v_i}\, dQ, \qquad (2)$$

where P(Q) is the operator for the dipole moment of the molecule, averaged over the electronic coordinates (the state of the electronic motion is assumed to be the ground state). This may be expanded as a power series in Q

$$P(Q) = \sum_l P_l Q^l \qquad (3)$$

and, neglecting terms quadratic in a, (2) may be written in the form

$$P_{v_j v_i} = \sum_l P_l\, (v_j | Q^l | v_i) + \sum_l P_l \sum_{v_s} [a_{v_j v_s}(v_s | Q^l | v_i) + a_{v_i v_s}\, (v_j | Q^l | v_s)]. \qquad (4)$$

Here

$$(v_j | Q^l | v_i) = \int u_{v_i} Q^l\, u_{v_i}\, dQ. \qquad (5)$$

For a given initial state v_i, the absorption of a photon of a given energy is associated with a transition to a fully determined state v_j which depends on v_i. If the latter is an excited state, then, in addition to the absorption of a light quantum, radiation of a quantum is also possible. With an increase in i, the probability of attaining an excited state increases. The ratio of the probabilities of the two processes is established by the quantum theory of radiation. The probability of radiation of a quantum with energy $h\nu$ within a single angle $d\Omega$ is determined, in the dipole approximation, by the following expression:[8]

$$w d\Omega = \frac{e^2 \nu}{\hbar m^2 c^3} |(P_e)_{ab}|^2 (n+1)\, d\Omega = (w_1 + w_2)\, d\Omega, \qquad (6)$$

where $(P_e)_{ab}$ is the matrix element, between the initial and final states of the system, of the projection of its momentum on the direction of polarization of the radiated photon, and n is the number of photons of a given energy, polarization, and direction of propagation existing prior to radiation. The quantities w_1 and w_2 correspond to the components n and 1 of the factor n + 1 (the induced and spontaneous parts of the radiation, respectively). For the probability of absorption, w_3, an expression analogous to w_1 holds.

Each act of absorption of a photon leads to a decrease in the intensity of the light, while an act of emission increases it. The effect resulting from a decrease in the intensity of the light beam, as compared with an increase in the thickness of the layer of substance penetrated, must be different. In view of this, the part of the radiation which is described by the component w_2 in (6) and corresponds to spontaneous radiation should not be counted, if the measurements are carried out, as is usual, in terms of the increase over the background, and the base line is plotted not only at the base of the absorption band but also at its maximum. Therefore, if there are states into which a transition is possible with the radiation or absorption of a light quantum of a given frequency, the corresponding expressions for w_1 and w_3 differ only in the values of the matrix elements $(P_e)_{ab}$ which determine the transitions to which reference has been made.

In our symbols, the probabilities of the absorption of a photon with a fixed direction of propagation and of its emission in the same direction differ only in the matrix elements $P^n_{v_j v_i}$ and $P^u_{v_n v_i}$, where v_j and v_n, which depend on v_i, are the final states for transitions involving absorption and radiation respectively. Thus, allowance for radiation shows that calculation of the factor determining the temperature dependence of the integrated intensity of an absorption band, in the case of a gas in thermal equilibrium, must be carried out with the help of the formula*

$$f(T) = \sum_{v_i} (w'^n_{v_j v_i} - w'^u_{v_n v_i}) \frac{N_{v_i}}{N} = \frac{\sum_{v_i} (w'^n_{v_j v_i} - w'^u_{v_n v_i})\, e^{-\frac{E_{v_i}}{kT}}}{\sum_{v_i} e^{-\frac{E_{v_i}}{kT}}} \qquad (7)$$

Here we have used

$$\frac{N_{v_i}}{N} = \frac{e^{-\frac{E_{v_i}}{kT}}}{\sum_{v_i'} e^{-\frac{E_{v_i'}}{kT}}}$$

for the relative number of molecules in the state with energy E_{v_i}. The quantities $w'^n_{v_j v_i}$ and $w'^u_{v_n v_i}$ differ from $(P^n_{v_j v_i})^2$ and $(P^u_{v_n v_i})^2$ only by factors independent of v.

Since in the general case the expression (6) leads to very awkward formulas, we shall consider below only certain special cases.

1. There is no mechanical or electro-optical anharmonicity. In this case (3) contains only terms no higher than the first degree in Q, and all $a_{v_j v_i} = 0$. Transitions corresponding to combination frequencies and overtones are forbidden, and for the fundamental frequencies we may set $w'^n_{v+1,\,v} = v + 1$ and $w'^u_{v-1,\,v} = v$, so that

$$f(T) = \frac{\sum_{v=0}^{\infty} [(v+1) - v]\, e^{-\beta v}}{\sum_{v=0}^{\infty} e^{-\beta v}} = 1, \quad \left(\beta = \frac{h\nu}{kT}\right). \qquad (8)$$

Thus, despite the conclusions of ref. 4, statistical theory which takes account of radiation does not lead to any temperature dependence of the intensities of bands corresponding to the fundamental frequencies of noninteracting molecules.*

2. The molecule possesses electro-optical anharmonicity, while mechanical anharmonicity does not play a substantial role. In this case, as before, all $a_{v_j v_i} = 0$, but in the expansion (3) there are terms of higher than first order in Q. Consequently, transitions involving excitation of combination frequencies and overtones are now allowed. We shall pay attention, in (3), to the lowest-order terms leading to the appearance of a given band. Then the previous result (8) is obtained for the fundamental frequencies.

Let us consider an overtone 2ν. Setting $w'^n_{v+2,\,v} = (v+1)(v+2)$ and $w'^u_{v-2,\,v} = v(v-1)$ for this case, we find, with the help of (7),

*Having in mind only the integrated intensity, but not the change in absorption coefficient with frequency, we ignore the insignificant change due to mechanical anharmonicity in the energies of the absorbed and emitted photons during transitions from different initial levels v_i.

*Stepanov and Gribkovskii[15] have arrived at this conclusion by another route.

$$f^{2\nu}(T)=2\frac{1+e^{-\frac{h\nu}{kT}}}{1-e^{-\frac{h\nu}{kT}}} \qquad (9)$$

In an analogous way, we have for the combination frequencies $\nu_1+\nu_2$ and $\nu_1-\nu_2$

$$f^{\nu_1+\nu_2}(T)=\frac{\sum_{v_1v_2}[(v_1+1)(v_2+1)-v_1v_2]\,e^{-(\beta_1v_1+\beta_2v_2)}}{\sum_{v_1v_2}e^{-(\beta_1v_1+\beta_2v_2)}}$$

$$=\frac{1-e^{-\frac{h(\nu_1+\nu_2)}{kT}}}{\left(1-e^{-\frac{h\nu_1}{kT}}\right)\left(1-e^{-\frac{h\nu_2}{kT}}\right)}; \qquad (10)$$

$$f^{\nu_1-\nu_2}(T)=\frac{\sum_{v_1v_2}[(v_1+1)v_2-v_1(v_2+1)]\,e^{-(\beta_1v_1+\beta_2v_2)}}{\sum_{v_1v_2}e^{-(\beta_1v_1+\beta_2v_2)}}$$

$$=\frac{e^{-\frac{h\nu_2}{kT}}-e^{-\frac{h\nu_1}{kT}}}{\left(1-e^{-\frac{h\nu_1}{kT}}\right)\left(1-e^{-\frac{h\nu_2}{kT}}\right)}; \qquad \left(\beta=\frac{h\nu_i}{kT},\ i=1,2\right). \qquad (11)$$

respectively.

In just the same way, it is not difficult to examine also the cases of bands corresponding to higher-order frequencies. Suppose that, as the result of a phototransition with the emission of a photon, the quantum numbers of the oscillators with the frequencies ν_ρ increase by s_ρ units ($\rho=1,2,\ldots$) while the quantum numbers of the oscillators with the frequencies ν_π decrease by s_π units. With the help of the functions

$$\left.\begin{aligned}K_{v_\rho}(s_\rho)&=(v_\rho+1)(v_\rho+2)\ldots(v_\rho+s_\rho),\ K_{v_\rho}(0)=1;\\ L_{v_\pi}(s_\pi)&=v_\pi(v_\pi-1)\ldots(v_\pi-s_\pi+1),\ L_{v_\pi}(0)=1\end{aligned}\right\} \qquad (12)$$

the temperature factor may be represented in the form

$$f(T)=\frac{\sum_v\left\{\prod_\rho K_{v_\rho}(s_\rho)\prod_\pi L_{v_\pi}(s_\pi)-\prod_\rho L_{v_\rho}(s_\rho)\prod_\pi K_{v_\pi}(s_\pi)\right\}e^{-\sum_\alpha\beta_\alpha v_\alpha}}{\sum_v e^{-\sum_\alpha\beta_\alpha v_\alpha}}$$

$$\left(\beta_\alpha=\frac{h\nu_\alpha}{kT}\right). \qquad (13)$$

The evaluation of the sums appearing in (13) may be carried out without difficulty if we use the relationships

$$Z_{1,2,\ldots}(n_1,n_2,\ldots)$$

$$=\frac{\sum_{v_1v_2\ldots}v_1^{n_1}v_2^{n_2}\ldots e^{-(\beta_1v_1+\beta_2v_2+\ldots)}}{\sum_{v_1v_2}e^{-(\beta_1v_1+\beta_2v_2+\ldots)}}=Z_1(n_1)Z_2(n_2)\ldots; \qquad (14)$$

$$Z_i(n)=\frac{\sum_{v=0}^{\infty}v^ne^{-\beta_iv}}{\sum_{v=0}^{\infty}e^{-\beta_iv}}=(1-e^{-\beta_i})(-1)^n\frac{\partial^n}{\partial\beta^n}\frac{1}{1-e^{-\beta_i}};$$

$$(i=1,2,\ldots). \qquad (15)$$

With the help of (12)-(15), it is not difficult to obtain the values of f(T) for any concrete case. The formulas (8)-(11) are special cases of (13).

The influence of temperature in cases where mechanical anharmonicity does not play a substantial role has been considered in ref. 4. Inasmuch as the temperature effect is different in the sense indicated above, which was not taken into account in ref. 4, the real dependence on T proves actually to be weaker. As for vibrational emission spectra and Raman spectra, the connection of the intensities of these spectra with temperature, within the framework of the assumptions which we have introduced, must be determined by the relationships previously obtained.[4,9] Thus, contrary to the generally accepted belief, the formulas describing the temperature dependence for the cases of absorption, emission, and Raman scattering prove to be different. Considering the different nature of these spectra, one must admit that the conclusion reached is entirely natural.

In those cases when the effect of mechanical anharmonicity may not be ignored, formulas (9)-(11) are at best only qualitatively correct.

3. Both electro-optical and mechanical anharmonicity exist. As was already noted above, the formulas derived from (7) are very awkward for an arbitrary case. Moreover, they contain unknown parameters—the mechanical anharmonicity constants—the number of which may be very large.[6] If we consider that the electro-optical anharmonicity constants are also unknown in the overwhelming majority of cases, it becomes understandable that it is not possible at present to obtain general formulas suitable for practical application. In our opinion, the problem must be solved separately for each specific case.

As an illustration, let us consider one example. Suppose we are dealing with a polar molecule, so that the term of zeroth order in Q in expansion (3) is different from zero. In many cases, the quantities $P_{1q}(v_q+1\,|\,Q_q\,|\,v_q)$ which determine the intensities of the fundamental vibrations (for example, the q-th) satisfy the inequalities*

*Thus, in the case of the very intense ν_3 vibration of the CCl_4 molecule,[10] the quantity $P_{1q}(1\,|\,Q_q\,|\,0)$ amounts to only 0.22 D altogether, according to the estimates appearing in ref. 11.

$$P_{1q}(v_q+1\,|\,Q\,|\,v_q)\ll P_0,\quad P_{1q}=\left(\frac{\partial P(Q)}{\partial Q_q}\right)_{Q_q=0}. \qquad (16)$$

Therefore it might be expected that the terms in (4) which contain P_0 may prove to be substantial, even though they enter into the correction terms. For the case $P^n_{v_q+1,\,v_q}$, these terms have the form

$$P_0[a_{v_q+1,\,v_q}(v_q\,|1|\,v_q)+a_{v_q,\,v_q+1}(v_q+1\,|\,1\,|\,v_q+1)]. \qquad (17)$$

If we restrict ourselves to taking account of the V′ terms in first-order perturbation theory, then

$$a_{v_q+1,\,v_q}=\frac{V'_{v_q+1,\,v_q}}{(E^0_{v_q+1}-E^0_{v_q})}=-a_{v_q,\,v_q+1},$$

in connection with which (17) reduces to zero; this is a coincidence (in the second approximation, it will be different from zero). For a totally symmetric vibration, V′ will contain terms linear in Q_q

$$V'_q=Q_q\sum_k b_{qk}Q_k^2. \qquad (18)$$

In the calculations, such matrix elements as

$$(V'_q)_{v_q+1,\,v_q}=\sqrt{\frac{\hbar}{2\omega_q}(v_q+1)}\sum_k b_{qk}\frac{\hbar}{2\omega_k}(v_k+1) \qquad (19)$$

for example, will be significant (all the reduced masses[6] are set equal to unity). Analysis of the last expression shows that the q-th vibration must be coupled with other

vibrations. Inasmuch as the intensities are determined by the formulas (7), vibrations with low frequencies ω_k will make a significant contribution to the temperature dependence (under conditions where the corresponding b_{qk} are not very small). This allows us to suppose that, when the inequality (16) is fulfilled, the influence of mechanical anharmonicity may prove to be substantial even for the fundamental vibrations—and not only for molecules containing light atoms, but sometimes also for molecules with heavy atoms, since the latter may possess relatively low frequencies ω_k.

There is no reason to write out here the corresponding formulas for the special case under consideration or any other one, since we know of no detailed studies on temperature dependence which were performed under appropriate conditions for a sufficiently wide temperature interval. If necessary, it is not difficult to obtain these formulas if, having written down the V′ terms (allowing for symmetry) and having determined the coefficients $a_{v_j v_s}$ which appear in (1) (with the help of the well-known methods of perturbation theory[7]), one then makes use of formulas (4), (5), (7), (14), and (15). It should also be noted that the effect of mechanical anharmonicity brings about a more abrupt increase in f(T) with temperature than when one allows for electro-optical anharmonicity alone, since allowance for the former leads to an increase in the number of quantum numbers of separate oscillators, on which $P_{v_j v_l}$ in (4) depends. The question of the relative role of mechanical and electro-optical anharmonicity remains as yet entirely unclarified. One may expect, for example, that in the case of two molecules of the same structure the effect of electro-optical anharmonicity will be more significant for the molecule with the less polar bonds, when the nonlinear terms in expansion (3) play a substantial role.*

*In just this way, the authors of ref. 12 succeeded in explaining the differences in the intensity ratios of vibrations of different orders as a function of the degree of polarity of the bond.

The fact that the locations of relatively high-order vibrations fit the serial formulas for harmonic oscillators fairly well (deviations therefrom are brought about exclusively by mechanical anharmonicity) may serve as an indirect indication of the relatively small role of mechanical anharmonicity in a number of cases.

COMPARISON OF THEORY WITH EXPERIMENT

The first attempt at carrying out a quantitative study for the purpose of experimental verification of the theory was undertaken in ref. 1. The temperature dependence of the total integrated absorption of the overlapping bands of the combination frequencies $\nu_1 + \nu_3$ and $2\nu_1 + \nu_4$ of carbon tetrachloride was obtained in the interval 20°-200°C. In this case, the phenomenon was somewhat complicated by the presence of Fermi resonance. As was shown in ref. 13, in comparing theory with experiment one should use the formulas which fix the temperature dependence of the more intense component. The temperature factor used in ref. 13 then has the form

$$f^{\nu_1+\nu_3}(T) = \left(\left[1 - e^{-\frac{h\nu_1}{kT}} \right) \left(1 - e^{-\frac{h\nu_3}{kT}} \right) \right]^{-1}$$

i.e., it differs from (10) by the factor

$$1 - e^{-\frac{h(\nu_1+\nu_3)}{kT}}$$

which is very close to unity* over the whole temperature

*Even at t = 200°C, this factor amounts to about 0.98.

interval employed in ref. 1. Consequently, the temperature trend observed in ref. 1 for the change in intensity is described equally well with the help of the function $f^{\nu_1+\nu_3}$ and with the help of expression (10). This fact, of course, is coincidental. The results of works 1 and 13 show in addition that, in the given case, electro-optical anharmonicity apparently plays the principal role.

The results of comparative quantitative studies of the intensities of the fundamental vibrations of a number of molecules in the temperature interval 25°-275°C are set forth in ref. 2. If we turn to the statistics of the results, it appears that, of 19 bands, 6 display practically no change of intensity with temperature, which agrees with expression (8); in 2 cases these changes somewhat exceed experimental error, and in the remainder quite significant temperature changes of the intensities are observed.

Reference 3 is devoted to the investigation, for the bands of the ν_1 and $\nu_1 + \nu_4$ vibrations of gaseous bromoform and $\nu_1 + \nu_4$ of gaseous chloroform, of the dependence which we are considering. Analogously to the case investigated in refs. 13 and 14, the frequency and temperature values proved to be such that the temperature factors of the earlier theory[4] and those obtained in the present work actually coincide in numerical value. The discrepancy between experiment and theory hardly exceeds the limits of error of the experiment. One may speak (especially for the $\nu_1 + \nu_4$ $CHBr_3$ vibration) only of a certain tendency to a more rapid increase of absorption with T in comparison with that predicted by the theory. The latter is to be ascribed, apparently, to the effect of mechanical anharmonicity, reinforced on account of the presence of the light hydrogen atom. The fact that the deviations from the serial formulas written down for a set of harmonic oscillators (at least for vibrations in which the C—H bond takes part) are in general significantly greater in the case of $CHCl_3$, for example, than in the case of CCl_4 serves as an indirect indication of the increase in the role of phenomena associated with mechanical anharmonicity in molecules of the type of $CHCl_3$ and $CHBr_3$ in comparison, let us say, with the CCl_4 molecule. It is not difficult to convince oneself of this by analysis of the frequency values presented in refs. 10 and 14.

In the opinion of the authors, further experimental investigations are necessary for final solution of the question of the correspondence of theory and experiment. Such investigations should be carried out over a wider range of substances and of vibrations of different orders. Particular attention should be paid to cases where the temperature interval and the frequency values are such that the theory predicts significant changes in the intensities.

REFERENCES

1. M. P. Lisitsa and V. N. Malinko, Ukrain. Fiz. Zhur. 3, 773 (1958); Opt. i Spektr. 6, 694 (1959), Optics and Spectroscopy 6, 450 (1959).
2. V. N. Smirnov and P. A. Bazhulin, Opt. i Spektr. 7, 193 (1959), Optics and Spectroscopy 7, 123 (1959).
3. M. P. Lisitsa and Yu. P. Tsyashchenko, Opt. i Spektr. 9, 742 (1960), Optics and Spectroscopy 9, 389 (1960).
4. M. V. Vol'kenshtein, M. A. El'yashevich, and B. I. Stepanov, "Kolebaniya molekul" (Molecular Vibra-

tions), Vol. 2. Gosudarst. Izd. Tekh. i Teoret. Lit., Moscow-Leningrad, 1949.
5. B. I. Stepanov and Ya. S. Khvashchevskaya, Doklady Akad. Nauk SSSR **116**, 588 (1957), Soviet Phys.-Doklady, **2**, No. 5, 457 (1957).
6. M. V. Vol'kenshtein, M. A. El'yashevich, and B. I. Stepanov, "Kolebaniya molekul" (Molecular Vibrations), Vol. 1. Gosudarst. Izd. Tekh. i Teoret. Lit., Moscow-Leningrad, 1949.
7. L. D. Landau and E. M. Lifshitz, "Kvantovaya mekhanika" (Quantum Mechanics). Gosudarst. Tekh. i Teoret. Izd., Moscow, 1949.
8. B. Heitler, "Kvantovaya teoriya izlucheniya" (Quantum Theory of Radiation). Izd. Inostrannoi Lit., Moscow, 1956. 3rd ed., Oxford Univ. Press, 1954.
9. G. Placzek, "Releevskoe passeyanie i Raman-effekt" (Rayleigh Scattering and Raman Effect). Ob''ed. Nauch. i Tekh. Izd., Kiev-Khar'kov, 1935.
10. M. P. Lisitsa and V. N. Malinko, Opt. i Spektr. **4**, 455 (1958).
11. V. L. Strizhevskii, Opt. i Spektr. **8**, 165 (1960), Optics and Spectroscopy **8**, 86 (1960).
12. N. E. Gaponova, M. P. Lisitsa, and Yu. P. Tsyachchenko, Opt. i Spektr. **8**, 465 (1960), Optics and Spectroscopy **8**, 245 (1960).
13. M. P. Lisitsa and V. L. Strizhevskii, Opt. i Spektr. **7**, 478 (1959), Optics and Spectroscopy **7**, 305 (1959).
14. M. P. Lisitsa and Yu. P. Tsyashchenko, Opt. i Spektr. **6**, 605 (1959), Optics and Spectroscopy **6**, 396 (1959).
15. B. I. Stepanov and V. P. Gribkovskii, Doklady Akad. Nauk SSSR **121**, 446 (1958), Soviet Phys.-Doklady **3** No. 4, 781 (1958).

INFRARED ABSORPTION AND RAMAN SPECTRA OF BIPROPENYL AND DIALLYL AND THE QUESTION OF ROTATIONAL ISOMERISM

Yu. A. Pentin, Yu. N. Panchenko, E. G. Treshchova, and Z. Sharipov

Received 8 April 1960

The Raman and infrared absorption spectra of bipropenyl (2, 4-hexadiene) were studied in the liquid and solid states in order to obtain new experimental data on the rotational isomerism of molecules with the bond type $\gg C-C\ll$. The spectra of liquid and solid diallyl (1, 5-hexadiene) were also obtained; this molecule has three single bonds (one of type $\gg C-C\ll$ and two of type $\gg C-C\ll$) which permit rotational isomerism. In both cases the existence of rotational isomerism was established and it was shown that the trans form is the more stable in the solid state; in the case of diallyl a rotational isomer with respect to the central C—C bond is indicated.

The question of the rotational isomerism of the conjugated hydrocarbon dienes (due to the presence in the molecule of a bond of the type $\gg C-C\ll$) has not yet been satisfactorily cleared up. It has usually been considered that for these compounds there are in principle two possible rotational isomers: the trans form, $\gg C-C\ll$, and the cis form, $\gg C-C\ll$. However this hypothesis cannot be considered to be satisfactorily established, particularly when it is realized that the atoms which are not directly bound are found for the plane configurations in an "eclipsed" position which is energetically unstable. Accepting this one can still assume a nonplanar structure of rotational isomers about a bond of the type $C_1\ll C_2-C_3\ll C_4$. In fact, the widespread notion of the planar structure of the molecules of the conjugated dienes is confirmed only in the case of a few of the simplest compounds (for example, 1, 3-butadiene).

The question as to whether rotational isomerism is in fact present in the molecules of any given diene, and whether the planar or the nonplanar configuration is the more stable energetically, depends to a large extent on what substitutes are attached to the C_2 and C_3 atoms and also to the C_1 and C_4 atoms, and should be considered in detail for each substance. In other words, the investigation of the general form of the potential function for internal molecular rotation with respect to a bond of the type $\gg C-C\ll$ is a complicated problem and we will not take it up here. For the simplest diene (1, 3-butadiene) we can assume that the potential curve of the molecule has the form shown in Fig. 1. The maximum of the potential energy should clearly correspond to the planar cis form (c), since the distances between the nuclei H ... H and C ... C of the two $=CH_2$ groups in this case are equal to ~1.8 and ~2.8 A, respectively, and these are significantly smaller than the corresponding sums of the Van der Waals radii (~2.4 and ~3.6 A). In the case of the planar trans form (t) this steric hindrance does not occur. It is possible that in 1, 3-butadiene the rotated or gauche-isomer (g_c), which approaches the cis form,

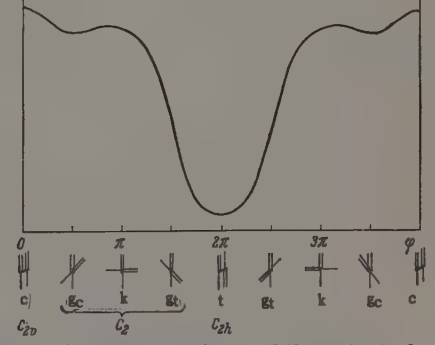

Fig. 1. Approximate form of the potential curve of the internal molecular rotation of the simplest diene. Below-schematic representation of the various spatial isomers of the molecule.

is present in negligible amounts. However, the existence of two rotational isomers for this molecule has not been conclusively demonstrated up to the present, and the minima on the potential energy curve which correspond to the form g_c may not even exist. For the case in which to each carbon atom (C_1, C_2, C_3, and C_4) a very bulky group is attached and the steric repulsion is large, it can be assumed that the structure can show only the "crosslike" form (k); this means that strictly rotational isomerism cannot occur. It is possible to also imagine intermediate cases of the occurrence of rotational isomers, the gauche form (g_c) approximating to the cis form and the gauche form (g_t) approximating to the trans form. The question of the azimuthal angles of the isomers g_c and g_t remains open in all cases.

It seems to us that there is a definite interest in studying the rotational isomerism of bipropenyl (2, 4-hexadiene), the molecule of which is next in complexity after 1, 3-butadiene, with the main objective of establishing whether such isomerism really exists for this molecule.

The other diene which we took up for investigation, diallyl (1, 5-hexadiene), does not have any conjugated double bonds, but it presents a complex case of the possible superposition of effects of rotational isomerism with respect to a bond of the type $\gtrless C-C \lessgtr$ and two bonds of the type $\gtrless C-C \lessdot$. The question of rotational isomerism with a bond of the latter type has been studied very little up to the present.

EXPERIMENTAL METHOD

One of the methods of establishing the presence of rotational isomerism with the aid of vibrational spectra is the comparison of the spectra for the liquid and solid phases; we have used this method in the present investigation.

The infrared spectra in the 700-1800 cm^{-1} region were studied with an IKS-2 double-beam spectrometer using a thermostatted absorption tube.[1] The optical slit width was 7-10 cm^{-1}. The calibration of the instrument was carried out with the spectra of ammonia, polystyrene, cyclohexane, and benzene. To obtain more precise values of the frequencies the spectra at room temperature were recorded also with an IKS-12 single-beam instrument.

The Raman spectra of the substances, with excitation by the 4358 A mercury line, were obtained with a homemade DFS-12 spectrometer with double monochromatisation. The high purity of the spectra thus obtained and the presence of only small aberrations made it easy to obtain the Raman spectra of the substances in the solid state. The spectra were excited with radiation from a low-pressure spiral mercury lamp. A high sensitivity FEU-17 photomultiplier served as the radiation detector. A special tube was constructed for obtaining spectra at different temperatures in the liquid and solid phases; a diagram of this is given in Fig. 2. The tube was cooled by passing cold nitrogen gas through it, the speed of flow being regulated by the heating of a nichrome spiral immersed in liquid nitrogen in a metal Dewar flask. The spectra were recorded after temperature equilibrium had been established. A copper-constantan thermocouple was used to measure the temperature.

Fig. 2. Sketch of a tube for obtaining Raman spectra of thermostatted liquids and solids. a—Vacuum jacket; b—thermostat jacket; c—substance tube.

The spectral slit width in the Raman investigations was 5-7 cm^{-1}, and the accuracy of the readings of the wavelength drum was 1 A or 4 cm^{-1}.

The physical constants of the bipropenyl and diallyl samples are compared in Table 1 with data from the literature. Bipropenyl was obtained by the isomerization of diallyl over calcium amide, and diallyl from allyl chloride by a Grignard-Würtz reaction. Both substances were distilled in a column with an efficiency of 80 theoretical plates.*

*The authors express their gratitude to I. V. Gastunska who furnished the alkadiene samples for the present investigation.

Table 1. Physical Constants of Bipropenyl and Diallyl

Substance	p (mm Hg)	$T_{boiling}$ (°C)	$T_{melting}$ (°C)	n_D^{20}	d^{20}
Biptopenyl	760	82.4—84.6	73	1.4550	0.7216
	760 [2]	80	—	1.4550	0.720
Diallyl	755	59.5—59.8	140	1.4045	0.6810
	760 [2]	59.46	140.68	1.4042	0.6923

EXPERIMENTAL RESULTS AND DISCUSSION

The infrared and Raman spectra of bipropenyl and diallyl obtained in the present investigation are reproduced in part in Figs. 3-6 and the frequencies are given in Tables 2 and 3. The spectra of the liquids agree very well with data in the literature;[2,3] the spectra of the substances in the solid phase have apparently not been studied before and have been obtained here for the first time.

Bipropenyl. This compound with two double bonds can have three geometrical isomers (configurations):*

*To distinguish configurations and conformations we designate the former with capital letters and the latter with lower case letters.

trans—trans (TT), trans—cis (TC) and cis—cis (CC),

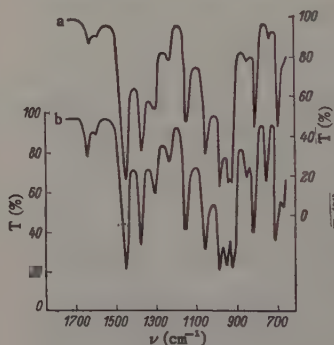

Fig. 3

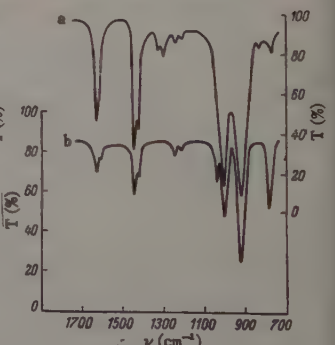

Fig. 4

Fig. 3. Infrared absorption spectrum of bipropenyl ($CH_3-CH=CH-CH=CH-CH_3$). Curve a—liquid at +20°C (sample thickness d ~ 0.02 mm); curve b—solid at −167°C.
Fig. 4. Infrared absorption spectrum of diallyl ($CH_2=CH-CH_2-CH_2-CH=CH_2$). Curve a—liquid at +20°C (d ~ 0.02 mm); curve b—solid at −170°C.

Table 2. Vibrational Frequencies of Bipropenyl (cm^{-1})

Infrared		Raman		Infrared		Raman	
Liquid	Solid	Liquid	Solid	Liquid	Solid	Liquid	Solid
		204	211	986	986	979	979
		268	262			1033	< 1030
		318	< 322	1054	< 1054		
438		430	< 430			1095	< 1095
		460	< 460	1150	1150	1157	1152
521						1170	< 1170
593		590	> 595	1234	1234	1238	> 1238
680	< 685					1270	< 1270
703	710	709	> 709			1280	1280
750	< 755			1302	1302	1299	1303
813	818	824	824	1373	1373	1378	> 1378
		834	< 834	1445	1445	1453	< 1453
854	< 854			1598	1598		
923	923	926	> 926		< 1640		
945	950	944	> 944			1656	1657
						1666	> —

Table 3. Vibrational Frequencies of Diallyl (cm^{-1})

Infrared		Raman		Isomer with respect to C_3-C_4	Infrared		Raman		Isomer with respect to C_3-C_4
Liquid	Solid	Liquid	Solid		Liquid	Solid	Liquid	Solid	
		249	249			1020	1026	< 1030	t
		355	< 355	t			1130	< 1134	t
		405	< 400	t			1187	< 1183	t
		422	> 422	g	1212	1212	1217	1212	tg
		532	< 540	g	1246	1246			t
552				t			1280	< 1276	t
615		614	< 614	tg	1301	> —	1299	> 1299	g
649				t	1325	> —			g
		691	692	tg			1334	< 1339	t
774	< 774			t	1419	1419	1416	1416	tg
832	> —	832	> 832	g	1445	1445	1442	1442	tg
912	912	913	?	tg	1630	1620	1617	1617	tg
		920	< 920	t	(not resolved)	1640	1642	1637	tg
995	> 995	996	991	tg					
(not resolved)									

nd, in addition, in each of these cases one can postulate ne existence of rotational isomers due to rotation about ne $\gg C-C \ll$ bond (conformations). Since it is very dif-cult to separate out any one of the geometrical isomers f bipropenyl in pure form and we were not able to do nis, the problem is complicated by the necessity of con-onsidering all possible configurations and conforma-ions. For a planar structure of the latter the isomers f bipropenyl would have the following form:

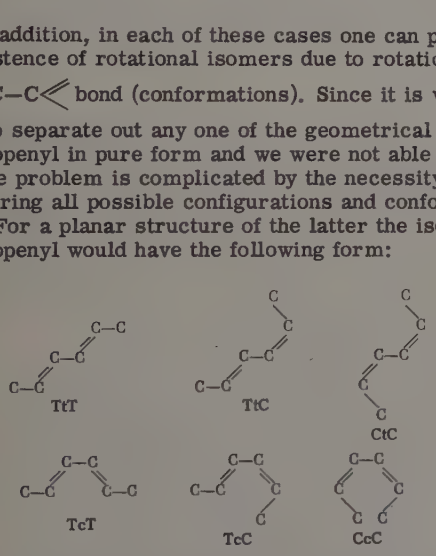

However, on the basis of the considerations which re mentioned above, we can be certain for the planar tructure of only the single isomer TtT (point group C_{2h}). enerally speaking the TT configuration of dipropenyl as almost the same steric factors as the 1, 3-butadiene olecule. Thus everything that was said above with eference to Fig. 1 evidently holds also in the present ase, that is, the second rotational isomer of this con-iguration, if it really exists, must be the isomer Tg_cT point group C_2). The steric strain of the plane confor-nations (except TtT) should be very great, changing in ne following way along the series of isomers: TcT < tC < TcC < CtC < CcC. It is possible therefore that he configurations TC and CC exist in the form of the

Fig. 5

Fig. 6

Fig. 5. Recordings of Raman lines of bipropenyl. a—Liquid at +20°C; b—solid at −160°C.
Fig. 6. Recordings of Raman lines of diallyl. a—liquid at +20°C; b—solid at −160°C.

conformations g or even k, that is, the presence of a strictly rotational isomer for these configurations is less probable than for configuration TT.

The number of observed vibrational frequencies in the infrared and the Raman spectrum of bipropenyl exceeds the calculated number for any one conformation and, in any case, for the conformation TtT (C_{2h}). This can be caused by either geometrical or a rotational isomer. Using data from the literature[5] for the characteristic frequencies in the infrared spectra of TT, TC, and CC configurations of conjugated diene systems, we can only suggest that bipropenyl is a mixture of all three molecular configurations (it is possible that there is a predominance of the TT and, in a lesser degree, of the TC configuration). It is difficult to reach a more definite conclusion in this matter, since in using the IKS-2 instrument certain absorption bands originating in different configurations and lying close together in frequency are not resolved.

A comparison of the infrared spectrum with the Raman spectrum shows that the rule of mutual exclusion holds for a number of vibrational frequencies; this indicates the existence in the mixture of highly symmetric molecular forms, one of which in particular could be the conformation TtT (C_{2h}). Comparing the spectra of liquid and of solid bipropenyl one notes the following. On cooling the bipropenyl a change in the intensity of certain bands in the infrared spectrum is observed. It is interesting to note that there is an increase in the intensities of the bands of precisely those vibrations (685, 755, 854, 1054, and 1640 cm^{-1}) which are inactive in the Raman spectrum. This undoubtedly indicates that on cooling the concentration of the most symmetrical conformation (evidently, TtT (C_{2h})) increases. Unfortunately we cannot say with certainty that a truly crystalline state rather than a "glass" was obtained when the bipropenyl was solidified. It is possible that it is just for this reason no bands of the less stable conformation were observed to disappear. In the investigation of the Raman spectrum of solid bipropenyl a regular change of the intensities of a number of lines was observed (indicated in the table by the signs >, <), while an analysis of the spectrum made possible a clear proof of the existence of a rotation isomer of bipropenyl since one of the bands of the valence vibrations of the double bonds (ω = 1666 cm^{-1}; cf. Fig. 5) disappeared completely in the crystallized substance. This fact can be explained only by the disappearance of one of the rotational isomers (conformations) and not by a change of

configuration. Actually, the height of the potential barriers for rotation around the single bond does not exceed a few kcal per mole, while the barriers between the geometrical CIS—TRANS isomers are of the order of tens of kcal per mole.

On comparing the data from the infrared and Raman spectra it is not difficult to come to the conclusion that, firstly, it can be considered as firmly established that true rotational isomerism for the bond type $\gg C-C \ll$ exists in the bipropenyl molecule, most likely in its TT-configuration and, secondly, the most stable conformation is apparently TtT (C_{2h}) and the least stable the "frozen out" configuration $Tg_cT(C_2)$. On the other hand, the TC and CC configurations apparently do not possess rotational isomers and occur in a single form.

Diallyl. As has already been pointed out the molecule of this compound has three single C—C bonds, and hindered internal rotation about these permits the effect of strictly rotational isomerism. Rotation about the central bond of the type $\gg C-C \ll$ can lead to the appearance of rotational isomers with trans and gauche arrangements of the vinyl groups, that is, with C_{2h} and C_2 symmetries, respectively, if the forms of the vinyl groups are not taken into account. This effect should clearly occur and should be considered first of all. At the same time one must expect that in the case of the trans as well as the gauche isomer, the symmetry can be destroyed and various different conformations can occur as a result of internal rotation about bonds of the type $\gg C-C \ll$. The question of rotational isomerism for bonds of this type was discussed previously by one of us[6] (cf. also ref. 7).

Sverdlov and his co-workers[8] have interpreted the Raman spectrum of diallyl assuming that the molecule belongs to the point-group C_2. At the same time there are no grounds for rejecting the possibility of the existence of the trans rotational isomer, C_{2h}, which can be even more stable. The discussion of these authors concerning the nonobservance of the rule of mutual exclusion is not sufficiently convincing since, in the first place, it is not supported properly by experiment and, in the second place, the possibility of a lowering of the symmetry because of internal rotation about the outer single bonds is not taken into account. It is also not clear why the authors did not consider that it is possible for several rotational isomeric forms to exist simultaneously. These considerations, along with data given below which were obtained in the present investigation, indicate that the interpretation of the spectrum of diallyl in ref. 8 is incorrect.

A comparison of the infrared and Raman spectra shows that certain frequencies are present only in one spectrum and certain are present only in the other (rule of mutual exclusion). Even more interesting is the result obtained when the spectra of the liquid and solid are compared. In Table 3 the bands for which the intensity changes by at least a factor of 2 to 4 on solidification are indicated by the signs $>$, $<$, and those whose intensity falls to zero are indicated by a dash. As a rule, the intensity increases for those bands which are observed only in the Raman spectrum or only in the infrared spectrum and decreases for the bands which are observed in both spectra. As an example Fig. 6 shows the recorder trace of two lines in the Raman spectrum for which the intensity ratio, I_{1280}/I_{1299}, changes approximately from 1:2.5 to 3.5:1 in going from the liquid to the solid. The first of these frequencies is not present in the infrared spectrum and clearly belongs to the trans isomer, whereas the second, which occurs in the infrared spectrum of the liquid and disappears on solidification, manifestly belongs to the gauche isomer. The situation is similar for a number of other frequencies. These data indicate that diallyl represents an equilibrium mixture of rotational isomers, and that on solidification the equilibrium shifts in the direction of increasing concentration of the more symmetrical trans isomer and of decreasing concentration of the gauche form. As a result of internal rotation around the outer single bonds there can be, generally speaking, no one trans and no one cis form. However, for the present we will refrain from going into the details of this question. On the basis of the above considerations we have attempted to assign the observed frequencies to the trans (t) and gauche (g) forms of the diallyl molecule. Those bands for which the intensity does not change or changes very slightly can obviously belong simultaneously to different isomers; these are designated tg in Table 3.

In all cases when we referred to intensity changes in the spectra of bipropenyl and diallyl in the transition from the liquid to the solid, it was meant that these changes occur gradually on lowering or raising the temperature of the liquid; i.e., on displacing the equilibrium of the rotational isomeric forms.

In conclusion the authors consider it a pleasant duty to express their gratitude to V. M. Tatevskii.

REFERENCES

1. Kh. Kesler, Yu. A. Pentin, E. G. Treshchova, and V. M. Tatevskii, Opt. i Spektr. 7, 301 (1959), Optics and Spectroscopy 7, 195 (1959).
2. F. D. Rossini, K. S. Pitzer, R. L. Arnett, R. M. Braun, and G. C. Pimentel, "Selected Values of Physical and Thermodynamical Properties of Hydrocarbons and Related Compounds." Carnegie Press, Pittsburgh, Pa., 1953.
3. W. G. Brown, D. F. Spooner, and M. R. Fenske, Analyt. Chem. 22, 1074 (1950).
4. E. R. Blout, M. Fields, and R. Karplus, J. Am. Chem. Soc. 70, 194 (1948);
H. Inhoffen, I. Heimann-Trosien, H. Munfeldt, and A. Krömer, Chem. Ber. 90, 187 (1957).
5. L. J. Bellamy, "The Infrared Spectra of Complex Molecules." Wiley, London, 1954;
E. R. Lippincott, C. E. White, and I. P. Siblia, J. Am. Chem. Soc. 80, 2926 (1958).
6. Yu. A. Pentin, Kand. Ph.D. diss., Moscow (1955).
7. M. V. Vol'kenshtein, "Konfiguratsionnaya statistika polimernykh tsepei" (Configurational Statistics of Polymeric Chains). Izd. Akad. Nauk SSSR, Moscow-Leningrad, 1959.
8. L. M. Sverdlov, M. G. Borisova, and N. V. Tarasova, Opt. i Spektr. 5, 354 (1958).

RAMAN SPECTRA OF VARIOUS CLASSES OF HYDROCARBONS
VII. Ditertiaryalkylmethanes C_{10}-C_{17}-Branched Alkanes with Two Quaternary Carbon Atoms Separated by a Methylene Group

E. G. Treshchova, V. M. Tatevskii, V. K. Daukshas, and R. Ya. Levina (pp. 63-68)

Received 21 December 1959

The Raman spectra of C_{10}-C_{17} hydrocarbons with two quaternary carbon atoms separated by a methylene group (ditertiaryalkylmethanes) were investigated. It is shown that the characteristic manifestations of the presence of quaternary carbon atoms and of groups containing a tertiary carbon atom at the end of a chain (found in the case of the lower hydrocarbons) hold also for paraffinic hydrocarbons with high molecular weight—up to $C_{17}H_{36}$. The manifestations characterizing the presence in a molecule of complex branching with two quaternary carbon atoms separated by a CH_2 group were found to occur irrespective of the length of the chain and the presence of simple branching in the molecule. The characteristic spectral manifestations of groups with quaternary and tertiary carbon atoms are not affected by the simultaneous presence of these groups in a molecule.

As a continuation of earlier work[1-3] on the regularities in the vibrational spectra of higher alkanes, we investigated a number of C_{10}-C_{17} hydrocarbons containing quaternary and tertiary carbon atoms—ditertiaryalkylmethanes (I): 3,3,5,5-tetramethylheptane, 4,4,6,6-tetramethylnonane, 5,5,7,7-tetramethylundecane, 2,2,4,4-tetramethylhexane, 2,2,4,4-tetramethylheptane, 2,4,4,6,6,8-hexamethylnonane, and 2,5,5,7,7,10-hexamethylundecane.

EXPERIMENTAL METHOD AND RESULTS

The hydrocarbons (I) were synthesized according to the following scheme:

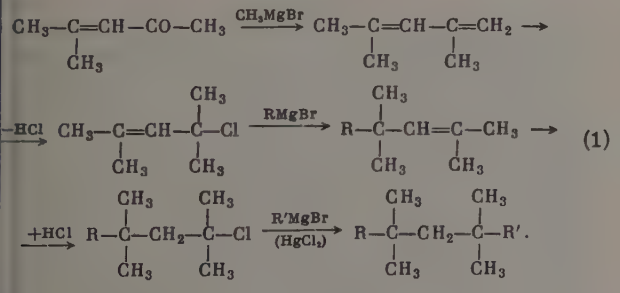

(1)

where either R = CH_3 and R′ = C_2H_5 or C_3H_7 or R = R′ = C_2H_5, C_3H_7, C_4H_9, iso-C_4H_9, and iso-C_5H_{11}.

The synthesis has been described in our earlier publications.[4-6] The compounds were purified first by distillation through a column of 35 theoretical plates and then chromatographically using a silica-gel column.

Some physicochemical constants of the hydrocarbons are given in Table 1.

The Raman spectra of the hydrocarbons were obtained with a three-prism spectrograph and a photoelectric detector (f = 300 mm, photomultiplier FEU-17 possessing an integrated sensitivity of 40 amp/lumen and dark current 3×10^{-10} amp). The methods of measurement and calculation were described earlier.[7]

Table 1. The Physical Properties of Ditertiaryalkylmethanes

General formula	R	R′	Name	B.P. (° C) (pressure in mm of Hg)	n_D^{20}	d_4^{20}	MR_D	Literature
$C_{10}H_{22}$	CH_3	C_2H_5	2,2,4,4-tetramethylhexane	148.8—149.1 (745)	1.4203	0.7449	48.37	[6]
$C_{11}H_{24}$	CH_3	C_3H_7	2,2,4,4-tetramethylheptane	58—58.5 (14)	1.4232	0.7522	52.93	[5]
»	C_2H_5	C_2H_5	3,3,5,5-tetramethylheptane	51 (6)	1.4309	0.7669	52.76	[4]
$C_{13}H_{28}$	C_3H_7	C_3H_7	4,4,6,6-tetramethylnonane	84 (9)	1.4378	0.7813	62.05	[4]
$C_{15}H_{32}$	C_4H_9	C_4H_9	5,5,7,7-tetramethylundecane	106 (7)	1.4420	0.7884	71.30	[4]
»	iso-C_4H_9	iso-C_4H_9	2,4,4,6,6,8-hexamethylnonane	62—63 (2)	1.4407	0.7852	71.38	[5]
$C_{17}H_{36}$	iso-C_5H_{11}	iso-C_5H_{11}	2,5,5,7,7,10-hexamethylundecane	92—92.5 (2)	1.4443	0.7926	80.62	[5]

The frequencies and intensities of the Raman lines of the alkanes from 150 to 1600 cm^{-1} are given in Table 2. The integrated intensities of the lines correspond to a a monochromator slit width of 35 cm^{-1} and are expressed as I_∞ according to the scale developed in ref. 8 and based on the intensity of the 802 cm^{-1} line of cyclohexane (500 units/mole). Table 2 also gives the I_a or analytical intensities obtained with equal entrance and exit slits (0.06 mm/0.06 mm or ~9 cm^{-1}/8cm^{-1}, i.e., at a total slit width of ~17 cm^{-1}). Optimum conditions were maintained during the intensity measurements.

The value of I_a for the standard 802 cm^{-1} line of cyclohexane was taken to be 320 units/mole. This value was obtained from a plot of the 802 cm^{-1} line intensity as a function of the monochromator slit width at constant entrance slit height (see Figure). Assuming the I_∞ = 500 units/mole for the 802 cm^{-1} line of cyclohexane, we measured the intensity of this line at constant entrance slit width and different exit slit widths (curve 1) and at equal entrance and exit slit widths (curve 2) as a function of slit width. If the asymptotic value of I_∞ in curve 1 is assumed to be 500 units/mole, then the point on curve 2 corresponding to a total slit width S ≈ 17 cm^{-1} (S_1 ≈ 9 cm^{-1}; S_2 ≈ 8 cm^{-1}) gives directly the value of 320 units/mole for the I_a of the 802 cm^{-1} line of cyclohexane.

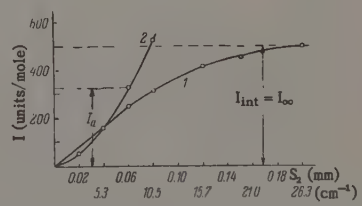

Plot of the intensity of the 802 cm^{-1} line of cyclohexane as function of S_2 the exit slit width of the monochromator. Curve 1—entrance slit width S_1 = 0.04 mm; curve 2—$S_1 = S_2$.

Table 2. Frequencies and Intensities of Lines in the Raman Spectra of Branched C_{10}-C_{17} Alkanes*

[C_{10}]-2,2,4,6-tetramethylhexane			[C_{11}]-2,2,4,4-tetramethylheptane			[C_{11}]-3,3,5,5-tetramethylundecane			[C_{12}]-4,4,6,6-tetramethylheptane			[C_{13}]-5,5,7,7-tetramethylnonane			[C_{15}]-2,4,4,6,6,8-hexamethylnonane			[C_{17}]-2,5,5,7,7,10-hexamethylundecane		
$\Delta\nu$ (cm^{-1})	I_a	I_∞	$\Delta\nu$ (cm^{-1})	I_a	I_∞	$\Delta\nu$ (cm^{-1})	I_a	I_∞	$\Delta\nu$ (cm^{-1})	I_a	I_∞	$\Delta\nu$ (cm^{-1})	I_a	I_∞	$\Delta\nu$ (cm^{-1})	I_a	I_∞	$\Delta\nu$ (cm^{-1})	I_a	I_∞
242	20	—	218	20	—	257	0	—	240	20	—	224; br.	25	—	242	30	—	242/ф	0	—
290	0	—	276/ф	40	65	329	20	—	291; br.	45	—	320; br.	63	95	295	20	—	257	0	—
322	30	—	308; m	25	—	387	20	62	340	50	—	380	0	—	329	30	—	300; diff.	25	—
385	0	—	340	35	—	406	0	—	397	0	—	397	0	—	387	20	—	398/ф	25	—
424	25	—	387	46	56	446	0	—	455	0	—	420	0	—	439	0	—	454	25	—
468	0	—	423	20	—	474	33	62	494; dbl.	50	92	493	0	—	480	0	—	474/ф	30	—
490	40	70	460	20	—	496			586; br.	25	—	586; br.	46	100	518	30	—	591; br.	30	—
519	0	—	496	32	44	544	33	50	627	0	—	675	20	—	603; br.	30	—	673	0	—
550	46	115	546	30	—	576	25	50	687	60	80	695	0	—	671	30	—	734	106	184
582	30	—	574	30	43	651	0	—	735; br.	158	325	735; br.	140	285	695	20	—	765	40	—
621	0	—	635	20	—	671	0	—	850	35	158	792	20	—	733	240	390	803	28	238
671	20	—	672	30	—	715; br.	160	390	873	47		822	0	—	764	40	—	825	130	
716; dbl.	183	450	735	220	415	729	25		884	30	—	854	75	—	822; br.	76	120	860	30	—
732			769	0	—	776	40	—	912	0	—	875	115	170	858	78	119	884	25	—
764	30	—	814	25	—	833	43	110	930	80	185	893			884	30	—	912; br.	50	150
787	30	—	849	30	—	840	43		996	20	—	910	40	120	914	99	185	932	40	208
843	40	135	862/ф	65	132	862	20	—	1040	90	230	930	50		936			956	100	
859	43		875			907	25	—	1101; br. ф	40	—	994	0	—	956	143	235	987	30	—
874	65	145	912	115	245	919	75	197	1138	30	98	1056	120	142	996	20	—	1015	40	—
912	122	315	929/ф			930; br.			1166	50		1090	60	110	1015	20	—	1040; br.	—	—
935																		1112; br./ф	60	90
970	30	—	952	30	120	974	50	80	1204; br.	105	275	1138; br.	60	95	1056	20	—	1142br.ф	35	200
996	20	—	978	35		1012	68	160	1223	60		1159; br.			1104/ф	44	75	1170/ф	65	
1020; dbl.	50	118	1023	20	—	1061	45	120	1258	40	—	1198	70	173	1140/ф	88	175	1198; br.	155	345
1068	48	82	1042	45	117	1138/ф	30	67	1304; dbl. ф	86	223	1241	40	—	1168/ф			1219	40	
1105; br.	30	—	1091	40	103	1170/ф	36	60	1350	40	150	1264	40	—	1196; br./ф	130	315	1241	35	—
1143	35	108	1104			1218	80	240	1381	60		1304; br.	100	230	1227	66		1268/ф	30	40
1168	30		1141 —	60	100	1227	58		1443; br.	400	730	1349/ф	20	—	1267	30	—	1306	60	—
1195; br./ф	96	220	1168br./ф			1296	70	—	1461			1380	45	—	1293	35	—	1342	90	287
1222	55		1191	185	219	1323	60	—				1408	25	—	1354	77	120	1380	60	
1250	148	230	1219			1383	55	100				1450; br./ф	353	720	1380	60	—	1442/ф	400	830
1296	40	—	1246	135	305	1443—	240	612							1442/ф	370	785	1463/ф		
1323	40	98	1296	50	—	1463; br.									1460/ф					
1354	40		1316	82	205															
1389	55	105	1323																	
1445	260	680	1352; br.	20	120															
1465			1385	74																
			1442	270	640															
			1463/ф																	

*Note: The meaning of ф in this table is not clear.

DISCUSSION OF RESULTS

The C_{10}-C_{17} alkanes investigated all have the general structure $R-\overset{CH_3}{\underset{CH_3}{C}}-CH_2-\overset{CH_3}{\underset{CH_3}{C}}-R'$ with two quaternary carbon atoms separated by a CH_2 group.

In five of the hydrocarbons investigated R = R′ while in the other two R and R′ are different: R = CH_3 and R′ = C_2H_5 or C_3H_7. It can be seen from the results presented in Table 2 that the spectra of the seven hydrocarbons are very similar.

Stepanov[9] has given a theoretical analysis of the relationship between the characteristic frequencies in Raman spectra and the chemical structure of branched paraffins. Through analysis of experimental results, Sheppard[10] and other authors[1-3] have established certain regularities in the Raman spectra of hydrocarbons; thus one can infer the absence or presence of various kinds of branching from the absence or presence of specific lines in the spectra.

It is possible to make the following conclusions from a comparison of the results obtained in this investigation with the relationships determined in the above-mentioned papers. The characteristic manifestation of the complex branching with quaternary carbon atoms in the observed spectra of the C_{10}-C_{17} paraffins is the presence of a very intense band in the 716-735 cm^{-1} region due to the completely symmetric vibration and the presence of bands of medium intensity in the 910-935 cm^{-1} and 1200-1240 cm^{-1} regions. The hydrocarbons C_{15}-2,4,4,6,6,8-hexamethylnonane and C_{17}-2,5,5,7,7,10-hexamethylundecane which contain, besides the group with quaternary carbon atoms, also simple branching, one or two CH_2 groups away from a quaternary carbon atom, exhibit in their spectra, apart from the enumerated bands, intense bands in the 800-825 cm^{-1} region characteristic of completely symmetric vibrations in molecules possessing simple branching and an intense band at 956 cm^{-1} indicating that the branching occurs at the end of a chain.

Thus, notwithstanding the presence of complex branching with two quaternary carbon atoms in the molecules of these hydrocarbons, the occurrence of simple branching with a tertiary carbon atom in the chain manifests itself quite definitely in their spectra. The bands in the 800-825 cm^{-1} region and the band at 956 cm^{-1} are absent or very weak in the spectra of the hydrocarbons which do not have branching with a tertiary carbon atom, namely 2,2,4,4-tetramethylhexane, 2,2,4,4-tetramethylheptane, 3,3,5,5-tetramethylheptane, 4,4,6,6-tetra-

methylnonane and 5,5,7,7-tetramethylundecane. The frequencies in the 1140-1170 cm^{-1} region, which characterize simple branching according to Stepanov and Sheppard, are present in the spectra of all the hydrocarbons and hence can not be considered as a reliable indication of the presence of simple branching. The same can be said of the low frequency bands of medium intensity in the 490-380 cm^{-1} region and belonging to the deformation vibrations of the hydrocarbon chain.

REFERENCES

1. E. G. Treshcheva, P. A. Akishin, and V. M. Tatevskii, Zhur. Anal. Khim. 3, 75 (1948).
2. E. G. Treshcheva, V. M. Tatevskii, T. I. Tantsyreva, A. A. Fainzilberg, and R. Ya. Levina, Zhur. Fiz. Khim. 25, 1239 (1951)
3. E. G. Treshcheva, V. M. Tatevskii, A. A. Fainzilberg, N. P. Shusherina, and R. Ya. Levina, Zhur. Fiz. Khim. 35, 1564 (1953).
4. R. Ya. Levina, Yu. S. Shabarov, V. K. Daukshas, and E. G. Treshcheva, Doklady Akad. Nauk SSSR 113, 1286 (1957).
5. R. Ya. Levina, Iu. S. Shabarov, and V. K. Daukshas, Zhur. Obshchei Khim. 28, 2049 (1958).
6. R. Ya. Levina and V. K. Daukshas, Zhur. Obshchei Khim. 29, 3550 (1959).
7. E. G. Treshcheva, V. M. Tatevskii, V. R. Skvarchenko, and R. Ya. Levina, Opt. i Spektr. 5, 553 (1958).
8. G. S. Landsberg, P. A. Bazhulin, and M. M. Sushchinskii, "The Basic Parameters of the Raman Spectra of Hydrocarbons." Izd. Akad. Nauk SSSR, Moscow, 1956.
9. B. I. Stepanov, Zhur. Fiz. Khim. 20, 197 (1946).
10. N. Shappard and M. Simpson, Quart. Revs. (London) 7, No. 1 (1953).

VIBRATIONAL SPECTRA OF ORGANIC COMPOUNDS CONTAINING ELEMENTS OF GROUP IV (Si, Ge, Sn)

I. Characteristic Absorption Bands in the Infrared Spectra of Silicon-Organic Compounds

N. A. Chumaevskii (pp. 69-78)

Received 31 March 1960

The infrared absorption spectra of a large group of silicon-organic compounds with various substitutions on the silicon atom have been investigated. A number of regularities have been established with regard to the specificities of the absorption bands of the investigated substances in the 2100-2300 cm^{-1} region and below 1300 cm^{-1}.

In the present work we present the results of an investigation of the infrared absorption spectra of a series of silicon-organic compounds consisting of alkylalkenylsilanes, tetrasubstituted disiloxanes, and also some alkylchlorosilanes.

Out interest in the compounds listed was aroused partly by our study of the products of the polymerization reaction of tetrasubstituted disiloxanes with difunctional unsaturated derivatives,[1] with acetylene, and with acetylene derivatives, and partly by the need for having as complete data as possible on the infrared absorption spectra of silicon-organic compounds for the purpose of using these data to solve various problems of chemical, analytical, and structural nature.

The most interesting portions of the infrared spectrum—those giving valuable information on the nature of the substitution on the silicon atom—are the region of frequencies below 1300 cm^{-1} and the 2100-2300 cm^{-1} region. In the present work, the examination of the characteristic bands in the infrared absorption spectra of silicon-organic compounds has been carried out with various bonds and groupings characterizing the substitution being used as examples.

1. THE Si-H BOND

The detection of Si-H bonds in silicon-organic compounds with the help of infrared absorption spectra gives rise to no difficulties at all.

The absorption bands of the valence vibrations of Si-H bonds lie in the 2100-2300 cm^{-1} region: for silane itself (SiH_4), ν_{SiH} = 2190 cm^{-1};[2,3] in the case of trichlorosilane, ν_{SiH} = 2262 cm^{-1} (see Fig. 4,e below).

For tetrasubstituted disiloxanes of the structure

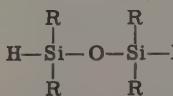

(R = CH_3, C_2H_5, C_6H_5) and for a series of alkylalkenylsilanes, the absorption bands of the Si-H valence vibrations lie in the 2120-2150 cm^{-1} region[1] (see also Fig. 1,a, b, c). The elevation of the ν_{SiH} frequency in the spectrum of $HSiCl_3$ in comparison with SiH_4 may be explained by the strong influence of the chlorine atoms on the Si-H bond.*

*Here one must take into account the change in the characteristics of the Si-H bond on account of the shift of the electron pairs according to the scheme 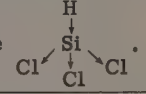 .

In the case of the alkylsilanes and the alkylalkenylsilanes, the stiffness of the Si—H bond becomes less than in SiH_4. It has been shown in ref. 4, on the basis of the series $(CH_3)_nSiH_{4-n}$ (n = 0-4), that the stiffness of the Si—H bond decreases with increasing number of CH_3 groups on the silicon atom, while the corresponding force coefficient $k_{q(Si-H)}$ diminishes (this explains the shift of ν_{SiH} toward the low-frequency side).

2. THE Si—Alk GROUPING (Alk = CH_3, C_2H_5, n-C_3H_7, n-C_4H_9)

The appearance of absorption bands in the region below 1265 cm^{-1} is characteristic for Si—Alk groupings (the frequency falls off in the order $CH_3 \rightarrow$ n-C_4H_9).

Absorption bands with frequencies of 1250-1258 cm^{-1} may serve as a reliable criterion for the presence of $Si-CH_3$ groupings in silicon-organic compounds (Fig. 1). For chlorosilanes, the corresponding frequency has a somewhat greater value (for example, for CH_3SiCl_3 it is 1267 cm^{-1}). When $Si-C_2H_5$ groupings are present in silicon-organic compounds, absorption bands in the region 1235-1240 cm^{-1} appear in the infrared spectra (Fig. 1).

In the case of n-propyl groups (the $Si-n-C_3H_7$ grouping), absorption bands around 1210 cm^{-1}, which are doublets (1205 and 1215 cm^{-1}), appear (Fig. 2). Double absorption bands, located around 1185 cm^{-1} (1180 and 1190 cm^{-1}), are also characteristic of $Si-n-C_4H_9$ groupings (Fig. 2). The doubling noted for the bands of the $Si-n-C_3H_7$ and $Si-n-C_4H_9$ groupings is in all probability associated with the presence of rotational isomers.

The intensities of the absorption bands produced by Si—Alk groupings may serve as a measure of the number of alkyl groups linked to a silicon atom (an estimate of the integrated band intensities for the Alk groups mentioned above has been carried out).

On the basis of the foregoing, the following conclusion may be made concerning the origin of the absorption bands in the region 1265-1180 cm^{-1} (Si—Alk groupings). These bands are to be assigned to deformation vibrations of the methylene group nearest the silicon atom, vibrations associated with a change in the H—C—H and H—C—Si angles (in the case of $Si-CH_3$, it will be $Si-CH_2-H$). The correctness of such an assignment follows from the fact that, for tetravinylsilane $(CH_2=CH)_4Si$ and for compounds in which there are isopropyl and isobutyl groups, bands with the frequencies characteristic for $Si-CH_2-R$ groupings (R = H, CH_3, C_2H_5, C_3H_7) are not observed (see, for example, Fig. 2,f). The frequency falls off as the alkyl group (of the Si—Alk grouping) lengthens, and also on going from Si to Ge and Sn (for $(CH_3)_3GeCH=CH_2$ it is 1237 cm^{-1}, and for $(CH_3)_3Sn-CH_2-CH=CH_2$ it is 1193 cm^{-1}).

3. THE $Si-CH=CH_2$ AND $Si-CH_2-CH=CH_2$ GROUPINGS

The absorption bands corresponding to the valence vibrations of the C=C bond ($\nu_{C=C}$) are most convenient

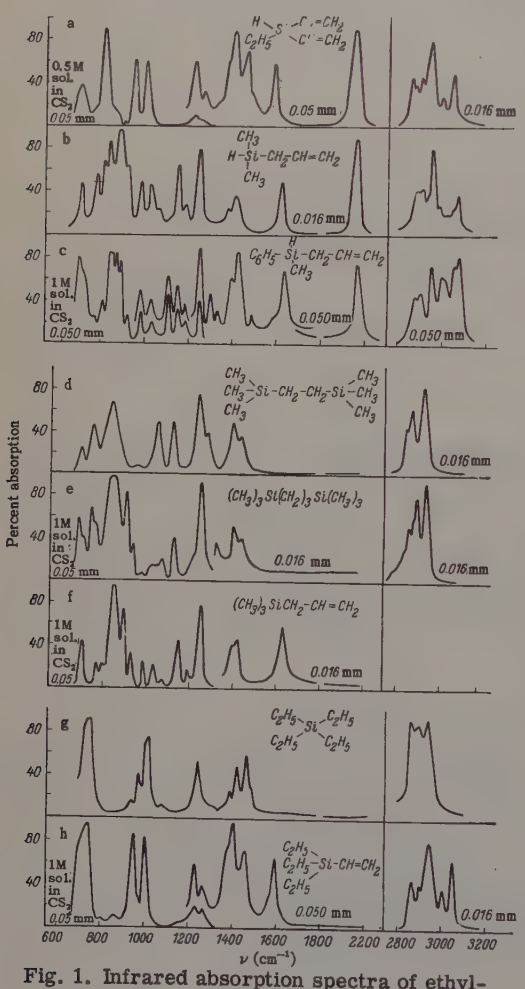

Fig. 1. Infrared absorption spectra of ethyldivinylsilane (a), dimethylallylsilane (b), phenylmethylallylsilane (c), 1,2-bis(trimethylsilyl)ethane (d), 1,3-bis(trimethylsilyl)propane (e), trimethylallylsilane (f), tetraethylsilane (g), and triethylvinylsilane (h).

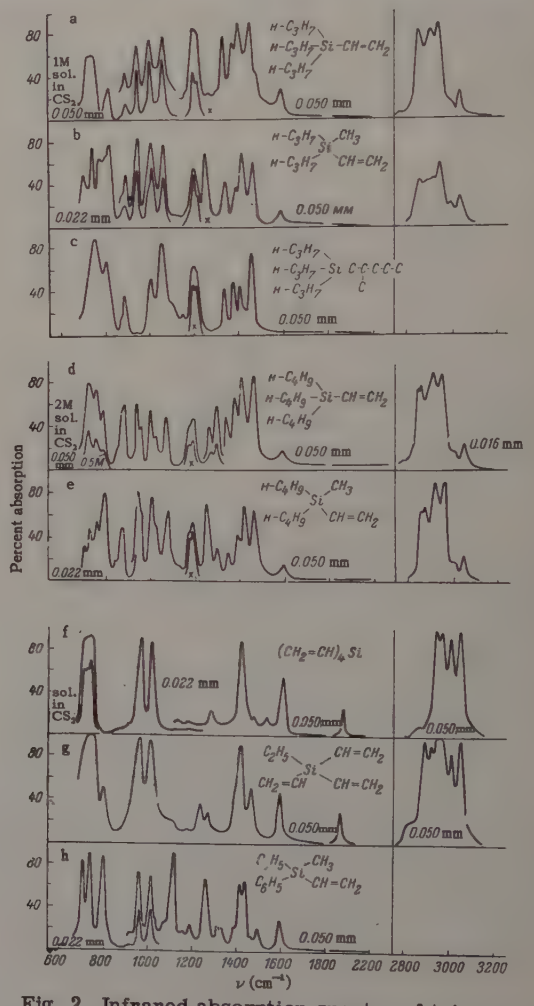

Fig. 2. Infrared absorption spectra of tripropylvinylsilane (a), methyldipropylvinylsilane (b), 2-methyl-1-(tripropylsilyl)pentane (c), tributylvinylsilane (d), methyldibutylvinylsilane (e), tetravinylsilane (f), ethyltrivinylsilane (g), and diphenylmethylvinylsilane (h).

or the recognition of a vinyl or allyl group attached to silicon atom. In the case of the vinyl group, $\nu_{C=C}$ = 595-1600 cm^{-1}, and in the case of an allyl group $\nu_{C=C}$ = 625-1635 cm^{-1}. It should be noted that, for olefins, isolated double bonds are represented by absorption bands in the region 1620-1680 cm^{-1} (this has been considered in detail in ref. 5). The low value of $\nu_{C=C}$ for the vinyl derivatives is apparently connected with a change in the force constants of the bonds close to the C=C, and also of the C=C bond itself, on account of σ,π-conjugation of the Si—C(σ) and C=C(π) bonds.

The absorption bands corresponding to the valence vibrations of the C—H bonds in terminal CH_2 groups (vinyl and allyl) may also serve for purposes of identification of alkenyl groups; it is better to make use of the bands belonging to the antisymmetric valence vibrations. For the terminal vinyl=CH_2 group ν_{as} = 3040-3050 cm^{-1} (closer to 3050 cm^{-1}), and for allyl, ν_{as} = 3070-3080 cm^{-1} (closer to 3080 cm^{-1}).

Aside from the bands already mentioned, the absorption bands in the 900-1200 cm^{-1} region are also of interest. When vinyl groups attached to a silicon atom are present in the compounds, there appear in the spectra (in the interval cited) two absorption bands around 955-980 and 1008-1010 cm^{-1}, and in the case of allyl derivatives there are bands around 1155-1158 and 1192-1195 cm^{-1} (Fig. 1,b, c; Fig. 2,d-h).

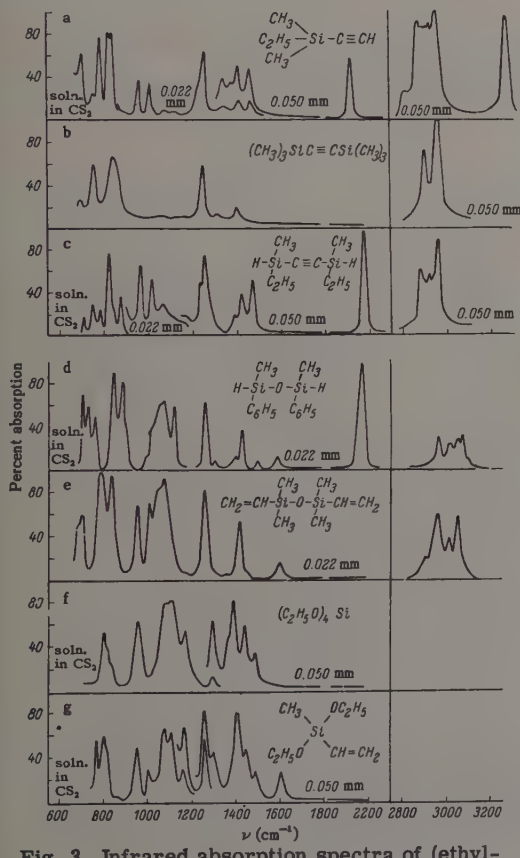

Fig. 3. Infrared absorption spectra of (ethyldimethylsilyl)acetylene (a), hexamethyldisilylacetylene (b), bis(methylethylsily)acethylene (c), dimethyldiphenyldisiloxane (d), divinyltetramethyldisiloxane (e), tetraethoxysilane (f), and methyldiethoxyvinylsilane (g).

4. THE Si—C≡CH AND Si—C≡C—Si GROUPINGS

We have investigated one compound containing the Si—C≡CH groupings—(ethyldimethylsilyl)acetylene, $C_2H_5(CH_3)_2Si—C\equiv CH$—and two compounds with the Si—C≡C—Si grouping—$(CH_3)_3Si—C\equiv C—Si(CH_3)_3$ and $CH_3(C_2H_5)HSi—C\equiv C—SiH(C_2H_5)CH_3$ (Fig. 3,a, b, c). For (ethyldimethylsilyl)acetylene, $\nu_{C\equiv C}$ = 2050 cm^{-1}; for monosubstituted acetylenes, $\nu_{C\equiv C} \approx$ 2080-2100 cm^{-1}. The valence vibration of the C—H bond in the ≡CH group has the frequency 3280 cm^{-1}. For compounds with the Si—C≡C—Si grouping, the $\nu_{C\equiv C}$ frequency does not appear in view of the symmetry of the molecule (for HC≡CH itself, the frequency $\nu_{C\equiv C}$ = 1974 cm^{-1} and is active only in the Raman spectrum).

5. THE Si—C BOND

In the infrared spectra of the compounds studied by us, vibrations of the Si—C bond are represented by absorption bands in the region 680-860 cm^{-1}.* In distinction to the absorption bands of C—C bonds, which are very weak and consequently have quite limited application for analytical purposes, the bands of Si—C bonds are more intense and are more readily found in the spectra. The pronounced intensity of the absorption bands of the Si—C bonds is brought about by their greater polarity in comparison with C—C.

*The results of the investigation of the region above 680 cm^{-1} are presented.

The position of the Si—C bands depends to a considerable degree on the nature of the substituents on the silicon atom. For compounds with Si—CH_3 groupings, the interval 700-860 cm^{-1} is characteristic. In this interval there are usually three bands: around 700, 760, and 850 cm^{-1}, which can be clearly seen when $Si(CH_3)_3$ groupings are taken as examples (see Fig. 1,d, e, f; Fig. 3,b). In the case of CH_3SiCl_3, there are absorption bands around 760 and 800 cm^{-1} (Fig. 4,f).

For $(C_2H_5)_4Si$ and for a series of compounds with Si—C_2H_5 groupings, absorption bands around 740 cm^{-1} appear (Fig. 1,g). The ν_{Si-C} absorption bands of vinyl derivatives lie in the same region: for $(CH_2=CH)_4Si$, ν_{Si-C} = 720 cm^{-1} (Fig. 2,f).

6. THE Si—O BOND

For the tetrasubstituted disiloxanes of structure

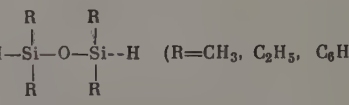

which we have studied (Fig. 3,d, e, f, g), the band of the valence vibrations of the Si—O bond (the Si—O—Si grouping) lies in the region 1060-1070 cm^{-1}, retaining its frequency unchanged also[1] for the polysiloxanes of structure

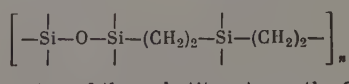

The character of the substituents on the Si Atom has practically no influence on the $\nu_{Si-O-(Si)}$ frequency. In groupings of the Si—O—C type, the $\nu_{Si-O-(C)}$ frequency is shifted to 1090-1100 cm^{-1} and, contrariwise, when one of the silicon atoms in Si—O—Si is replaced by a titanium atom, $\nu_{Si-O-(Ti)}$ is shifted to 912 cm^{-1} (on the basis of

Table 1. Frequencies of the Valence Vibrations of the Si—Cl Bond (cm^{-1})

								Character of of the vibration
481	484	469	467	493	450	458	491	ν (Si—Cl)$_s$
—	—	538	540	589	572	586	579	ν (Si—Cl)$_{as}$

tetrakis(diphenylmethylsiloxy)titanium and di(triethylsiloxy)titanium oxide, according to our data). For the cyclic polysiloxanes of structure 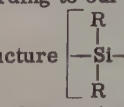 , the regularities associated with the changes in the Si—O frequency for different n have been noted in refs. 6 and 7.

7. THE Si—Cl, Si—Cl_2, AND Si—Cl_3 GROUPINGS

For dimethylbutylchlorosilane and diethylpropylchlorosilane (Fig. 4,a, b), the presence of intense absorption bands around 481 and 484 cm^{-1} respectively is characteristic; these bands are due to the ν_{Si-Cl} vibration. In the case of dimethyldichloro- and methylethyldichlorosilane, absorption bands at 469 cm^{-1} ($\nu_{s\,(Si-Cl)}$) appear in the infrared spectra. In the spectra of the trichlorosilanes, there are also two absorption bands each, $\nu_{s\,(Si-Cl)}$ (type A) and $\nu_{as\,(Si-Cl)}$ (type E) (see Table 1), the position of which depends on the character of the alkyl groups. In the general case, one may consider that the interval 450-490 cm^{-1} is characteristic for $\nu_{s\,(Si-Cl)}$ and the interval 540-600 cm^{-1} for $\nu_{as\,(Si-Cl)}$.

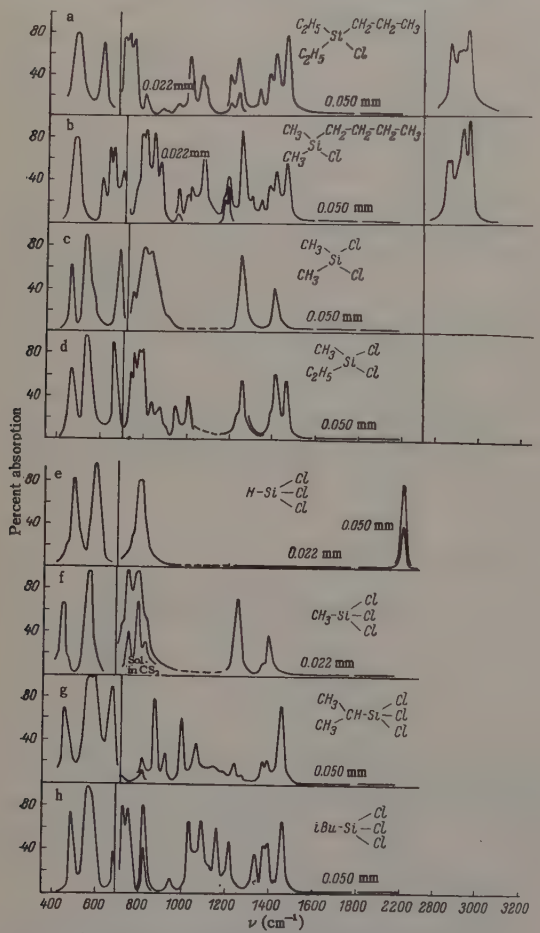

Fig. 4. Infrared absorption spectra of diethylpropylchlorosilane (a), dimethylbutylchlorosilane (b), dimethyldichlorosilane (c), methylethyldichlorosilane (d), trichlorosilane (e), methyltrichlorosilane (f), isopropyltrichlorosilane (g), and isobutyltrichlorosilane (h).

Attention should be paid to the incorrect assignment of the vibration frequency of the Si—Cl bond in ref. 8, the authors of which suppose that the intense absorption band with the frequency 810 cm^{-1} in trichlorosilane $HSiCl_3$, ethyldichlorosilane $(C_2H_5)HSiCl_2$, and diethylchlorosilane $(C_2H_5)_2$—SiCl is associated with the vibrations of the Si—Cl bond (reference to this work is made in Bellamy's monograph[8]). For $HSiCl_3$, the band at 802 cm^{-1} (Fig. 4,e) is characteristic; it is due to the δ(H—Si—Cl) vibration associated with the deformation of the angle 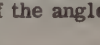 .

Among the works on chlorosilanes, one should also note ref. 9, in which a large body of data on the Raman spectra of several alkyltrichlorosilanes is presented.

In Table 2 are given the absorption band frequency values which are characteristic for the various functional groups attached to the silicon atom.

Table 2. Frequencies of the Absorption Bands of Various Functional Groups Attached to a Silicon Atom

Functional group	ν (cm^{-1})	Class of compound
H—	2125—2150	Tetraalkyldisiloxanes
	2262 ($HSiCl_3$)	Alkylalkenylsilanes
CH_3—	1250—1258	Alkylalkenylsilanes
	1260—1267	Methylchlorosilanes
C_2H_5—	1235—1240	Alkylalkenylsilanes
n.-C_3H_7—	1207—1210	"
	(double)	
n.-C_4H_9—	1185—1187	"
	(double)	
C_6H_5—	1110—1120	Phenyl-substituted silanes
CH_2=CH—	955	Alkylvinylsilanes
	1008	
C=C (vinyl)	1595—1600	"
$=CH_2$ (terminal vinyl)	3040—3050	"
CH_2=CH—CH_2—	1155	Alkylallylsilanes
	1192	
C=C (allyl)	1625—1635	"
$=CH_2$ (terminal allyl)	3070—3080	"
—C≡C	2050	$C_2H_5(CH_3)_2SiC{\equiv}CH$
≡CH (monosubst.)	3285	"
C—	680—860	Alkylalkenylsilanes
Si—O—	1060—1070	Tetraalkyldisiloxanes
C—O—	1090—1100	Ethoxysilanes
Cl—	480—485	Alkylchlorosilanes
Cl_2—	469	Dialkyldichlorosilanes
	540	
Cl_3—	450—490	Alkyltrichlorosilanes
	570—600	

As for the frequencies of the valence and deformation vibrations of the CH_2 and CH_3 groups (the region around 3000 and 1450 cm^{-1}), their values remain practically the same as for hydrocarbons.

EXPERIMENTAL PART

The study of the infrared absorption spectra was carried out with the help of three instruments—two double-beam VIKS M-3 spectrophotometers with NaCl and LiF

prisms and a single-beam IKS-12 spectrometer with a KBr prism (certain bands (marked by crosses) were gone over with an NaCl prism on the latter instrument also). The spectral slit width for the instrument with an NaCl prism in the 1000 cm^{-1} region amounted to 10 cm^{-1}, with an LiF prism in the 3000 cm^{-1} region amounted to 6 cm^{-1}, and for the IKS-12 amounted to about 4 cm^{-1}. The spectra were studied at various layer thicknesses, which are indicated on the spectrograms (where there are no indications of the layer thickness, the substance was placed between two tightly-clamped salt windows). Some of the substances were studied in the form of solutions in carbon disulfide (the region below 1300 cm^{-1}), as a result of the high intensity of certain absorption bands of the silicon-organic compounds.

The author is grateful to I. V. Obreimov for his interest in the work, to V. F. Mironov and A. M. Polyakova for those substances obtained from them for which a need arose in the course of the work, and to R. A. Isaeva and E. D. Vlasov for their help in the work.

REFERENCES

1. A. M. Polyakova and N. A. Chumaevskii, Doklady Akad. Nauk SSSR 130, No. 5, 1037 (1960).
2. W. B. Steward and H. H. Nielsen, J. Chem. Phys. 2, 712 (1934); Phys Rev. 47, 828 (1935).
3. C. H. Tindal, J. W. Straley, and H. H. Nielsen, Proc. Natl. Acad. Sci. USA 27, 208 (1941).
4. I. F. Kovalev, Doklady Akad. Nauk SSSR 134, 559 (1960), Soviet Phys.-Doklady 5, No. 5 in press.
5. L. Bellamy, "Infrakrasnye spektry molekul" (Infrared Spectra of Complex Molecules). Izd. Inostrannoi Lit., Moscow, 1957. Wiley, London, 1954.
6. N. Wright and M. J. Hunter, J. Am. Chem. Soc. 69, 803 (1947).
7. C. W. Young, P. C. Servais, C. C. Currie, and M. J. Hunter, J. Am. Chem. Soc. 70, 3758 (1948).
8. R. E. Richards and H. W. Thompson, J. Chem. Soc. 124 (1949).
9. V. A. Kolesova and M. G. Voronkov, Chem. listy 51 (81), 4, 686 (1957).

THE VIBRATIONAL SPECTRA OF SILICATES
II. Infrared Absorption Spectra of Silicates and Germanates with Chain Anions

A. N. Lazarev and T. F. Tenisheva (pp. 79-85)

Received 20 April 1960

The absorption spectra of metasilicates and metagermanates containing one or two XO_4 tetrahedra per repeating unit of the chain are considered.

INTRODUCTION

The existence of complex anions in the form of infinite chains with one, two, three, four, five, or seven XO_4 tetrahedra per repeating unit has been shown by x-ray investigations of silicates, germanates, phosphates, and arsenates.[1] The number of internal chain vibrations which possess nonzero intensity equals $3pq - 4$, where q is the number of atoms in the "chemical" unit link of the chain, and p is the number of such links in the repeating unit.[2] Therefore, the spectra of chains with different numbers of XO_4 tetrahedra in the repeating unit must differ substantially, which affords a possibility of judging the structure of the chain from spectroscopic data. For the interpretation of the spectra of metasilicates and metagermanates, we have used the one-dimensional crystal model, which has been successfully employed to determine the selection rules (with the help of the theory of one-dimensional space groups) in the spectra of crystalline high polymers.[2-4] In assigning the frequencies in the spectra, we also took account of the results of the investigation of "model" silicon-organic compounds and silicates with Si_2O_7 groups[5,6] and the calculations of the frequencies of the pyroxene chain carried out by Stepanov and Prima.[7] In discussing the spectra we have paid attention to the data existing in the literature on the infrared reflection spectra and the Raman spectra of metasilicates.[8,9]

Sp

SPECTRA OF THE METAGERMANATES OF GROUP I METALS

The infrared absorption spectra of three crystalline metagermanates were investigated: Cu_2GeO_3, Na_2GeO_3, and Li_2GeO_3.

The metagermanates were obtained by fusion of germanium dioxide with the carbonate of the corresponding alkali metal (or with cupric oxide). After being briefly held at a temperature 50° above the melting point, the platinum crucible with the melt was quickly cooled. The homogeneity of the crystals obtained was checked by microscopic and x-ray phase analysis. In the preparation of Cu_2GeO_3, part of the copper was reduced, but large crystals of the metagermanate formed on the surface of the melt.

According to x-ray data,[10] the chain of germanium-oxygen tetrahedra in Cu_2GeO_3 contains one tetrahedron per repeating unit (four atoms) and has the following symmetry elements (Fig. 1) (aside from the identity element and pure translation along the chain axis): a plane of symmetry σ_x perpendicular to the chain axis, a plane of symmetry σ_y in which the Ge and —O— atoms lie, and a twofold axis of symmetry C_2. Thus the symmetry properties and selection rules for the eight nonzero fundamental vibrations of the chain are determined by the C_{2v} factor-group of the one-dimensional space group.[3,4] The four valence vibrations belong to symmetry types A_1 (two), B_1, and B_2 (Table 1). Of these four frequencies for the limiting vibrations of an infinite chain, three may be compared, in a qualitative description, with the triply degenerate vibration of an isolated GeO_4 tetrahedron, and one with its totally symmetric (breathing) vibration (Table 2). The form of the vibrations, naturally, is somewhat different. Thus, in the absorption spectrum of Cu_2GeO_3 (Fig. 2), the 868 cm^{-1} band may be ascribed to the vibration of type B_2 and the 724 and 780 cm^{-1} bands to the vibrations of types B_1 and A_1 which correspond to the F_2 vibration of the free GeO_4 tetrahedron. We ascribe the somewhat less intense band at 630 cm^{-1} to the vibration of type A_1 which corresponds to the breathing vibration of the isolated tetrahedron (i.e., to the symmetric GeOGe

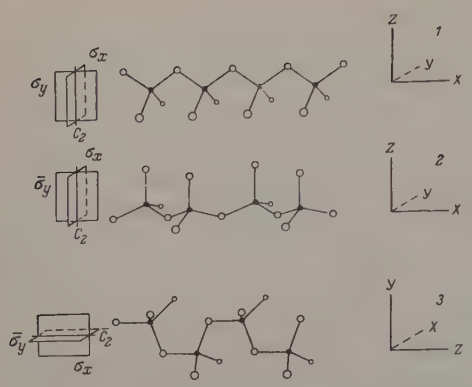

Fig. 1. Various forms of chains of types $(XY_3)_\infty$ and $(X_2Y_6)_\infty$ and their symmetry elements. 1—$(XY_3)_\infty$ (Cu_2GeO_3 structure); 2—$(X_2Y_6)_\infty$ (pyroxene structure); 3—$(X_2Y_6)_\infty$ (Li_2GeO_3 and Na_2GeO_3 (Li_2SiO_3 and Na_2SiO_3) structure). Symbols: C_n and σ_i—axes and planes of symmetry; $\overline{C}_n$ and $\overline{\sigma}_i$—screw axes and glide-reflection planes.

vibration in the chain).* The intense broad band around 535 cm^{-1} is probably associated with deformation vibrations of the chain, which are close in frequency to the vibrations of the metal-oxygen polyhedra, and therefore are not considered within the framework of the isolated-chain model.

*The proposed interpretation is in satisfactory correspondence with the possible values for the frequencies of the GeO_4 ion. The spectrum of this ion has not been described, but the frequencies 676 and 770 cm^{-1} have been obtained for the ion $(H_2GeO_4)^{2-}$ in the absorption spectrum of SrH_2GeO_4.[15]

Table 1. Symmetry Types and Number of the Valence Vibrations of Chains of Types $(XY_3)_\infty$ and $(X_2Y_6)_\infty$

Factor group	Symmetry elements			Selection rules		Orientation of the change in dipole moment (with respect to the chain axis)		Number of tetrahedra (atoms) in the repeating unit	
C_{2v}	C_2	σ_x	σ_y					1 (4)	2 (8)
Symmetry types of the vibrations	Characters			Ram.	IR	C_2 axis ⊥ chain axis	C_2 axis ∥ chain axis	Number of valence vibrations	
A_1	+1	+1	+1	P	a	⊥	∥	2	3
A_2	+1	−1	−1	DP	i	—	—	—	1
B_1	−1	+1	−1	DP	a	⊥	⊥	1	3
B_2	−1	−1	+1	DP	a	∥	⊥	1	1

*Symbols: Ram.—Raman spectrum, IR—infrared absorption spectrum; characteristics of the vibration: a—active, i—inactive; P—polarized, DP—depolarized.

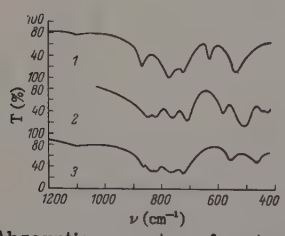

Fig. 2. Absorption spectra of metagermanates (pressed discs with KBr). Curve 1—Cu_2GeO_3 (7 mg); curve 2—Li_2GeO_3 (5 mg); curve 3—Na_2GeO_3 (5 mg). Sample weight for all was 2 gm for a diameter of 25 mm.

Table 2. Valence Vibrations of XY_4 Groups and of Chains Formed by Them

Structure	Symmetry group (factor-group)	Symmetry types of the vibrations*							
XY_4 tetrahedron	T_d	F_2						A_1	
Chain of tetrahedra $(XY_3)_\infty$	C_{2v}	B_2 as_{XYX}		B_1 as_{YXY}		A_1 s_{YXY}		A_1 s_{XYX}	
Chain of tetrahedra $(X_2Y_6)_\infty$ (pyroxene structure; C_2 axis ⊥ to chain axis)	C_{2v}	B_2 as'_{XYX} ω_4	B_1 as_{XYX} ω_6	B_1 as'_{YXY} ω_7	A_1 as_{YXY} ω_3	A_1 s_{YXY} ω_2	A_2 s'_{XYX} ω_8	B_1 s'_{YXY} ω_5	A_1 s_{XYX} ω_1
Chain of tetrahedra $(X_2Y_6)_\infty$ (Na_2GeO_3 and Na_2SiO_3 structure; C_2 axis ∥ chain axis)	C_{2v}	B_1 as'_{XYX}	A_1 as_{XYX}	B_2 as'_{YXY}	A_2 as_{YXY}	A_1 s_{YXY}	B_1 s'_{XYX}	B_1 s'_{YXY}	A_1 s_{XYX}

*Symbols: s—symmetric, as—antisymmetric (vibrations within the isolated XYX or XY_3 group are being considered); the prime denotes vibrations which are opposite in phase in adjoining XYX or XY_3 groups; ω_i is the numbering of the vibrations of the pyroxene chain in Stepanov and Prima's work.[7]

The more complicated appearance of the spectra of Na_2GeO_3 and Li_2GeO_3 may be associated with differences in the form of the chains. In these crystals,[11,12] the chains contain, like the pyroxenes, two tetrahedra per repeating unit, but all the X—O—X bonds lie in one plane (Fig. 1), and the chain axis is a twofold screw axis. The vibrational spectrum of the chain may be considered on the basis of the factor-group C_{2v} obtained by excluding translational elements from the one-dimensional space group. In connection with the doubling of the unit cell of the chain in comparison with Cu_2GeO_3, there must be observed in the spectrum eight valence vibrations, of which six correspond to the triply degenerate and two to the breathing vibration of the GeO_4 tetrahedron (these two vibrations correspond to the breathing of the two tetrahedra in one repeating unit "in phase" and "in opposite phase"). One (type A) falls in the low-frequency region of the spectrum.

The assignment of the observed frequencies is given in Table 3. The group of intense bands between 700 and 870 cm^{-1} is associated with the anticipated five (or six) OGeO (symmetric and antisymmetric) and GeOGe (antisymmetric) vibrations. Then the bands at 582 and 506 cm^{-1} in the Li_2GeO_3 spectrum (557 and 464 cm^{-1} in the Na_2GeO_3 spectrum) may be ascribed to two vibrations (A_1 and B_1) of the types ν_s(GeOGe) and ν_{as}(GeOGe). It may here be supposed that the type A_1 vibration has a higher frequency than B_1 does. We have obtained the Raman spectrum of a glass close to potassium metagermanate in composition (48% K_2O, 52% GeO_2), and we have found the following frequencies: 840, 790 (on a background of the 860-780 cm^{-1} band), 505, and a weaker little band around 370 cm^{-1}. This allows us to ascribe the frequencies 840, 790 and 505 cm^{-1} in K_2GeO_3 to valence vibrations of type A_1, the last of these frequencies apparently corresponding to the 582 and 557 cm^{-1} bands in the Li_2GeO_3 and Na_2GeO_3 spectra (since there is a tendency toward a lowering of the frequencies on going from Li to Na and, probably, to K). An approximate calculation of the pyroxene chain according to the formulas of ref. 7, with the replacement of Si atoms by Ge, also gives $\nu_{A_1} > \nu_{B_1}$. Thus, for $k_{Ge-O^-} = k_{Ge-O(Ge)} = k$, the frequency values are expressed in the following way in terms of k: $0.285 \times k^{1/2}$, $0.270 \times k^{1/2}$, $0.146 \times k^{1/2}$ (A_1); $0.285 \times k^{1/2}$, $0.270 \times k^{1/2}$, $0.105 \times k^{1/2}$ (B_1); $0.360 \times k^{1/2}$ (B_2); $0.182 \times k^{1/2}$ (A_2).

Table 3. Frequencies in the Absorption Spectra of Metagermanates (cm^{-1})*

Compound	Cu_2GeO_3	Li_2GeO_3	Na_2GeO_3
Structure of the anion	$(GeO_3)_\infty$ chain	$(Ge_2O_6)_\infty$ chain	
Ge-O deformation vibration?	535 vs	427 m 447 m	— —
GeO_4 tetrahedron $(GeO_3)_\infty$ chain			
A_1 ν_s(GeOGe)	630 m A_1	506 vs** 582 s	464 m B_1 557 m A_1
F_2 ν_s(OGeO)	724 vs A_1	707 vs 761 vs	721 s A_2 770 vs $2A_1$,
F_2 ν_{as}(OGeO)	780 vs B_1	809 vs 820 vs	$2B_1$,
F_2 ν_{as}(GeOGe)	868 vs B_2	848 vs 857 vs	835 s 866 s B_2

*Symbols for band intensities: vs—very strong, s—strong, m—medium intensity.
**It is possible that there are poorly-resolved secondary maxima around 520 and 482 cm^{-1}.

ALKALI METASILICATES

In crystals of alkali metasilicates there are planar chains of tetrahedra, similar to the chains in the alkali metagermanates but characterized, apparently, by somewhat larger values of the SiOSi angles than for GeOGe.[13,14] These chains possess the same symmetry elements and contain two tetrahedra per repeating unit, in consequence of which the number of valence vibrations and their distribution among the symmetry types is the same as in the germanates (Tables 1 and 2). The absorption spectra of Li_2SiO_3 and of Na_2SiO_3 are presented in Fig. 3.* An

*The samples of crystalline and glassy alkali metasilicates were prepared by Yu. A. Shmidt and were subjected to microscopic and x-ray checking.

attempt at the interpretation of the spectra of given in Table 4. As in the case of the alkali metagermanates, the vibrations of the metasilicate chains may more expediently be classified as vibrations of the SiOSi and O^-SiO^- groups and not by matching them with the vibrations of the isolated SiO_4 tetrahedron. (For the correspondence between the two methods of description, see Table 2.) This ensues from the following considerations. It follows from the calculations of Stepanov and Prima[7] that, in the pyroxene chain, the two lowest-frequency vibrations are ν_s(SiOSi)(A_1) and $\nu_{s'}$(SiOSi)(A_2) (in the al-

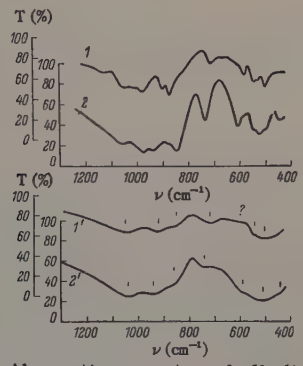

Fig. 3. Absorption spectra of alkali metasilicates (pressed discs with KBr). Curve 1—Na_2SiO_3 (crystalline, 5 mg); curve 2—Li_2SiO_3 (crystalline, 5 mg); curve 1′—Na_2SiO_3 (glassy, 5 mg); curve 2′—Li_2SiO_3 (glassy, 5 mg).

kali metasilicate chains, these vibrations are related to symmetry types A_1 and B_1). In just the same way, it has been shown, in the study of the $SiO_4 \rightarrow Si_2O_7$ transition,[5] that when the breathing vibration of the tetrahedron is split, only one component falls in the low-frequency region of the spectrum—this may be considered as the ν_s(SiOSi) vibration—but the other component appears in the region 850-1100 cm^{-1}.

One may expect that, in the spectra of glassy metasilicates, two bands must be contained in the region 580-740 cm^{-1} if there exists in the chain of tetrahedra the same repeating unit as in the crystal, even though with some distortions. If the repeating unit is different or the distortions in the shape of the chain are so great that it is impossible to pick out groups of tetrahedra oriented in an approximately repeating fashion, then the number of bands in the spectrum in the indicated region may be different, or there will appear only one washed-out band in the whole region. The spectrum of glassy Li_2SiO_3, presented in Fig. 3, permits us to confirm that two bands in the indicated frequency range are retained during the transition to glass. The spectrum of glassy Na_2SiO_3 proved to be so washed-out that this conclusion cannot be made with full certainty; however, the Raman-spectrum

Table 4. Frequencies (cm^{-1}) in the Infrared Spectra of Metasilicates with $(Si_2O_6)_\infty$ Anions*

Structure type	Alkali metasilicates					Pyroxenes					
Compound	Li_2SiO_3		Na_2SiO_3		Symmetry of the vibration	$NaFe^{III}Si_2O_6$ (aegirite)	$CaFe^{II}Si_2O_6$ (hedenbergite)	$CaMgSi_2O_6$** (diopside)	$(MgFe)_2Si_2O_6$** (bronzite)	$NaAlSi_2O_6$*** (jadeite)	Symmetry of the vibration
	кристалл	glass	crystal	glass							
Si-O deformation vibrations (and M-O valence vibrations in the pyroxenes)	447 m 500 s 521 s	440 s — 510 vs	452 s — 534 s	— 490— —520 s	— — —	467 s 507 s 545 s	466 vs 492 vs 518 vs	— 511 519	— — 523	442 463—500 532	— — —
SiO_4 tetrahedron $(Si_2O_6)_\infty$ chain	545 m	—	545 s	545 s	—	560 s	—	564	557	590	—
A_1 ν_s (SiOSi)	(587 vw)						(616 ?)				
F_2 $\nu_{s'}$ (SiOSi)	605 m	595 m	583 m (667 vw)	?	A_1	639 m	624 m	645	647	663	A_1
A_1 $\nu_{s'}$(OSiO)	736 m	740 m	716 m	720 m	B_1	725 w	663 m	677	—	744	A_2
ν_s(OSiO)	847 vs	860 s	873 s	850 s	B_1						B_1
ν_{as}(OSiO)	879 s	—	898 s	—	A_1	864 s	860 vs	—	877	858	A_1
F $\nu_{as'}$(OSiO)	—	—	—	—	A_2	897 s	912 vs	930	934	926	A_1
$\nu_{as'}$(SiOSi)	942 vs	940 vs	976 s	920 s	B_2	950 vs	959 vs	970	970	—	B_1
$\nu_{as'}$(SiOSi)	973 vs	—	1007 s	—	A_1	1004 vs	1056 vs	1014	1014	995	B_1
	1055 s	1040 vs	1043 s	1050 s	B_1	1059 vs	1089 vs	1117	1104	1064	B_2
			(1117 w)			(1414 s)****					

*The frequencies of weak bands not related to fundamental vibrations of the chains are enclosed in parentheses. Symbols for band intensities: vs—very strong; s—strong; m—medium; w—weak; vw—very weak.
**Reflection spectra according to the data of Matossi.[8]
***Absorption spectra according to the data of Kolesova.[15]
****Band of the CO_3 ion.

data existing in the literature confirm the presence of a band around 600 cm^{-1}.[9] The fact that this band is polarized serves as confirmation of the assignment given in Table 4.

SPECTRA OF THE PYROXENES

Metasilicates with the pyroxene structure represent quite an extensive group of minerals. We have confined outselves to consideration of the spectra of the two pyroxenes investigated by us—aegirite $NaFe^{\cdots}Si_2O_6$ and hedenbergite $CaFe^{\cdot\cdot}Si_2O_6$—and of the reflection spectra of diopside $CaMgSi_2O_6$ and bronzite $(Mg,Fe)_2Si_2O_6$ presented in the work of Matossi.[8] The number of valence vibrations of the pyroxene chain and their distribution among the symmetry types may be obtained with the help of the factor-group isomorphous with C_{2v}, as in the case of the alkali metagermanates and metasilicates. However, in the pyroxene chain the C_2 axis is perpendicular to the chain axis; this must lead to differences in the spectrum, which may be discovered during investigations in polarized light (see Table 1). One may expect the appearance of six bands in the 800-1100 cm^{-1} region and two bands corresponding to the vibrations ν_s(SiOSi) and $\nu_{s'}$(SiOSi).* The frequencies in the spectra of the pyroxenes (Fig. 4) and their assignment are given in Table 4. The spectrum of an aluminum-containing pyroxene—jadeite—is presented there also. It has been shown by Kolesova that the vibration frequencies of the Al—O bond lie in the 750 cm^{-1} region for silicates containing Al atoms in the skeleton (the complex anion), and diminish significantly on going over to compounds in which the Al atoms play the role of cations.[15] Inasmuch as the Al atoms in jadeite do not enter into the anion and are relatively weakly bonded to the O atoms, it may be that the 663 and 744 cm^{-1} bands are due to vibrations of the pyroxene chain and that the Al—O vibration frequencies lie around 600 cm^{-1} and below.

*One of these vibrations belongs to type A_2, which is inactive in the infrared spectrum of the chain. However, allowance for the symmetry of position (site-symmetry) of the complex ions in the pyroxene crystals lifts this prohibition.

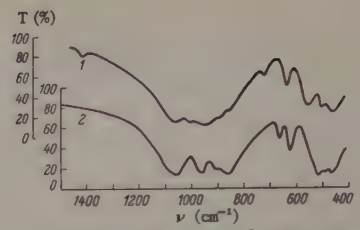

Fig. 4. Absorption spectra of pyroxenes (pressed discs with KBr). Curve 1—aegirite $NaFe^{\cdots}Si_2O_6$ (5 mg); curve 2—hedenbergite $CaFe^{\cdot\cdot}Si_2O_6$ (5 mg).

CONCLUSION

Comparison of the spectra of metagermanates and metasilicates possessing different numbers of XO_4 tetrahedra in the repeating unit of the chain testifies to the possibility of investigating the structure of these and similar compounds by spectroscopic methods. In this connection, the greatest interest in the spectra of the metasilicates is presented not by the 800-1100 cm^{-1} region, since the number of frequencies in this region in the spectra of the chains is large and a complete identification of them is difficult, but by the 550-750 cm^{-1} region, which usually does not contain absorption bands in the spectra of orthosilicates. The number of frequencies in this region which correspond to a symmetric vibration of the SiOSi group apparently enables us to judge of the number of tetrahedra in the repeating unit of the chain. The methods described, however, may be applied only to specimens in which the vibration frequencies of the metal-oxygen bonds are sufficiently low, and these vibrations must not interact strongly with the valence vibrations of the chain.

A discussion of the spectra of silicates containing three and more SiO_4 tetrahedra in the repeating unit will be published later.

REFERENCES

1. N. V. Belov, Mineral. Sbornik, L'vovsk. Geol. Obshchestra No. 13, 23 (1959);
F. Liebau, Acta Crust. **12**, 177 (1959).
2. C. J. Liang, S. Krimm, and G. B. B. M. Sutherland, J. Chem. Phys. **25**, 543 (1956).
3. C. J. Liang, J. Mol. Spectrosc. **1**, 61 (1957).
4. M. C. Tobin, J. Chem. Phys. **23**, 891 (1955).
5. A. N. Lazarev, Opt. i Spektr. **9**, 195 (1960), Optics and Spectroscopy **9**, 103 (1960).
6. A. N. Lazarev and M. G. Voronkov, Opt. i Spektr. **8**, 614 (1960), Optics and Spectroscopy **8**, 325 (1960).
7. A. M. Prima, Trudy Inst. Fiz. i Mat., Akad. Nauk Belorus.SSR, No. 2, 124 (1957);
B. I. Stepanov and A. M. Prima, Opt. i Spektr. **4**, 734; Ibid. **5**, 15 (1958).
8. C. Schaefer, F. Matossi, and K. Wirtz, Z. Physik. **89**, 210 (1934).
9. Ya. S. Bobovich, O. P. Girin, and T. P. Tulub, Doklady Akad. Nauk SSSR **105**, 61 (1955);
Ya. S. Bobovich and T. P. Tulub, Opt. i Spektr. **2**, 174 (1957); Uspekhi Fiz. Nauk **66**, 3 (1958), Soviet Phys.-Uspekhi **1**, No. 1, 1 (1958).
10. J. Genetti, Bull. soc. chim. Belges **63**, 209 (1954).
11. H. Hahn and U. Theune, Naturwiss. **44**, 33 (1957).
12. J. Ginetti, Bull. soc. chim. Belges **63**, 460 (1954).
13. A. Grund and M. Pizy, Acta Cryst. **5**, 837 (1952).
14. G. Donnay and J. D. H. Donnay, Am. Mineralogist **38**, 163 (1953);
H. Seemann, Acta Cryst. **9**, 251 (1956).
15. V. A. Kolesova, Opt. i Spektr. **6**, 38 (1959), Optics and Spectroscopy **6**, 20 (1959).

ON THE MECHANISM OF THE TRANSITION OF EXCITED ORGANIC MOLECULES INTO THE METASTABLE STATE

G. A. Mokeeva and B. Ya. Sveshnikov (pp. 86-90)

Received 21 April 1960

The influence of temperature on the duration of fluorescence and phosphorescence and on the relative emission of phosphorescence of five organoluminors, of which three have α- and β-phosphorescence, and two only β-phosphorescence, has been investigated. It is shown that for the first three luminors, a rise in temperature leads to an increase of the emission of phosphorescence and a decrease of the duration of fluorescence. Both these phenomena are explained by the assumption that the probability of transition of the excited molecule into the metastable state depends on the supply of vibrational energy in the molecule.

The fundamental achievement of Jablonski's scheme[1] was the explanation of the nature of the two phosphorescences (which differ in the spectral location of the bands) of organic molecules. The question of the mechanism by which the molecule gets into the metastable (phosphorescent) state was not considered by him. This mechanism was considered in detail for the first time in the article of Lewis, Lipkin, and Magel.[2] These authors propose that the molecule passes into the phosphorescent state directly from those levels which it occupies as the result of excitation; the conversion of all energy of excitation of the molecule into vibrational energy is the intermediate step in the transition into the phosphorescent state. At a certain stage of degradation of the vibrational energy, the molecule can get into the phosphorescent state. Similar views can be found also in the article of Terenin,[3] in which the nature of the metastable state of organic molecules was explained.

In 1947 and 1948, it was shown by one of us[4] that the excited molecule gets into the phosphorescent state from the fluorescent state, that is, after conversion into heat of the excess vibrational or electronic energy, obtained in the process of excitation, not during the process of conversion. Thus the hypothesis was advanced that the indicated transition is accomplished with a probability r, not depending on time as does the probability of radiation.

In accordance with this hypothesis and additional assumptions that probabilities (frequencies) of nonradiating deactivation (quenching) of fluorescent (q_1) and phosphorescent (q_2) levels do not depend on time, and that static quenching is absent, formulas were obtained[5] connecting the values of the relative quantum emission of phosphorescence (φ) with probabilities of different transitions between the fluorescent, phosphorescent, and normal levels

$$\varphi = \frac{p\rho r\tau_1\tau_2}{p(1+\rho r\tau_1\tau_2)+r\pi\tau_2} + \frac{r\pi\tau_2}{p(1+\rho r\tau_1\tau_2)+r\pi\tau_2}, \qquad (1)$$

where p and π are probabilities of radiation transitions from fluorescent and phosphorescent levels to a normal level; ρ is the probability of transition from the fluorescent level to the phosphorescent level on account of thermal fluctuations. The durations of fluorescence (τ_1) and phosphorescence (τ_2) are determined by the following expressions:

$$\tau_1 = (p+q_1+r)^{-1} \text{ and } \tau_2 = [\pi+q_2+\rho(1-r\tau_1]^{-1}. \qquad (2)$$

In those cases where $\rho = 0$, that is, where there is only long wavelength phosphorescence (β-phosphorescence),

$$\varphi = \frac{r\pi\tau_2}{p+r\pi\tau_2}. \qquad (3)$$

On the contrary, at $\rho \gg \pi$ or when there is only short wavelength phosphorescence (α-phosphorescence),

$$\varphi = \frac{\rho r\tau_1\tau_2}{1+\rho r\tau_1\tau_2}. \qquad (4)$$

The experiments of Lewis, Lipkin and Magel showed that in the temperature range 186°-258° the duration of phosphorescence changes very little with temperature. These results served as an important argument in favor of two assertions: firstly, that the transition from the phosphorescent level to the normal level with radiation is a spontaneous process, and secondly, that over the indicated temperature range, temperature quenching, which depends upon the lifetime of the molecule in the metastable state, is practically absent. If all other forms of quenching are absent ($q_2 = 0$), then

$$\varphi = \frac{r}{p+r}. \qquad (5)$$

The same result is obtained also for α-phosphorescence where $\rho \gg \pi$, if an additional assumption is made that quenching is absent at the fluorescent level ($q_1 = 0$).

As the probability of spontaneous emission from the fluorescent level to the normal level (p) does not depend upon temperature, so from (3), (4), and (5) it follows that if r likewise does not depend upon temperature, then the largest value of the emission of phosphorescence can be expected at low temperatures.

However, the results of certain experiments carried out in our laboratory in the years 1955-1957 contradicted this trivial deduction. Thus, Kudryashov found that by excitation in the anti-Stokes region of luminescence of sugar candies activated by acridine orange, the relative emission of phosphorescence falls to zero on going from room temperature to the temperature of liquid air. A little later Pilipovich noticed that the emission of phosphorescence of boric phosphorus, activated by fluorescein, at room temperature appreciably exceeds the emission of these phosphors at the temperature of liquid air. And finally, Bauer and Baczynski,[6] studying with the same phosphors the dependence of the relative emission of phosphorescence upon the wavelength of the exciting light, arrived at the conclusion that the probability of the transition from the labile to the metastable state is greater for high vibrational levels than for low levels. These observations prompted us to a more detailed investigation of the influence of temperature on the relative emission of phosphorescence.

As the object for our investigation, organoluminors having two bands of luminescence were taken—boron-glycerine activated by fluorescein, sugar candy activated by tripaflavin, and acridine orange—and also organolumi-

nors having one band of luminescence—sugar candy activated by aesculin, and boric phosphorus activated by phthalimide. For the excitation of the colored luminors, the mercury lines at 407 and 436 millimicrons were used; for the colorless—313 and 366 millimicrons.

The relative emission of phosphorescence is equal to the ratio of the number of quanta radiated in phosphorescence over a short time interval (short in comparison with its lifetime), immediately after stopping the excitation, to the total number of quanta radiated for the same time interval during excitation. For the determination of emission we used two arrangements. The first technique used a double-chopper phosphoroscope, monochromator, and galvanometer. In the second arrangement, the galvanometer was replaced by an oscilloscope having a screen with a prolonged luminescence, and the Becquerel phosphoroscope was replaced by a shutter for quick stopping of the excitation.* Finally, in this case, when

*Simultaneously with stopping of excitation, the light filter which reduced the luminescence was removed so that readings on the screen of the oscilloscope for phosphorescence are sufficiently large.

the spectra of both kinds of luminescences are not overlapping, the relative quantum emission of phosphorescence can be determined straightforwardly from the spectrum of the total luminescence. For the determination of the duration of phosphorescence, the arrangement described earlier[7] was used, but the duration of fluorescence was measured with the aid of a phase fluorometer.[8]

In the Figure is presented the spectra of total luminescence and phosphorescence of the luminors activated by tripaflavin, acridine orange, aesculin, and phthalimide at 20° and −183°,* and in the Table are presented our

*Spectra of luminescence of the boron-glycerine luminor led to another article.[9]

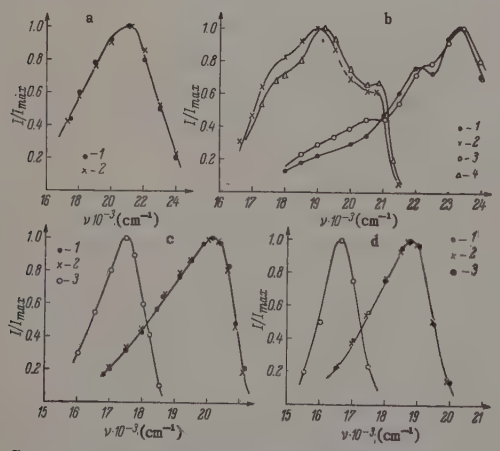

Spectra of radiation of organoluminors at different temperatures. A—phthalimide in boric acid (C = 5 × 10⁻³ gm/gm) 1—phosphorescence at t = 20°C, 2—phorphorescence at t = −183°C; B—aesculin in sugar candy (C = 5 × 10⁻⁴ gm/gm) 1—total luminescence and 2—phosphorescence at 20°C, 3—total luminescence and 4—phosphorescence at −183°C; C—tripaflavin (C = 1 × 10⁻⁴ gm/gm) and D—acridine orange (C = 5 × 10⁻⁵ gm/gm) in sugar candy 1—total luminescence and 2—phosphorescence at t = 20°C, 3—phosphorescence at t = −183°C.

Luminor	φ_{ph} (expt.)		τ_{ph} (sec)		$\tau_{11} \cdot 10^6$ (sec)		φ_{ph} (calc.)
	20°	−183°	20°	−183°	20°	−183°	20°
Phthalimide in boric acid (C = 5 · 10⁻³ gm/gm)	1	1	1.25	1.5	—	—	—
Aesculin in sugar candy (C = 5 · 10⁻⁴ gm/gm)	0.05	0.13	0.35	1.2	4.15	4.4	—
Fluorescein in boron-glycerine (C = 5 · 10⁻⁴ gm/gm)	0.4	0.2	0.85	2.8	4.35	4.9	0.30
Tripaflavin in sugar candy (C = 1 · 10⁻⁴ gm/gm)	0.16	0.06	0.3	2.5	5.6	6.0	0.13
Acridine orange in sugar candy (C = 5 · 10⁻⁵ gm/gm)	0.12	0.025	0.24	2.1	5.6	6.0	0.085

values of the relative emission and the duration of phosphorescence and also the duration of fluorescence. The Table begins with boric phosphorus activated by phthalimide. These phosphors have only phosphorescence; as the duration of phosphorescence remains essentially unchanged with temperature, evidently in the metastable level there is no quenching during the time interval. In order to examine whether there are other kinds of quenching, and in particular quenching at the labile level, a comparison was made of the emission of luminescence of these phosphors at 20° and −183° when there is complete absorption of the exciting light; and it is shown that it practically does not change. However, in the case of the luminors which have both bands of phosphorescence, a very important increase of emission of phosphorescence is observed on changing from the temperature of liquid air to room temperature. Simultaneously the duration of fluorescence grows shorter, that is, there is a temperature extinction of fluorescence.

From expressions (1) and (4) it is evident that the increase of emission of phosphorescence with an increase in temperature in the given case can be explained only on account of an increase with temperature of the r value, that is, of the probability of the transition from the fluorescent to the metastable state. But the increase of r with temperature must be considered as temperature quenching of fluorescence and must lead to a decrease in the duration of fluorescence. From this it follows that the value of the probability of transition into the metastable state at any temperature whatsoever (r) is connected with the value of this probability for very low temperatures (r_0) by the relation:

$$r = \frac{\tau_{10} - \tau_{11}}{\tau_{10}\tau_{11}} + r_0, \qquad (6)$$

where τ_{10} is the value of the duration of fluorescence for the temperature of liquid air, and τ_{11} is the value for some temperature at which perceptible temperature quenching of fluorescence exists.

Let us assume that for the last three organoluminors mentioned in the Table, the temperature quenching at the metastable level is absent at all temperatures ($q_2 = 0$), and at the fluorescent level other temperature quenching is absent, except the increase of r with increasing temperature ($q_1 = 0$). By these assumptions, r_0, that is, the probability of the transition from the fluorescent to the phosphorescent state at the temperature of liquid air, is easily determined from (5)

$$\varphi_0 = \frac{r_0\tau_{10}}{1 + r_0\tau_{10}}, \qquad (7)$$

where for the values φ_0 and τ_{10}, data is taken from the Table.

Now, having determined r for room temperature from the value of τ_{11}, that is,

$$\tau_{11} = \frac{1}{p + r}, \qquad (8)$$

nd having calculated ρ from (2), it is not difficult to find he expected value of the relative emission of phosphores-ence φ for room temperature; these values led to the ast column of the Table. It is easy to see that they are ear enough to the experimental values (first column).

Aesculin, having only β-phosphorescence at all tem-eratures, the emission and duration of luminescence rops with an increase of temperature. As there is like-vise a change of duration of fluorescence, so also there s a temperature quenching of fluorescence, treated in ccord with the above-stated as the increase of the prob-bility of the transition of the molecule into the meta-stable state.

It is possible to carry out the quantitative calcula-ions of the expected value of emission at room temper-ture in that case, only if it is assumed that the changes f the relative emission of phosphorescence as a result f quenching on the metastable level are proportional to he changes of the duration of phosphorescence. By such n assumption, we obtain a value of 0.07 (experimental alue 0.05) for relative emission.

We think that the results of the temperature experi-ments explained in this paper, together with the data of udryashov, Bauer, and Baczynski on the anti-Stokes xcitation of organoluminors, gives completely conclu-sive evidence for the statement that the probability of the transition into the metastable state does depend on the supply of vibrational energy of the excited molecule.

REFERENCES

1. A. Jablonski, Nature **131**, 839 (1933); Z. Physik **94**, 38 (1935).
2. G. Lewis, D. Lipkin, and Th. Magel, J. Am. Chem. Soc. **63**, 3005 (1941).
3. A. N. Terenin, Acta Physico-chim. URSS **18**, 210 (1943).
4. B. Ya. Sveshnikov, Doklady Akad. Nauk SSSR **58**, 49 (1947).
5. B. Ya. Sveshnikov, Zhur. Eksptl. i Teoret. Fiz. **18**, 878 (1948).
6. R. Bauer and A. Baczynski, Bull. acad. polon. sci. **6**, 2, 113 (1958).
7. V. A. Pilipovich and B. Ya. Sveshnikov, Opt. i Spektr. **4**, 116 (1958).
8. A. M. Bonch-Bruevich, V. A. Molchanov, and V. I. Shirokov, Izvest. Akad. Nauk SSSR, Ser. Fiz. **20**, 496 (1956).
9. G. A. Mokeeva and B. Ya. Sveshnikov, Opt. i Spektr. **9**, 601 (1960), Optics and Spectroscopy **9**, 317 (1960).

ELECTROLUMINESCENCE OF A POWDERED ZnS:Cu:Mn ELECTROLUMINOR IN A DC FIELD

V. N. Favorin and G. S. Kozina (pp. 91-95)

Received 2 September 1959

Luminescence characteristics in a dc field are given for solid electroluminescent layers prepared from a ZnS:Cu:Mn phosphor mixed with melamine-formaldehyde and alkyd resins. A mechanism is described which explains the results obtained.

Polycrystalline zinc sulfide compressed between lectrodes or placed in a semiconducting medium (tri-resylphosphate) is known to be capable of luminescing n a dc field. The intensity of this electroluminescence s very low and emission is observed only at isolated oints.[1]

We observed bright electroluminescence under dc oltage in a layer prepared from the yellow ZnS:Cu:Mn hosphor placed in a dielectric medium.[2-4] This lumi-escence occurs in a solid or a liquid dielectric and is bserved when manganese is included as one of the ac-ivators of the electroluminor.

The so-called "green" ZnS:Cu phosphors also ex-ibit a weak electroluminescence in a dc field. It appears s individual scintillating blue points.

We give below the dc luminescence characteristics f solid electroluminescent layers prepared from a ZnS:Cu:Mn phosphor mixed with melamine-formaldehyde nd alkyd resins. As electrodes, we used a layer of tin xide on glass and an evaporated layer of aluminum.

1. THE SPECTRAL CHARACTERISTICS OF THE LUMINESCENCE IN A DC FIELD

Figure 1 shows the spectral characteristics of the ZnS:Cu:Mn phosphor in a dc (curve 1) and ac fields of different frequencies (curves 2 and 3). We see from this figure that the short wavelength emission bands observed in an ac field are absent in the dc case. We may conclude, therefore, that dc luminescence is governed essentially by the manganese centers.

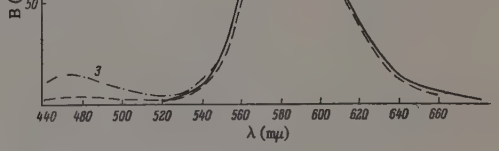

Fig. 1. Spectral characteristics of the ZnS:Cu:Mn electroluminor in a dc field (curve 1) and in ac fields of different frequencies (curve 2, 400 cycles, curve 3, 3000 cycles).

Thus all of the characteristics given below for a ZnS:Cu:Mn phosphor in a dc field refer solely to emission by manganese centers.

2. TIME VARIATION OF THE BRIGHTNESS OF LUMINESCENCE AND THE CONDUCTIVITY CURRENT THROUGH THE LAYER IN A DC FIELD

The brightness B of luminescence in a dc field and the conductivity current J through a solid layer of phosphor in a dielectric (a mixture of alkyd and melamine-formaldehyde resins) decrease with time. (See Fig. 2.) These time variations are observed only at fairly high conductivity currents (above 10^{-5} amp/cm^2) and increase with the current. After the voltage has been maintained for a definite length of time (aging), the values of the brightness and the current become stabilized. These changes in the properties of the electroluminescent layer are irreversible and are apparently connected with irreversible changes in the structure of the layer caused by the passage of the dc current.

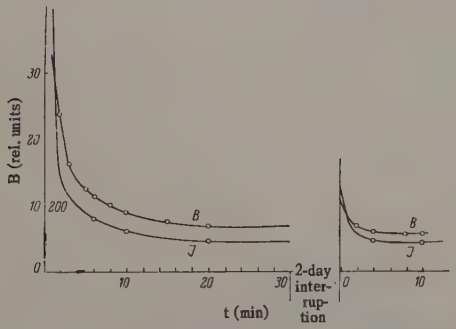

Fig. 2. Time variation of B, the brightness of luminescence in a dc field, and of J, the conductivity current through the layer.

Simultaneously with the irreversible changes in the properties of the layer, we also observed reversible changes, which are apparently connected with polarization processes. After the termination of the field action and a "rest period," the electroluminescent brightness increases somewhat but soon falls again to the former level. (See Fig. 2.)

The irreversible changes in the layer caused by passage of the dc current manifest themselves not only in changes in brightness and conductivity, but also in changes in the dependence of these quantities on the applied field.

3. THE DEPENDENCE ON VOLTAGE OF THE BRIGHTNESS OF LUMINESCENCE AND OF THE CONDUCTIVITY CURRENT THROUGH THE LAYER

Figure 3 shows a log-log slot of the brightness B and the conductivity current J of the ZnS:Cu:Mn phosphor in a dielectric as a function of the average voltage of the field. These values are given for the layer prior to aging (curves 1 and 2) and after aging for one hour at maximum voltage (curves 3 and 4). The same figure shows also the characteristic B(E) for excitation of the layer by a sinusoidal ac field (curve 5).

In the voltage range studied, B(E) and J(E) are exponential functions of E:

$$B = KE^{\alpha},$$

$$J = ME^{\beta}.$$

A comparison of the curves presented in Fig. 3 shows the following:

(a) The nonlinearity of the characteristics B(E) and

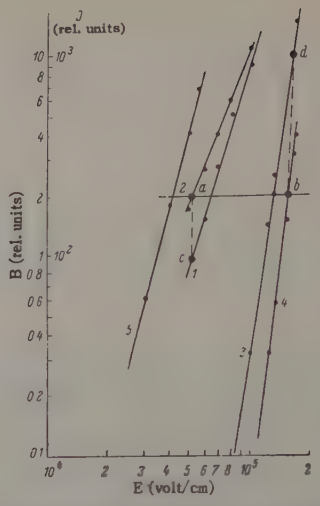

Fig. 3. The brightness B and conductivity current J as functions of E, the voltage gradient across the layer. Before aging: curve 1—B(E), $\alpha = 3.3$; curve 2—J(E), $\beta = 2.6$. After aging: curve 3—B(E), $\alpha = 7$; curve 4—J(E), $\beta = 8.2$, curve 5—B(E) in an ac field, $\alpha = 4$.

J(E), which is determined by the exponents α and β, increases with aging.

(b) These exponents are almost the same; in the process of aging, however, β increases faster than α.

(c) The exponent α of an aged electroluminescent layer is much higher in the case of a dc than an ac field.

4. BRIGHTNESS IN A DC FIELD AS A FUNCTION OF THE CONDUCTIVITY CURRENT THROUGH THE LAYER

The experimental data presented above lead to the following power dependence of the brightness B on the current J

$$B = LJ^{\frac{\alpha}{\beta}},$$

where L is a constant coefficient. Since α and β have different rates of variation during the aging process, the exponent in the B(J) characteristic decreases, passing through unity. (See Fig. 4.) Figure 4 contains curves showing the brightness as a function of the conductivity current through the layer before and after aging (curves 1 and 2, respectively). Since in the working range of brightness, the values of the exponent are close to one, and since brightness and current show similar decrease with aging time, we may assume that the conductivity current through the layer is one of the main factors determining luminescence in a dc field.

5. THE RESISTANCE OF ELECTROLUMINESCENT LAYERS

The characteristics of layer conductivity presented in Fig. 3 indicate that the resistance of the layer varies with voltage according to a law differing from Ohm's law and that this law changes as the layer ages. The layers investigated consist of three parts ZnS:Cu:Mn phosphor and one part resin mixture. It follows from Fig. 5 that the specific resistivities of the layer components differ

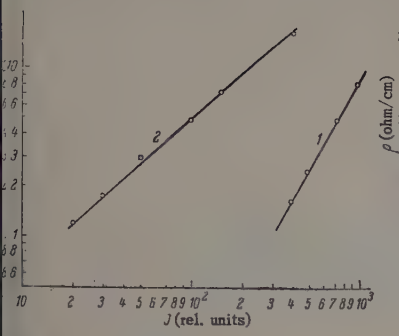

Fig. 4

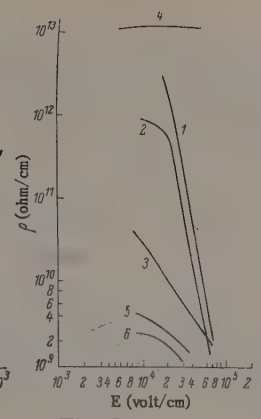

Fig. 5

Fig. 4. The brightness B as a function of the conductivity current J for a layer before aging (curve 1, $\alpha/\beta = 1.75$) and after aging (curve 2, $\alpha/\beta = 0.87$).

Fig. 5. The specific resistivity ρ as a function of the field intensity for an aged layer (curves 1 and 2), for a layer before aging (curve 3), for the dielectric layer (curve 4), and for a layer of compressed phosphor (curve 5).

ry several orders of magnitude and vary little, if at all, ·ith the field intensity across the layer. (See curve 4 for ne layer with resin mixture and curve 5 for the com·ressed phosphor without binder.) A mixture of com·onents with such different resistivities has a sharply ecreasing characteristic $\rho(E)$. (Curves 1 and 2 refer o aged layers with binders consisting of a resin mixture nd a silicone-type lacquer, respectively.) This type of (E) function may be explained by a redistribution of the oltage between thin high-resistivity resin layers and elatively high-conductance phosphor crystals. As a re·ult, high voltage gradients arise across the layers and ring about a decrease in their resistance according to ·ohl's law.

The apparent conflict between this assumption and ne $\rho(E)$ curve for the dielectric layer given in Fig. 5 nay be explained as follows: When the conductivity of nis layer is measured, the breakdown of the layer starts t lower voltage gradients (due to local defects) than hose acting on the interlayers of the electroluminescent ayer. A numerical calculation of the effective voltages s not possible because of lack of information concerning ne functional dependence $\rho(E)$ at high gradients.

. CONCLUSION

The experimental data reported here indicate that he dc electroluminescence of layers made of ZnS:Cu:Mn hosphor coincides with the appearance of conductivity n the layers under the action of high potential gradients. The brightness is determined by the conductivity current: for a fixed value of this current, the brightness depends on the voltage across the layer. (See Figs. 3 and 4.)

The dependence of dc brightness on voltage is expressed by a power law with a higher exponent than in the case of ac electroluminescence of the same layer.

The mechanism of dc electroluminescence[1] consists apparently in the excitation of characteristic activator centers (manganese) by electrons coming from the electrodes, passing through the supporting medium and entering the crystal, and in the emission of radiation when the excited centers return to the initial state. The necessary conductivity across the intervening dielectric layer appears under the action of high field gradients. The more pronounced dependence of brightness on voltage observed here, as compared with that observed under ac conditions, can apparently be explained as follows: As the voltage across the layer increases, there is an increase not only in the local voltage gradients, i.e., in the energy of the exciting electrons, but there is also a rapid increase in the number of these exciting electrons (conductivity electrons).

The marked brightness increase which is observed in the course of aging of the layer, provided the conductivity current is kept constant, indicates that in an aged layer the voltage acting on a phosphor crystal increases. It follows from simple considerations, however, that this increase in the acting voltage does not correspond to an increase of the average voltage across the layer. In order to keep the magnitude of the conductivity current the same, the average voltage across the layer must be increased several fold. (See, for example, the abscissas a and b of curves 2 and 4 in Fig. 3.) When this is done, the brightness of luminescence of the aged layer increases by a factor of only ten (the ratio d/c of the ordinates of curves 3 and 1). This is much smaller than the expected brightness increase.

Thus the distribution of voltages between the phosphor crystal and the dielectric interlayer varies in the course of aging. This is due to an increase in the absolute value of the phosphor resistance accompanied by a simultaneous increase in the ratio of the resistance of the dielectric medium to that of the phosphor.

The authors express their deep appreciation to F. M. Pekerman and her collaborators for their extensive work in developing and preparing phosphor samples capable of electroluminescence in a dc field.

REFERENCES

1. P. Zalm, Philips Research Repts. 11, 353, 417 (1956).
2. V. N. Favorin, G. S. Kozina, and L. K. Tikhonova, Opt. i Spektr. 7, 703 (1959), Optics and Spectroscopy 7, 420 (1959).
3. G. S. Kozina, V. N. Favorin, and I. D. Anisimova, Opt. i Spektr. 8, 218 (1960), Optics and Spectroscopy 8, 112 (1960).
4. G. S. Kozina and L. P. Poskacheeva, Opt. i Spektr. 8, 215 (1960), Optics and Spectroscopy 8, 110 (1960).

THE REFLECTION OF RADIATION FROM AN INFINITE FLAT SURFACE ILLUMINATED BY A POINT SOURCE
I. Characteristics of the Radiation Field

B. A. Grigoriev, A. G. Ershov, and V. A. Uvarov (pp. 96-103)

Received 3 October 1959

The radiation field and its characteristics are investigated theoretically for ideally scattered reflection and for directional reflection from an infinite flat surface. It is assumed that scattering within the medium occupying the half-space above the reflecting surface can be neglected, and that only directional absorption of radiation by the medium has to be taken into consideration.

An investigation of the radiation field due to reflection from an infinite flat surface illuminated by a point source is of practical interest for the solution of many problems in illumination technology involving the use of strong light sources, and also in the study of many problems in geophysics and astrophysics. In the literature,[1-6] more consideration has been given to the scattering and reflection of parallel beams of light transmitted through a scattering medium and incident upon a reflecting surface. The scattering and reflection of the radiation emitted by a point source have been considered only in part,[7,8] and require further investigation.

The general solution of this problem should consider not only the different characteristics of reflection (the form of the indicatrix, the dependence of the coefficient of reflection upon the angle of incidence and upon the coordinates, etc.) but also the scattering of radiation by the medium occupying the half-space above the reflecting surface. Such scattering not only exerts a direct influence on the radiation field, but also leads to multiple reflection from the surface. In a number of cases of practical importance and theoretical interest where the role of scattering is relatively small, one can restrict the investigation to direct and reflected radiation, taking the medium into consideration only as a factor reducing the intensity of the radiation.

Such is the problem in its simplified form; it will be considered here under the assumption that the following conditions are fulfilled:*

*In the following the terminology of illumination technology as recommended by the Committee for Technical Terminology of the Academy of Sciences of the USSR[9] will be used.

1. A point source of radiation is located above the reflecting surface at a finite distance from it. Shadowing of the reflected radiation by the source itself is not considered.

2. The flat, infinite reflecting surface is a perfect scatterer, its indicatrix of reflection obeys Lambert's law.

3. The reflection coefficient of the surface is constant; it does not depend upon the angle of incidence nor on the coordinates.

4. The half-space above the reflecting surface is filled with an inhomogeneous isotropic medium which does reduce the intensity of the radiation.

5. The reduction of intensity is characterized by directional transmission which obeys Bouguer's law.

6. The inhomogeneity of the medium is characterized by the presence of two layers, parallel to the reflecting surface, which have different coefficients of absorption but identical refractive indices.

For comparison, the analogous problem for directional reflection is considered.

Obviously, these conditions can only be really fulfilled for monochromatic radiation. However, in many cases they can be fulfilled sufficiently well for radiation of a given spectral composition if the optical coefficients are known and the selectivity of the absorbing medium is negligible. One should keep in mind, however, that one obtains somewhat lower values for the amount of reflected radiation at an arbitrary point above the reflecting surface if one neglects the scattering of radiation by the medium, and considers only single reflection.

The characteristics of the radiation should be described by functions involving the amount of radiation incident upon the absorbing area of a flat, opaque detecting element which is located above the reflecting surface. The independent variables are the position and orientation coordinates of the source relative to the plane of the receiver and the height of the latter above the reflecting surface. The radiation field will be investigated within the domain where the shadow produced by the receiver element does not exert a noticeable influence upon the radiation incident upon the reflecting surface. In the following, a transition will be made from dimensional to dimensionless characteristics.

Diagrams characterizing the general case of the position and orientation of the point source and the detecting element are shown in Figs. 1 and 2 (the dimensionless geometric parameters considered below are given in parentheses in the figures). A cartesian coordinate system is used whose origin is chosen in such a way that the center of the detecting element (of surface area ds_0) is located on the axis oz at the point (P(O,O,1).

The xoy-plane coincides with the reflecting surface. The normal n to the plane of the detecting element, passing through its center, is in the plane zoy and intersects the axis oy at A. The angle between the axis oz and the normal n (measured from the top downward) will be denoted by $\psi (0 \leq \psi \leq \pi)$. The plane containing the surface of the detecting element intersects the plane xoy along a straight line parallel to the axis ox (or coincident with it), and intersects the axis oy at the point D. This line is described by the equation $y = b$, where

$$b = l \operatorname{cotan} \psi. \qquad (1)$$

The point source is located at the point $I(x_0,y_0,z_0)$. An arbitrarily chosen element of the reflecting surface (of area ds) is located on the plane xoy at the point K(x,y,o); the normal n_1 passes through the center of this

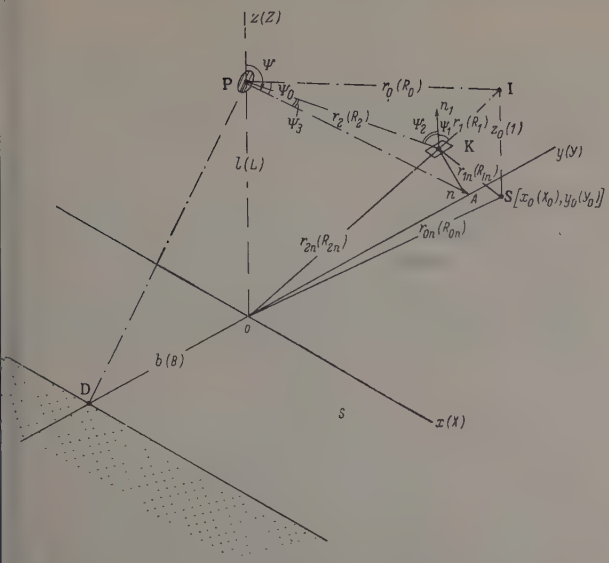

Fig. 1. Coordinate system and location of the point source and detecting element for $1 > z_0$ ($L > 1$). The section of the plane from which reflected radiation cannot reach the receiver is covered with dots. Solid lines are in the plane xoy (XoY); broken lines are above the plane xoy (XoY).

ement. Other notations should be clear from Figs. 1 d 2 (projections on the plane xoy are indicated by the pplementary subscript n).

The location and orientation of the radiating source lative to the plane of the receiver and the height of the ter above the reflecting surface are determined by the antities x_0, y_0, z_0, ψ, and l. In view of the symmetry the detector relative to the plane zoy, all the possible riations of the location of the source are taken into sideration if one transposes its projections in the st and fourth quadrant of the plane xoy, i.e., $0 \leq x_0 \leq$, $-\infty \leq y_0 \leq +\infty$.

In a number of cases, the surface of the receiver n be illuminated only by reflected radiation (the condi- n that it can be reached by primary radiation is $0 \leq$ $\leq 1/2\,\pi$). There are two limiting positions of the sur- e of the receiver parallel to the plane xoy; in one it not reached by any reflected radiation ($\psi = 0$: the sur- e is turned in the direction opposite to the plane xoy); d in the other it is reached by the reflected radiation m the whole reflecting surface ($\psi = \pi$: the surface is ing the plane xoy).

The domain S on the plane xoy from which the re- cted radiation is "collected" on the surface of the re- iver is partly defined (according to the condition $0 \leq$ $\leq 1/2\,\pi$) by the straight line $y = b$. Therefore, the llowing conditions are fulfilled within the domain S: $\leq x \leq +\infty$ and $b \leq y \leq +\infty$. In turn, because of Eq. (1), has the limiting values $b = +\infty$ for $\psi = 0$ and $b = -\infty$ $\psi = b$.

The reflected ray reaches the plane of the receiver $0 \leq \psi_1 \leq 1/2\,\pi$ and $0 \leq \psi_2 \leq 1/2\,\pi$. The first of these nditions is always fulfilled for finite distances from e source according to the formulation of the problem $< z_0 < \infty$), and does not impose any additional limita- n on the domain S. The second condition will always fulfilled unless the receiver is located on the reflecting rface itself ($l = 0$). One should therefore postulate a nimum value, $l_{min} > 0$, especially since for values of l of the same order of magnitude as the linear dimensions of the detector, the shadow caused by the detector on the reflecting surface can affect the quantity of radiation reaching the detector.* No further limitation of the domain S is then imposed by the second condition.

*Calculation shows that if one does not wish to permit a reduction of more than 10% in the quantity of reflected radiation due to shadowing, one should postulate $l_{min} = 3\sqrt{dS_0}$.

The plane which divides the absorbing medium into two layers of different absorption coefficients passes through either point P (if $z_0 > 1$), or point I (if $z_0 < 1$).*

*It is assumed that there is no reflection from the surface separating these layers.

Let us denote the absorption coefficient along the direct ray r_0 by k_0 (cm^{-1}), along the direct ray r_1 by k_1 (cm^{-1}), and along the reflected ray r_2 by k_2 (cm^{-1}). Because of the relation

$$k_1 = \frac{1}{z_0}\left[k_0 (z_0 - l) + k_2 l\right]. \qquad (2)$$

it is sufficient if two of these coefficients are given (k_0 and k_1 or k_2).

At the point P where the receiver element is located, the quantity of direct radiation from the point source incident upon a surface normal to the direct ray is given by the expression

$$H_0 = \frac{W}{4\pi r_0^2} e^{-k_0 r_0} \ (\text{cal/cm}^2), \qquad (3)$$

if the conditions of the problem are fulfilled; W (cal) is the energy radiated by the point source (H_0 can be called the quantity of direct normal radiation).

The total quantity of radiation H incident upon one side of the detecting element consists of the sum of the direct and reflected radiation; that is

$$H = H_0 \cos\psi_0 + H_\rho. \qquad (4)$$

If direct radiation does not strike the receiver ($\psi_0 > 1/2\,\pi$), the term $H_0 \cos\psi_0$ should not be considered; then $H = H_\rho$.

According to Lambert's law, the luminosity of an arbitrarily chosen element of the reflecting surface at

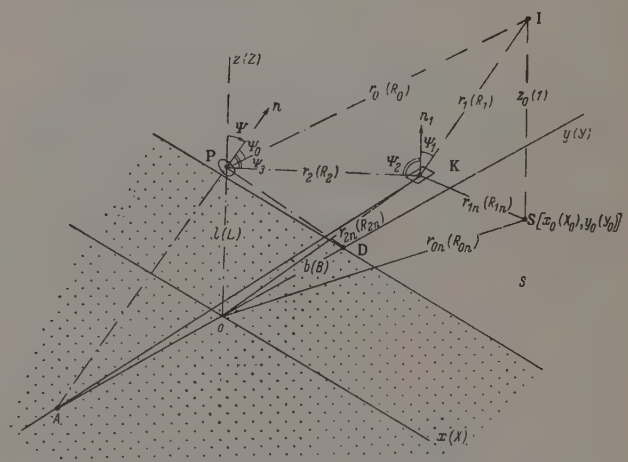

Fig. 2. Coordinate system and location of the point source and detecting element for $1 > z_0$ ($L > 1$). For symbols, see caption for Fig. 1.

any instant of time can be determined from the expression

$$B = \frac{\rho}{\pi} E \cos\psi_1 e^{-k_1 r_1} \text{ (cal/cm}^2 \text{ sec sterad)}, \quad (5)$$

E (cal/cm^2 sec) is the direct normal illuminance at the point K where the element of the surface is located; ρ is the coefficient of reflection, and it is assumed that there is no attenuation of the radiation.

For the value of the corresponding element of luminous flux reflected from the surface element under consideration, which is incident upon the plane of the receiver element, one obtains

$$dF_\rho = B \cos\psi_2 \, ds \, d\Omega \, e^{-k_2 r_2} \text{ (cal/sec)}, \quad (6)$$

where

$$d\Omega = \frac{ds_0 \cos\psi_3}{r_2^2} \text{ (sterad)}, \quad (7)$$

is the element of solid angle occupied by the detector as seen from point K.

The amount of reflected radiation incident on a unit area of the receiver from an arbitrarily chosen element of the reflecting surface during the time element $d\tau$ is

$$dH_\rho = \frac{dF_\rho}{ds_0} d\tau \text{ (cal/cm}^2\text{)}. \quad (8)$$

Considering Eqs. (5) to (7), one can replace Eq. (8) by

$$dH_\rho = \frac{\rho}{\pi} E \frac{\cos\psi_1 \cos\psi_2 \cos\psi_3}{r_2^2} \exp(-k_1 r_1 - k_2 r_2) \, ds d\tau. \quad (9)$$

The quantity of reflected radiation incident upon one side of the receiver during the time interval 0 to τ is obtained by integration of expression (9) over the time τ and the domain S

$$H_\rho = \frac{\rho}{\pi} \int_S \int_0^\tau E \frac{\cos\psi_1 \cos\psi_2 \cos\psi_3}{r_2^2} \exp(-k_1 r_1 - k_2 r_2) \, ds d\tau. \quad (10)$$

Taking into consideration that in Eq. (10), only E can be a function of τ, and that

$$\int_0^\tau E d\tau = \frac{W}{4\pi r_1^2}, \quad (11)$$

and using further the obvious relations $\cos\psi_1 = z_0/r_1$ and $\cos\psi_2 = l/r_2$, one can put Eq. (10) into the form

$$H_\rho = \frac{\rho W}{4\pi^2} \int_S \frac{z_0 l \cos\psi_3}{r_1^3 r_2^3} \exp(-k_1 r_1 - k_2 r_2) \, ds. \quad (12)$$

Let us introduce the dimensionless modulus of the reflected radiation, M, choosing the product of the reflection coefficient ρ and the quantity of direct normal illumination H_0 at point P as the scaling factor for the dimensionless transformation; i.e.

$$M = \frac{H_\rho}{H_0 \rho}. \quad (13)$$

Making use of Eqs. (2), (3), and (12), we transform Eq. (13) into

$$M = \frac{r_0^2}{\pi} \int_S \frac{z_0 l \cos\psi_3}{r_1^3 r_2^3} \times \exp\left\{k_0 r_0 - k_2 r_2 - r_1\left[k_0\left(1 - \frac{l}{z_0}\right) + \frac{k_2 l}{z_0}\right]\right\} ds. \quad (14)$$

One can also introduce a dimensionless modulus for the total illumination N, which is obtained by transforming Eq. (4):

$$N = \frac{H}{H_0} = \cos\psi_0 + \rho M. \quad (15)$$

Using Eqs. (4), (14), and (15), the expression for the total quantity of illumination of the one-sided, flat detector element can be written in the form

$$H = H_0(\cos\psi_0 + \rho M) = H_0 N. \quad (16)$$

A transformation of the geometric parameters and absorption coefficients into dimensionless form can be carried out, if one chooses as the scaling factor of the dimensionless transformation the height of the point source above the reflecting surface (the coordinate z_0); one can then obtain dimensionless coordinates of length and area

$$X = \frac{x}{z_0}, \quad Y = \frac{y}{z_0}, \quad Z = \frac{z}{z_0},$$

$$X_0 = \frac{x_0}{z_0}, \quad Y_0 = \frac{y_0}{z_0}, \quad Z_0 = 1,$$

$$R_0 = \frac{r_0}{z_0}, \quad R_1 = \frac{r_1}{z_0}, \quad R_2 = \frac{r_2}{z_0}, \quad (17)$$

$$L = \frac{l}{z_0}, \quad B = \frac{b}{z_0},$$

$$dS = \frac{ds}{z_0^2}, \quad dS_0 = \frac{ds_0}{z_0^2},$$

and also the criteria of Bouguer*

*Because of Eq. (2), $Bu_1 = Bu_0(1 - L) + Bu_2 L$.

$$Bu_0 = k_0 z_0, \quad Bu_1 = k_1 z_0, \quad Bu_2 = k_2 z_0. \quad (18)$$

The dimensionless characteristics of the radiation field can thus be represented in the form of relations between the moduli of the reflected and total radiation and the dimensionless geometric parameters, the criteria of Bouguer, and the coefficient of reflection.

If Eqs. (17) and (18) are used, expression (14) for the modulus of the reflected radiation can be given the following form:

$$M = \frac{R_0^2 L}{\pi} \int_S \frac{\cos\psi_3}{R_1^3 R_2^3} \exp\{Bu_0 R_0 - Bu_2 R_2 - R_1[Bu_0(1 - L) + Bu_2 L]\} \, ds. \quad (19)$$

We shall carry out further transformations by expressing all of the geometric parameters in terms of quantities describing the orientation and location of the emitter and the detector, at the same time replacing integration over the area by a double integral over the coordinates.

From the geometry of the triangles APK (see Figs. 1 and 2) one sees that

$$\cos\psi_3 = \frac{Y \sin\psi - L\cos\psi}{\sqrt{X^2 + Y^2 + L^2}}. \quad (20)$$

The domain S in the plane XoY is partly defined by the straight line Y = B where, according to Eq. (1),

$$B = L \operatorname{cotan}\psi. \quad (21)$$

The remarks made above concerning the limiting values of the angles and coordinates are naturally still valid after the transition to dimensionless parameters.

Taking into consideration Eqs. (20) and (21), and also the obvious geometrical relations and the identity dS = dX dY, one can replace Eq. (19) by

$$M=\frac{L\left[X_0^2+Y_0^2+(L-1)^2\right]}{\pi}$$

$$\times\int_{B}^{+\infty}\int_{-\infty}^{+\infty}\frac{(Y\sin\psi-L\cos\psi)}{(X^2+Y^2+L^2)^2\left[(X-X_0)^2+(Y-Y_0)^2+1\right]^{\frac{3}{2}}}$$

$$\times\exp\left\{Bu_0\sqrt{X_0^2+Y_0^2+(L-1)^2}-Bu_2\sqrt{X^2+Y^2+L^2}\right.$$

$$\left.-\sqrt{(X-X_0)^2+(Y-Y_0)^2+1}\left[Bu_0(1-L)+Bu_2L\right]\right\}dYdX. \quad (22)$$

From the relations in the triangles API (see Figs. and 2) we obtain

$$\cos\psi_0=\frac{Y_0\sin\psi-(L-1)\cos\psi}{\sqrt{X_0^2+Y_0^2+(L-1)^2}}. \quad (23)$$

is not difficult to verify that for $0<\psi\leq\pi$, the direct adiation is incident on the surface of the receiver, and hat the receiver is illuminated by reflected radiation if ot $\psi\leq Y_0/(L-1)$. For $\psi=0$ (if $L\leq 1$) this illumination is independent of the coordinates of the emitter.

Expressions (22) and (23) show that M and N are unctions of the same four dimensionless geometrical arameters X_0, Y_0, ψ, L, and of the two criteria of ouguer, Bu_0 and Bu_2 (or Bu_1).

Let us now obtain expression for the moduli of radiation in case of directional reflection, using the coordinate system defined above.

If $x_0=y_0=0$, the reflected radiation will reach the urface of the receiver only for $1>z_0$, since for $1<z_0$ he direct ray is intercepted by the opaque detector.

The quantity of the reflected illumination on one ide of the flat detector element is

$$H_\rho^*=\frac{\rho W\cos\psi_3}{4\pi(r_1+r_2)^2}\exp(-k_1r_1-k_2r_2). \quad (24)$$

fter introduction of the dimensionless geometrical arameters and of the criteria of Bouguer, the modulus or reflected radiation can be written in the form

$$M^*=\frac{R_0^2\cos\psi_3}{(R_1+R_2)^2}$$

$$\times\exp\left\{Bu_0R_0-Bu_2R_2-R_1\left[Bu_0(1-L)+Bu_2L\right]\right\}. \quad (25)$$

he modulus for the total radiation (analogous to Eq. 15)) is

$$N^*=\frac{H^*}{H_0}=\cos\psi_0+\rho M^*. \quad (26)$$

The total quantity of illumination on one side of the at detector element is, by analogy with Eq. (16),

$$H^*=H_0(\cos\psi_0+\rho M^*)=H_0N^*. \quad (27)$$

From geometrical considerations, one can conclude nat

$$R_2=LR_1, \quad (28)$$

$$\cos\psi_3=\frac{Y_0\sin\psi-(L+1)\cos\psi}{\sqrt{X_0^2+Y_0^2+(L+1)^2}}. \quad (29)$$

For $0<\psi\leq\pi$, directionally reflected radiation is incident on the surface of the receiver (i.e., $0\leq\psi_3\leq 1/2\,\pi$) if the condition

$$\operatorname{ctg}\psi\leq\frac{Y_0}{(L+1)}.$$

is fulfilled. Making use of Eqs. (28), (29), and also of the obvious geometrical relations, one can write instead of Eq. (25)

$$M^*=\frac{\left[Y_0\sin\psi-(L+1)\cos\psi\right]\left[X_0^2+Y_0^2+(L-1)^2\right]}{\left[X_0^2+Y_0^2+(L+1)^2\right]^{3/2}}$$

$$\times\exp\left\{Bu_0\sqrt{X_0^2+Y_0^2+(L-1)^2}\right. \quad (30)$$

$$\left.-\frac{\sqrt{X_0^2+Y_0^2+(L+1)}}{(L+1)}\left[2LBu_2+Bu_0(1-L)\right]\right\}.$$

Expressions (26) and (30) show that the moduli of radiation are functions of the same quantities for directional reflection as for ideally scattered reflection.

The calculation of the total or the reflected illumination in terms of the corresponding moduli, and of the quantity of direct normal illumination, do not present difficulties except at points located in the immediate vicinity of the emitter, where one should use expressions (4), (12), and (24).

REFERENCES

1. K. Ya. Kondrat'ev, "Luchistyi teploobmen v atmosfere (Radiative Heat Exchange in the Atmosphere)." GIMIZ, Leningrad, 1956.
2. K. Ya. Kondrat'ev, "Luchistaya energiya solntsa (Radiant Energy of the Sun)." GIMIZ, Leningrad, 1954.
3. E. S. Kuznetsov, Izvest. Akad. Nauk SSSR, Ser. Geogr. 6, 613 (1940).
4. E. V. Pyaskovskaya-Fesenkova, "Issledovanie razzeyaniya sveta v zemnoi atmosfere (Investigation of the Scattering of Light in the Earth's Atmosphere)." Izd. Akad. Nauk SSSR, Moscow-Leningrad, 1957.
5. I. I. Minin, and K. S. Shifrin, Trudy Glav. Geofiz. Observ. issue 68, 5 (1957).
6. E. M. Feigel'son, Trudy Inst. Fiz. Atmos. 1, 1 (1958).
7. V. V. Sobolev, "Perenos luchistoi energii v atmosferakh zvezd i planet (Transfer of Radiative Energy in the Atmospheres of Stars and Planets)." Gosudarst. Tekh. i Teoret. Izd., Moscow-Leningrad, 1957.
8. V. V. Meshkov, "Osnovy svetotekhniki (Principles of Illumination Technology)," Part 1. Gosenergoizdat, Moscow, 1957.
9. "Terminologiya svetotkehniki (Terminology of Illumination Technology)." Edited by the Academy of Sciences of the USSR, Moscow-Leningrad, 1957.

EXPERIMENTAL STUDY OF THE INTENSITY DISTRIBUTION IN THE SPECTRUM OF DIFFRACTION GRATINGS FOR POLARIZED LIGHT

E. A. Yakovlev and F. M. Gerasimov (pp. 104-112)

Received 21 March 1960

The reflecting properties of a large number of diffraction gratings were investigated for polarized light. The gratings were prepared on thin layers of various metals with grooves having a steplike profile. It was found in all cases that the intensity distribution curves of light with the electric vector parallel to the grooves are displaced toward the shorter wavelengths relative to the curves for light with the electric vector perpendicular to the grooves. The displacement is directly proportional to the square of the wavelength, and inversely proportional to the grating constant. Because of this displacement of the curves, a characteristic change of the degree of polarization of the diffracted light along the spectrum is observed. It has been found that replicas prepared on organic glass or on a layer of gelatine do not have this property.

The intensity distribution of light by gratings with grooves of a steplike profile has been theoretically treated by many authors. However, the derived formulas do not consider the state of polarization of the incident light. As was shown in the paper by Rohrbaugh et al.,[1] in which the intensity distribution was investigated in the microwave range in an echelette with a constant of 10 mm, these formulas give satisfactory agreement with experiment only for polarized radiation with the electric vector perpendicular to the grating grooves.

It was pointed out in the paper by one of us[2] that there is a considerable change in the degree of polarization along the spectrum in the region of high concentration of light diffracted by a grating with a steplike profile. One can conclude from the diagrams given in the present paper for the intensity distribution obtained with a grating with 600 grooves/mm, as well as from the diagrams of the ratio of the reflection coefficients in polarized light, that the aforementioned property of the grating is the result of a relative displacement of the curves for the intensity distribution of light polarized parallel and perpendicularly to the grooves.

Curves for the intensity distribution similar to those observed in ref. 2 were also obtained by Jamaguchi and collaborators[3] during the measurements of the transmission of a spectrometer with an echelette of 75 grooves/mm in the wavelength range from 2 to 19μ. There was, however, in the quoted paper no analysis of the results obtained.

We undertook a more detailed experimental study of the displacement of the light intensity distribution for a large number of gratings in the range between 0.4 and 1.7μ. The results obtained are given in the present paper.

THE MEASUREMENT OF THE INTENSITY DISTRIBUTION

The measurement of the reflection coefficients of the gratings in polarized light was made with a special spectrophotometric apparatus, the scheme of which is shown in Fig. 1. The grating under investigation 7 was illuminated by a parallel beam of linearly polarized light from a monochromator with a grating 2 (3 is the exit slit, 4 is the lens). The diffracted light was focused by the lens 8 on the surface of a photoelement 9. The reflection coefficient was determined as the ratio of the flux diffracted from the grating to the flux reflected by a plane aluminum mirror 6 that was introduced into the beam in place of the grating. An incandescent bulb 1 served as the light source. A Rochon prism 5 was used for polarization of the light. A selenium photocell was applied for measurements in the visible range, a silver sulfide cell for the infrared up to 1.3μ, and a lead sulfide above 1.3μ. The photocurrent was measured with a mirror galvanometer 10. The spectrum band separated by the monochromator was 70 A wide in the visible region and 140 A wide in the infrared region.

Altogether about 40 plane gratings of our own make (with 200, 300, 600, and 1200 grooves/mm) were investigated. Most of them were prepared on aluminum layers which were deposited on glass by evaporation in vacuum, with grooves having a steplike profile. Therefore the gratings gave a high concentration of light in the direction of specular reflection from the groove planes, the angles of inclination of which had values of from 4° to 64° for the different gratings.

The measurements of the reflection coefficients $\rho_{\parallel}$ and $\rho_{\perp}$ for different wavelengths were made in the maximum concentration region with light with the electric vector parallel and perpendicular to the grooves. More detailed data for some gratings differing from one another by the grating constant and by the angle of inclination of the working surfaces are given in the Table.

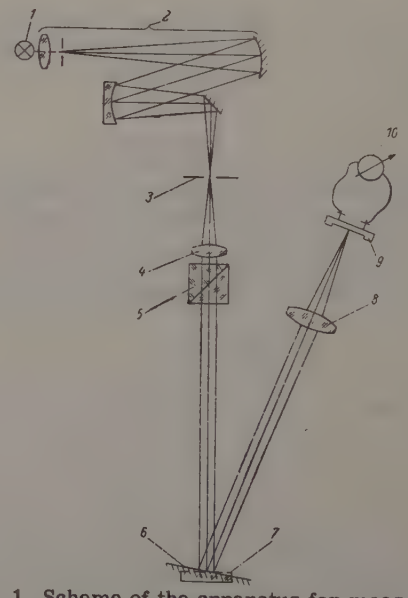

Fig. 1. Scheme of the apparatus for measuring the reflection coefficients of gratings in polarized light.

Grating No.	No. of grooves mm	Angle of the working side of the groove**	Spectrum order	Position of the concentration maximum**** Wavelength (μ) ⊥	∥	u	Relative displacement of the maximum (μ)	Reflection coefficient in the maximum (%)**** ⊥	∥	u
	200	4°30′	I	0.750	0.750	0.750	—	80	76	78
	300	8°30′	I	0.950	0.850	0.883	0.100	79	80	79
			II	0.465	0.445	0.450	0.020	62	72	66
*	300	11°30′	II	0.675	0.585	0.625	0.090	64	72	58
			III	0.427	0.410	0.410	0.017	46	55	51
	300	20°00′	II	1.080	0.980	1.033	0.100	87	82	80
			III	0.712	0.675	0.689	0.037	78	80	77
			IV	0.531	0.517	0.523	0.014	68	75	71
			V	0.426	0.416	0.420	0.010	65	72	66
*	600	10°30′	I	0.590	0.520	0.550	0.070	84	80	82
	600	19°00′	I	1.080	0.840	0.917	0.240	89	89	80
			II	0.516	0.456	0.500	0.060	72	63	64
	600	24°00′	I	1.295	0.950	1.160	0.345	98	84	84
			II	0.653	0.560	0.600	0.093	85	75	75
			III	0.445	0.400	0.425	0.045	62	65	60
*	600	31°30′	II	0.900	0.710	0.800	0.190	70	61	59
			III	0.570	0.483	0.525	0.087	48	56	50
***	600	19°30′	I	0.900	1.100	1.030	0.200	97	87	89
		64°00′	III	0.980	0.790	0.930	0.190	82	54	49
			IV	0.725	0.625	0.700	0.100	46	52	39
			V	0.626	0.544	0.550	0.082	32	49	28
	1200	21°00′	I	0.575	0.450	0.550	0.125	90	80	75
	1200	31°30′	I	0.475	0.800	0.700	0.325	97	86	80
*	1200	38°00′	I	1.000	0.650	0.850	0.400	87	76	60

*The gratings do not have a smooth intensity distribution curve for the perpendicular component.

**The inclination angle of the working side is calculated from the position of the maximum of the perpendicular component in the highest order measured for a given grating.

****Measurements made on two sides of the normal corresponding to reflection from the deep and the even sides of the groove.

*****Symbols for the state of polarization of light incident on the grating: ⊥, ∥ – electric vector perpendicular and parallel to the grooves, respectively; u – unpolarized light.

Figure 2 gives the results of the measurements of the reflection coefficients for different wavelengths in four orders of the spectrum from grating No. 4 (300 grooves/mm). The measurements were made for normal incidence of light. The scales along the abscissa axes were selected in such a way that the wavelengths in the overlapping orders which correspond to the same diffraction angle are on the same vertical line. Points represent the measured values of the reflection coefficients; the curves are the theoretical intensity distributions according to the formula given in ref. 4. The theoretical curves are adjusted to the experimental values for the ordinate. Under these conditions, for each state of polarization separately, the experimental points fit the theoretical curves fairly well. The curves for the parallel and for the perpendicular components display in all orders well-defined main maxima of unequal intensity that are displaced relative to each other. The curve $\rho_{\parallel}$ (dashed) is displaced toward the shorter wavelengths relative to the curve $\rho_{\perp}$ (continuous). The reflection coefficient at the maximum for both polarization states increases with decreasing order of the spectrum. Furthermore, the intensity of the perpendicular component increases more rapidly.

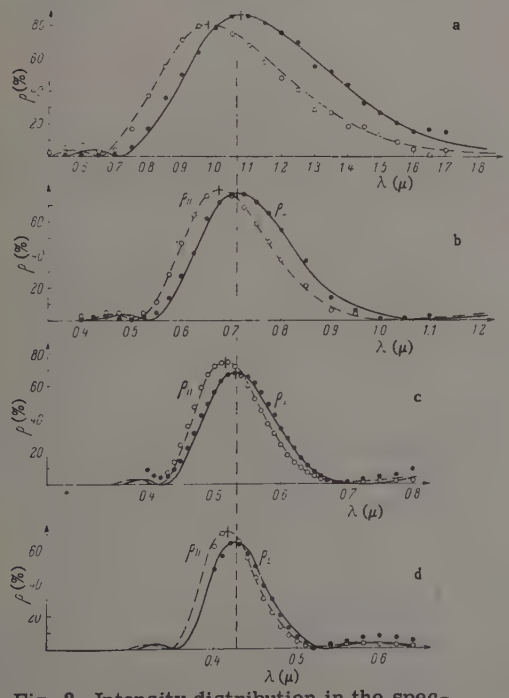

Fig. 2. Intensity distribution in the spectrum of grating No. 4 (300 grooves/mm) in polarized light. Spectrum order: a—II; b—III; c—IV; d—V.

A similar intensity distribution was observed for all other gratings. However, for some gratings the curves for the perpendicular component were less smooth than those for the parallel component (Fig. 3). This applies particularly to gratings with a relatively small reflection coefficient at the maximum. The decrease of the reflection coefficient could be caused by the surface defects of the reflecting sides of the grooves such as very small scratches or protrusions in the direction of the grooves. These defects apparently cause a change in the energy distribution for the component with the electric vector perpendicular to the grooves.

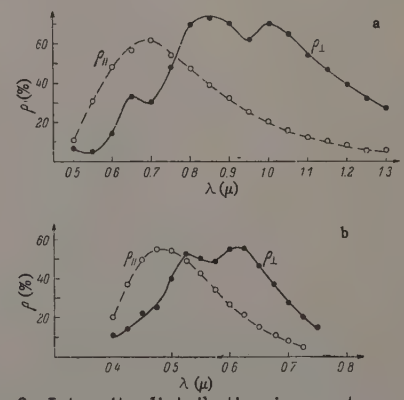

Fig. 3. Intensity distribution in spectrum of grating No. 4 (600 grooves/mm). Order of the spectrum: a—II; b—III.

The irregularities of the curve $\rho_{\perp}$ make it difficult to determine accurately the position of the concentration maximum. Therefore, the wavelengths of the maximum given in the Table were determined according to the general shape of the experimental curve by comparing it with the theoretical curve which was calculated for the given case. The values of the relative displacement of the maxima for the two states of polarization obtained in this manner are also given in the Table. By comparing these values for gratings with different constants in approximately the same wavelength range, one can see that they are larger for gratings with 1200 grooves/mm and smaller for those with 300 grooves/mm. Furthermore, the displacement does not depend on the order of the spectrum when the curves to be compared are in the same wavelength range. Within the errors of measurement, there is no displacement of the curves in the visible range for gratings of 200 grooves/mm. In the overlapping orders of a given grating, the displacement of the maximum increases for lower orders. This is clearly seen in Fig. 2, where the positions of the maxima are marked on the curves by short vertical lines.

Figure 4 depicts the dependence of the displacement of maxima $\Delta\lambda$, relative to $\lambda_{0\perp}$, on the value of $\lambda_{0\perp}/d$ ($\lambda_{0\perp}$ is the wavelength of the maximum for the perpendicular component, d is the grating constant). The displacements are given relative to $\lambda_{0\perp}$ because the maxima for the perpendicular component in the overlapping orders correspond approximately to the same diffraction angle (Fig. 2) and, as follows from comparison with the data of ref. 1, their position in the spectrum is sufficiently accurately given by the angle of the specular reflection from the working side of the groove, whereas the maximum for the parallel component is displaced toward the shorter wavelengths. The relationship given in Fig. 4 is almost linear and can therefore be represented by

$$\frac{\Delta\lambda}{\lambda_{0\perp}} = \alpha \frac{\lambda_{0\perp}}{d}, \qquad (1)$$

where α is the slope of the straight line.

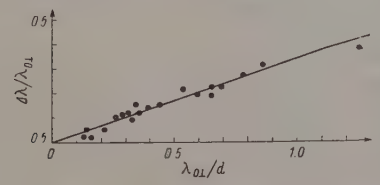

Fig. 4. Relative displacement of the maxima of the concentrated polarized light vs $\lambda_{0\perp}/d$. $\alpha = 0.34$ (see Eq. 1).

It follows that the displacement of the maxima expressed in wavelengths is directly proportional to the square of the wavelength, and inversely proportional to the grating constant.

In Fig. 5, a and b, the intensity distribution in the spectrum of grating No. 9 (600 grooves/mm) in the vicinity of the minima of light concentration is given, as well as the spectrograms obtained in that region with a source of continuous spectrum. The wavelength scale for both the diagram and the spectrogram is the same.* The dark

*This is not the case in the figure as printed.

parts of the spectrograms in both polarizations correspond to the minima in the curves for the intensity distribution. The figure shows that the minima are displaced relative to each other in the same direction as the main maxima, but the displacement is smaller than for the maxima (see Table). The displacements of the minima which were determined for several gratings, fit the plotted line well (Fig. 4) and, consequently, follow the established relationship.

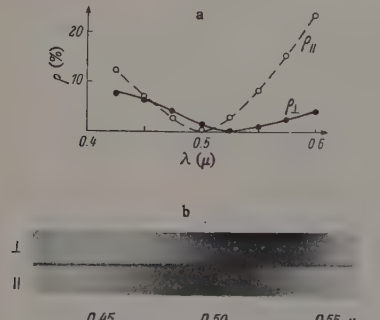

Fig. 5. Intensity distribution in the vicinity of the minima of light concentration for grating No. 9 (600 grooves/mm).

It is natural to suppose that this relationship is valid not only for the maxima and minima, but also for all wavelengths. In that case, the distance between the corresponding points of the curves $\rho_{\parallel}$ and $\rho_{\perp}$ must change along the spectrum, and therefore the displaced curve ($\rho_{\parallel}$) will be deformed. This conclusion is actually confirmed qualitatively. The experimental curves $\rho_{\parallel}$ for the gratings with 1200 grooves/mm are, as a rule, narrower than the theoretical ones, whereas the curves $\rho_{\perp}$ are close to the latter. This effect is not observed in gratings with a smaller number of grooves/mm, apparently because of the smaller displacements.

A decrease of the reflection coefficient for the unpolarized light, in comparison with the reflection coefficient for each of the polarized components separately, is one of the consequencies of the displacement of the intensity distribution curves. This effect is considerable in gratings with a large number of grooves/mm, as the Table shows.

POLARIZATION OF LIGHT BY A GRATING IN THE REGION OF HIGH CONCENTRATION

Another consequence of the displacement of the intensity distribution curves is the partial polarization of the diffracted light, with the degree of polarization changing considerably along the spectrum. Figure 6 depicts the dependence of the ratio $\rho_{\perp}/\rho_{\parallel}$ on the wavelength for grating No. 4 in the range of high concentration. The curves are calculated from the measured values of $\rho_{\parallel}$ and $\rho_{\perp}$ (see Fig. 2). For comparison, in the same figure the dependence of the reflection coefficients on the wavelength is given for unpolarized light. The diagram shows that the ratio $\rho_{\perp}/\rho_{\parallel}$ increases approximately linearly with the wavelength, passing through unity in the vicinity of the maximum of concentration.* Within the limits of

*The dependence of the ratio of the reflection coefficients on the wavelength is less regular in gratings which do not have a smooth curve for $\rho_{\perp}$ (Fig. 3).

the halfwidth of the maximum, shown in Fig. 6 by dashed lines, the ratio $\rho_{\perp}/\rho_{\parallel}$ changes with the increase of the relative displacement of the curves—greater for the lower orders. There are regions in the vicinity of the minima where the light is strongly polarized and changes from one state of polarization to another in a narrow wavelength range.

In order to eliminate the possibility of errors in the determination of the ratio $\rho_{\perp}/\rho_{\parallel}$, due to some parts of the apparatus which may themselves polarize light to some extent, this ratio was also measured directly with a visual polarization photometer that was built according to the above-described apparatus. The photometer setup is shown in Fig. 7. The square shaped entrance aperture 2 is illuminated by the scattered monochromatic light from a diffuse source 1. The image of the entrance aperture is observed in the light diffracted by the grating 4, through a Wollaston prism 3, and an analyzer 5. In the field of view of the photometer, two images of the entrance aperture are seen in light of the same wavelength which, at a certain position of the prism, form an extension of one another. The light of one of them is polarized parallel, and that of the other perpendicularly to the grating groove.

The brightness of the fields is equalized, just as it is done in the usual polarization photometers, by rotating the analyzer until the separation line disappears. Inasmuch as the beams leaving the Wollaston prism have the same intensity, the square of the tangent of the angle of rotation of the analyzer determines the ratio of the reflection coefficients in both states of polarization. In the given

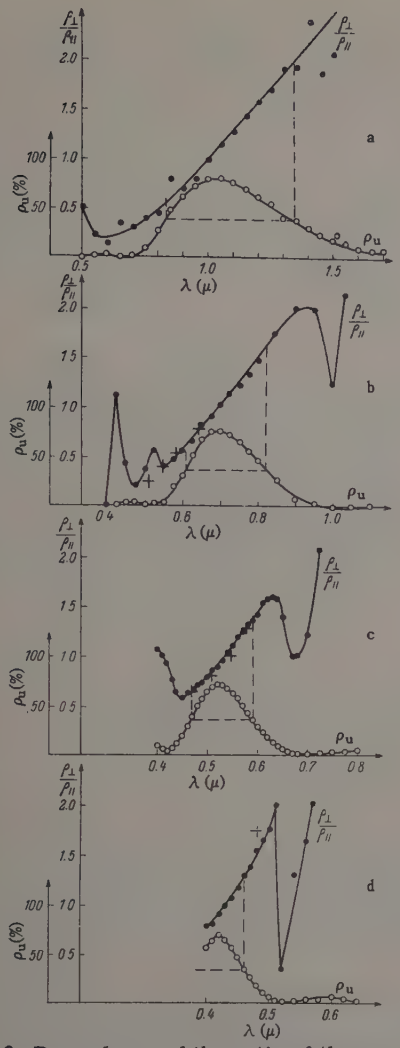

Fig. 6. Dependence of the ratio of the reflection coefficients $\rho_\perp/\rho_\parallel$ on wavelength for four spectral orders for grating No. 4 (300 grooves/mm). Spectrum order: a—II; b—III; c—IV; d—V. Visual observations are indicated by crosses. The curves ρ_u represent the reflection coefficient for unpolarized light.

eme, the light enters the analyzer from only a very ll part of the grating, thus permitting inspection of change in the polarizing properties along its surface. The measurements were made in the visible range the bright lines of cadmium and mercury. The es of $\rho_\perp/\rho_\parallel$ obtained for a number of gratings are in sfactory agreement with the results of photometric surements (see Fig. 6).

LUENCE OF THE GRATING MATERIAL ON THE SHIFT OF THE INTENSITY DISTRIBUTION CURVES

Metals, as it is well known, polarize light under ain conditions. Furthermore, the character of the rization depends both on the nature of the metal and he properties of the thin oxide—and other films that are always present on its surface. It was natural to suppose that the displacement of the intensity distribution curves in the gratings is also somehow connected with the properties of the metal on which they are cut. In order to check this assumption, one of the gratings with 1200 grooves/mm, cut on silver, was covered first with a thin layer of aluminum, and then with gold, by vacuum vaporization. Before each deposition, the measurements of the intensity distribution were made by the method described above. The diagrams given in Fig. 8, which were based on these measurements, show that in the transition from one metal to another, the essential features of the curves are retained. Only the amount of displacement of the maxima and their position in the spectrum change, and this could be connected not only with the nature of the metal, but also with the change in the microgeometry of the grooves because of the repeated depositions.

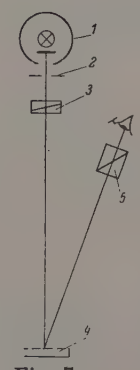

Fig. 7

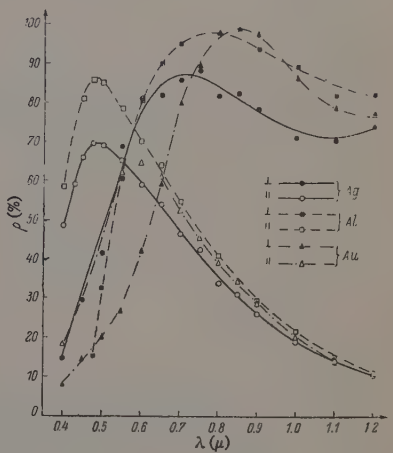

Fig. 8

Fig. 7. Setup for visual measurements of the ratio of the reflection coefficients in polarized light.
Fig. 8. Intensity distribution in spectrum of a grating cut on a layer of silver and covered with aluminum and gold.

An original grating and its reflection replica obtained on a layer of organic glass, and then covered with aluminum, have similar intensity distribution curves with well developed main maxima in both polarizations (Fig. 9). The displacement of the curves is about the same in both cases. The same replica, before it was covered with aluminum, had a dependence of the ratio $\rho_\perp/\rho_\parallel$ on the

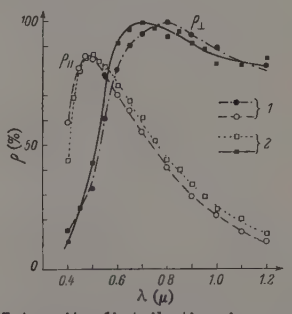

Fig. 9. Intensity distribution in spectrum of an original grating and that of its replica covered with aluminum. Curves 1—original; curves 2—replica.

wavelength (according to the measurements in the visible part of the spectrum with the arrangement shown in Fig. 7) that was expressed by a straight line parallel to the axis of abscissas, with an ordinate smaller than unity, that is, the replica polarized light uniformly along the spectrum. This indicates that there is no displacement of the intensity distribution curves in this case, and that the observed polarization of light is produced by other causes. Replicas made on gelatine layers behave similarly.

These experiments, as well as the above-mentioned results by other authors, demonstrate that the phenomenon of displacement of the intensity distribution curves is characteristic only of metal gratings. Furthermore, the displacement does not directly depend on the changes of the physical properties of metals produced by the strong deformations which are created in the process of cutting the grooves.

CONCLUSION

The reflecting properties of blazed gratings are not confined to the above described displacement of the intensity distribution curves which leads to changes in the degree of polarization along the spectrum: As well as the phenomena mentioned, there is a considerable chang along the spectrum in the phase difference between the components polarized parallel and perpendicularly to the grooves, which causes the peculiar character of elliptic polarization. One can hope that further experimental and theoretical study of these phenomena will lead to a deepe understanding of the physical properties of diffraction gratings, which will prove useful in practical spectroscopy.

REFERENCES

1. J. H. Rohrbaugh, C. Pine, W. G. Zoellner, and R. D. Hatcher, J. Opt. Soc. Am. 48, 710 (1958).
2. F. M. Gerasimov, I. A. Tel'tevskii, S. S. Naumov, S. N. Spizharskii, and S. V. Nesmelov, Opt. i Spektr. 4, 779 (1958).
3. A. Jamaguchi, I. Ichishima, and S. Mizushima, Spectr chim. Acta, 12, 294 (1958).
4. A. Sommerfeld, "Lectures on Theoretical Physics, Vol. 4, Optics" Academic Press, New York, 1954.

THE EFFECT OF OBJECT THICKNESS ON PHASE CONTRAST

Radu Grigorovich and Radika Manaila (pp.113-119)

Received 13 April 1960

Relationships are derived for the luminance of the image of phase objects of finite thickness in the field of a phase contrast microscope. The effect of depth is appreciable in the case of large aperture objectives and objects which are wide compared with their thickness and with the wavelength of light. The relationships found are confirmed experimentally.

INTRODUCTION

The elementary theory of phase contrast in its initial formulation, given by Zernike,[1] was based on several simplifying assumptions, as follows: (a) The microscope objective has an infinite aperture and has no aberrations, so that the whole diffraction pattern of the object contributes to forming the image, in accordance with Lummer's theory; (b) the change of phase and the absorption introduced by the phase plate are independent of λ (the phase plate has no dispersion); (c) the phase plate is infinitesimally narrow, so that the undeviated ray and the rest of the light diffracted by the object are sharply differentiated from each other, with an arbitrary object width and also with an arbitrary width of diffraction pattern; (d) the phase change introduced by the object is small ($\sin \varphi \approx \varphi$) and independent of λ; (e) the object is sharply focused over its whole thickness.

In practice, none of these conditions is rigorously satisfied. The effect of finite aperture (a) and dispersion of the phase plate (b) are easily calculated.[2] The effect of the finite width of the phase plate (c) is that there is only a partial separation of the undeviated ray from the rest of the diffracted light, in consequence of which a reduction in contrast occurs toward the center of the image of the phase object (the center effect). This effect has been studied in detail theoretically and experimentally with linear objects and linear[3] and annular[4] phase plates.

Doubts have been expressed[5] about the validity of the elementary theory for strongly dephasing objects (d). In an earlier paper,[6] we were able to show that these doubts were not well founded. In fact, crystals of NH_4Cl up to 3μ thick show pronounced color under phase contrast. Comparison of the results of some microcolorimetric measurements with the elementary theory shows qualitative agreement. In principle, quantitative discrepancies from the theory may arise as a result of deviation from any one of conditions (a) to (e).

Earlier studies[7] showed that in the case considered, the center effect (c) and dispersion of the phase plate (b) caused the observed discrepancies from theory.

In the present paper we will consider the effect of depth only; this effect is, of course, superimposed on all of the other effects cited above.

We had at our disposal a Carl Zeiss (Jena) Lumipan microscope with four objectives, positive phase contrast (Phako) and an annular phase plate, with the following magnifications and apertures: 10×/0.30, 20×/0.40, 40×/0.65, and 90×/0.25 oil immersion.

We derived our relationships with a view toward applicability to this actual case.

In order to avoid the laborious averaging required for the case of a phase annulus,[4] we will treat the object as linear and the circular boundaries of the annulus as squares, two sides of which are parallel to the object and equal in length to the diameter of this circular boundary. Thus, only the two sides of the phase plate parallel to the object contribute to the contrast. This approximation gave results which were in satisfactory agreement with Schmidt's exact calculations.[4]

The dimensions of the phase plate of the objectives espond to the optimum conditions recommended by ike,[8] that is, the mean diameter of the annulus is half the aperture diameter and the width is 1/15 the ture.

ORY

We will assume a linear phase object of width l and igibly small thickness situated with its center at the O (Fig. 1), conjugate with the observation point P, enter of its image.

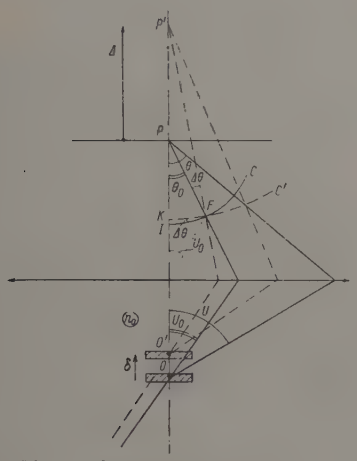

Fig. 1. Phase change occurring with change in focus.

Let the phase shift introduced by the object be $d\varphi$. diffraction pattern in the focal plane of the objective stributed about the intensity maximum, which is in irection of the incident beam, making an angle of u_0 the optical axis.

In our case, two maxima occur at $\pm u$, and the distri- n of amplitude and phase in the focal plane is given e function:

$$g(v)=\frac{1}{2}e^{id\varphi}\left[\frac{\sin(v-v_0)}{v-v_0}+\frac{\sin(v+v_0)}{v+v_0}\right], \tag{1}$$

e:

$$v=\frac{\pi l n_0 \sin u}{\lambda} \tag{2}$$

variable related to the direction of propagation u of rave diffracted by the object and n_0 is the refractive of the immersion medium (if there is one).

In the absence of any influences on the intermediate e, the amplitude and phase at the center P of the e will be obtained without additional dephasing as esult of the superposition of waves radiating from ocal plane. This is shown in Fig. 1, where the focal ne" is a sphere with center at P. The angle θ be- n the optical axis and the direction of propagation of rave after refraction at the objective is related to the esponding angle before refraction by the relationship:

$$\sin\theta\approx\theta=\frac{1}{\alpha}n_0\sin u, \tag{3}$$

e α is the magnification of the objective.

If we now move the object along the optical axis by all amount δ (to the point O′), the image moves the nce (from P to P′)

$$\Delta=\delta\beta=\delta\alpha^2, \tag{4}$$

where β is a longitudinal magnification of the objective. The focal "plane" is now centered at point P′; its intersection with the plane of the paper in Fig. 1 is the arc C′. The distances KP′ and FP′ are therefore equal.

If we continue observations at the point P, the wave traveling along the optic axis at an angle θ to the axis has the amplitude and phase given by Eq. (1) at all points of the curve C′, and consequently at the points K and F also. But while the wave traveling along the optic axis covers the distance KP in reaching P, the wave traveling at an angle covers the distance FP = IP. A path difference $d = IK = \Delta\theta^2/2$ thus appears between the two waves.

Using Eqs. (2), (3), and (4), we have for the phase shift between two waves traveling at angles θ and θ_0 to the optical axis:

$$\psi=\frac{2\pi}{\lambda}(d-d_0)=\frac{\lambda\delta}{\pi l^2}(v^2-v_0^2)=A(v^2-v_0^2). \tag{5}$$

If we observe a thin object having phase contrast, using a phase plate of width Δv_0 and transmission coefficient h^2, which introduces a phase shift γ between the undeviated wave and the remaining diffracted light, then besides the undeviated wave a part of the diffracted light in the range $\pm v_0 - \Delta v_0/2$, $\pm v_0 + \Delta v_0/2$ undergoes a reduction in amplitude by a factor h; the remaining diffracted wave undergoes phase shifts of γ and ψ, due respectively to the effect of the phase plate and to the effect of the angle between the direction of propagation of the wave and the optic axis. The amplitude and phase at the center of the image are given by:

$$dj=h\pi+\frac{1}{2}(e^{id\varphi}-1)\left\{e^{i\gamma}\left[\int_{-2v_0}^{-v_0-\frac{\Delta v_0}{2}}g(v)\,e^{i\psi}dv+\int_{-v_0+\frac{\Delta v_0}{2}}^{v_0-\frac{\Delta v_0}{2}}g(v)\,e^{i\psi}dv+\int_{v_0+\frac{\Delta v_0}{2}}^{2v_0}g(v)\,e^{i\psi}dv\right]+h\left[\int_{-v_0-\frac{\Delta v_0}{2}}^{v_0+\frac{\Delta v_0}{2}}g(v)\,e^{i\psi}dv+\int_{v_0-\frac{\Delta v_0}{2}}^{v_0+\frac{\Delta v_0}{2}}g(v)\,e^{i\psi}dv\right]\right\} \tag{5′}$$

This equation is rigorously satisfied only if the image of the annular diaphragm in the following focal plane is infinitesimally narrow and is centered on the phase plate, or when its width is finite if the function g(v) is linear or constant in the region of the phase plate. In the case of wide objects, the deviations from the calculated values obtained from the above expression may be considerable.

An object of finite thickness δ may be treated as made up of thin layers lying one on another and introducing a phase shift $\varphi = \Sigma d\varphi$. Assuming that sharp focus adjustment is made for the middle of the object in depth, in the preceding expression we should replace $d\varphi$ by φ and average the integrals over the range $[-\Delta A/2, +\Delta A/2]$ where as in Eq. (5), $\Delta A = \lambda\delta/\pi l^2$.

By symmetry, the imaginary parts of the integrals vanish and the expression for the amplitude and phase in the center of the image takes the form:

$$f=h\pi+(e^{i\gamma}-1)\left\{e^{i\gamma}\left[\frac{1}{\Delta A}\int_{-\frac{\Delta A}{2}}^{+\frac{\Delta A}{2}}dA\cdot\int_{0}^{v_0-\frac{\Delta v_0}{2}}g(v)\cos A(v^2-v_0^2)\,dv+\frac{1}{\Delta A}\int_{-\frac{\Delta A}{2}}^{+\frac{\Delta A}{2}}dA\cdot\int_{v_0+\frac{\Delta v_0}{2}}^{2v_0}g(v)\cos A(v^2-v_0^2)\,dv\right]\right.$$

$$+\frac{h}{\Delta A}\int_{-\frac{\Delta A}{2}}^{+\frac{\Delta A}{2}} dA \cdot \int_{v_0-\frac{\Delta v_0}{2}}^{v_0+\frac{\Delta v_0}{2}} g(v)\cos A\left(v^2-v_0^2\right)dv\Bigg\}$$

$$=\pi\left[h+\left(e^{i\varphi}-1\right)\left(e^{i\gamma}I_1+hI_2\right)\right], \qquad (6)$$

and the illumination at the center of the image, except for a factor of π^2 becomes

$$B=\frac{|f|^2}{\pi^2}=h^2+2(1-\cos\varphi)\left[\overline{I_1^2}-h^2I_2(1-I_2)-hI_1\cos\gamma(1-2I_2)\right]$$
$$-2hI_1\sin\gamma\sin\varphi. \qquad (7)$$

In the absence of dispersion in the phase plate ($\gamma = \pm\pi/2$), we have:

$$B=h^2+2(1-\cos\varphi)\left[\overline{I_1^2}-h^2I_2(1-I_2)\right]\mp 2hI_1\sin\varphi, \qquad (8)$$

and when the effect of depth is negligibly small (A = 0) averaging the integrals becomes unnecessary and they take the form $I = \int g(v)dv$ and the averaging sign over the I's vanishes:

$$B=h^2+2(1-\cos\varphi)\left[I_1^2-h^2I_2(1-I_2)\right]\mp 2hI_1\sin\varphi. \qquad (9)$$

The minus sign in front of the last terms in Eqs. (8) and (9) corresponds to positive phase contrast.

EXPERIMENT

Analysis of Eqs. (7) to (9) shows that in the case of the coloring in NH_4Cl crystals which we studied,[6] the effect of depth is negligible chiefly because the width of the crystals was relatively large (2.5-4 μ) and the objective used for the studies (×40) relatively weak. Therefore we now chose objects and experimental conditions better adapted for detecting the depth effect.

Firstly we chose from a preparation of NH_4Cl crystals in air four long prismatic crystals with widths ranging from 0.34 to 2.43 μ. Under the weak objective, all showed the same saturated blue coloring. Equation (7) shows that their thicknesses must have been almost identical and equal to 1.00 ± 0.01 μ, since even a small deviation in thickness would have caused a large change in chromaticity. The observations were made with 20× and oil immersion 90× objectives in quasi-monochromatic light obtained by using two Schott (Jena) filters (BG 12 and VB 5). The spectrum of the transmitted light has a sharp maximum at 485 mμ. Between 460 and 510 mμ the contrast $C = (B - h^2)/h^2$ between the background and the image is a linear function of λ, so that using only one wavelength in the calculation is perfectly valid.

The contrast was measured both photographically and visually. In general, the values obtained photographically agreed with the visual results, but the scatter was greater for the photographic values than for the visual ones because of the difficulty of sharply focusing on the photographic plate in such weak light.

Visual observations, more exact and easily reproducible, were made with an optical wedge, cemented to the micrometer of the eyepiece and moving in the plane of the scale (Fig. 2).

The wedge, calibrated by means of a microphotome was partly covered by the image of the crystal Cr. This measurement was achieved by moving the stage until the luminance of the crystal was equal to that of the background.

Results obtained by the two authors individually were reproducible and agreed with each other.

Figure 3 compares the calculated and measured figures averaged over 10 to 15 measurements. Curves 1 and 2 were computed from Eqs. (8) and (9) considering and neglecting the effect of depth for the 90× objective. Curve 3 corresponds to the 20× objective. The effect of depth is not felt in this case. The integrals I_1, I_2, $\overline{I}_1$, $\overline{I}_2$ were evaluated graphically; the transmission of the phase annulus was measured with an FEU-17 photomultiplier in monochromatic light obtained with an interference filter. The photocurrent i indicated by the apparatus was measured as a function of the aperture a of the image of the annular diaphragm of the microscope illumination system. The monotonic increase of i(a) along the curve broke off when the image of the diaphragm intersected the phase annulus and the curve went through a maximum when the image and the annulus coincided (Fig. 4). The transmission was obtained from the relationship $h^2 = i_0/i_m$.

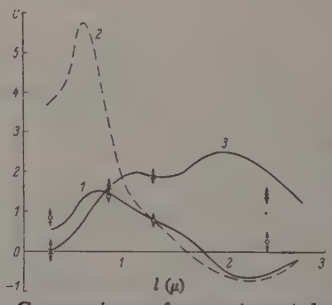

Fig. 3. Comparison of experimental and theoretical contrast data. Curve 1—90×, depth effect present; curve 2—90×, depth effect absent; curve 3—20×.

In order to obtain the best possible correspondence between theory and experiment, we used the value 0.996 for the thickness of the crystal and n = 1.653 from the Tables. The good agreement between the experimental points and the theoretical curve which takes account of the depth effect is clear evidence of the existence of this effect and of the validity of the relationships derived above.

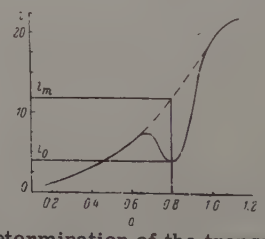

Fig. 4. Determination of the transmission of the phase annulus.

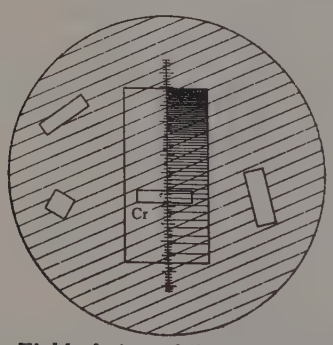

Fig. 2. Field of view of the ocular for visual measurements of the contrast between the background and the image.

The deviations observed for the widest crystal can attributed to the finite width of the annular diaphragm, was shown earlier.

We also studied typical biological phase objects, a ure of Bacillus anthracus in water, with a diameter of . In this case the phase change was slight, the dis- sion of the phase plate was negligibly small, and since coloring was observed it was convenient to work with te light, using the photographic method.

The center effect was always considerable, while the th effect appeared only with the 90× objective.

Objective		10×	20×	40×	90×
h^2		0.39	0.37	0.35	0.34
Calculated contrast	no depth effect	—0.569	—0.628	—0.658	—0.624
	with depth effect	—0.569	—0.627	—0.652	—0.580
Measured contrast		—0.533	—	—0.653	—0.578
Contrast with correction for halation		—0.579	—	—	—

In the Table the computed and experimental results compared. If we assume that n = 1.359 for bacillus toplasm, the contrast values obtained for 40× and 90× ectives agree very well with the values obtained from (8), which takes account of the depth effect; however, contrast for the 10× case was definitely low.

The reason for this discrepancy must be sought in halation effect. In fact, the images of bacilli obtained n the 10× objectives are very narrow and darker than background. If we plot the density of the image meas- d with a microphotometer as a function of the distance rom the center of the image, we get a curve resembling nverted arrowhead, without (Fig. 5a) any uniformly ght plateau at the center. The broader image of an olitude object obtained with the same objective (Fig. has such a flat region.

The reason for this difference is background light ttered by the grains of the plate into the dark region he image; this is the halation effect, well known in tography.

The effect causes the sharp boundaries between the ongly and weakly illuminated regions to become dif- e and to shift towards the dark region.

By superimposing the curve of Fig. 5a on that of .. 5b so that their lower parts coincide, we can esti-

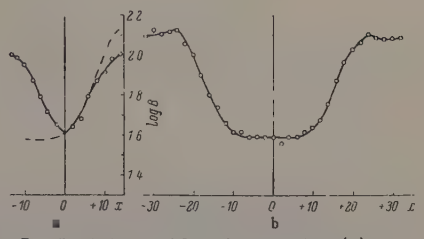

Fig. 5. Variation of brightness for (a) a narrow phase object and (b) a wide amplitude object photographed with 10× objectives.

mate actual contrast values given in the last line of the Table, which agree better with theory. Consequently, for the case where the image is small and darker than the background, the halation effect can considerably reduce the contrast.

CONCLUSION

We feel that in the present paper we have succeeded in demonstrating the existence of a previously undescribed deviation from the elementary theory of phase contrast. This deviation is the depth effect arising when a phase object is not in sharp focus over all of its depth. This effect is usually negative in the case of high power objectives and objects whose widths are comparable with the wavelength of light and with their thickness.

REFERENCES

1. F. Zernike, Physica 9, 686 (1942).
2. A. Bennett, X. H. Oxterberg, H. Jupnik, and O. W. Richards, "Phase Microscopy." Wiley, New York, 1951.
3. H. Wolter, Ann. Physik 7, 33, 147 (1950).
4. U. Schmidt, Ann. Physik 16, 68 (1955).
5. A. Frey-Wyssling, Naturwiss. 39, 145 (1952); Ibid. 40, 517 (1953).
6. R. Grigorovici and R. Manaila, Rev. opt. 37, 281 (1958).
7. R. Grigorovici and R. Manaila, Stud. Cercet. Fiz. 11 711 (1960).
8. F. Zernike, Physica 9, 974 (1942).

ON THE CHROMATIC FIELD ABERRATIONS IN ELECTRON MICROSCOPES

V. N. Vertsner and Yu. V. Vorob'ev (pp. 120-126)

Received 25 March 1960

On the basis of recent data on magnetic lenses, a calculation has been made of the chromatic field aberrations in an electron microscope (aberration in magnification and error in rotation). The chromatic field aberrations in an EM-3 electron microscope have been investigated for the case where replicas of diffraction gratings served as the objects.

The chromatic field aberrations in an electron microscope (and specifically the aberrations in magnification and rotation) were first investigated by Morito[1] and Kanaya.[2] These authors did not have at their disposal the information in recent research on magnetic lenses and they were therefore obliged to use for their calculations a close approximation of the magnetic field in the form of a bell-shaped curve. In view of the fact that there are indications in the literature that such an approximation can lead to a considerable discrepancy with the experimental data, we considered it necessary to carry out both a calculation and an experimental verification of the chromatic field aberrations on the basis of the data on magnetic lenses obtained recently. Naturally, in doing this we had to change both the method of calculation and the experimental method.

CALCULATION OF CHROMATIC FIELD ABERRATION IN MAGNIFICATION IN THE TWO-LENS SYSTEM OF AN ELECTRON MICROSCOPE

Let us begin with the computation of the chromatic aberration in the magnification of the objective. Let us introduce two fundamental solutions of the paraxial equation U(Z) and V(Z), where V(Z) is the mirror image of U(Z) relative to the plane of symmetry of the field of the objective and U(Z) is determined by the initial conditions $U(-\infty) = 1$ and $U'(-\infty) = 0$. Furthermore, let us designate by Z_0 the distance of the second focal plane from the center of the lens, and by f_0 and f_1 the first and second focal distances (Fig. 1). Let us place the object in the first focal plane of the objective where $Z = -Z_0$. Then the equation of the main trajectory for the condition that the object is illuminated by a parallel beam of electrons will have the form

$$r = CU(Z).$$

If the point under consideration on the object is at the distance h from the axis, then the equation of the main trajectory passing through this point will be written in the form

$$r(Z) = h\frac{U(Z)}{U(-Z_0)}.$$

If, now, we employ the Wronskian

$$U(Z)V'(Z) - U'(Z)V(Z) = \frac{1}{f_1},$$

then, since $V(-Z_0) = 0$ and $V'(-Z_0) = 1/f_0$, we have

$$U(-Z_0) = \frac{f_0}{f_1} \qquad (1)$$

and

$$r(Z) = h\frac{f_1}{f_0}U(Z).$$

Now let us change the current in the objective. Then the equation of the main trajectory passing through the same point on the object will have the form

$$r^{(1)}(Z) = h\frac{U^{(1)}(Z)}{U^{(1)}(-Z_0)},$$

where the symbol (1) indicates that all of the values are calculated for the changed current in the objective. When the current in the objective is changed, the position of the focal plane also is changed, i.e., $Z_0^{(1)} = Z_0 + \Delta Z_0$.

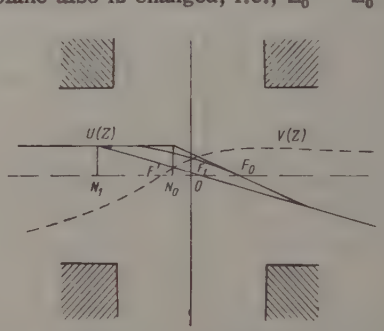

Fig. 1. $Z_0 = F_0O$; $f_0 = F_0N_0$; $f_1 = F_1N_1$.

Considering ΔZ_0 as small, by expansion in a Taylor series we obtain

$$U^{(1)}(-Z_0) = U^{(1)}(-Z_0^{(1)}) + \Delta Z_0 U^{(1)\prime}(-Z_0).$$

From the Wronskian, in a manner cimilar to that above, we obtain

$$U^{(1)}(-Z_0^{(1)}) = \frac{f_0^{(1)}}{f_1^{(1)}}.$$

Thus, neglecting the infinitesimal values of higher order, we have

$$U^{(1)}(-Z_0) = \frac{f_0^{(1)}}{f_1^{(1)}} + \Delta Z_0 U'(-Z_0)$$

and

$$r^{(1)}(Z) = -h\frac{U^{(1)}(Z)}{f_0^{(1)} + \Delta Z_0 f_1^{(1)} U'(-Z_0)} \cdot f_1^{(1)}. \qquad (2$$

Determining the fundamental solution for sufficiently large values of Z outside the field of the objective, we have

$$U^{(1)}(Z) = -\frac{1}{f_1^{(1)}}(Z - Z_1^{(1)}).$$

Substituting this expression in $r^{(1)}(Z)$ and assuming

$$f_0^{(1)} = f_0 + \Delta f_0,\ f_1^{(1)} = f_1 + \Delta f_1,\qquad Z_1^{(1)} = Z_1 + \Delta Z_1,$$

we obtain

$$r^{(1)}(Z) = +h\left\{-\frac{Z - Z_1}{f_0} + \frac{Z - Z_1}{f_0}\left[\frac{\Delta f_0}{f_0} + \frac{\Delta Z_0}{f_0} \times f_1 U'(-Z_0)\right] - \frac{\Delta Z_1}{f_0}\right.$$

re we have neglected infinitesimals of higher order.

On the other hand, from formula (1) for large values Z we have

$$r(Z) = -h\frac{Z - Z_0}{f_0}.$$

Thus, in the plane of the image for the objective n $Z = Z_b$ (by definition of the magnification m_0) we e

$$m_0 = -\frac{Z_b - Z_0}{f_0}$$

consequently the expression for the relative chro- ic aberration in magnification has the form

$$\frac{\Delta m_0}{m_0} = \frac{r'(Z_b) - r(Z_b)}{r(Z_b)} = -\frac{\Delta f_0}{f_0} - \frac{\Delta Z_0}{f_0} f_1 U'(-Z_0), \quad (3)$$

re we have neglected the quantity $\Delta Z_1/m_0 f_0$, which is ll for large values of the magnification m_0.

For the chromatic aberration in the magnification of projection lens the derivation is considerably simpler. ually the magnification of the projection lens is de- mined by the formula

$$m_p = \frac{\bar{H}}{f_{1p}},$$

re $\bar{H}$ is the distance from the center of the projection to the screen and f_{1p} is the second focal distance of projector.

From this formula we have

$$\frac{\Delta m_p}{m_p} = -\frac{\Delta f_{1p}}{f_{1p}}. \quad (4)$$

Thus, since the total magnification of the microscope s equal to the product of the magnifications of the ob- ive and the projector ($m = m_o m_p$), the total relative nge in the magnification of the whole system may be tten in the form

$$\frac{\Delta m}{m} = \frac{\Delta m_0}{m_0} + \frac{\Delta m_p}{m_p} = -\left\{\frac{\Delta f_0}{f_0} + \frac{\Delta Z_0}{f_0} f_1 U'(-Z_0) + \frac{\Delta f_{1p}}{f_{1p}}\right\}.$$

The relative change in magnification is connected n the coefficient of chromatic aberration in magnifica- . C_m by the simple relationship

$$\frac{\Delta m}{m} = C_m \frac{\Delta V}{V}.$$

Similar relationships exist for the objective and pro- or individually.

For the purpose of actual calculation of the coeffi- nts C_m for the objective and projector of the EM-3 ctron microscope we made a numerical computation he trajectories for different values of the excitation rent. The graphs of the aberrations are given in Fig. where C_{m_0} is the coefficient of chromatic aberration magnification of the objective and C_{m_p} is the corre- nding coefficient of the projector.

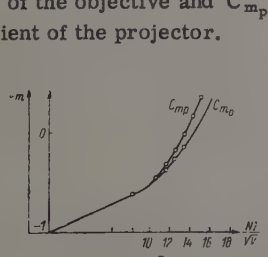

Fig. 2

Comparison of the values of the chromatic aberra- ns with the experimental values (see below) shows t actually correction of the aberrations is achieved at large values of the excitation currents in the lenses. This result should be attributed to the effect of saturation of the pole pieces, which is not taken into account in the calculations.

CHROMATIC ERROR IN ROTATION

With variations in the accelerating voltage in an electron microscope not only the magnification, but also the angle of rotation of the image changes. It is known that the angle of rotation of the image of a magnetic lens is determined by the formula

$$\theta = \sqrt{\frac{e}{8m_0 V}} \int_{-\infty}^{+\infty} B dZ = \mu_0 \sqrt{\frac{e}{8m_0}} \frac{NI}{\sqrt{V}} = 0.1863 \frac{NI}{\sqrt{V}};$$

$$\int_{-\infty}^{+\infty} B dZ = \mu_0 NI, \quad (6)$$

where θ is measured in radians, NI in amperes, and V in volts.

The calculation of the angle of rotation of the image by the field of the objective presents some difficulties, since usually the object is within the field of the objective lens and for the formation of the image only a part of the objective field is used. Therefore the angle of rotation of the image of the objective should be calculated by the formula

$$\theta_{ob} = \sqrt{\frac{e}{8m_0 V}} \int_{-Z_0}^{+\infty} B dZ = 0.1863 \frac{(NI)_e}{\sqrt{V}}, \quad (7)$$

where the integration should start only from the first focal plane, in which the object is located. By $(NI)_e$ we designate the number of ampere turns actually used in the objective for the formation of the image.

The relationship of the angles of rotation of the image in the objective (ob) and the projection (pr) lenses is given in Fig. 3.

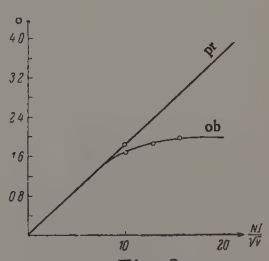

Fig. 3

Knowing the chromatic error in magnification and the angle of rotation, it is easy to calculate how these errors affect the quality of the image. For this purpose let us consider a point on the object at a distance h from the axis of the objective. When the accelerating voltage is changed by the amount ΔV, the image of this point will be shifted on the screen in a radial direction by the amount Δmh. Furthermore, the angle of rotation of the image will be changed by the amount

$$\Delta\theta = \Delta\theta_{ob} + \Delta\theta_{pr}.$$

According to formulas (6) and (7)

$$\Delta\theta_{pr} = -\frac{1}{2}\theta_{pr}\frac{\Delta V}{V}, \quad \Delta\theta_{ob} = -\frac{1}{2}\theta_{ob}\frac{\Delta V}{V},$$

whence

$$\Delta\theta = -\frac{1}{2}(\theta_{pr} + \theta_{ob})\frac{\Delta V}{V},$$

and as a result of the rotation the image of the point on the screen is turned around the axis for the distance $\Delta\theta h$. Thus the square of the total chromatic error imparted to the object will have the value

$$\Delta^2 = h^2(C_{in}^2 + C_\theta^2)\left(\frac{\Delta V}{V}\right)^2,$$

where

$$C_\theta = -\frac{1}{2}(\theta_{ob} + \theta_{pr}).$$

Let us note that in present day electron microscopes, in which the field of view constitutes not more than 2-3 μ and $\Delta V/V < 5 \times 10^{-5}$, these errors are small. They play a very important role, however, in the inspection and balancing of electron microscopes.

EXPERIMENTAL INVESTIGATION OF CHROMATIC FIELD ABERRATIONS IN AN ELECTRON MICROSCOPE

In an electron microscope with a nonachromatic optic, as a result of the superposition of the two field aberrations the images of the points will appear in the form of arcs[3] formed with radii of angle β, the magnitude of which can be found from the ratio

$$\operatorname{ctg}\beta = \frac{C_m}{C_\theta}. \qquad (8)$$

The angle β may vary from 0° to 180°, depending on the relative weight of the chromatic errors in magnification and rotation. Having determined the angle β, we can find, from Eq. (8), the ratio of the coefficients of the chromatic field aberrations.

From the same equation it follows that when there is no chromatic field error in magnification, $\cot\beta = 0$ (i.e., the angle $\beta = 90°$). In this case when the accelerating voltage is changed, the points of the object will be represented by arcs having a common center. In practice, the procedure for exciting the two lenses is usually selected so that compensation of the chromatic field error in magnification occurs (then by counterconnection of the windings of the lenses a substantial lowering of the chromatic field error of rotation also is accomplished).

The choice of the procedure for achromatization is usually made more precise by experimental means. To make the choice of the exciting conditions easier, an alternating sinusoidal voltage that substantially increases the chromatic error is applied to the accelerating voltage. By the method indicated below, the angles β for different values of excitation of the objective are determined from photographs and the one at which $\beta = 90°$ is selected from them. Since when the exciting conditions for the objective are changed, its focal distance changes, a corresponding simultaneous change in the position of the object is required. Usually films with perforations or objects with small particles (in particular, particles of carbon black) are used as the object. The voltaic center of the image (which remains motionless when the acceleration is changed) is brought, as far as possible, to the center of the final image.

For the determination of the angle β we have developed a comparatively simple experimental method which has been tested on the EM-3 electron microscope. As objects, instead of those mentioned above, we used diffraction-grating replicas shadowed with gold. If the voltaic center is approximately at the center of the image, then when an alternating component is applied and the lens windings are suitably connected (with complete elimination of the error in magnification), the image of the striations of the diffraction grating appears distinct only on the line passing through the voltaic center and perpendicular to the striations. The images of the gold particles will have the form of arcs of circles with a center coinciding with the voltaic center (see Fig. 4).

Fig. 4

In the absence of compensation of the chromatic field error in magnification, the line joining the distinct sections of the image of the striations will not coincide with the perpendicular to the striations, and the angle between them will be equal to $90° - \beta$ (Fig. 5).

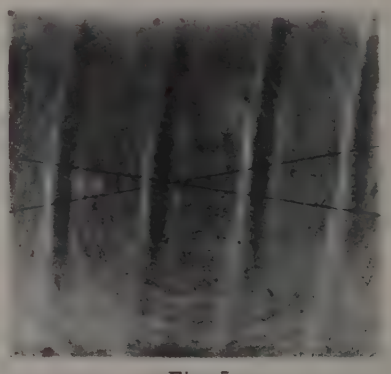

Fig. 5

For the experimental determination on the EM-3 microscope of the magnitude of the current in the objective lens at which the chromatic aberration in magnification appears to be compensated, an alternating component with a frequency of 50 cps and an amplitude of 1600 volts was applied to the accelerating voltage. Initially, the direction of the current in the objective and the projection lenses was consistent, i.e., the chromatic errors of rotation

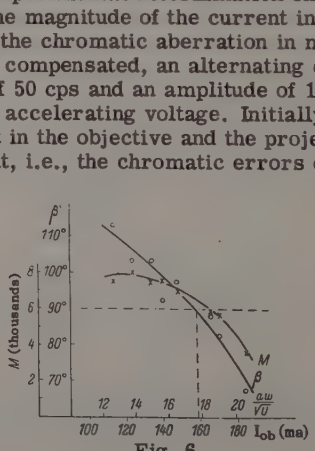

Fig. 6

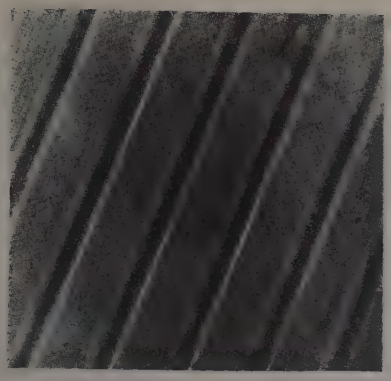

Fig. 7

ere additive. A graph (Fig. 6) that was constructed of ne relationship of the angle β to the excitation of the ojective showed that compensation of the field error in agnification ($\beta = 90°$, Fig. 4) occurs at a current of 158 a in the objective. The current in the projection lens as selected as 62.5 ma from the condition $C_{mp} = 0$ (in accordance with the curves of Fig. 2). On the same graph (Fig. 6) is shown the change in magnification M of the microscope versus the excitation of the objective. From the data presented it is seen that when $\beta = 90°$, the magnification will be 6000. The photograph in Fig. 4 was obtained at a magnification of 6000 times when an additional voltage with an amplitude of 1600 volts was applied to the accelerating voltage, and the chromatic error in magnification was compensated, but the lenses were so connected that the rotations were additive. The chromatic error of rotation in this case was a maximum. The photograph in Fig. 7 was obtained under the same conditions, but with the lenses counterconnected, i.e., with the minimum total chromatic field error possible in the presence of the alternating component of the accelerating voltage of 1600 volts.

REFERENCES

1. N. Morito, J. Appl. Phys. **25**, 986 (1954).
2. K. Kanaya, Repts. Elec. Communs. Lab., Nippon Telegr. and Teleph. Public Corp., No. 548, 20 (1955).
3. S. Katagiri, Rev. Sci. Instr. 26, 870 (1955).

NONSELECTIVE OPTICO-ACOUSTICAL RECEIVER OF RATIATION WITH A CAPACITOR MICROPHONE

N. A. Pankratov and E. F. Vasil'ev* (pp. 127-130)

*N. A. Pankratov developed the receiver, E. F. Vasil'ev the amplifier.

Received 19 April 1960

A receiver with a capacitor microphone was built, based on preceding theoretical and experimental investigations which had demonstrated that the threshold sensitivity of (selective and nonselective) optico-acoustical receivers does not depend on the type of microphone used. The receiver has its highest threshold sensitivity at low frequencies, where it has practically the same sensitivity as a receiver with an optical microphone. A basic scheme of an amplifier with high frequency input is described.

Radiation receivers based on the optico-acoustical ffect, that is, based on pressure pulsations of a gas ctuated by a chopped radiation flux and observed with a icrophone of some type or another, are widely used at resent in engineering and in spectroscopy. In the nonelective version of the receiver the radiation is absorbed either by a layer of black pigment,[1,2] or by a very in metal film deposited on an organic substrate,[3] or by arbonized down.[4] The heat is transferred from the reeiver to the surrounding gas by thermal conductivity nd it is conducted away to the walls of the chamber. The nreshold of sensitivity of the receiver is limited by luctuations in the gas pressure, caused by an energy xchange between the gas, the absorber, and the walls. here is, moreover, through the entrance window, a raiative exchange between the absorbing film and the exerior.

A number of research workers have concerned themelves with the theory of the optico-acoustical receiver.[5-10] he properties of receivers provided with various types f microphones have been compared in theoretical and xperimental publications by one of the authors of this aper, and it has been shown that the threshold of reeiver sensitivity is determined by the type of physical ffect on which its action is based and not by the type of microphone used.[7,8,11-13] The only condition set forth for the microphone consists in the latter being capable of transmitting to the input of the amplifier a signal which corresponds to the pressure fluctuations of the gas. From this point of view electrodynamic, capacitor, and optical microphones are of equal value when they are optimized. In the case of a selective receiver the corresponding threshold sensitivity is realized at low frequencies if a capacitor or an optical microphone is used, and at high frequencies if an electrodynamic receiver is employed.

The optical microphone has until now been the type most successfully used in the nonselective version of the receiver.[5,13] When the first attempt was made to apply the more simply constructed capacitor microphone, described in ref. 2, the receiver sensitivity was not found to be high enough, but for reasons other than fundamental.

A capacitor microphone was also tested in 1952, in the course of investigations mentioned above, in connection with the comparison of several types of microphones as applied to the task of measuring extremely weak fluxes of radiation. The membrane of this microphone had the same thickness as the membrane of an optical microphone and it was covered with a layer of antimony. The fixed electrode was placed at a distance of 20 μ from the membrane. Amplification of the signal developed by

the microphone was obtained by means of an amplifier with an input stage of the electrometer type. This combination of a receiver and an amplifier did not yield the expected result as the noise level was determined by the amplifier itself, and not by the receiver chamber, because of the poor quality of the amplifier. An increase in the polarizing voltage on the microphone did not lead to an appreciable increase in sensitivity, as the membrane stretched and stuck under the action of the voltage.

Further work was done in two directions. In one case the receiver was the same as described above, but a high frequency connection was provided for signal amplification. In the other case microphones with stiff membranes and amplifiers with electrometer input were used.

In the present paper we present results obtained with a high frequency connection of the capacitor microphone.

CONSTRUCTION OF THE RECEIVER

The construction of the receiver is explained in Fig. 1a and b. The radiation enters through window 1 and is absorbed by a layer of aluminum deposited on an organic film substrate in cavity 2. This film is attached to a brass ring 3, glued to the entrance window. A metallized membrane is stretched over another brass ring 4, the metallic layer being in contact with the ring. The membrane is covered by a layer of either antimony or silver. A brass electrode 5 is placed parallel to the membrane. Grooves and openings as shown in Fig. 1b are arranged on the front plane surface of the electrode. The openings connect the small volume under the membrane to the large volume behind the electrode and thus decrease the elastic resistance of the gas under the membrane. The grooves give some decrease in the gas friction caused by the displacement of the gas from the center to the edges of the membrane during its flexures. The electrode is fixed in an isolation ring 6, made out of plexiglass. The gap between the electrode and the membrane is 10-15 μ wide. The microphone capacitance is 4-6 pf. It withstands a polarizing voltage of 5-15 volts. To obtain maximum sensitivity the tension of the membrane must be such (as shown later) that the elasticity of the membrane is equal to the elastic resistance of the gas in the chamber, that is, it must have the value of 1.6×10^4 dyne/cm (if the membrane has a higher tension, the polarizing voltage may reach 100-150 volts.)

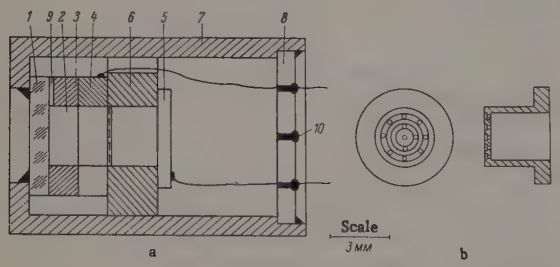

Fig. 1

The receiver is located in a shielding housing 7, closed off by cover 8. The volumes in front of and behind the membrane are connected by a compensating channel 9 to compensate for slow changes in temperature. The length and cross section of the channel are chosen such that there is no noticeable flow of gas out of the volume in front of the membrane when an intermittent flux of radiation is measured. Opening 10 is used for evacuation of the receiver and for filling it with xenon. A scale is shown on the drawing for comparison.

AMPLIFIER LAYOUT

In Fig. 2 is represented a block diagram of the amplifier used for amplification of the signal developed in the receiver. The receiver 1 is connected to one arm of a balanced AC bridge 2, which is powered by a high frequency generator 3. The balance of the bridge is periodically disrupted when an intermittent flux of radiation enters the receiver and the high frequency voltage is thus amplitude modulated. This voltage is amplified by amplifier 4 and then enters the detector 5 from the output of which the envelope of the carrier is taken off. That is, a voltage is taken off which has the interruption frequency of the radiation flux falling on the receiver. This signal is amplified by a low frequency amplifier 6, detected by the synchronous detector 7, and then enters the terminal dc current indicator device 8. Oscilloscope 9 serves to control the ac signal. The low frequency amplifier can be used either as a broad band amplifier or as a narrow band amplifier tuned to a frequency of 10 cps. A reference voltage supplied by a reference generator 10, mounted on the same axis as motor 11, is applied to the synchronous detector in the required phase.

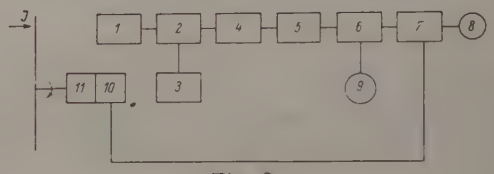

Fig. 2

The frequency of the supply voltage, stabilized by quartz, is 320 kc. The high frequency voltage on the capacitor microphone is 7 volts when the bridge is balanced. The band-pass of the bridge power amplifier channel $\Delta f_{0.7} = 7$ kc.

The high frequency amplifier has an amplification coefficient of 14.3×10^3. The low frequency amplifier has an amplification coefficient of 100 and a variable band-pass width—a narrow $\Delta F_{0.7} = 0.15$ cps for a resonant frequency of 10 cps, and a large $\Delta F_{0.7} = 3$ kc. The component of carrier frequency can be compensated down to the noise level of the power supply, which is of the order of 2-3 μv at the output of the bridge. A stable state of compensation was such that the ratio of the levels of carrier frequency at the input and the output of the bridge had a value of 1.5×10^5 at a bridge output level of the carrier frequency component of 100 μv.

An amplifier with a high frequency bridge was described in ref. 4; it was intended as a means of connecting ordinary capacitor microphones in radio broadcasting installations. It was used in refs. 2, 15 to amplify signals developed by optico-acoustical receivers with a capacitor microphone. The high frequency method of connecting a microphone, as shown in ref. 14, is more complex than the use of an electrometer input, but it also has a number of advantages. The microphone has a relatively small capacitive impedance at high frequencies, and therefore the isolation requirements for the microphone itself and its mounting are considerably reduced. Preamplification takes place at high frequency and consequently low frequency noise, caused by the flicker effect of the cathode of the first tube, does not appear. The noise coming in, together with the supply voltage from the high frequency generator is partially compensated in the arms of the bridge when it is balanced.

RESULTS OF MEASUREMENTS

A measurement of the sensitivity of the described receiver was made as follows: the signal from a Hefner candle was fed into the receiver which had in this case a diaphragm 1 mm in diameter installed in front of it. The low frequency amplifier was operating in the wide band-pass mode and the signal was observed and read on the screen of a cathode ray oscilloscope EO-7. Next, the weak noise value was registered with a closed receiver. The bandwidth of the low frequency amplifier was in this case equal to 0.15 cps. The radiation flux equivalent to the root mean square noise and the specific sensitivity of the receiver were calculated from the obtained data.

It was determined from the data that individual samples of receivers with an input window 3 mm in diameter had a root mean square noise of $1\text{-}2 \times 10^{-10}$ watts, with an amplifier band-pass of 0.15 cps at a modulation frequency of 10 cps. These receivers were then only two to four times worse in threshold sensitivity than receivers with an optical microphone.

The specific sensitivity of the tested receivers had a value of approximately 400 volts/watt (it is equal to 30,000-40,000 volts/watt in receivers with an optical microphone). The specific sensitivity refers to the output of the bridge circuit to which the microphone is connected, and it corresponds to a modulation depth of 10% at a 100-μv level of the carrier frequency. The time constant of the receiver is 0.01 sec with its chamber filled with xenon, as in a receiver with an optical microphone.

It should be pointed out that the noise measured at the output of the whole receiving apparatus is basically determined by the generator noise, inasmuch as the same noise is observed when the microphone is replaced by a capacitor of the same capacitance and quality. The highest sensitivity was obtained in this scheme when the bridge was slightly detuned, when the detection is noticeably improved, with an appearance in the detector of a component of the carrier frequency. One can expect an increase in sensitivity of the receiving system and a decrease in the amount of noise introduced by the generator if synchronous detection at high frequencies is used and an exact balancing is realized.

Taking into account that the capacitor microphone is much simpler than the optical, it can be concluded that receivers with this type of microphone will find a large number of applications in those cases in which it is necesssry to interrupt at a low frequency the radiation flux to be measured.

The authors are grateful to M. L. Veingerov for his interest and his guidance of this work.

REFERENCES

1. S. M. Luchin, Zhur. Tekh. Fiz. 16, 1115 (1946).
2. P. F. Weber, Optik, 152 (1950).
3. M. Golay, Rev. Sci. Instr. 18, 347 (1947).
4. A. N. Terenin and N. G. Yaroslavskii, Izvest. Akad. Nauk. SSSR, Ser. Fiz. 9, 203 (1945).
5. M. Golay, Rev. Sci. Instr. 20, 816 (1949).
6. N. A. Pankratov, L. N. Galkin, Zhur. Opt.-Mekh. Prom. No. 1, 67 (1957).
7. N. A. Pankratov, Zhur. Opt.-Mekh. Prom. No. 2, 16 (1957).
8. N. A. Pankratov, Opt. i Spektr. 2, 662 (1957).
9. A. O. Sall', Opt. i Spektr. 6, 219 (1959), Optics and Spectroscopy 6, 139 (1959).
10. K. Josihara. Sci. of Light (Tokyo) 7, 789 (1959).
11. N. A. Pankratov and L. M. Vinogradova, Opt. i Spektr. 7, 789 (1959), Optics and Spectroscopy 7, 464 (1959).
12. N. A. Pankratov, Opt. i Spektr. 8, 109 (1960), Optics and Spectroscopy 8, 53 (1960).
13. N. A. Pankratov, Zhur. Opt.-Mech. Prom. No. 1, 37 (1960).
14. I. I. Zaalberg van Zelst, Philips Tech. Rev. 9, 357 (1948).
15. A. Girard, Recepteur pneumatique de rayonnement (Pneumatic radiation receiver). Fifth Meeting and Conference of the International Commission for Optics, Stockholm, 1959.

ON THE INFLUENCE OF THE NATURE OF THE SOLVENTS ON THE CHARACTER OF THE BAND OF THE CARBONYL GROUP IN THE INFRARED SPECTRA OF CARBONYL COMPOUNDS

T. V. Yakovleva, A. G. Maslennikova, and A. A. Petrov (pp. 131-133)

Received 12 April 1960

In a series of works by domestic and foreign investigators, it has been shown that the band of the valence vibrations of the carbonyl group in infrared and Raman spectra consists of at least two bands differing in frequency and intensity.[1-6] In other works, the influence of solvents on the frequency and intensity of the band of the carbonyl group is noted.[7-11] However, no systematic study has been carried out concerning the influence of the nature of the solvents on the character of the band of the carbonyl group.

We have established that solvents may be divided into three types according to their influence on the contour of the band of the carbonyl group. In solvents of the first type, to which polar substances (nitromethane, chloroform, alcohols, toluene) belong, there appears in dilute solutions only one (lower-frequency) band of the carbonyl group. In solvents of the second type (carbon tetrachloride, carbon disulfide, benzene), both bands of the carbonyl group appear. And finally, in solvents of the third type, to which nonpolar substances belong (hexane, oxtane, cyclohexane), there appears only a higher-frequency band of the carbonyl group (see Table 1 and Figure).

In the literature, there is no unanimity of opinion with respect to the causes of the splitting of the carbonyl group frequency in the infrared spectra of aldehydes and ketones. This splitting has been ascribed to rotational isomerism,[5] Fermi resonance,[10,12] enolization and association of the enols with the carbonyl compounds,[2] association between the molecules of the carbonyl compound and of the solvent,[10,13] dipole interaction,[14] and other causes.[4]

The first hypothesis is not consistent with the presence of two bands in the spectrum of acetone. Fermi resonance cannot depend on the nature of the solvent. Enol forms can exist, in the case of the simplest aldehydes and ketones, only in very small concentrations, and therefore explanation of the splitting as a result of enolization likewise does not withstand criticism.

It is most probable that the splitting of the band of the carbonyl group in the infrared spectra is connected with association. If we accept this explanation, then the higher frequency, the one which is preserved in dilute solutions of aldehydes and ketones in nonpolar solvents, may be assigned to the vibrations of the unassociated carbonyl group, while the lower frequency, the one which is preserved in the spectra of solutions in polar solvents, is assigned to the vibrations of the associated carbonyl group.

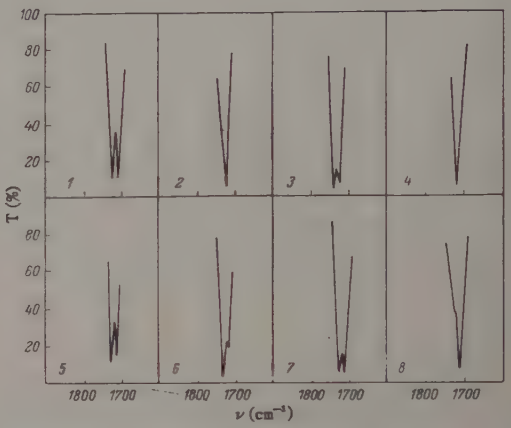

Contours of the absorption band of the carbonyl group. 1—methyl propyl ketone; 2—methyl propyl ketone in octane; 3—methyl propyl ketone in benzene; 4—methyl propyl ketone in toluene; 5—cyclohexanone; 6—cyclohexanone in cyclohexane; 7—cyclohexanone in carbon tetrachloride; 8—cyclohexanone in chloroform.

A change in the concentration of the solutions within the limits indicated in Table 2, with simultaneous proportional change in the layer thickness (i.e., while keeping the same number of molecules of the carbonyl compound

Table 1. Vibration Frequencies (cm^{-1}) of the Carbonyl Group in the Infrared Spectra of Carbonyl Compounds and Their Solutions

Solvent	Substance							
	Acetone	Methyl ethyl ketone	Methyl propyl ketone	Diethyl ketone	Pinacolone	Cyclohexanone	Acetophenone	Benzophenone
	1714 1728	1715 1726	1712 1724	1715 1728	1714 —	1715 1727	1682 1695	1670 —
Hexane	— 1726	— 1726	— 1724	— 1724	1715 —	— 1725	— 1692	1674 —
Octane	— 1726	— 1724	— 1726	— 1724	1714 —	— 1722	— 1693	1673 —
Cyclohexane	— 1724	— 1724	— 1724	— 1722	1712 —	1714 1724	— 1692	1670 —
Carbon tetrachloride	1718 1726	1715 1723	1714 1724	1715 1723	1712 —	1713 1723	— 1690	1670 —
Carbon disulfide	1717 1726	1718 1728	1712 1726	1718 1726	1715 —	1716 1725	— 1694	1668 —
Benzene	1718 1725	1713 1724	1714 1724	1715 1722	1714 —	1713 1722	— 1690	1668 —
Toluene	1714 —	1713 1723	1712 —	1713 1724	1713 —	1717 1724	— 1686	1669 —
Chloroform	1713 1724	1712 1723	1714 —	1715 —	1708 —	1709 1727	1682 1691	1660 —
Nitromethane	1716 —	1714 —	1712 —	1713 —	1708 —	1710 —	— 1685	1667 —

Note: The data were obtained with the help of an IKS-15 spectrophotometer in 1% solutions, at a layer thickness of 0.25 mm. The pure ketones were studied at a layer thickness of 0.01 mm.

Table 2. Vibration Frequencies of the Carbonyl Group in the Infrared Spectra of Solutions of Various Concentrations

Substance and solvent	Concentration (%)	Layer thickness (mm)	Frequency (cm^{-1}) "polar"	Frequency (cm^{-1}) "nonpolar"
Acetone in CCl_4	1	0.5	1718	1726
	0.5	1.0	1718	1726
	0.1	5.0	1718	1726
	0.05	10.0	1718	1726
Cyclohexanone in CCl_4	1	0.5	1713	1723
	0.5	1.0	1713	1723
	0.1	5.0	1713	1723
	0.05	10.0	1713	1723
Acetone in hexane	1	0.5	—	1724
	2	0.25	—	1724
	5	0.1	—	1724
	15	0.032	—	1724
Cyclohexanone in $CHCl_3$	1	0.5	1709	—
	2	0.25	1709	—
	5	0.1	1709	—
	15	0.032	1709	—

the path of the light beam), does not affect the shape of e absorption band of the carbonyl group. This indicates at the percentage of associated molecules is not changed ereby. Since more than two bands are sometimes observed in the 1700 cm^{-1} region in the spectra of concentrated solutions of carbonyl compounds in thick layers, e may suppose that these compounds are capable of ring associated structures of several types.

The regularity here considered has been studied ough many examples. In Table 1 are presented the ta for two symmetric aliphatic ketones (acetone and ethyl ketone), two unsymmetric aliphatic ketones ethyl propyl ketone and pinacolone), an unsaturated one (mesityl oxide),* an aliphatic-aromatic ketone

*Translator's note: Mesityl oxide is not included in Table The error is in the original.

etophenone), and an aromatic ketone (benzophenone). an be seen from the table that, along with the general gularity considered above, the separate carbonyl compounds manifest their own peculiarities. In the case of acolone, only one frequency is observed. In the spectrum of acetophenone in chloroform, two bands of roughly equal intensity appear. In the spectrum of benzophenone, there is only one carbonyl group frequency regardless of the solvent and within the concentration limits of 1-4%. These and other deviations from the general rule are apparently connected with structural peculiarities of the carbonyl compounds and of the solvents, which in some cases favor and in others inhibit association. Thus, for example, the presence of a branched radical in the alpha position to the carbonyl group (pinacolone) inhibits association.

We have not succeeded in establishing any definite dependence between such properties of the solvents as dielectric constant or dipole moment and the character of the spectrum of carbonyl compounds in them.

REFERENCES

1. E. Gray and C. Mangin, J. phys. radium **15**, 9 (1954).
2. E. Gray and M. M. Bottreau, Compt. rend. acad. sci. **240**, 2134 (1955).
3. E. Gray, Cahiers phys. No. 71-72, 71 (1956).
4. F. J. Taboury, Cahiers phys. No. 73, 24 (1956).
5. P. Mirone and V. Lorenzelli, Atti accad. naz. Lincei. Mem., Classe sci. fis., mat. e nat. **24**, 54 (1958).
6. Cl. Mangin and M. M. Bottreau, Compt. rend. acad. sci. **242**, 2637 (1956).
7. V. M. Chulanovskii and Kim Den Dok, Izvest. Akad. Nauk SSSR, Ser. Fiz. **18**, 720 (1954).
8. V. M. Chulanovskii, Doklady Akad. Nauk SSSR **101**, 457 (1955).
9. M. L. Josien and J. Lascombe, J. chim. phys. **52**, 162 (1955).
10. C. L. Angell, Trans. Faraday Soc. **52**, 1178 (1956).
11. Tsibomura, J. Chem. Soc. Japan **77**, 962 (1956).
12. A. W. Baker, J. Phys. Chem. **60**, 1660 (1956).
13. E. J. Hartwell, R. E. Richards, and H. W. Thompson, J. Chem. Soc. 1436 (1948).
14. J. Lecomte, E. Gray, and F. J. Taboury, Compt. rend. acad. sci. **224**, 907 (1947).

REMARKS ON NEGATIVE ABSORPTION

S. G. Rautian and I. I. Sobel'man (pp. 134-135)

Received 29 April 1960

This article considers the possibility of obtaining gative absorption in electronic transitions of organic lecules by means of optical methods of excitation.*

consideration of this question has recently been published.[1] However, the models used for the calculations ere did not consider a series of important characteristics of real molecules which are known to have the possility of exhibiting negative absorption.

e scheme of levels for these molecules (for example, omatic hydrocarbons) consists of singlet (S_0, S_1, S_2, ...) d triplet (T_1, T_2, ...) terms (see Figure). The most effective excitation occurs in the singlet levels, since the ansition between ground singlet and triplet levels occurs only as a violation of the selection rules. However, is well known[2] that, as the result of nonradiative transitions the triplet level T_1 can be occupied, after which the pulation of S_0, S_1, and T_1 are determined by the Boltzmann distribution involving the vibrational states. At sufficiently low temperatures (~100°K) only the lowest vibrational states of S_0, S_1, and T_1 are populated. Thus, for comparatively high-energy vibrational states of S_0, transitions to which from S_1 and T_1 correspond to maximum intensity in the fluorescence and phosphorescence

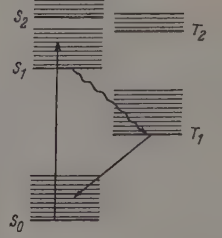

spectra, the forced emission increases the absorption, i.e., negative absorption occurs.

In order to observe negative absorption, certain conditions must be fulfilled. First of all, it is necessary that the excited molecules do not absorb the radiation at the frequency where the absorption is to be measured. It is known[3] that singlet-singlet absorption is practically continuous, i.e., for transitions $S_0 \rightarrow S_1$ negative absorption apparently is not detectable. Analysis of published data on triplet-triplet absorption[4] shows that for many molecules (e.g., naphthalene, anthracene, naphthacene, and their halogen derivatives), the frequencies of the $T_1 \rightarrow T_2$ transitions are somewhat greater than for the $S_0 \rightarrow T_1$ transitions, i.e., the conditions mentioned are fulfilled.

The second condition is the requirement of a large quantum yield for phosphorescence. Accordingly,[5] the quantum yield for phosphorescence for the molecules mentioned is relatively high and increases with decreasing quenching time, which, in turn, is favored by the introduction into the molecules of heavy atoms (I, Br).

It is necessary, finally, to have a sufficiently high concentration of excited atoms in order that the negative absorption will be observable with reasonable sample thicknesses. The determination of the value of the coefficient of negative absorption is given by the simple formula

$$|k| = \frac{\lambda_p^2}{8\pi\Delta\nu} \frac{bN}{1+b\tau}, \qquad (1)$$

where λ_p and $\Delta\nu$ are average wavelength and width of the phosphorescence spectrum, N is the number of molecules per cm^3, τ is the quenching time for phosphorescence, and b is the probability of excitation. Formula (1) is obtained on the assumption that the quantum yield of phosphorescence is equal to 1. The probability of excitation is

$$b = \int \frac{E_\nu}{h_\nu} k_\nu d\nu, \qquad (2)$$

where ν is the frequency of the exciting light, E_ν the intensity on the sample of light at frequency ν, and k_ν the coefficient of singlet-singlet absorption. Assuming $\lambda_p \approx 1\ \mu$, $\Delta\nu \approx 3 \times 10^{13}\ sec^{-1} = 10^3\ cm^{-1}$, $k_\nu N = 20\ cm^{-1}$, $\tau = 10^{-4}$ sec, $\nu = 10^{15}\ sec^{-1}$, we obtain $|k| = 3 \times 10^{-4} E\ cm^{-1}$, where E is the integrated light intensity, expressed in watts/cm^2. Thus, if $E = 30$ watts/cm^2, for a sample thickness $l \approx 10$ cm we obtain $|k|l = 0.1$. This value is sufficiently large for observation and for use in "masers."

The high energy of the exciting radiation and the low value of the energy yield of phosphorescence can lead to a significant heating of the sample. Consequently, it was necessary to use a pulse method (length of the impulse ~0.01 sec). Besides, sufficiently intense sources of excitation radiation must be pulsed.

The difficulties mentioned are associated with the large width $\Delta\nu$ of the phosphorescence spectrum. In this connection we were interested in applying the method of Shpolskii.[6]

We carried out an analogous analysis of other compounds, which were characterized by narrow luminescence lines (salts of the rare earths, organic complexes with ions of the rare earths, uranyl compounds). However, knowledge of the terms and quantum yields for these compounds is insufficient to decide about their practical utility for displaying negative absorption.

REFERENCES

1. A. P. Ivanov, Opt. i Spektr. 8, 352 (1960), Optics and Spectroscopy 8, 183 (1960).
2. "Applications of Spectroscopy in Chemistry," V. Vesta (ed.). Izd. Inostrannoi Lit., Moscow, 1959.
3. A. Gillem and E. Shtern, "Electronic Absorption Spectra of Organic Compounds." Izd. Inostrannoi Lit., Moscow, 1959.
4. D. S. McClure, J. Chem. Phys. 19, 670 (1951); Ibid. 23, 1772 (1955);
G. Porter and F. J. Wright, Trans. Faraday Soc. 51, 1205 (1955);
D. R. Craig and I. G. Ross, J. Chem. Soc. (London) 1589 (1954).
5. E. H. Gilmore, G. E. Gibson, and D. S. McClure, J. Chem. Phys. 20, 829 (1952); Ibid. 23, 399 (1955);
V. L. Ermolaev and K. K. Svitashev, Opt. i Spektr. 7, 664 (1959), Optics and Spectroscopy 7, 399 (1959).
6. E. V. Shpolskii, Uspekhi Fiz. Nauk 68, 51 (1959), Soviet Phys.-Uspekhi 2, 378 (1959).

METALLIC MIRRORS WITH AN ENHANCED REFLECTION COEFFICIENT

E. I. Levitina (pp. 135-138)

Received 3 May 1960

In current practice reflective coatings evaporated in vacuum onto polished glass surfaces find wide use. For this application aluminum is most generally used, since it has a high reflection coefficient in the whole visible spectrum, good adhesion to glass, and completely satisfactory durability in most atmospheric conditions. The reflection coefficient of aluminum for white light reaches 89-90%.

It has been shown theoretically by a series of authors that with the deposition of a pair of transparent dielectric films on a metal it is possible to increase the reflection coefficient of the metal substantially on account of the phenomenon of light interference in thin films.[1,2]

Among the materials for films which increase the reflection of aluminum mirrors, magnesium fluoride and zinc sulfide, and also aluminum oxide and titanium dioxide obtained by anodic oxidation or hydrolysis of the ester of orthotitanic acid, have been suggested.[3-5]

Besides aluminum reflecting layers, chromium, nickel, palladium, and rhodium layers likewise are beginning to be used in equipment construction. Such layers differ advantageously from aluminum by high chemical stability and mechanical strength, but have a significantly lower reflection coefficient. An increase in the reflecting power of such mirrors would have substantial value.

In the present work such a problem was solved by depositing films of silica and titanium dioxide, obtained by hydrolysis of ethyl esters of orthosilicic and orthotitanic acids, on metallic reflecting layers by a method which is used for "clarifying" optics.[6] The application of

ch multilayer coatings for increasing the reflecting wer of glass and semitransparent aluminum layers s been described.[7,8]

Experiments were carried out with plane-parallel ecimens of mirror glass with a diameter of 45 mm d a thickness of 5 mm. The following method of prep- ration of mirrors was used. Aluminum layers were posited by evaporation in vacuum immediately after lishing the glass surface.

For the preparation of nickel reflecting layers on a er of nickel obtained by evaporation in vacuum (R = -50%), a nickel layer of about 0.15 μ thickness was posited electrolytically from a bath of the usual com- sition. Likewise palladium mirrors were prepared ctrolytically by a method described earlier.[9] With s objective, a layer of nickel was first deposited on glass by evaporation of the metal in vacuum, and n that layers of electrolytic nickel and palladium were posited. The palladium layer was about 0.1 μ thick. certain cases palladium mirrors were obtained on ers of chromium and palladium by evaporation in uum. Rhodium mirrors prepared electrolytically on ers of nickel on glass were supplied to us by A. I. vat. The method of preparation of these mirrors has en described previously.[10]

With the objective of seeking the conditions for max- um increase in the reflection coefficient of mirrors, dependence of the reflection coefficient was studied h respect to the thickness of the silica and titanium xide films, which was determined by two basic fac- s—the concentration of the esters and the speed of ation of the mirror samples.[11] The speed of rotation samples was constant in all experiments.

After deposition of each of the coatings the mirrors re annealed at a temperature of 120-220° for a period 2-3 hr. In Fig. 1 the experimental data for chromium, kel, palladium, and aluminum mirrors are presented.

In the Table the reflection coefficients obtained for white light are presented for the mirrors without films and with interference coatings.

Reflecting layer	Reflection coefficient (%)	Reflection coefficient with silica and titanium dioxide films (%)
Chromium	50—53	65—67
Nickel	60—63	72—75
Palladium	65—67	75—77
Rhodium	72—75	82—85
Aluminum	88—89	91—92

The results of spectral measurements are presented in Fig. 2. Calculation of the reflecting power of the metallic mirrors[4] gives values near to those observed experimentally if the optical constants of the metal and dielectric films are known to sufficient accuracy. Calculation of the thickness of the interference films by empirical formulas[11] shows that for the achievement of maximum reflection the thickness of the silica film should be approximately 1000 A and the thickness of the titanium dioxide film should be about 2000 A.

The interference films should be deposited on a freshly prepared mirror immediately after the corresponding preliminary preparation of the surface (this applies especially to aluminum mirrors). Considerable difficulties occurred in the development of a method for depositing layers of silica and titanium dioxide on nickel and nickel-palladium mirrors. Layers of silica and to an even greater extent titanium dioxide showed a tendency to disintegrate and peel. The observed defects were associated with the interaction of hydrochloric acid, present in the esters of the orthosilicic and orthotitanic acids, with metallic nickel. The effect is increased even more for nickel-palladium mirrors (probably because of the presence of the galvanic nickel-palladium pair). It is possible to obtain better adhesion of the layers either by acceleration of the hydrolysis of the esters as a result of rapid heating of the mirrors with films or by the use

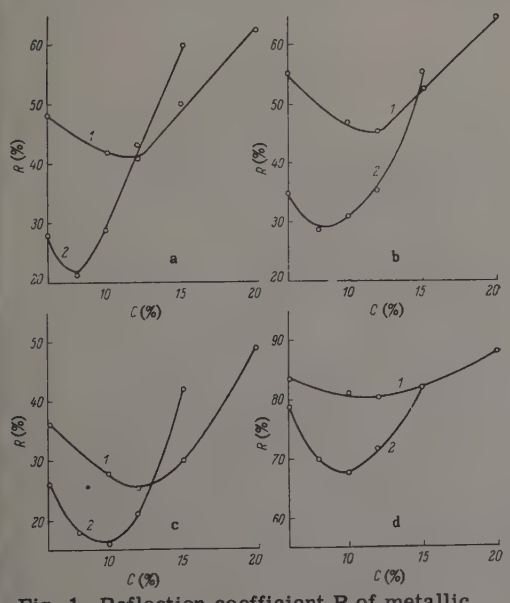

Fig. 1. Reflection coefficient R of metallic mirrors as a function of the concentrations C of esters of orthosilicic acid (curves 1) and orthotitanic acid (curves 2) which determine the thickness of silica and titanium dioxide films. Metals: a—nickel; b—palladium; c—chromium; d—aluminum.

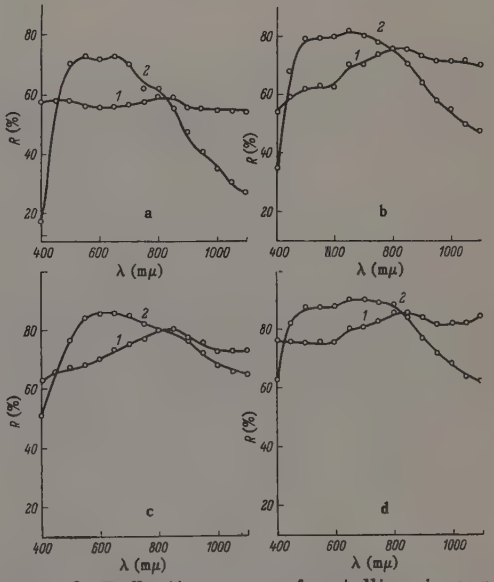

Fig. 2. Reflecting power of metallic mirrors without films (curves 1) and with silica and titanium dioxide films (curves 2). Metals: a—chromium; b—nickel; c—palladium; d—rhodium.

of palladium mirrors on chrome palladium layers on glass.

Deposition of the interference coatings not only increases the reflecting power of the mirrors, but in a significant measure increases their stability in corrosive media and their mechanical strength. The latter holds especially for aluminum mirrors. Thus, after 3-5 hr testing in a corrosion chamber with periodic moisture condensation and a drop in temperature from 50 to 35° in the course of each hour (cycle), a layer of aluminum on glass completely disintegrates. After 100 hr an aluminum mirror of the same type, with films of silica and titanium dioxide still does not show a trace of corrosion, and furthermore, the mirror retains the initial high reflection coefficient. The reflection coefficients of aluminum mirrors with films were lowered only to 89% after exposure for 1 hr in a 10% solution of caustic soda, whereas a metallic layer on the mirror without films is completely dissolved under the same conditions in 30-45 sec. Aluminum mirrors with films can remain for an hour in concentrated sulfuric acid without a change in reflection coefficient, whereas mirrors without films are completely dissolved in 20-30 min.

The mechanical durability of aluminum mirrors with interference films is not inferior to that of anodically oxidized mirrors. Likewise the chemical stability of nickel mirrors is substantially increased. Nickel mirrors have a reflection coefficient of about 8% after exposure of 20 hr in an atmosphere of moist hydrogen sulfide, whereas such mirrors with films retain a reflection coefficient of the order of 75% after 100 hr.

Reflecting layers of nickel, palladium, and chromium are completely dissolved in concentrated nitric acid in 17, 45, and 60 min, respectively, whereas mirrors with films still retain reflections of 42, 46, and 68% after 60 min.

In concentrated sulfuric acid a reflecting layer of nickel on glass is completely dissolved in 10 min, the reflection of palladium mirrors falls to 58% (from 65-67%) in an hour, and that of chromium mirrors to 47% (from 50-59%), whereas mirrors with films retain a high reflecting power—73, 72, and 64%, respectively, after an hour.

The method of deposition of interference films of silica and titanium dioxide is very simple. Moreover, the observed effect of increase in reflecting power and durability of mirrors on deposition of two interference films deserves definite attention.

T. S. Tatarinova took part in this work.

REFERENCES

1. R. Messner, Optik **2**, 228 (1947).
2. F. Abeles, Compt. acad. sci. **224**, 733 (1947).
3. A. F. Turner, J. Opt. Soc. Am. **36**, 711 (1946).
4. G. Hass and A. P. Bradford, J. Opt. Soc. Am. **44**, 810 (1954).
5. M. A. Validov, Zhur. Opt.-Mekh. Prom. No. 1, 31 (1958).
6. I. V. Grebenshchikov, A. G. Vlasov, B. S. Neporent, and N. V. Suikovskaya, "Prosvetlenie Optiki." Gosudarst. Tekh. i Teoret. Izd., 1946.
7. T. N. Krylova, Opt. i Spektr. **4**, 217 (1958).
8. K. I. Tarasov, Opt. i Spektr. **6**, 94 (1959), Optics and Spectroscopy **6**, 54 (1959).
9. A. G. Samartsev, N. V. Andreeva, and A. I. Kvyat, Zhur. Opt.-Mekh. Prom. No. 10, 25 (1958).
10. A. I. Kvyat, Ph.D candidate's dissertation, Leningrad, 1955.
11. G. A. Aleksandrov, Zhur. Opt.-Mekh. Prom. No. 1, 25 (1958).

MAGNETIC RESONANCE SPECTRA OF F^{19} IN AROMATIC COMPOUNDS WITH SUBSTITUENTS CONTAINING FLUORINE

V. F. Bystrov, E. Z. Utyanskaya, and L. M. Yagupolskii (pp. 138-141)

Received 6 June 1960

In recent years a large number of aromatic compounds with various substituents containing fluorine have been synthesized. Certain of them find use in technology as light-fast dyes, photosensitizers, and drugs.

In this investigation, the magnetic resonance spectrum of F^{19} nuclei of some substituents containing fluorine in aromatic rings was studied. Chemical shifts were measured relative to the fluorine resonance line in benzotrifluoride and expressed in terms of the quantity

$$\delta = \frac{H_i - H_r}{H_r} \cdot 10^6,$$

where H_i and H_r are the resonance values of the external magnetic field for F^{19} nuclei in the group investigated and in the reference material ($C_6H_5CF_3$), respectively. For expressing the chemical shifts relative to F_2 the quantity 493.3, which corresponds to the shift of the resonance in $C_6H_5CF_3$,[1] was added.

A cylindrical ampule of the material to be studied was placed in a radiofrequency coil above an ampule of the reference compound. The effective volume of the reference compound was about 20 mm^3, that of the sample about 80 mm^3. The samples were pure liquids or solutions of the solid compound. No correction for the diamagnetic susceptibility of the sample was made. The NMR apparatus and method of measurement have been described in detail previously.[2] The intensity of the permanent magnetic field was 4530 gauss. The resolving power of the apparatus for measuring chemical shifts was about 1×10^{-6}; the precision of the measurements $\pm 0.3 \times 10^{-6}$. For measurement of the spin-spin interaction constant, the resolution was about 2×10^{-7}, which was achieved by mechanical rotation of the sample and by reduction of the effective volume to about 4 mm^3. All measurements were made at room temperature. Examples of the spectra are given in Figs. 1 and 2.

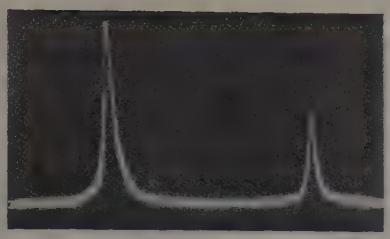

Fig. 1. Oscillogram of the absorption signals from F^{19} in the molecule F– –SO_2CF_3 (chemical shift between signals $\delta = 19.7 \times 10^{-6}$).

Experimental values of the chemical shifts in the ups investigated are given in Table 1. The resonance nals of the compounds indicated were single narrow s, which indicates the chemical equivalence of the rine atoms in each group.

Fig. 2. Recorded absorption signal from F^{19} in the SCF_3-group of the molecule 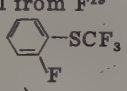 (spin-spin interaction equals 4.6 cps).

The electronegativity of the substituents in the ben- ring decreases in the order $SO_2CF_3 > CF_3 > SCF_3 >$ F_3 and 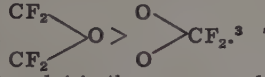 .[3] The magnetic screening e F^{19} nuclei in these groups decreases in the order $CF_3 > CF_3 > OCF_3 > SCF_3$ and 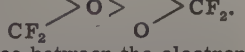 . easy to see the correspondence between the electron nity of the substituent and the screening of the fluorine ei in the group. The SCF_3 and OCF_3 groups are ex- ions relative to each other. Since a change of the par- netic term in the magnetic screening constant[4] is the f cause of the chemical shift in fluorine compounds, paramagnetic term increases from the SO_2CF_3-group e SCF_3-group in the series given above. The large amagnetic term of the magnetic screening constant of rine in the $C_6H_5SCF_3$ molecule in comparison with $_5OCF_3$ can perhaps be explained in the following way. magnitude of the paramagnetic term is inversely portional to the averaged energy difference of the ecular electrons in the ground and excited states. In $C_6H_5SCF_3$ molecule the 3p-valence electrons of di-

Table 1

Compound	$C_6H_5SCF_3$	$C_6H_5C{\equiv}CCF_3$		$C_6H_5OCF_3$	$C_6H_5CH{=}CHCF_3$			$C_6H_5SO_2CF_3$
Chemical shift relative to F_2	472.9	479.3	480.1	489.0	493.5	493.8*	499.8	509.4

*Measured in a solution of ethanol at a concentration of 1.5 mole/liter.

valent sulfur take part in bond formation. The minimum excitation energy of these electrons is less than the minimum excitation energy of the 2p-valence electrons which take part in forming the bonds of the divalent oxygen in the $C_6H_5OCF_3$ molecule.

The data on the dissociation constants of carboxylic acids indicate that a carbon atom forming a triple bond is appreciably more electronegative than one forming a double or aromatic bond. This bond, in turn, is somewhat more electronegative than a carbon atom forming a saturated σ-bond.[5,6] Table 2 compares the dissociation constants of the acids with the fluorine chemical shifts in the corresponding trifluoromethyl derivatives. It is easy to see that the chemical shift of fluorine in the CF_3-group decreases with an increase of the electronegativity of the carbon to which the CF_3-group is attached.

Table 2

Carboxylic acid	Dissociation constant $K \times 10^5$ (ref. 5)	Trifluoromethyl derivative	δ
$CH_3CH_2CH_2COOH$	1.50	CF_3-group on the aliphatic carbon atom	495±7 [7]
$C_6H_5CH_2CH_2COOH$	2.19		
$C_6H_5CH{=}CHCOOH$ { trans-	3.65	$C_6H_5CH{=}CHCF_3$	493.5
cis-	13.2		
C_6H_5COOH	6.27	$C_6H_5CF_3$	493.3 [1]
		β-$C_{10}H_7CF_3$	493.8
$CH_2{=}CHCOOH$	5.56	CF_3-group on the ethylene carbon atom	485 [7]
$C_6H_5C{\equiv}CCOOH$	590	$C_6H_5C{\equiv}CCF_3$	479.3

In addition, we studied the effect of different substituents in the benzene ring on the chemical shift of fluorine in fluorine-containing groups. The results of the measurements are given in Table 3. The chemical shifts are measured relative to the corresponding fluorine-containing group in the unsubstituted compound. Analysis of the data shows that with the introduction of various substituents, the chemical shift of fluorine changes little. Since the spectral ranges are narrow and do not overlap, one can use measurements of the chemical shifts to determine the presence of the indicated groups in newly synthesized compounds.

For the ortho-substituents of the fluorobenzenes, the resonance line of the fluorine in the SCF_3-, OCF_3-, and SO_2CF_3-groups splits into two components (Fig. 2). This is caused by the indirect spin-spin interaction with the

Table 3

X / Compound	p-NH_2	p-$NHCOCH_3$	m-$NHCOCH_3$	o-$NHCOCH_3$	p-F	m-F	o-F	p-Cl	p-Br	p-NO_2	Spectral range
$XC_6H_4SO_2CF_3$ . . .	+0.8[a,b]	—	—	—	—0.1	—0.3	—0.7	—0.3[c]	—0.6[c]	—0.7[b,c]	508.7—510.2
$XC_6H_4CF_3$	—	—	—0.5[a,b]	—2.2[b]	—0.4[8]	+0.5[8]	—	0.0[1]	—	—	491.1—493.8
$XC_6H_4OCF_3$	—0.2[a]	—0.1[a,b]	—0.2[b]	—0.3[b]	+0.8	+0.7	+1.8	0.0	—	—	488.7—490.8
$XC_6H_4SCF_3$	+0.6	—	+0.8[a,b]	+0.9[a,b]	+0.6	—0.5	—0.9	0.0	—0.3	—0.9[a,c]	472.0—473.8

*These measurements were made in solution.
Solvent: a – ethanol; b – nitromethane; c – nitrobenzene.

fluorine in the ring. The spin-spin interactions equal 4.6, 4.4, and 9.4 cps, respectively. The splitting for the corresponding meta- and para-fluorobenzenes is not observed with an apparatus of this resolving power. This is explained by the much smaller spin-spin interaction in meta- and para-fluorobenzenes, which was shown for fluorine derivatives of benzotrifluoride.[8] The resonance line of the CF_3-group in $C_6H_5CH = CHCF_3$ is split into two components because of the indirect spin-spin interaction between the F^{19} nuclei in the CF_3-group and the protons at the α-carbon atom. The spin-spin interaction equals 4.7 cps.

Only one narrow line is observed for the compound 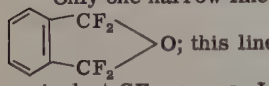 ; this line corresponds to the chemically equivalent CF_2-groups. In the case of 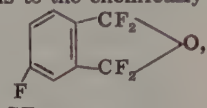 , however, the resonance line from the 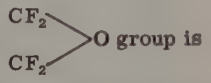 group is split into two components separated by 6.5×10^{-7}. The width of each component is greater than the instrumental broadening, and represents an unresolved multiplet. Evidently, the presence of fluorine in the ring leads to a nonequivalence of the CF_2-groups, which also causes the formation of an unresolved multiplet structure.

REFERENCES

1. H. S. Gutowsky, D. W. McCall, B. R. McGarvey, and L. H. Meyer, J. Am. Chem. Soc. **74**, 4809 (1952).
2. V. F. Bystrov, L. L. Dekabrun, Yu. N. Kil'yanov, A. U. Stepanyants, and E. Z. Utyanskaya, Prib. i Tekh. Ekspt. No. 1 1961. (Instruments and Experimental Techniques, in press.)
3. L. M. Yagupol'skii, V. F. Bystrov, and E. Z. Utyanskaya, Doklady Akad. Nauk SSSR **135**, No. 2 (1960).
4. N. F. Ramsey, Phys. Rev. **78**, 699 (1950); A. Saika and C. P. Slichter, J. Chem. Phys. **22**, 26 (1954).
5. J. F. J. Dippy, Chem. Revs. **25**, 151 (1939).
6. C. K. Ingold, "The Mechanism of Reactions and the Formation of Organic Compounds." Izd. Inostrannoi Lit., Moscow, 1959.
7. P. M. Borodin and F. I. Skripov, Izvest. Vyssh. Ucheb. Zaved., Ser. Radiofiz. **1**, No. 3, 37, No. 4, 69 (1958).
8. R. E. Richards and T. Schaefer, Trans. Faraday Soc. **54**, 1447 (1958).

THE SPECTRA AND LUMINESCENCE KINETICS OF CaF_2:Tb SINGLE CRYSTALS

P. P. Feofilov (pp. 142-144)

Received 25 July 1960

In an article[1] on the luminescence spectra of artificial fluorite single crystals (CaF_2) activated by rare earth elements (RE), we noted the presence in the CaF_2:Tb spectra of two similar sequences of the line groups displaced by about 5800 cm^{-1} relative to each other. These sequences, located in the 380-480 mμ (L') and 490-660 mμ (L) regions, respectively (See Fig. 1a), were correlated with two types of luminescence centers, whose existence was established[1] for all rare earth ions introduced into the fluorite single crystals. Further investigation has shown, however, that this correlation, which placed terbium in a unique position with regard to the other RE, was mistaken. In the latter case the groups of lines, while differing considerably in structure, have approximately the same position in both types of spectrum. It actually turned out that in CaF_2:Tb, as well as in all other CaF_2:RE crystals, the difference between the so-called type I and type II spectra is relatively small and reduces to a difference in the structure of individual groups of lines. (See Fig. 1b.)

The presence of two sequences in the CaF_2:Tb luminescence spectra should apparently be considered as being due to transitions from two electronic levels of the excited state of the Tb^{3+} ion to levels of the fundamental state, which is known[2] to be an inverted ^7F multiplet. The lower excited level (~20,500 cm^{-1}) can be interpreted[3] as being $^5D_4$. The next level, whose position (~26,500 cm^{-1}) is known from absorption spectra,[4] has not been classified.[2] This is illustrated in the energy level diagram shown in Fig. 2. The Table gives the locations of the four most clearly isolated groups of lines in the L and L' luminescence spectra. The positions of the long wavelength groups in both sequences (the 2-0 and 2'-0' groups) cannot be indicated with sufficient accuracy for the following reasons: The distances between groups decrease towards the longer wavelengths, the multiplet splitting becomes comparable with the splitting of the levels in the field of the crystal, and the groups begin to overlap. As shown in the Table, the difference between the frequencies of corresponding groups of lines remains approximately constant. No better agreement can be expected, since the groups of lines cover a range of 300-500 cm^{-1} and the position of the "center of gravity" of the group can be determined with only limited accuracy. The relative intensity of the two sequences varies greatly from one

Fig. 1. Luminescence spectra of CaF_2:Tb single crystals. a—Portion of the spectrum at room temperature; b—the structure of groups 5 and 4 in the two types of spectrum at −183°C.

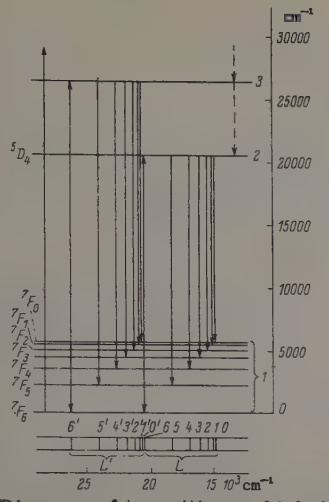

Fig. 2. Diagram of transitions which determine the luminescence of CaF_2:Tb crystals.

ıple to the next. This also was the reason for the er- ous assignment of the sequences to two types of spec- While the interpretation of two sequences of groups ines can be settled uniquely from spectral analysis, itional investigation is necessary to establish the hanism of the process. Indeed, two different mecha- ms may give spectrally identical results: (1) The elec- excited to a level above 3 (see Fig. 2) may lose its rgy rapidly and find itself in states 3 or 2, from which ontaneous transition with the probability p_{31} or p_{21} occur to the levels of system 1. (2) The excited elec- may go first to level 3. From there, transitions are sible either directly to the levels of system 1 (prob- ity p_{31}), giving rise to the luminescence L', or to el 2 (probability p_{32}), from which the electron can re- to the ground state with the probability p_{21}. This s rise to the luminescence L. In order to have the ation intensities in the two sequences L' and L com- able, (which, as a rule, is actually the case) it is ob- sly necessary that the probabilities p_{31} and p_{32} be parable. The 3 → 2 transition may be accompanied adiation (infrared), or it may be radiationless. Its bability p_{32} is apparently considerably different for erent crystal samples.

Position of Bands in the CaF_2:Tb Luminescence Spectrum

Frequencies of the "center of gravity" of each band				
N of band	ν (cm⁻¹)	N of band	ν' (cm⁻¹)	$\nu' - \nu$ (cm⁻¹)
6	20500	6'	26300	5800
5	18300	5'	24100	5800
4	17000	4'	22900	5900
3	16100	3'	21700	5600

We can easily satisfy ourselves as to the following: If in the case of the first mechanism the luminescence in both sequences must decay according to the exponential law $I = I_0 \exp(-t/\tau)$ with $\tau = 1/p_{21}$ and $\tau' = 1/p_{31}$, then in the stepwise second process, exponential decay with $\tau' = 1/(p_{31} + p_{32})$ will occur only in the short wavelength sequence L'. The longer wavelength luminescence L will decay according to the complex law

$$I = I_0 \frac{\tau' e^{-\frac{t}{\tau'}} - \tau e^{-\frac{t}{\tau}}}{\tau' - \tau},$$

where, as in the first case, $\tau = 1/p_{21}$.

Our preliminary kinetic investigations, which we carried out by means of a "tau meter,"[5] have shown that a purely exponential decay with $\tau' = 2 \times 10^{-3}$ sec occurs in the short wavelength sequence. (Filters were used to isolate the 5'-4' groups.) At the same time, a sharp deviation of the decay curve from the exponential form and a two- to threefold increase in the average afterglow duration is observed in the long wavelength region of the spectrum. (Filters were used to isolate the 5 or 5-0 line groups.)

Thus a study of the spectra and kinetics of luminescence of CaF_2:Tb single crystals shows that the luminescence processes are stepwise in nature. It also shows that due to the weak interaction of excited states, thermal equilibrium between them cannot become established even during a time interval of 10^{-3} sec, which is enormously long on the molecular scale. As a result, the excited state contains not only ions at the lowest level, but a comparable number of ions with an energy excess of 5800 cm⁻¹ as well.

We have also observed the absence of a thermal distribution over the levels of the excited state in a series of other crystals activated by rare earths and uranium.[6]

REFERENCES

1. I. V. Stepanov and P. P. Feofilov, Doklady Akad. Nauk SSSR 108, 615 (1956), Soviet Phys.-Doklady 1, No. 4, 350 (1956).
2. M. A. El'yashevich, "Spektry redkikh zemel' (Rare Earth Spectra)." Gosudarst. Izd. Tekh. i Teoret. Lit., Moscow, 1953.
3. H. F. Geisler and K. H. Hellwege, Z. Physik **136**, 293 (1953).
4. W. Prandtl and K. Scheiner, Z. annorg. u. allgem. Chem. **220**, 107 (1934); Ibid. **232**, 267 (1937).
5. N. A. Tolstoi and P. P. Feofilov, Uspekhi Fiz. Nauk **41**, 44 (1950).
6. L. M. Belyaev, G. F. Dobrzhanskii, O. V. Sokolova, and P. P. Feofilov. Doklady na IX Soveshchanii po Lyuminestsentsii (Proceedings of the Ninth Conference on Luminescence) Kiev, 1960.

O P T I K A I S P E K T R O S K O P I Y A

Volumes I through V

Some of the papers in the 1956 through 1958 volumes of "Optika i Spektroskopiya" have been translated. These are listed below, and information as to their availability may be obtained from the sources of translations given hereafter. The capital letters in parenthesis at the end of each translation identify its source.

ACSIL
Admiralty Centre for
Scientific Information
and Liaison
Queen Anne's Mansions
London, S.W.1, England

AEA
Industrial Group HQ
Risley, Lancs.
England

AEC
Atomic Energy Commission
Technical Information Servi
P.O. Box 62
Oak Ridge, Tennessee

AEI
Associated Electrical
Industries, Ltd.
Research Laboratory
Aldermaston, Berks.
England

AERE
United Kingdom Atomic Energy
Research Establishment
Harwell, Nr. Didcot
Berks., England

ASLIB
8 Palace Gate
London, W.8, England

ATS
Associated Technical
Services, Inc.
P.O. Box 271
East Orange, N.J.

CEA
Commissariat a l'Energie
Atomique
Bellevue
Seine et Oise, France

CNRS
Centre National des Re-
searches Scientifiques
Bellevue
Seine et Oise, France

CSIRO
Commonwealth Scientific and
Industrial Research Organ-
ization, 314 Albert Street
East Melbourne, Australia

COURTAULDS LTD.
Foleshill Road
Coventry
England

DSIR HQ
Department of Scientific an
Industrial Research Head-
quarters Library, Chester
House, 5-11 Regent Street
London, S.W.1, England

INDUSTRIAL GROUP HQ
Risley, Warrington
Lancs., England

INFOSEARCH
242 Willesden Lane
London, N.W.2, England

INSDOC
Hillside Road
New Delhi, 12, India

LC
Photoduplication Service
Publication Board Project
Library of Congress
Washington 25, D.C.

LLU
Department of Scientific and
Industrial Research Lending
Library Unit, 20 Chester Tce.
Regents Park, London, N.W.1
England.

NRC
National Research Council o
Canada, The Library
Sussex Drive
Ottawa, Canada

OTS
Office of Technical Services
225 D Street, S.E.
Washington, D.C.

PILKINGTON BROTHERS, LTD.
Research Department
St. Helens, Lancs.
England

PROGIL
10 C...

ROWNTREE
Robert F. Rowntree
90 East Norwich Avenue
Columbus 1, Ohio

SL
Science Library, The Keeper
Science Museum Library
South Kensington
London, S.W.7, England

...sociati...
...on Cente..., John
...ar Library, 86 East
Randolph Street
Chicago, Illinois

FILLER MATERIAL - NOT IN RUSSIAN ORIGINAL

nslations Sources

TF
Taylor and Francis, Ltd.
Red Lion Court, Fleet St.
London, E.C.4, England

ME I (1956)

LNOVICH, V.M.
eory of the Intrinsic Optical Activity of lecular Crystals. I. Classical Theory. C or SLA)
LNOVICH, V.M. and FAIDYSH, A.N.
gration and Transmission of Electron Ex- tation Energy from the Base Material to e Impurity in Molecular Crystals in the esence of two types of Excitons. C or SLA)
LNOVICH, V.M. and FAIDYSH, A.N.
fluence of Reabsorption on the Quantum eld of the Luminescence of Solid So- tions of Organic Compounds. SIR HQ and ACSIL)
IANGEL'SKAYA, V.A. et al
simple method for the Determination of e Transmission of Certain Optical Mater- ls in the Schumann Spectrum Range. NFOSEARCH)
V, N.G. et al
eory of the Superfine Structure of Rota- onal Spectra of Molecules Caused by the ectric 2^4-Polar Moment of the Nucleus. SIRO)
RCHUKOVA, N.R. and DUBROVSKII, G.B.
fect of Variating Argon Pressure in ectrolodeless discharge on the Re- ction of the Wavelength of the Red ne of Cd^{114}. (LLU; SL and NRC)
TDI
ectres d'Absorption des Homologues du nzene. (PROGIL)
YSH KUCHEROV, I.Ya. and TERSKII, in the Transfer of lution of SLA)

f band

MONOV,
tle not available. (ATS)
INSKAYA, D.A. et al
frared Spectra of Sodium Silicate asses and their Relationship with the ructure. (INFOSEARCH)

GALANIN, N.L. and CHIZHIKOVA, Z.A.
Transfer of Excitation Energy in Anthracene Crystals Containing Naphthacene as Impurity (ACSIL)
GRUDINKINA, N.P.
Absorption of Ultra-violet Radiation by Water (INFOSEARCH)
IVANOV, A.P. et al
Spectrophotometric study of Mixtures of Powdered Objects. (INFOSEARCH)
KALITEEVSKII, N.I. and CHAIKA, M.P.
The Ratio of the Magnetic Spin and Quadrupole Moments of the Nuclei U^{233} and U^{235}. (AEC)
KALITEEVSKII and TAIVA
Magnetic Spin. (AERE)
KISELEV, B.A.
Double Monochrometer with Diffraction Gratings (INFOSEARCH)
KITAEVA, V.F. and SOBOLEV, N.N.
Shape and Width of Lines in D.C. Arc Spectra. (AERE)
KOLOMITSOV, Yu.V. et al
Contactless Interference Method for the Control of Spherical Lens Surfaces. (INFOSEARCH, LLU)
KOLYADIN, A.I.
Anomalous Scatter of Light in Glass. (INFOSEARCH)
KORONKEVICH, V.P.
Dispersion of Air in the Visible Region of the Spectrum. (NRC and LLU)
LANDSBERG, G.S., SHATENSHTEYN, A.I. et al
Vibration Spectra of Diphenyl and Decadeutero-Diphenyl. (OTS)
LOTKOVA, E.N. et al
Infrared and Raman Spectra of Boric Anhydride. I. (INFOSEARCH)
NIKITINA, O.N.
Consideration of the Overlapping of the line-band Spectrum in the Analysis of Silica. (INFOSEARCH)
NOSKOV, M.M. et al
Measurement of Optical Constants of Metals in the Infrared Spectrum Region using Multiple Reflections. I. Theoretical Foundations of the Procedure. (INFOSEARCH)
OGANOV, M.N., STRIGANOV, A.R. and SOBOLEV, Yu.P.
Atomic Spectrum of Americium. (AERE and AEC)

FILLER MATERIAL - NOT IN RUSSIAN ORIGINAL

VOLUME I - Cont'd

PALITSYNA, I.A.
Modification of SF-4 Spectrophotometer for the High-speed Automatic Recording of Spectra. (INFOSEARCH)

RASKIN, Sh.Sh.
On the Raman Spectra of Complex Compounds of Antimony Trichloride with Benzene and some of its Derivatives. (LC or SLA)

RAUTIAN, S.G.
Illumination of a Spectrograph by a Three-Dimensional Light Source. (INFOSEARCH)

SHEREMET'EV, G.D.
Optical Properties of Uranium Hexafluoride. I. Absorption Spectra in the Visible and Neighboring Ultraviolet Region. (AEC)

STEPANOV, B.I.
Negative Luminescence and Negative Photo-effect. (INFOSEARCH)

STRIGANOV, A.R. and KOROSTYLEVA, L.A.
Atomic Spectra of Plutonium (AERE and AEC)

WEINBERG, G.V., ZAIDEL, A.N. and PETROV, A.A.
Spectral Analysis of Isotopic Compositions of Hydrogen-Deuterium Mixtures. (INDUSTRIAL)

YAROSLAVSKII, N.G., ZHELUDOV, B.A. and STANEVICH, A.E. A Recording Spectrometer for the Long Wave Infrared Region (ROWNTREE)

ZAKHAROVA, V.M. and KAGAN, Yu.M.
Investigation of the Discharge Parameters and the Character of the Excitation of Ion Lines at High Current Densities. (ACSIL)

VOLUME II (1957)

AGRANOVICH, V.M.
Theory of the Intrinsic Optical Activity of Molecular Crystals. II. Quantum Theory. (LC or SLA)

AKIMOV, A.I.
A Nomogram for use in Spectrum Analysis of Rare Earth Elements by the Addition Method. (SLA)

ANDREYESHCHEV, E.A. and ROZMAN, I.M.
Luminescence Spectra of Plastic Scintillators with Triphenylpyrazoline. (LC or SLA)

BAKHSHIYEV, N.G.
A new Principle of Spectrometry. (LC or SLA)

BRANDI, V.L.
Title not available. pp 323-329 (SLA)

BROUDE
Spectres d'Absorption des Homologues du Benzene. III. Absorption de la lumiere par les Benzene Dialcoyles (PROGIL)

BULANIN, M.O.
The Structure of Absorption Bands of Liquid H_2O, D_2O and HDO Determined by the Structure of the Molecules. (NRC)

DEIGEN, M.F.
Contribution to the Theory of Impurity Centres in Isotropic Homopolar Crystals. (PILKINGTON)

FEDOROV, F.I.
Optics of Magnetic Crystals. II. Binormals and Biradials. Optical Surfaces. III. Uniaxial and Unirefractive magnetic Crystals. (LC or SLA)

GROMOV, V.A.
New Method of Exciting Spectra in an atomic beam. (LC or SLA)

IVANOV, A.P.
Some Problems of Spectrophotometry of Light-scattering Media. (CSIRO)

KAGAN, Y.M. and PEREL, U.I.
On the Motion of Ions and the Shape of their Lines in the Positive Column of a Discharge. I. (AERE and AEI)

KARD, P.G.
The Analytical Theory of Optical Properties of Multi-layer Dielectric Coatings. (LC or SLA)

KIZEL, V.A. and STEPANOV, A.F.
Reflection of Light from a Liquid Surface and its connection with the Process of Crystallization. (LC or SLA)

LEONTOVICH, A.M.
Absorption Spectra of Crystals of Plutonium Salts. (LC or SLA)

LUSHCHIK, Ch.B.
New Methods of Investigation of Relaxation Processes and Trapping Centers in Crystal Phosphors. (LC or SLA)

LISITSA, M.P. and TSVELYKH, N.G.
Optique des coughes fines--phasage dans la reflexion de la lumiere par les couches minces d'argent, de germanium, de tellure et de selenium. (CEA)

MARKOVA, Z.A.
Application of Infrared Spectroscopy to the Study of some Olefine Absorption on Alumino-Silicate Catalyst. (SLA)

MAZING, M.A. and MANDEL'SHTAM, F.L.
On the Spectral Line Broadening and Shifting a gas Discharge Plasma. (AEI and SL)

RASHBA, E.I.
Theory of Strong Interactions of Electron Excitations with Lattice Vibrations in Molecular Crystals. (LC or SLA)

FILLER MATERIAL - NOT IN RUSSIAN ORIGINAL

ME II - Cont'd

AN, I.M.
pendence of the Luminescence Yield of astic Scintillators with Triphenylpyra- line on Temperature. (LC or SLA)
OVSKY, L.M. et al
ructure of Alkali-Halide Phosphors and echanism of Luminescence Process (INSDOC)
ROV, T.A. et al
frared Spectrum and Molecular Structure Phosphorus Oxide. I. (DSIR)
INIKOV, K.D. et al
uble Refraction of Fluoride Films NSDOC)
AREVSKI, I.N. and RYAZANOV, A.N.
spersion se le Saute de Phase des llicules Minces d'Aluminium.
NRS)
L'KOVSKII, A.A.
lculation of a Thin Multilayer Plate a one-layer Plate with an Effective fractive Index. (LC or SLA)

ME III (1957)

KA, M.P.
minosite d'un Spectrometre a Interfero- tre Fabry-Perot. (LC or SLA)
EN, M.F. and SHUL'MAN, L.A.
the Theory of Electron Spin Resonance f-Centers in Ionic Crystals (Continuum del of f-Center -- "Smoothed Function")
TS)
RIEVSKII, O.D., NEPORENT, B.S. and TIN, V.A.
gh-speed Infrared Spectrometer for the 8 - 3.0 μ Bank. (SLA)
PERIN, D.Yu.
plication of the Theory of Aberrations High Orders to the Calculation of tical Systems. (SLA)
V, E.I.
tle not available. Pp 115-122
TS)
HIN, V.L.
e Contribution of Soviet Science to minescence Research. (ACSIL)
NOVA, N.V. and RAUTIAN, G.N.
w Tables for Calculating Chromaticity -ordinates. (SLA)
OV, M.N.
Comparison of Low-Inertia Receivers Infrared Radiation. (ACSIL)

OSIPOV, B.
Hyperfine Structure of the Rotational Transition l=3:4 of the CH_3I^{127} Molecule. (CSIRO)
OSTROVSKII, Yu.I. and PENKIN, N.P.
Relative f-Values of the Spectral Lines of Scandium. (LC or SLA)
PENKIN, N.P. and FRISH, S.E.
The Emission and Absorption Spectra of Uranium. (AERE)
SHATALOV, A.A.
Photochemical Conversion of Color Centers in Heated Alkali-Halide Crystals. (LC or SLA)
SIDOROV, T.A. and SOBOLEV, N.M.
Infrared and Raman Spectra of Boron Oxide. II. Infrared Spectra and Molecular Structure. (PILKINGTON)
SMIRNOV, L.V.
Study of Molecular Dichroism by Means of an Artificial Orientation of the Molecules. (AEC)
VAINSHTEIN, L.A.
The Calculation of Atomic Wave Functions and Oscillator Strengths with an Electronic Computer. (AERE)
ZEMSKOV, E. and VESELAGO, V.
Stark Effect in Rotational Spectra of Molecules of the Asymmetrical Top Type in the Presence of Quadrupole Interaction (the case re=eQq). (CSIRO)

VOLUME IV (1958)

AGRANOVICH, V.M.
On the Capture of "Free" Excitons by Impurities in Molecular Crystals. (OTS)
BARCHUKOV, A.I. and BASOV, N.G.
Measurement of Frequencies and Intensities of Hyperfine Structure Lines of CH_3I (J=0→1 Transition). (LC or SLA)
BARCHUKOV, A.I., MURINA, T.M. and PROKHOROV, A.M.
Microwave Spectrum and Rotational Constants of the C_2H_5Cl Molecule. (LC or SLA)
BARCHUKOV, A.I. and PROKHOROV, A.M.
Microwave Spectrum of the CH_3GeH_3 Molecule. (LC or SLA)
BASOV, N.G. and OSIPOV, B.D.
Lines of Emission for the F=5/2-3/2, J=1, K=1 Transition of the Rotational Spectrum of the CH_3I^{127} Molecule. (LC or SLA)
BATARCHUKOVA, N.R.
Comparative Investigations of the Metrological Qualities of the Spectral Lines of ^{206}Pb and ^{114}Cd. (LC or SLA)

FILLER MATERIAL - NOT IN RUSSIAN ORIGINAL

VOLUME IV - Cont'd

CHARNAYA, F.A.
Investigation of the Instantaneous Brightness of a Flash Discharge. (AEC)

FAIDYSH, A.N.
Experimental Proof of the Theory of the Transfer of Excitons by Diffusion. (LC or SLA)

FRISH, S.E. and YAKHONTOVA, V.E.
New Data Regarding the Excitation Functions of Helium Lines. (DSIR)

GALANIN, M.D. and CHIZHIKOVA, Z.A.
On the Quenching of Luminescence of Organic Substances upon Excitation by α-particles. (LC or SLA)

GALANIN, M.D.
On the Causes for the Dependence of the Luminescence Yield of Organic Substances on the Energy of the Ionizing Particles. (LC or SLA)

GERASIMOV, F.M., TEL'TEVSKII, I.A., et al
Diffraction Gratings from the State Optical Institute. (LC or SLA)

GURVICH, I.M.
Rayonnement d'un Tube d'Impulsion Puissant au Moment de l'Explosion. (LC or SLA)

IRISOVA, N.A.
Radiospectroscopic Investigation of CH_3GeCl_3 (LC or SLA)

IVANOV, A.P.
Theoretical Investigations of the Behavior of Luminescent Radiation of Dispersed Luminescent Particles. (LC or SLA)

JBANKOV, R.G.
Infrared Spectra of Cellulose Fibres. (COURTAULDS)

KAGAN, Yu.M. and PEREL, V.I.
On the Motion of the Ions and the Profile of the Spark Lines in the Positive Column of a Discharge. II. Radical Motion of the Ions in a low pressure Discharge. (AEC)

KAGAN, Yu.M. and PEREL, V.I.
On the Motion of Ions and the Shape of their Lines in the Positive Column of a Discharge. III. The directed motion of Ions in a Discharge at Arbitrary Pressure. (AERE)

KATS, M. and SEMENOV, B.Z.
The Absorption and Luminescence Spectra of Nickel-Activated Alkali-Halide Crystals. (LC or SLA)

KRYLOVA, T.N.
Multilayer Dielectric Coatings with a High Coefficient of Reflectance on Glass Surfaces. (LC or SLA)

LUBCHENKO, A.F. and RASHBA, E.I.
On the Excitonic States of a Molecular Crystal containing Different Molecules. (OTS)

LYZINA, L.A.
Method of Precipitation of Solid Dye Layers from Solutions; Corrections due to the Reflectance made in Absorption Measurements of these layers. (LC or SLA)

NIKITIN, V.A.
Relationship between the Scanning Speed and the Resolving Power of a Spectral Instrument. (LC or SLA)

PARFIANOVICH, I.A.
Interaction between Electrons and the Activator in NaCl-Ni and NaCl-Cu Phosphors. (LC or SLA)

PEDOS, F.Z. and SVENTITSKII, N.S.
A Low-voltage Vacuum pulsed Discharge for Exciting Spectra. (DSIR)

PROTAS, I.R.
Plates for Vacuum Ultraviolet Photography. (LC or SLA)

ROZMAN, I.M.
On the Theory of Quenching of Fluorescence of Solutions. (NRC)

ROYEV, L.M., FILIMONOV, V.N. and TERENIN, A.N.
Changes in the Infrared Spectra of Molecules Interacting with the Adsorption Centers of a Silica-Alumina Catalyst. (ATS)

SEVCHENKO, N.A. and FLORINSKAYA, V.A.
Infrared Spectral Transmittance of Porous and Quartzoid Glasses. (LC or SLA)

SEVCHENKO, N.A. and FLORINSKAYA, V.A.
Reflection Spectra of Quartz Crystal Plates cut at Different Angles to the Optical Axis within the 7-24$_\mu$ Wavelength Range.(LC or SLA)

SHIROKSHINA, Z.V. and SUIKOVSKAYA, N.V.
Preparation of Infrared Transmitting Films. (LC or SLA)

SIDOROV, T.A.
Infrared Spectra at Low Temperatures and the Structure of Quartz and Crystobarlite. (PILKINGTON)

SLYUSAREV, G.G. and KULIKOVSKAYA, N.I.
Distribution of Light Energy Changed in the Diffraction Pattern by Variable Transmittance Filters. (LC or SLA)

STEPANOV, B.I. and PRIMA, A.M.
Vibrational Spectra of Silicates. I. (PILKINGTON)

TAGIROV, R.B.
A Method of Measuring the Reflection Coefficient of Mirrors. (LC or SLA)

TARASOVA, L.I. and FEOFILOV, P.P.
Polarization of Luminescence and the Nature of Luminescent Centers in NaCl-Ag and KCl-Tl Crystals. (LC or SLA)

TOLSTOI, N.A.
Possibility of Using Pulse Lamps for Studying the Relaxations of Luminescence of Photoconductivity. (LC or SLA)

FILLER MATERIAL - NOT IN RUSSIAN ORIGINAL

LUME IV - Cont'd.

CORETS, A.S.
Absorption and Scattering of Light in Pigments (LC or SLA)
EMENKO, V.A.
Luminescence of Cadmium Sulfide Crystals. (LC or SLA)
IDEL, A.N.
Determination de la composition Isotopique d'apres les Spectres d'Absorption. (CEA)

LUME V (1958)

LCHUKOV, A.I. and PROKHOROV, A.M.
Quadrupole Coupling, Dipole Moment and Barrier of Internal Rotation of the CH_3GeH_3 Molecule as Determined from its Rotational Spectrum. (LC or SLA)
LYANIN, V.B.
Multiplet Splitting of the Ground Term of the Holmium Atom. (OTS)
HKOVA, C.P., RAZUMOVSKAYA, L.P. and FRISH, [illegible] A simplified method of Spectral Analysis of Inert Gases for purity. (AERE)
TLER, G.I.
Infrared Polarization Filters. (LC or SLA)
TISHIN, M.T.
Optical Constants of Germanium in Region 2-25μ (PILKINGTON)

KOVARSKII, V.A.
Theory of Non-Radiation Transitions in an F-Center. (ATS)
MOROZ, L.P.
Imaging of Separate Objects by an Aberration less Optical System in a Field which is more or less luminant than the Objects Themselves. (LC or SLA)
PEDOS, F.Z. and SVENTITSKII, N.S.
Excitation des spectres dans la Region du Vide par une Decharge pulsee a basse tension. (CEA)
SINEL'NIKOV, K.D. and RYAZANOV, A.N.
Resolving Power of Optical Systems Increased (LC or SLA)
TITUSHINA, V.P. and FABRIKANT, V.A.
Etude de la Divergence du Flux de Rayonnement de la Raie 2537A d'une Decharge dans le Mercure. (LC or SLA)
VOYEVODSKII, V.V., MOLIN, Yu.N. and CHIBRIKIN, B.M. Spectra of Electron Paramagnetic Resonance of Cr-Aromatic Compounds with Various Substitutes. (OTS)
YAROSLAVSKII, N.G. and STANEVICH, A.E.
The Rotational Spectrum of H_2O in the long Wavelength Region of the Infrared 50-1500μ (200-7 cm^{-1}) (ROWNTREE)

THIS LIST WILL BE BROUGHT UP TO DATE FROM TIME TO TIME

bruary 20, 1961

FILLER MATERIAL - NOT IN RUSSIAN ORIGINAL

THE OPTICAL SOCIETY OF AMERICA

Why should you join OSA?

There is no other association of opticists in existence to promote and disseminate knowledge in this field. The Optical Society of America was organized in 1916 "to increase and diffuse the knowledge of optics in all its branches pure and applied, to promote the mutual interests of investigators of optical problems, of designers, manufacturers and users of optical instruments and apparatus of all kinds, and to encourage co-operation among them".

What about the advantages of membership?

You receive three monthly publications:

THE JOURNAL OF THE OPTICAL SOCIETY OF AMERICA: *This is the official publication of OSA*

OPTICS AND SPECTROSCOPY: *an English translation of the leading scientific journal of the USSR Academy of Sciences in this field*

PHYSICS TODAY: *as OSA is a member society of the American Institute of Physics, OSA members receive this publication**

From JOSA and OPTICS AND SPECTROSCOPY you will not only learn what your American colleagues are doing, but also discover what the Russians are working on in your field. Together these two journals publish the work of American and Russian scientists in all branches of optics and spectroscopy, including X-ray, ultraviolet, visible, infrared and microwave, filters, lens design, thin layer optics, geometric optics, electron optics, diffraction gratings, electroluminescence, wave mechanics, thermal radiation backgrounds, detectors, infrared polarizers, and their many applications in science and industry.

You will also receive announcements and programmes of all meetings (OSA holds at least two a year) and, even if you cannot attend many of these, you will know what is going on in your area. And you can submit a paper and have it given by proxy.

Who can join?

OSA invites to membership all who are interested in any branch of optics, either in research, in teaching, in optical applications, in the manufacture and distribution of optical equipment of all kinds, or in physiological and medical optics.

What are the membership dues? $13.00 per annum.

How can you join?

Write Dr. Mary E. Warga, Executive Secretary, Optical Society of America, 1155 16th Street, N. W., Washington 6, D. C., for an application form.

*OSA members may also subscribe to other AIP publications at a reduced rate.

OPTICAL SOCIETY *of* AMERICA

1155 SIXTEENTH STREET, N. W. WASHINGTON 6, D. C.

(FILLER MATERIAL - NOT IN RUSSIAN ORIGINAL)

OPTICAL SOCIETY *of* AMERICA

THE OPTICAL SOCIETY OF AMERICA was organized in 1916 "to increase and diffuse the knowledge of optics in all its branches, pure and applied, to promote the mutual interests of investigators of optical problems, of designers, manufacturers and users of optical instruments and apparatus of all kinds and to encourage cooperation among them." The Society cordially invites to membership all who are interested in any branch of optics, either in research, in instruction, in optical applications, in the manufacture and distribution of optical equipment of all kinds, or in physiological and medical optics.

APPLICATION FOR MEMBERSHIP

Full Name .....Date of Birth .....

Present Professional Position .....

.....

Previous Professional Positions *(with approximate dates)* .....

.....

.....

.....

Education *(List Colleges and Universities attended and degrees received, with dates)*

.....

.....

.....

Chief Publications in Optics *(Titles and journal references. Need not be complete.)*

.....

.....

.....

.....

.....

.....

.....

I wish my subscriptions to the Journal of the Optical Society of America and to the Russian translation journal, Optics and Spectroscopy, to begin January first of ☐ the current year ☐ next year

....., 19..... .....

(Date) *(Signature of Applicant)*

Please print or type your name and address in the space below, exactly as they should appear on the addressograph stencil, which will accommodate no more than four typewritten lines with thirty-one characters or spaces in each line. The Executive Secretary should be notified promptly of all changes of address.

.....

.....

.....

.....

All journal subscriptions date from January 1. Dues are assessed and the journals delivered for the complete calendar year in which application is made unless the applicant requests that the subscriptions begin on January 1 of the following year. Do not send payment of dues with this application. Bill will be sent by the American Institute of Physics after the applicant is elected.

FILLER MATERIAL - NOT IN RUSSIAN ORIGINAL

SPONSORS

We recommend that the applicant named on the reverse be elected to membership.

.....
Member

.....
Member

ACTION BY MEMBERS OF BOARD OF DIRECTORS

Elected to Associate Membership by approval of the undersigned.

.....
.....
.....
Directors

EXCERPTS FROM THE BY-LAWS RELATIVE TO MEMBERSHIP AND DUES

(As Amended January 1, and September 11, 1959)

Eligibility: Any person who is interested in optics is eligible for Associate Membership.

Any person who has been an Associate Member for three years, or has contributed materially to the advancement of optics, is eligible for Regular Membership.

Any person who has served with distinction in the advancement of optics is eligible for transfer to the class of Fellow.

Any person who has rendered eminent service in the advancement of optics may be elected to Honorary Membership.

Application for Membership: Applications for membership must state the candidate's name and qualifications for membership and must be signed by two Associate, Regular, Fellow, Emeritus or Honorary Members of the Society.

Election to Membership: Applications from individuals for membership shall be considered first as applications for Associate Membership and shall be acted upon as such. Applicants shall become Associate Members when their duly prepared applications have received the written approval of three members of the Board of Directors.

Associate Members will automatically become Regular Members at the conclusion of three years as Associate Members. Associate Members may also be transferred to Regular Membership before the completion of the three-year period at any regular meeting of the Board of Directors by a two-thirds vote of the members of the Board present.

Regular Members may be transferred to the class of Fellow at any regular meeting of the Board of Directors by a two-thirds vote of the members of the Board present. The number of Fellows shall at no time exceed one-tenth of the total membership of the Society, except that no one who has been transferred to the class of Fellow shall be displaced from that class because of a reduction in the total number of members in the Society. Fellows shall pay the same dues as Regular Members.

Honorary Members may be elected at any regularly called meeting of the Board of Directors by the unanimous vote of the entire Board. In case any members of the Board are not in attendance their ballots must be obtained by the Executive Secretary. The number of Honorary Members shall at no time exceed five

Duties and Privileges: On payment of their dues,* as determined from time to time by the Board of Directors, Associate Members have the following privileges: The right to attend meetings and receive the Journal of the Society and such other publications as the Board of Directors may direct.

On payment of their dues,* as determined from time to time by the Board of Directors, Regular Members and Fellows have the following privileges: The right to vote, hold office, attend meetings, and receive the Journal of the Society and such other publications as the Board of Directors may direct.

Honorary Members pay no dues. They have the following privileges: The right to vote, hold office, attend meetings, and receive the Journal of the Society and such other publications as the Board of Directors may direct.

Termination of Membership: Membership in the Society may be suspended or terminated by vote of the Board of Directors. Failure to pay dues for one year shall be deemed sufficient cause for suspension or termination of membership.

---

* By action of the Board of Directors, effective April 1, 1959, the annual dues are: Associate Members, $13.00; Fellows and Regular Members, $17.00.

FILLER MATERIAL - NOT IN RUSSIAN ORIGINAL

TRANSLITERATION OF CYRILLIC CHARACTERS

used by the Optical Society of America

А	а	a	Р	р	r
Б	б	b	С	с	s
В	в	v	Т	т	t
Г	г	g	У	у	u
Д	д	d	Ф	ф	f
Е	е	e	Х	х	kh
Ж	ж	zh	Ц	ц	ts
З	з	z	Ч	ч	ch
И	и	i	Ш	ш	sh
Й	й	i	Щ	щ	shch
К	к	k	Ъ	ъ	″
Л	л	l	Ы	ы	y
М	м	m	Ь	ь	′
Н	н	n	Э	э	e
О	о	o	Ю	ю	yu
П	п	p	Я	я	ya

(FILLER MATERIAL - NOT IN RUSSIAN ORIGINAL)

EDITOR'S NOTE

Comments on the scientific content of the translated Russian articles published in OPTICS AND SPECTROSCOPY are invited. They should be addressed as a Letter to the Editor of the Journal of the Optical Society of America and forwarded to the Editor of that journal, Dr. D. B. Judd, National Bureau of Standards, Washington 25, D. C.

UNIVERSITY OF ILLINOIS 3
LIBRARY
UNDERGRADUATE DIV
NAVY PIER GRAND AVE
CHICAGO 11 ILL

VOL. X, NO. 1 OPTICS AND SPECTROSCOPY JANUARY 1961

CONTENTS

(Numbers in parentheses are original Russian page numbers.
These Russian page numbers are also quoted at the head of each paper.)

The Size of Atomic Electron Shells as a Function of Atomic Number . . . . . V. S. Korol'kov 1 (3)
Measurement of the Absolute Values of the Oscillator Strengths for the Resonance Lines of Calcium, Strontium, and Barium Ions . . . . . Yu. I. Ostrovskii and N. P. Penkin 3 (8)
Spectral Determination of the Isotopic Composition of Lithium . . . . . A. N. Zaidel', A. N. Razumovskii, and M. P. Chaika 7 (15)
On the Use of the Curves $\nu = f(Z_X)$ in the Study of the Vibrational Spectra of Tetrahedral Molecules and Ions of the Form $X(Hal)_4$ . . . . . I. N. Godnev and A. M. Aleksandrovskaya 14 (27)
Calculation of the Integrated Intensities of the Infrared Bands of Isotopically Substituted Methanes. VIII . . . . . L. M. Sverdlov 17 (33)
Calculation and Interpretation of the Vibrational Spectra of Isobutane . . . . . T. I. Kuznetsova and M. M. Sushchinskii 20 (41)
On the Temperature Dependence of the Intensities of Vibrational Absorption Bands in Gases . . . . . M. P. Lisitsa and V. L. Strizhevskii 23 (48)
Infrared Absorption and Raman Spectra of Bipropenyl and Diallyl and the Question of Rotational Isomerism . . . . . Yu. A. Pentin, Yu. N. Panchenko, E. G. Treshchova, and Z. Sharipov 27 (55)
Raman Spectra of Various Classes of Hydrocarbons. VII. Ditertiaryalkylmethanes C_{10}–C_{17}–Branched Alkanes with Two Quaternary Carbon Atoms Separated by a Methylene Group . . . . . E. G. Treshchova, V. M. Tatevskii, V. K. Daukshas, and R. Ya. Levina 31 (63)
Vibrational Spectra of Organic Compounds Containing Elements of Group IV (Si, Ge, Sn) I. Characteristic Absorption Bands in the Infrared Spectra of Silicon-Organic Compounds . . . . . N. A. Chumaevskii 33 (69)
The Vibrational Spectra of Silicates. II. Infrared Absorption Spectra of Silicates and Germanates with Chain Anions . . . . . A. N. Lazarev and T. F. Tenisheva 37 (79)
On the Mechanism of the Transition of Excited Organic Molecules into the Metastable State . . . . . G. A. Mokeeva and B. Ya. Sveshnikov 41 (86)
Electroluminescence of a Powdered ZnS:Cu:Mn Electroluminor in a dc Field . . . . . V. N. Favorin and G. S. Kozina 43 (91)
The Reflection of Radiation from an Infinite Flat Surface Illuminated by a Point Source. I. Characteristics of the Radiation Field . . . . . B. A. Grigoriev, A. G. Ershov, and V. A. Uvarov 46 (96)
Experimental Study of the Intensity Distribution in the Spectrum of Diffraction Gratings for Polarized Light . . . . . E. A. Yakovlev and F. M. Gerasimov 50 (104)
The Effect of Object Thickness on Phase Contrast . . . . . Radu Grigorovich and Radika Manaila 54 (113)
On the Chromatic Field Aberrations in Electron Microscopes . . . . . V. N. Vertsner and Yu. V. Vorob'ev 58 (120)
Non Selective Optico-Acoustical Receiver of Radiation with a Capacitor Microphone . . . . . N. A. Pankratov and E. F. Vasil'ev 61 (127)

SHORT COMMUNICATIONS

On the Influence of the Nature of the Solvents on the Character of the Band of the Carbonyl Group in the Infrared Spectra of Carbonyl Compounds . . . . T. V. Yakovleva, A. G. Maslennikova, and A. A. Petrov 64 (131)
Remarks on Negative Absorption . . . . . S. G. Rautian and I. I. Sobel'man 65 (134)
Metallic Mirrors with an Enhanced Reflection Coefficient . . . . . E. I. Levitina 66 (135)
Magnetic Resonance Spectra of F^{19} in Aromatic Compounds with Substituents Containing Fluorine . . . . . V. F. Bystrov, E. Z. Utyanskaya, and L. M. Yagupolskii 68 (138)
The Spectra and Luminescence Kinetics of CaF_2:Tb Single Crystals . . . . . P. P. Feofilov 70 (142)